STUDIES ON INTERACTION OF NIOBIUM AND PROTACTINIUM WITH HYDROUS OXIDES

By

SHRI MADHUSUDAN GHOSH
CHEM01201304020

Bhabha Atomic Research Centre

A Thesis submitted to the

Board of Studies in Chemical Science

In Partial fulfillment of requirements for the degree of

DOCTOR OF PHILOSOPHY

of

HOMI BHABHA NATIONAL INSTITUTE

July, 2019

Homi Bhabha National Institute

Recommendations of the Viva Voce Committee

As members of the Viva Voce Committee, we certify that we have read the dissertation prepared by **Mr. Madhusudan Ghosh** entitled **"Studies on interaction of niobium and protactinium with hydrous oxides"** and recommend that it may be accepted as fulfilling the thesis requirement for the award of Degree of Doctor of Philosophy.

Chairman - Dr. P D Naik PDNaik **Date:** 06.01.2020

Guide / Convener – Dr. K K Swain **Date:** 06.01.2020

External examiner – Prof. Manoj Shrivastava Shrivastava **Date:** 06.01.2020

Member 1- Dr. C. P. Kaushik **Date:** 6/1/2020

Member 2- Dr. Neetika Rawat Neetika Rawat **Date:** 06.01.2020

Member 3- Dr. S. Mishra **Date:** 06-01-2020

Technology adviser - Dr. Remya Devi PS **Date:** 06.01.2020

Final approval and acceptance of this thesis is contingent upon the candidate's submission of the final copies of the thesis to HBNI.

I/We hereby certify that I/we have read this thesis prepared under my/our direction and recommend that it may be accepted as fulfilling the thesis requirement.

Date: 06.01.2020
Place: BARC, MUMBAI.

(Signature)
Guide

STUDIES ON INTERACTION OF NIOBIUM AND PROTACTINIUM WITH HYDROUS OXIDES

By

SHRI MADHUSUDAN GHOSH
CHEM01201304020

Bhabha Atomic Research Centre

A Thesis submitted to the

Board of Studies in Chemical Science

In Partial fulfillment of requirements for the degree of

DOCTOR OF PHILOSOPHY

of

HOMI BHABHA NATIONAL INSTITUTE

July, 2019

Homi Bhabha National Institute

Recommendations of the Viva Voce Committee

As members of the Viva Voce Committee, we certify that we have read the dissertation prepared by **Mr. Madhusudan Ghosh** entitled **"Studies on interaction of niobium and protactinium with hydrous oxides"** and recommend that it may be accepted as fulfilling the thesis requirement for the award of Degree of Doctor of Philosophy.

Chairman - Dr. P D Naik PDNaik	**Date:** 06.01.2020
Guide / Convener – Dr. K K Swain	**Date:** 06.01.2020
External examiner – Prof. Manoj Shrivastava Shrivastav	**Date:** 06.01.2020
Member 1- Dr. C. P. Kaushik	**Date:** 6/1/2020
Member 2- Dr. Neetika Rawat Neetika Rawat	**Date:** 06.01.2020
Member 3- Dr. S. Mishra	**Date:** 06-01-2020
Technology adviser - Dr. Remya Devi PS	**Date:** 06.01.2020

Final approval and acceptance of this thesis is contingent upon the candidate's submission of the final copies of the thesis to HBNI.

I/We hereby certify that I/we have read this thesis prepared under my/our direction and recommend that it may be accepted as fulfilling the thesis requirement.

Date: 06.01.2020
Place: BARC, MUMBAI.

(Signature)
Guide

STATEMENT BY AUTHOR

This dissertation has been submitted in partial fulfillment of requirements for an advanced degree at Homi Bhabha National Institute (HBNI) and is deposited in the Library to be made available to borrowers under rules of the HBNI.

Brief quotations from this dissertation are allowable without special permission, provided that accurate acknowledgement of source is made. Requests for permission for extended quotation from or reproduction of this manuscript in whole or in part may be granted by the Competent Authority of HBNI when in his or her judgment the proposed use of the material is in the interests of scholarship. In all other instances, however, permission must be obtained from the author.

Madhusudan Ghosh

(Madhusudan Ghosh)

DECLARATION

I, hereby declare that the investigation presented in the thesis has been carried out by me. The work is original and has not been submitted earlier as a whole or in part for a degree / diploma at this or any other Institution / University.

Madhusudan Ghosh

(Madhusudan Ghosh)

List of Publications arising from the thesis

Published

1. **“**Sorption of niobium on colloidal silica and the effect of humic acid”, **M. Ghosh**, Remya Devi P. S, Rakesh Verma and A. V. R. Reddy, J. Radioanal Nucl Chem. **2015**, 306/1., 147-153.
2. “Interaction of niobium with iron-oxide colloids and the role of humic acid” **M. Ghosh**, K.K. Swain and Rakesh Verma, J. Environ. Radioactivity, **2017**, 178/179., 101-109.
3. “Sorption of Nb(V) on Pyrolusite (β-MnO_2): effect of pH, humic acid, ionic strength, equilibration time and temperature” **M. Ghosh**, Remya Devi PS, KK Swain. Appl. Radiat. Isot. **2019**, 154., 108887 (1-8).
4. “Thermodynamic and Spectroscopic investigation of Nb(V) and Pa(V) sorption on colloidal Silica” **M. Ghosh**, A. K. Yadav, Remya Devi P.S, K. K. Swain, Rakesh Verma, S. N. Jha, D. Bhattacharyya. Environ. Earth Sci. **2020**, 79., 32 (1-12).

Communicated

1. “Effect of different physico-chemical factors on sorption of Pa(V) on iron oxides” **M Ghosh**, Remya Devi PS, KK Swain. Appl. Radiat. Isot.(ARI_2019_1108) under review

Chapters in books

Published

1. “Sorption of Protactinium (V) on silica colloid and the effect of humic acid” **M. Ghosh** and R Verma, “Thorium-Energy for the future: select papers from ThEC2015” by AK Nayak and Bal Raj Sehagal (Springer; 1st ed. **2019**, ISBN-13: 978-9811326578) pp. 125-139. *https://doi.org/10.1007/978-981-13-2658-5_8.*

Other publications:

Conferences/Symposia

1. “Sorption of ^{231}Pa on silica and the effect of humic acid” **M. Ghosh** and Rakesh Verma, Thorium Energy Conference 2015 (ThEC15) October 12 -15, **2015**, Mumbai.

2. “Sorption of Nb(V) on Pyrolusite (β-MnO_2): Effect of pH, humic acid, ionic strength and temperature” **M. Ghosh**, Remya Devi PS, KK Swain, NUCAR-2019, January 15-19, **2019**, Mumbai.

Madhusudan Ghosh

(Madhusudan Ghosh)

Dedicated to

My Family

ACKNOWLEDGEMENTS

From the depth of my heart, I express my sincere gratitude to the Almighty for all the blessings till date and forthcoming.

Firstly, I would like to express my sincere gratitude to my guide Dr. K K Swain, Analytical Chemistry Division (ACD), Bhabha Atomic Research Centre (BARC) for the continuous support of my Ph.D study and related research, for his patience and motivation,. His guidance helped me in all the time of research and writing of this thesis.

I sincerely acknowledge the support and guidance of Dr. H. Pal, Associate Director (A), Chemistry Group and Head, Analytical Chemistry Division for improvement of quality of the thesis.

I am greatly indebted to my mentor Dr. R. Verma, Former Head, Nuclear Analytical Methods Section, ACD, BARC, for encouragement, critical suggestions and posing challenging question throughout my work and this help me a lot to improve the quality of work.

It is with immense gratitude that I acknowledge the insightful comments, suggestions and encouragement rendered by my Doctoral Committee consisting of eminent scientists Dr. P D Naik (Chairman), Dr. C P Kaushik, Dr. Neetika Rawat, Dr. S Mishra along with my mentor Dr. Remya Devi PS.

I thank my fellow labmates Aditi A. Dalvi, Nicy Ajith, Trupti A. Chavan, for their support during the experiments and for valuable inputs for this thesis. I thank Dr. R.K. Singhal, Dr. M.K. Dey, Dr. A.K. Satpati, Dr. H. Basu and all other colleagues of ACD, BARC, for facilitating a healthy and cheerful working environment.

I earnestly thank the team members of BL-9, beam facility, Indus-2, Raja Ramanna Centre for Advanced Technology (RRCAT) for co-operation during the XAFS experiments. Special thanks to Dr. S.N. Jha and Dr. A.K.Yadav for their help.

There is no need for formal word of thanks for my entire family for their love and continuous support - both spiritually and materially and who have stood beside me through journey.

Finally, I thank all those who have helped me directly or indirectly in the successful completion of my thesis. Anyone, whose contribution is not mentioned in the above list, is also acknowledged.

Madhusudan Ghosh

(Madhusudan Ghosh)

LIST OF ABBREVIATION

Nuclear Fuel Cycle	NFC
Ammonium Di-uranate	ADU
Fast Breeder Test Reactor	FBTR
Pressurized Heavy Water Reactor	PHWR
Low Level Waste	LLW
Intermediate Level Waste	ILW
High Level Waste	HLW
High Efficiency Particulate Absorber	HEPA
Humic Substances	HS
Humic Acids	HA
X-Ray Absorption Fine Structure	XAFS
Time Resolved Laser Fluorescence Spectroscopy	TRLFS
X-Ray Photoelectron Spectroscopy	XPS
Distribution Coefficient	k_d
X-Ray Diffraction	XRD
Brunauer-Emmett-Teller	BET
High Purity Germanium Detector	HPGe
Dynamic Light Scattering	DLS
Energy Dispersive X-Ray Fluorescence	EDXRF
Energy Dispersive X-Ray Spectrometry	EDS
Fourier Transfomed Infrared Spectroscopy	FTIR

CONTENTS

Page No.

CHAPTER I

CHAPTER II:

Sorption of niobium and protactinium on colloidal silica

Chapter III

Sorption of niobium and protactinium on iron oxides

Chapter IV

Sorption of Nb and Pa on manganese dioxide

Chapter V

Evaluation of sorption mechanism using Thermodynamic studies and X-Ray Absorption Fine Structure (XAFS)

Chapter VI

Summary and future perspectives

SYNOPSIS

Since the discovery of radioactivity, it finds application in various fields of science & technology. It has enriched our society in several areas namely power production, medical science, agriculture, industry and strategic applications. In the field of power production, the term Nuclear Fuel Cycle (NFC) is used to describe the entire cycle starting from the mining of uranium to the reprocessing of spent fuel and the final disposal of the radioactive waste. The process from mining to fuel fabrication is called Nuclear Front End, whereas the reprocessing and waste management is termed as Nuclear Back End of the NFC. The main source of high-level radioactive waste is the fission products in the spent fuel from nuclear reactors. Other sources of radioactive waste arise from nuclear weapons testing, decommissioning of nuclear facilities and the waste from radioactive laboratories. It has been envisaged that high-level waste originating from the nuclear reprocessing plant will be stored underground in geological repositories after suitable treatment [1]. The main objective of underground storage of radioactive waste is to isolate it from the environment for a long period of time to avoid any possible release to cause any undue radiation exposure [2].

Nowadays, the back end of the NFC has become the most concerned and challenging research area in the nuclear industry, although there are standard protocols in place for the management and disposal of radioactive waste. The concern is due to any possible unwanted release and migration of radionuclides [3], more specifically those radioisotopes that have high yield in the fission/activation process and long half-life [4]. In general, the factors affecting the release and migration of the radionuclides in the environment are precipitation, complexation and sorption processes. Precipitation process takes the radionuclides in solid phase, thereby limits the concentration in the solution phase and thus retards their release and migration. Complexation of the radionuclides with organic and inorganic ligands present in aqueous medium can increase the release and migration of the species due to increased solibilization of the complexes. This increases the concentration of the radionuclides in the mobile phase. Attachment of radionuclides to mineral or rock surfaces in contact with aqueous phase, called the sorption process, can reduce the migration process substantially [5]. Based on the above three processes, most of the existing literature suggests that the tri and tetravalent radioisotopes cause no major hazard, as they have very high tendency to get sorbed onto the material engineered for their isolation and also in host rocks [6]. Earlier, a two-phase model, consisting of a mobile and a stationary phase, was used to explain the migration of radionuclides in aquatic system. However, a recent study reveals the migration of ^{239}Pu upto a distance of about 1.3 km in 30 years from the Nevada test site [7]. Penrose et al. [8] have studied the behaviour of Pu and Am in the Mortandad canyon and observed the migration rate of these radionuclides of about 0.5 km y^{-1} from the source. The two-phase model was unable to explain such fast and long-distance migration of radionuclides observed in previous cases. Another drawback of the two-phase model is its inability to explain the migration of radionuclides which have very low aqueous solubility. It was suggested that the colloids present in groundwater provide an additional phase causing enhanced migration [7]. Therefore, a three-phase model consisting of a mobile phase, a stationary phase and suspended colloids in mobile phase has been introduced to explain the enhanced migration of radionuclides and other contaminants in groundwater [9, 10].

The most important natural ligands found in groundwater are the humic acids. The presence of humic acid may affect the sorption and migration of radionuclides in the groundwater [11, 12]. It is reported that the anthropogenic actinides are about 10 times more concentrated in humic acid fraction than in the overall topsoil [13]. The complexation of humic acids with radionuclides increases the mean residence time of actinides in the mobile phase, which in turn reduces the sorption of the radionuclides to the stationary phase and thus enhances their migration. Humic acids can also affect the sorption behaviour of radionuclides by altering the oxidation state e.g. U(VI) to U(IV) and Np(V) to Np(IV) [13].

Oxides, especially those of Si, Al, and Fe, occur as colloids in groundwater. Various aspects of colloids that facilitate the transport of radionuclides in natural groundwater systems have been reviewed by Patera et al. [14]. Extensive work has also been carried out to understand the sorption of radionuclides on several minerals which include hydrous oxides of Fe [14-17], Mn [18], Si and Al [19], montmorillonite [20], bentonite [21] etc., studied for several radioisotopes like U, ^{239}Pu, ^{244}Cm, ^{241}Am, ^{60}Co, ^{152}Eu, ^{230}Th, ^{90}Sr, ^{137}Cs and so on.

Literature regarding leaching, sorption and migration of niobium (^{94}Nb) and protactinium (^{231}Pa) [22-24] are scanty and this motivated us to carry out extensive sorption studies for these two radionuclides in different hydrous oxides of Si, Fe and Mn, present in aquatic systems. The effect of pH, naturally occurring humic acid ligands, ionic strength, equilibration time and temperature on the sorption behaviour of ^{94}Nb and ^{231}Pa nuclides on silica, iron oxides and manganese dioxide have been evaluated. The sorption mechanism has been elucidated based on the classical sorption data (ionic strength and temperature dependent sorption study) and the spectroscopic evidences (Extended X-ray Absorption Fine Structure) obtained from the present study. In the PhD thesis, the work has been presented and discussed in six chapters, briefly described as follows.

Chapter 1: Introduction

This chapter provides the general introduction of the thesis encompassing the basic aspects of the element niobium (Nb) and protactinium (Pa). The course, in which ^{94}Nb and ^{231}Pa are generated in the nuclear industry, may be described as follows. Zirconium-niobium (Zr-Nb) alloy is used as pressure tubes in nuclear power reactors [25] because of its excellent mechanical strength [26] and very high resistance to hydride attack. ^{94}Nb (half-life: 2.03 x 10^4 y) is generated in the pressure tube by the (n,γ) reaction of the stable isotope ^{93}Nb. The presence of ^{94}Nb, along with other fission and activation products in discharged pressure tubes, results in large radiation field. The short and medium-lived radioisotopes (half-life: ≤ 1.5 y) decay off after 8-10 years of cooling [27]. ^{94}Nb activity remains for a prolonged period due to the long half-life.

Thoria is irradiated in a nuclear reactor for the production of fissile isotope ^{233}U via (n, γ) nuclear reaction of ^{232}Th and subsequent beta decay of ^{233}Th. Along with ^{233}U, ^{231}Pa (half-life: 3.27 x 10^4 y) is also generated via (n, 2n) nuclear reaction of ^{232}Th and consecutive beta decay [28]. After extraction of ^{233}U, ^{231}Pa remains in the aqueous phase along with other actinides. This aqueous phase is considered as high-level radioactive liquid waste. The severe concern in the handling and management of this high-level waste is the presence of ^{231}Pa, because the isotope is both long-lived and alpha-emitting [29]. ^{94}Nb and ^{231}Pa are thus two important radionuclides in radioactive waste and could have long term radiological impact. Chemical properties of these two elements and their comparisons are discussed in this chapter, which are the basis of the present thesis work.

Chapter 2: Sorption of ^{94}Nb and ^{231}Pa on colloidal silica

Sorption of niobium (Nb) and protactinium (Pa) on silica colloids was studied using radiotracer (^{94}Nb and ^{231}Pa) in the pH range of 2-11 in $NaClO_4$ medium, adopting batch equilibration method. Gamma activity measurements were carried out using high purity germanium (HPGe) detector coupled to 8k channel analyzer. Silica was characterized using X-ray diffraction (XRD), light scattering and surface area measurements. The point of zero charge for silica colloids was about pH 2. It is found that both Nb and Pa were strongly sorbed on silica colloids in the pH range of 3 to 9 in $NaClO_4$ medium. The sorption is lower (70-80 %) below pH 3 and above pH 9. There is no significant change in the sorption behaviour of both Nb and Pa on silica colloids in the presence of humic acid between pH 3 to 9. However, there is a small increase in the sorption below pH 2 and a small reduction in sorption above pH 10.

The pH dependent sorption phenomenon observed can be explained in terms of the chemical species of Nb and Pa exist at different pH condition and the variation in the zeta potential of silica at different pH. Literature reports suggest that both the elements exist as single positively charged species below pH 3 and this was confirmed in the case of Pa by determining the average charge (~ +1) in dilute $HClO_4$ medium (0.1 to 3M). Coulombic repulsion between the positively charged Pa and positive surface charge on silica colloids may be the reason for the lower sorption below pH 3. The strong sorption on silica colloids in the pH range 3 to 9 was assigned to the surface complexation between neutral species of Nb/Pa with the silanol groups of silica colloids. In basic pH, both Nb and Pa exist as negatively charged species and the zeta potential of silica is highly negative. Therefore, coulombic repulsion between them reduces the sorption of Nb/Pa on silica colloids in the alkaline condition.

The slight increase of sorption below pH 2 in the presence of humic acid (HA) may be due to sorption of humic acid on silica causing a reduction in surface charge of the colloids. In basic medium, carboxylate groups of humic acid may undergo complexation with Nb/Pa, increasing the concentration of the metal ions in the solution, and thus reducing their sorption on silica colloids.

Chapter 3: Sorption of ^{94}Nb and ^{231}Pa on various iron oxides

In this Chapter, results on the sorption of Nb and Pa on various iron oxide colloids are reported along with the effect of pH, ionic strength, humic acid and temperature on the sorption process. Iron oxides viz. goethite (FeOOH), hematite (α-Fe_2O_3), and magnetite (Fe_3O_4) were chemically synthesized and characterized by XRD, particle size, surface area, and zeta potential measurements. Results show that the sorption of Nb on all the three iron oxides was low (10-20 %) at pH 1, increased to ~ 90% at pH 8 and decreased marginally above pH 8. Presence of humic acid resulted in increased sorption of Nb/Pa on iron oxides in acidic medium, whereas the reverse was observed in basic medium. In acidic medium (pH 1), it is observed that the sorption is decreased with an increase in the ionic strength, and the effect of ionic strength is found to be strongest in the case of goethite, and least in the case of hematite. In basic medium (pH 10), the effect of ionic strength on sorption is quite negligible for all three oxides. From the above observations, it is inferred that the sorption in acidic pH occurs mainly due to ion-exchange between positively charged species of Nb/Pa and the surface –OH groups on the iron oxides. In basic pH, ion exchange phenomenon cannot contribute to the sorption, because the existence of Nb/Pa as the anionic species, causing a reduction in the sorption. Thermodynamic parameters viz. activation energy, enthalpy, entropy, free energy, and sticking probability were estimated to understand the mechanism of the sorption process. Although the enthalpy is found to be positive, the free energy change is overall negative, suggesting the sorption process to be an entropy-driven phenomenon. The sorption process followed pseudo-second-order kinetics and the sticking probability model of sorption indicated that the process is indeed chemisorption. The dissolution study of iron oxides shows that the iron concentrations in the supernatant in the case of goethite and hematite are negligible throughout the pH range, whereas ~3 % magnetite got dissolved in acidic pH. The solubility of magnetite in the acidic region may be due to the presence of Fe(II) in its structure which partially goes to the solution phase. From the above studies, it is clear that sorption is not influenced by the dissolution of goethite and hematite in acidic pH, though a mild effect exists in the case of magnetite.

Chapter 4: Sorption of ^{94}Nb and ^{231}Pa on manganese dioxide

The sorption of Nb/Pa on synthesized manganese dioxide has been described in this Chapter. The effects of pH, ionic strength, humic acid, temperature and equilibration time were investigated in a series of batch equilibrium experiments. The synthesized oxide was characterized using XRD, Fourier transform infrared (FTIR) spectroscopy, Scanning electron microscopy (SEM), surface area, particle size, and zeta potential measurements. The sorption is found to be affected by solution pH, ionic strength and humic acid. The sorption is high in neutral and near neutral pH zone (~ 96 %) but lower sorption is observed both in acidic pH (70-80 %) and basic pH (~ 85 %) conditions. Sorption decreases in acidic pH with an increase in ionic strength and reverse effect is seen in basic pH, although the effect in the latter case is less prominent. From the above results, it is inferred that the mechanism of sorption is the physisorption or outer sphere complexation at acidic pH and chemisorption or innersphere complexation at basic pH conditions. Presence of humic acid enhances the sorption in acidic pH, which indicates that mineral bound humic acid facilitates the sorption process at low pH whereas at higher pH, the dissolved humic acid complexes with Nb/Pa causing a decrease in sorption on manganese dioxide. The sorption process is found to be endothermic in acid medium but the positive entropy change makes the free energy of the sorption process negative and hence the process is spontaneous. However, the sorption in basic medium is exothermic and the high magnitude of enthalpy change indicates that the sorption process follows the chemisorption mechanism. Kinetics of the sorption is found to follow pseudo first order rate under acidic pH whereas pseudo second order rate under basic pH. Pseudo first order fitting under low pH condition suggests the physisorption mechanism whereas pseudo second order kinetic fitting proposes the chemisorption mechanism at high pH condition.

Chapter 5: Evaluation of sorption mechanism using Extended X-ray Absorption Fine Structure (EXAFS)

The sorption experiments discussed in the previous chapters were carried out using tracer solutions of ^{94}Nb and ^{231}Pa in nanomolar (nM) concentration, which is not sufficient for EXAFS studies as the method require higher concentration. Due to the constraints of handling radioactivity at the EXAFS facility, inactive Nb solution was used in elevated concentration (mM) for the sample preparation. Nb sorbed silica samples at pH 1.2, 6.5 and 10.5 were prepared and kept hydrated, to keep the bonding feature intact. Complete drying of the samples were avoided because it may change the binding features.

The EXAFS measurements were carried out at the Energy-Scanning EXAFS beamline (BL-

9) at the Indus-2 Synchrotron Source (2.5 GeV, 100 mA) in Raja Ramanna Centre for Advanced Technology (RRCAT), Indore, India. X-ray absorption spectrometry (XAS) measurements were performed in transmission mode placing the slurry sample in a transparent glass cuvette in the beam path. The experiments were performed at Nb K-edge energy. The same absorption edge position for all three pH condition suggests identical oxidation state for Nb.

The Fourier transform EXAFS spectra of Nb-SiO_2 at pH 1.2 suggests that there are two O atoms nearest to Nb at a distance 1.98 Å, indicating the presence of niobyl group as $[O{=}Nb{=}O]^+$ in hydrated condition. The other two O atoms at 2.08 Å may correspond to Nb-O bond which is longer and less rigid. The same amplitudes of different k-weighted spectra for the first and second peaks confirm similar atomic species in both the coordination shells. The second co-ordination shell also contains two O atoms with an average distance of 2.43 Å, which are the characteristics of equatorial water molecules around Nb. From the analysis of the EXAFS data at pH 1.2, it is obvious that there is no nearby Si atom upto 3.46 Å and the EXAFS data could be fitted satisfactorily with oxygen coordination shells.

It is inferred that there is no chemical bond formation between colloidal silica and Nb present in aqueous media. This finding also explains the low sorption of Nb on colloidal silica at pH 1.2. Hence the sorption at lower pH may be attributed to physisorption or ion exchange mechanism.

Although the systems at pH 6.5 and pH 10.5 have the same type of environment in the first coordination shell, the analysis suggests the presence of Si atom in the second coordination sphere. This implies the formation of chemical bond between silica and Nb atoms via oxygen bridge. The formation of chemical bonds between Nb and Si leads to high sorption of Nb onto silica at these pH conditions. The Si atom density around Nb atom at pH 6.5 and pH 10.5 are found to be about 1.32 and 1.65, respectively.

The EXAFS data of Nb sorbed hematite at three different pH (1, 6 and 10) also confirmed that at pH 1, Nb is not coordinated with Fe atom whereas at pH 6 and at pH 10, Nb is coordinated with 0.5 and 2 numbers of Fe atoms at 2.93 Å and 2.72 Å distances, respectively. These findings support the physisorption mechanism in acidic pH and chemisorption mechanism at neutral and basic pH conditions.

Chapter 6: Summary and future perspectives

In this Chapter, a brief summary of the research work carried out under the PhD programme has been presented, highlighting the major observations and suggesting the future perspectives of the present investigation.

The major outcomes of the present study are as follows:

(i) The sorption of both ^{94}Nb and ^{231}Pa in the acidic range is low and follow physisorption mechanism. The sorption is however quantitative in neutral or near neutral pH region and suggested to chemisorption mechanism. These propositions have been established based on ionic strength and temperature dependent sorption data as well as from the EXAFS spectroscopic evidences.

(ii) The quantitative sorption in neutral to near neutral pH region indicates that in the natural aquatic condition the migration of these two radionuclides is mainly assisted by the colloids present in the medium.

(iii) The naturally occurring complexing ligand i.e. humic acid, can alter the Nb/Pa sorption both in acidic and basic region, either by its self-absorption onto the colloids or by its complexation with the radionuclides at those respective pH conditions.

Future perspective of the present investigation:

(i) EXAFS investigation in Nb sorbed pyrolusite systems can provide more information on the sorption mechanism.

(ii) More detailed spectroscopic investigations on the sorption behaviour of Nb/Pa on iron oxides of mixed oxidation state (magnetite) and studies in regards to changing of metal ion oxidation states can provide more insight of the sorption process.

(iii) Utilization of laser-based fluorescence techniques to study the sorption mechanisms in very low concentration level of the radionuclides can provide more relevant information.

(iv) Sorption study of ^{94}Nb and ^{231}Pa on naturally occurring bentonite, clay minerals and soil samples are worth to be investigated in regard to the migration of radionuclides in aquatic systems.

References

1. Geological disposal of radioactive waste: An overview of the current status of understanding and development. Organization for economic cooperation and development (OECD), 1984, OECD publication service, Paris.
2. F.R. Rinderknecht, H. Geckies, T. Schafe, Bentonite erosion and colloid mediated transport of radionuclides in advection controlled system, Dissertation Karlsruher, Karlsruher Institut fur Technologie (KIT) (2017).

3. M.J. Apted, Radionuclide release from high-level nuclear-waste packages, J. Radioanal. Nucl. Chem. 142/1 (1990) 321-330.
4. D.J. Wiggins, J.A. Franz, Mobility of organic complexes of some NON-TRU fission and activation products: A selective review, PNL-2607 (UC-70), (1978) Pacific Northeast Laboratory, USA.
5. W. Stumm, J.J. Morgan, Aquatic Chemistry: Chemical Equilibria and Rates in Natural Waters. 3rd Edition, (1996) John Wiley & Sons, New York.
6. A.B. Khasanova, N.S. Shcherbina, S.N. Kalmykov, Yu. A. Teterin, A.P. Novikov, Sorption of Np(V), Pu(V), and Pu(IV) on colloids of Fe(III) oxides and hydrous oxides and MnO_2, Radiochemistry 49/4 (2007) 419-425.
7. A.B. Kersting, D.W. Efurd, D.L. Finnegan, D.J. Rokop, D.K. Smith, J.L. Thompson, Migration of Plutonium in ground water at the Nevada test site, Nature 397 (1999) 56-59.
8. W.R. Penrose, W.L. Polzer, E.H. Essington, D.M. Nelson, K.A. Orlandilini, Mobility of Plutonium and Americium through shallow aquifer in a Semiarld region, Environ. Sci. Technol 24/2 (1990) 228-234.
9. J.F. McCarthy, J.M. Zachara, Subsurface transport of contaminants, Environ. Sci. Technol. 23/5 (1989) 496-502.
10. B.D. Honeyman, Colloidal culprits in contaminants, Nature 397 (1999) 23-24.
11. S. Sachs, G. Bernhard, Influence of humic acids on the actinide migration in the environment: suitable humic acid model substances and their application in studies with uranium-a review, J. Radioanal. Nucl. Chem. 290 (2011) 17-29.
12. H. Geckies, T. Stumpf, Annual report on waste disposal, KIT SR-7617 (2011) KIT Scientific Publishing, Karlsruhe, Germany.

13. G. Buckau, Humic substances in performance assessment of nuclear waste disposal: actinide and iodine migration in the far field, 3rd Technical progress report, FZKA 7070 (2005) Karlsruhe Institute of Technology, Karlsruhe, Germany.
14. E.S. Patera, D.E.Hobart, A. Meijer, R.S. Rundberg, Chemical and physical processes of radionuclide migration at yucca mountain Nevada, J. Radioanal. Nucl. Chem. 142/1 (1990) 331-347.
15. T.D. Waite, J.A. Davis, T.E. Payne, D.A. Waychunas, N. Xu, U(VI) adsorption on ferrihydrite: application of a surface complexation model, Geochim. Cosmochim. Acta. 58/24 (1994) 5465-5478.
16. A.L. Sanchez, J.W. Murray, T.H. Sibley, The adsorption of Pu (IV)/(V) on goethite, Geochim. Cosmochim. Acta 49 (1985) 2297-2307.
17. B.A. Powell, R.A. Fjeld, D.I. Kaplan, J.T. Coates, M.S. Steven, Pu(V)O_2^+ adsorption and reduction by hematite and goethite, Environ. Sci. Technol. 39/7 (2005) 2107-2114.
18. J.L. Means, D.L. Krerer, M.R. Borcsik, D.O. Duguid, Radionuclide adsorption by manganese oxides and implication for radioactive waste disposal, Nature 274 (1978) 44-47.
19. E.R. Sylwestera, E.A. Hudsona, P.G. Allen, The structure of uranium (VI) sorption complexes on silica, alumina, and montmorillonite, Geochim. Cosmochim. Acta 64/14 (2000) 2431-2438.
20. E. Hartmann, H. Geckeis, T. Rabung, J. Lützenkirchen, T. Fanghäne, Sorption of radionuclides onto natural clay rocks, Radiochim. Acta 96 (2008) 699-707.

21. S.C. Rasai, J.W. Juang, Comparison of linear and nonlinear forms of isotherm models for Strontium sorption on sodium bentonite, J Radioanal and Nucl. Chem, 243/3 (2000) 741-746.
22. S. Kulmala, M. Hakanen, Sorption of protactinium on rocks in ground waters from Posiva investigation sites (POSIVA 98-12) (1998) University of Helsinki, Finland.
23. Y. Sakamoto, T. Ishii, S. Inagawa, Y. Gunji, S. Takebe, H. Ogawa, T. Sasaki, Sorption characteristics of actinium and protactinium onto soils, J. Nucl. Sci. and Technol., S3 (2002) 481-484.
24. H. Ervanne, M. Hakanen, J. Lehto, Modelling of niobium sorption on clay minerals in sodium and calcium perchlorate solutions, Radiochim. Acta, 102/9 (2014) 839-847.
25. H.G. Weidinger, Zr-Alloys, the nuclear material for water reactor fuel: A survey and update with focus on fuel for pressurized water reactor systems, 7th Int. Conf. on WWER Fuel Performance, Modelling and Experimental Support (2007) Albena, Bulgaria.
26. M. Howe-Grant, Kirk–Othmer encyclopedia of chemical technology, Vol-17, 4th ed. (1996) Wiley, New York, pp. 449-450.
27. S. Gangotra, P.M. Ouseph, S. Anantharaman, K.C. Sahoo, Gamma spectrometry studies on irradiated zircaloy pressure tubes, ZIRC-2002 (2002) BARC, Mumbai, India, pp. 658-674.
28. R.H. Rainey, J.G. Moore, Laboratory development of the acid Thorex process for recovery of consolidated edison Thorium reactor fuel. Oak Ridge National Laboratory, U.S. Atomic Energy Commission, ORN L-3155 (1962).
29. IAEA TECDOC-1450, Thorium fuel cycle - Potential benefits and challenges. Vienna, Austria (2005).

LIST OF FIGURES

Chapter-III

Chapter-IV

Chapter-V

LIST OF TABLES

Page No.

Chapter-I

Chapter-II

Chapter-III

Chapter-IV

Chapter-V

CONTENTS

Page No.

CHAPTER I

CHAPTER II:

Sorption of niobium and protactinium on colloidal silica

Chapter III

Sorption of niobium and protactinium on iron oxides

Chapter IV

Sorption of Nb and Pa on manganese dioxide

Chapter V

Evaluation of sorption mechanism using Thermodynamic studies and X-Ray Absorption Fine Structure (XAFS)

Chapter VI

Summary and future perspectives

LIST OF FIGURES

Page No.

Chapter-I

Chapter-II

Chapter-III

Chapter-IV

Chapter-V

LIST OF TABLES

Page No.

Chapter-I

Chapter-II

Chapter-III

Chapter-IV

Chapter-V

Chapter VI

Summary and Future Perspectives

6.1. Summary

In this thesis, the sorption studies of ^{94}Nb and ^{231}Pa on silica, iron oxides and manganese dioxides are described. The sorption studies were carried out in batch method. The effect of pH, humic acid and equilibration time on sorption, are also studied. The sorption mechanism is evaluated using classical sorption studies like ionic strength and temperature dependent sorption phenomena and XAFS spectroscopic investigation of the Nb sorbed silica and hematite at different pH. A summary of the above research has been presented in this chapter, highlighting the major observations and the future perspectives.

The major conclusions, drawn from the present studies are:

(i) Silica particles, one of the most abundant, naturally occurring, inorganic colloidal particles, display a range of important interactions with various metal ions and radionuclides. Both Nb and Pa are strongly associated with colloidal silica especially in the neutral pH to mildly basic pH region. So, in natural aquatic conditions, there is a high chance of association of these two radionuclides on silica colloids and therefore strong probability of colloid assisted migration. Humic acid has negligible effect on the sorption in neutral pH, but increases the sorption in acidic pH and decreases the sorption in basic pH. So, in ternary system interaction of Nb/Pa with humic acid can govern the sorption on silica in acidic and basic pH conditions. The results of this study will be useful for modeling the migration behaviour of Nb and Pa in natural aquatic stream.

(ii) The sorption of Nb/Pa on all the three iron oxides was low (~ 10-20 %) at pH 1, increased to ~ 90 % at pH 8 and decreased marginally above pH 9. Humic acid affects the sorption in acidic and basic medium either by its self-absorption onto the colloids or its complexation with the radionuclides at those respective pH conditions. In acidic medium, the sorption decreases with increase in ionic strength, which indicates the possibility of physisorption i.e., the sorption either by electrostatic interaction or by ion exchange phenomenon. In basic medium, the insensitive nature of sorption with respect to ionic strength indicates the formation of covalent bond between Nb/Pa species and iron oxides surfaces. The sorption followed pseudo-first order-order kinetics at acidic pH but pseudo second order in basic pH conditions. The sticking probability values indicate that the sorption follows physisorption at acidic pH and chemisorption at basic pH. The activation energy for the sorption in acidic pH is positive, which indicates that the energy is required to happen the sorption. In basic medium, the negative activation energy signifies that the sorption is spontaneous and does not require any activation energy. The sorption is not influenced by the dissolution of hematite and goethite but do mildly in the case of magnetite in the pH range 1-2, where the solubility of magnetite is near about 3 % of its initial weight. This study is important to understand the probable migration of ^{94}Nb and ^{231}Pa during underground storage of radioactive waste.

(iii) Both Nb and Pa are strongly sorbed on manganese dioxide even in acidic pH, but the sorptions become quantitative in neutral to near neutral pH region. The high sorption on manganese dioxide may be due to the low PZC and high surface area of the oxide. In acidic pH, mineral bound humic acid enhances the sorption of Nb and Pa, in higher pH, dissolved humic acid complexes with Nb/Pa and reduces the sorption. The sorption strongly depends on ionic strength of the medium at low pH, infers the outer sphere complexation but mild dependence on ionic strength in basic pH reinforces the probability of innersphere complexation. The sorption in acidic pH is endothermic, but the positive entropy change makes the endothermic sorption process spontaneous. In basic pH, the sorption is exothermic and spontaneous. The high magnitude of the enthalpy value suggests the formation of covalent bond between manganese dioxide surfaces and the species of Nb/Pa. Pseudo first order fitting in low pH suggests the high probability of physisorption whereas pseudo second order kinetic fitting proposes the probability of chemisorption at high pH.

(iv) The sorption mechanisms of Nb and Pa on silica and hematite were evaluated based on ionic strength, temperature dependent sorption studies and the XAFS studies of the Nb sorbed silica and hematite at different pH. The ionic strength dependent sorption of Nb(V) and Pa(V) on silica and hematite, primarily indicates the Outer Sphere Surface complexation which is solely governed by electrostatic forces. On the contrary, the inertness of sorption with ionic strength indicates Inner Sphere Surface Complexation in neutral and basic medium which is governed by electron sharing or bond formation. Enthalpy changes associated with the sorption process at different pH further supports the observation of the ionic strength results. EXAFS study of the Nb sorbed colloidal silica at different pH clearly shows that in acidic pH, Nb is not coordinated with Si atom, whole coordination is satisfied by oxygen atom only. In neutral and basic medium, Nb is bonded with one to two Si atom at 3.44 Å and 3.5 Å distances respectively. In the case of hematite in acidic pH, there is no evidence of Nb and Fe bonding but in neutral and basic medium, Nb is coordinated with 0.5 and 2 numbers of Fe atoms at 2.72 Å and 2.88 Å distances respectively. So in the present study, there is a good resonance among the chemical, thermodynamic and spectroscopic data which together establish the physisorption nature in acid medium and chemisorptions in neutral and basic medium.

So in general, the sorption of both ^{94}Nb and ^{231}Pa in the acidic range is low and follow physisorption mechanism. The sorption is however quantitative in neutral or near neutral pH region and suggest to chemisorption. These propositions have been established based on ionic strength and temperature dependent sorption data as well as from the XAFS spectroscopic evidences. The quantitative sorption in neutral to near neutral pH region indicates that in the natural aquatic conditions the migration of these two radionuclides is mainly assisted by the colloids present in the medium. The naturally occurring complexing ligand i.e. humic acid, can alter the Nb/Pa sorption both in acidic and basic region, either by its self-absorption onto the colloids or by its complexation with the radionuclides at those respective pH conditions.

6.2. Future perspectives

Future perspective of the present investigation:

(i) XAFS investigation in Nb sorbed pyrolusite systems can provide more concrete information regarding molecular level bond formation or surface complexation during the sorption process.

(ii) Detailed spectroscopic and electrochemical investigations on the sorption behaviour of Nb/Pa on iron oxides of mixed oxidation state (magnetite) and studies in regards to changing of metal ion oxidation states can provide more insight of the sorption process.

(iii) Utilization of laser-based fluorescence techniques to study the sorption mechanisms in very low concentration level of the radionuclides can provide more relevant information as compared to the spectroscopic techniques which performed at elevated concentration level where the chances of formation of hydrolysed polymeric species or precipitation exist.

(iv) Sorption studies of ^{94}Nb and ^{231}Pa on naturally occurring bentonite, clay minerals and soil samples are worth to be investigated in regard to the migration of radionuclides in aquatic systems, as they are the sorbents present in the geosphere, retard the migration process of the radionuclides.

Abstract

Name of Candidate:	Shri. Madhusudan Ghosh
Name of the Constituent Institution:	Homi Bhabha National Institute
Enrollment Number:	CHEM 01201304020
Title of the Thesis:	Studies on interaction of niobium and protactinium with hydrous oxides
Board of Studies:	Chemical Sciences

The back end of the Nuclear Fuel Cycle (NFC) has become the most concerned and challenging area sice several incidents were reported regarding the release and migration of radionuclides having high yield in the fission/activation process and long half-life. The radionuclides focused in the thesis work are ^{94}Nb and ^{231}Pa, two important radionuclides produced in nuclear reactors. The sorption behaviour of these radionuclides on silica, iron oxides (Goethite, Hematite and Magnetite) and manganese dioxide colloids and the effect of pH, humic acid, ionic strength, temperature, equilibration time were studied in detail.^{94}Nb radiotracer was prepared from irradiated Zr-Nb pressure tube and ^{231}Pa radiotracer from siliceous cake, a waste of monazite process plant. The sorption is high for silica and manganese dioxide even at acidic pH but low in the case of iron oxides. Classical methods such as ionic strength and temperature dependent sorptions, were used to explain the sorption mechanism. Extended X-ray Absorption Fine Structure (EXAFS) study of the inactive Nb sorbed on silica and hematite at different pH conditions has been used to elucidate sorption mechanism and correlated with the classical sorption data. The sorption of both ^{94}Nb and ^{231}Pa in acidic range follow physisorption mechanism and in neutral or near neutral pH follow chemisorption mechanism. Naturally occurring complexing ligand humic acid can alter the sorption in acidic and basic region either by itself getting sorbed onto colloid or by complexing with radionuclides.

The work is very important as ^{94}Nb and ^{231}Pa are the two isotopes generated in appreciable quantity in irradiated Zr-Nb pressure tube and in thorium based nuclear fuel respectively but very less studied. The ^{94}Nb tracer preparation explored a new possibility of reusing Zr after separation of the long lived ^{94}Nb isotopes. The quantitative sorption of the radionuclides in neutral to near neutral pH region indicates in the natural aquatic condition there is a high probability of migration of these two radionuclides as pseudo colloids.

Chapter I

Introduction

1.1. Historical aspect of radioactivity

Uranium (U) was discovered in 1789 in the mineral pitchblende by M H Klaproth and the only interest on U was that it is an element, till Henry Becquerel discovered the special feature of the element called radioactivity in 1896. Thorium was discovered in 1829 by Norwegian mineralogists Morten Thrane Esmark, but its radiological properties got attention in the early stage of 20th century. The scenario changed drastically after the discovery of neutron by James Chadwick in 1932 which introduced new concept in radioactivity like nuclear fission of uranium and artificial transformations of the naturally occurring elements. In 1934 research on nuclear fission by emirate scientists like Otto Hahn, Lise Meitner, Enrico Fermi and Oppenheimer came out with controlled fission of U for power production in nuclear reactor and uncontrolled fission for the production of deadly nuclear weapons. The artificial transformation and fission of U resulted generation of variety of radioisotopes which can be classified as transuranic isotopes, not present in nature, and the active isotopes of the elements, present on their own in the nature.

The advantages of nuclear energy production are dragging back by its own creation of long lived radio isotopes which causes radiation hazards and because of that these days the back end of the Nuclear Fuel Cycle (NFC) has also become the most concerned and challenging research area in nuclear industry, although there are number of standard protocols for the management and disposal of the radioactive wastes are in place.

1.2. Sources of radioisotopes

1.2.1. Radioisotopes in nature

There are three radioactive series of radio isotopes, which are the main sources of radioactivity in nature. All the end products in the series shown above are radioactive. The end products of all the three series, as shown in Table 2.1 are, however not radioactive, mere stable isotopes. Apart from these other radioisotopes like ^{3}H, ^{14}C, ^{7}Be, ^{38}S, ^{81}Kr, ^{40}K etc present in atmosphere also contributes to natural radioactivity.

Table1.1: Natural radioactive series: Parent isotopes, half lives and their stable daughter isotopes

Series	Parent isotope	Half-life (y)	Stable daughter isotope
4n	Thorium (^{232}Th)	1.40×10^{10}	^{208}Pb
4n+2	Uranium (^{238}U)	4.47×10^{9}	^{206}Pb
4n+3	Uranium (^{235}U)	7.04×10^{8}	^{207}Pb

1.2.2. Uranium Mining and milling

Starting from mining of uranium ore upto preparation of yellow cake or Ammonium Diuranate (ADU) is the part of U mining and milling process. Preparation of uranium dioxide or metallic uranium or uranium alloy comes under the part of fuel fabrication. The production of large quantity of nuclear fuel is associated with the generation of large amount of radioactive waste which contains U, Th and their active daughter products. The management of these wastes is a challenge and they are generally stored in tailing ponds which are kept well isolated from environment.

1.2.3. Thorium Mining and milling

Although thorium (Th) is not a fissile isotope, but mining of thorium is carried out with the motif of production of fissile isotope ^{233}U upon irradiation of thorium in nuclear reactor. The main ore of thorium is monazite. The mining of thorium is generally easier than uranium as it can be extracted from open pit monazite deposits. Management of Th mine tailings is also simpler because most of the daughter products are short lived e.g, ^{220}Rn (half-life: 55 s), daughter product of thorium, compared to the equivalent daughter product of uranium, ^{222}Rn (half-life: 3.8 d). However, the radioactivity of the mined products is much higher for thorium than for uranium, because of the thorium decay chain product ^{208} Tl, which emits 2.6 MeV gamma rays. So the trailing product of thorium mining process also stored safely so that it cannot come in contact with surrounding environment.

1.2.4. Nuclear reactor

Nuclear energy contributed more than 10% of the total electricity consumed in the world and nearly 449 nuclear power plant (NPP) providing this huge energy and the number of the NPP rising year after year. Along with NPP, there are about 227 research reactors throughout the world which are used for different nuclear research and the production of various useful radioisotopes. These huge number of nuclear reactor operations generates large quantity radioactive waste (IAEA database). In India 22 NPP and 5 research reactors are operating till date.

The "Nuclear Fuel Cycle" (NFC) related to the production of power using nuclear fission, starts from the mining of Uranium and ends with the radioactive waste treatment and disposal. The process from mining, enrichment and the preparation of fuel assembly is called "Front End" and the reprocessing/treatment of spent fuel and the management of radioactive waste and their proper disposal comes under the term "Back End". Each step of the NFC involves generation of some sort of radioactive waste. The block diagram of NFC is shown in Figure 1.1.

1.2.5. Spent fuel reprocessing

The spent nuclear fuel contains fission products, activation products, minor actinides, plutonium along with uranium. As a protocol, the spent nuclear fuel is kept as such for 1.5 years for the decay of the short lived radioisotopes. After that, the spent fuel is reprocessed for the extraction of U and Pu and the process involved is known as PUREX process. The residue remains after the extraction of U and Pu, contains many long lived radioisotopes, including minor actinides as are given in the following Table 1.2 and 1.3.

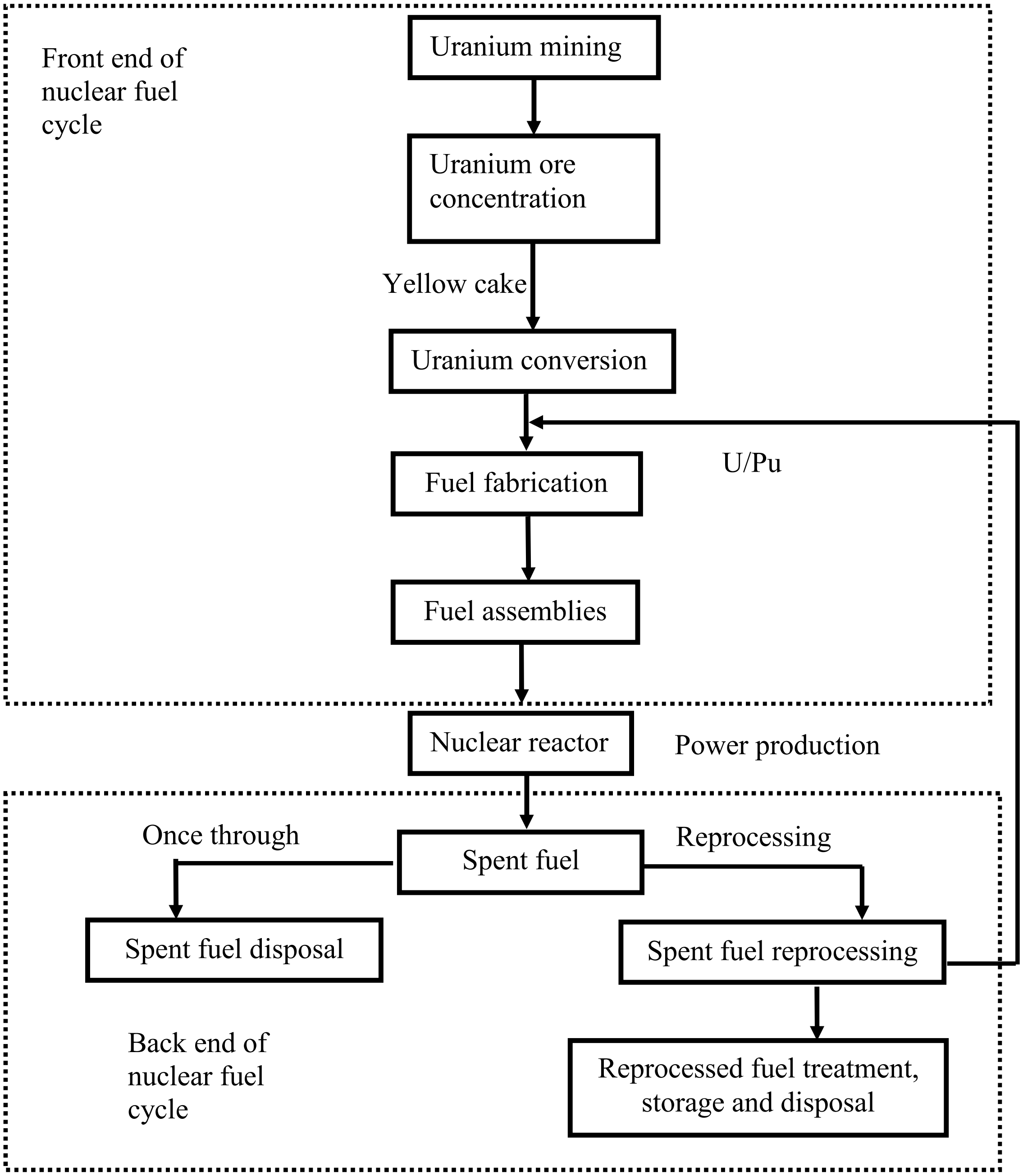

Figure 1.1: Block diagram of Nuclear Fuel Cycle

Table 1.2: List of important radionuclides having high fission yield and long half lives [1]

Radionuclides	**Yield (%) ^{235}U(n, f)**	**Half-life (y)**	**Radiation energy (keV)**
^{135}Cs	6.726	2 x 10^6	β (20)
^{137}Cs	6.23	30.17	β (500, 1200), γ (662)
^{99}Tc	6.074	2.1 X 10^5	β (300)
^{90}Sr	5.772	28.5	β (500, 2300)
^{93}Zr	6.375	1.5 x 10^6	β (60)
^{144}Ce	5.45	284 d	β (300, 3000), γ (133, 697)
^{125}Sb	0.025	2.77	γ (426, 601)
^{129}I	0.853	1.57 x 10^7	β (200), γ (40)
^{107}Pd	0.191	6.5 x 10^6	β (30)
^{147}Pm	2.255	2.62	β (200)
^{154}Eu	0.000017	8.8	β (100, 200), γ (123)
^{155}Eu	0.03328	4.96	γ (87, 105)
^{151}Sm	0.5314	88.8	β (77)
^{126}Sn	0.1084	2.3 x 10^5	β (4050), γ (414, 666, 695)

India own large reservoir of thorium which is about 25% of the world's thorium reserve. Thorium is being utilized as blanket material in Fast Breeder Test Reactor (FBTR) for the generation of fissile isotope ^{233}U. In fact India is operating a 30 kW ^{233}U fueled research reactor named "Kamini".

The process of extracting ^{233}U from irradiated Thoria is called THOREX process [3]. Similar to PUREX process, in the THOREX process also large quantity of radioactive waste is generated. The main concern regarding the radioactive waste of THOREX process is the daughter products of ^{232}U or more specifically ^{208}Tl, having intense gamma ray of energy 2.6 MeV. Proper categorization of the radioactive waste is required in view of proper segregation, treatment, storage and final disposal.

Table 1.3: List of important long lived transuranic isotopes [2]

Radionuclides	Half-life (y)	Radiation energy (MeV)
^{238}Pu	87.7	α (5.499)
^{239}Pu	2.4×10^{4}	α (5.155)
^{240}Pu	$6.55 X 10^{3}$	α (5.168)
^{241}Pu	14.4	β (0.02)
^{237}Np	2.1×10^{6}	α (4.788)
^{241}Am	432.6	α (5.486)
^{243}Am	7.37×10^{3}	α (5.275)
^{244}Am	18.11	α (5.805)
^{245}Cm	8.5×10^{3}	α (5.362)

1.2.6. Accidental failure of nuclear reactor and Nuclear weapons testing

Chernobyl accident (1986) and Fukushima Daiichi nuclear disasters (2011) are the two main notorious nuclear disasters which caused huge release of radioactivity in the environment and the associated contaminations in large area. Several incidents are also reported regarding the release/leakage of high level radioactive wastes like Hanford site in US, Mayak reprocessing plant in USSR.

More than 2000 nuclear devices have been tested in atmosphere, underground or in under water and these results the spread of large amount of radioactivity in the environment. Along with that, the nuclear powered submarine accidents also contributing radioactive contamination in the sea water.

1.3. Classification of radioactive waste and it's management

The radioactive wastes generated in the nuclear facilities can be classified according to their physical states i.e, solid, liquid and gaseous radioactive wastes.

1.3.1. Solid radioactive waste

Solid radioactive wastes can be categorized as the combustible, non-combustible, compressible and non-compressible wastes. Non-combustible wastes generally consist of activated reactor components like pressure tube, control rods, equipments used for reprocessing etc. Combustible wastes are generally incinerated for volume reduction. For compressible wastes, volume reduction is achieved by hydraulically operated baling press. The combustible and compressible categories of the waste have an appreciable contribution to solid waste and generally are of low activity. Based on activity level solid radioactive wastes are further classified into four categories as shown in the following Table 1.4.

Table 1.4: Categorization of solid waste based on dose at surface as per BARC Safety Council [4]

Category	Radiation dose (D) on the surface of waste package (mGh^{-1})	Remarks
I	$D \leq 2$	Beta Gamma emitters
II	$2 < D \leq 20$	
III	$20 < D$	
IV	Alpha bearing waste	Alpha emitters dominate

1.3.2. Liquid radioactive waste

The liquid radioactive waste generated in the nuclear fuel cycle can be categorized as [5,6]

LLW (Low level waste): Activity < 1mCi/L, generated from R&D work in radiological laboratories, washings of contaminated equipments etc. The radioisotopes generally concentrated by precipitation, ion exchange, membrane separation and by evaporation and finally dispose of the lean solution.

ILW (Intermediate Level Waste): Activity limits 1mCi/L to 1Ci/L, generated in the evaporation and condensation of high level radioactive waste. This type of waste is immobilized in cement matrix and stored in shallow trenches.

HLW (High Level Waste): Activity >1Ci/L are generated in reprocessing of the spent fuel. Although the volume is below 5% of the total liquid waste, but it contains more than 90% of the total activity. This type of waste generally vitrified in suitable glass matrix and then for interim storage and finally it supposed to dispose off in deep geological repository.

1.3.3. Gaseous radioactive waste

The gaseous radioactive wastes are classified based on their activity level as given in the following Table 1.5. Gaseous fission products or the gaseous isotopes generates from the decay of parent isotopes are the main origin of this type of waste. They are generally scavenged by High Efficiency Particulate Absorber (HEPA) or by activated charcoal [4, 5].

Table 1.5: Classification of gaseous radioactive wastes based on activity level

Category	Activity limit (A) (Bqm^{-3})	Remarks
I	$A \leq 3.7$	Beta Gamma emitters
II	$3.7 < A \leq 3.7 \times 10^4$	
III	$3.7 \times 10^4 < A$	

1.4. Fate of long lived radioisotopes in environment

In order to protect future generations and the environment, the high level radioactive wastes must be isolated from geosphere with all safety measures, at least for 100000 years. Study reveals that the leach and migration of the radionuclides in the environment mostly occurs through aqueous mobile phase. Penrose et al. [7] have studied the behaviour of Pu and Am in the Mortandad canyon and observed the migration of these radionuclides to a distance of 3.39 km from the source. Once the radionuclides come into aquatic system after its accidental release, migration of these radionuclides become a function of several parameters like sorption onto solid aquifer in contact with mobile phase, ground water mobility and complexation of the radionuclides with inorganic and organic complexing agents present in the mobile phase and also on the colloids dispersed in the mobile phase. Unless or until the radionuclides get sorbed into stationary phase, they tend to migrate.

1.5. Complexation of radionuclides in natural aquatic system

1.5.1. Inorganic complexing anions

The inorganic anions present in aquatic system are carbonate (CO_3^{2-}), bicarbonate (HCO_3^-), nitrate (NO_3^-), sulphate (SO_4^{2-}), chloride (Cl^-), phosphate (PO_4^{3-}) and fluoride (F^-) and their concentration varies place to place [2]. The solubility definitely depend upon the concentration of these inorganic complexing anions, specially carbonate complex, as its concentration and complexation ability favours the phenomenon and the tendency amplifies at higher pH, which is evident from the fact that U predominantly exists as carbonate species in sea water [8]. If the concentrations of the anions are insignificant, then hydrolysed species of those radionuclides generally predominates. This hydrolysis also depends on the effective charge/ionic potential of that ion; more the effective charge higher will be the hydrolysis tendency. Generally the hydrolysis become more effective in neutral to mildly basic medium compared to that of the acidic medium.

1.5.2. Humic substances

Besides the inorganic complexing anions, organic complexing anions also present in natural aquatic system which collectively called as humic substance (HS). It generates from the degradation of mainly plant residues and the mechanism of the formation discussed in detail by Stevenson [9]. Depending on the source of material and the decomposition stage, HS can have molecular weight range 2600-136000 Dalton and for the same reason HS has very complex molecular structures which can not be specifically defined. A hypothetical structure of humic acid is shown in **Figure 1.2.** Based on the water solubility, HS can be classified as Falvic Acid (FA), Humic Acid (HA) and Humin. HA contains several functional groups like carboxylic, phenolic, Enolic and quinine groups attached to various aromatic rings. FA has higher O content compared to that of the HA, indicating that FA contains more oxygen containing functional groups compared to that of HA. Their concentration varies from 0.1 mg L^{-1} in deep groundwater to 50 mg L^{-1} in swamp waters compared to 0.5–1.2 mg L^{-1} in oceans. Owing to their very high molecular weight, in high concentration they usually agglomerate and form colloids and also get sorbed onto inorganic colloids present in water. Because of the presence of both –COOH and phenolic –OH groups, humic acid acts as a polybasic acid. The pKa values corresponding to the two types of the acidic groups are known to be ~ 4.0 and ~ 9.0 respectively [10].

Humic acid play a vital role on radionuclide sorption and migration, as it can alter the total capacity of mineral oxides as well as the speciation of the radionuclides. It was observed that anthropogenic actinides concentrations are 10 times higher in humic acid fraction compared to that of the overall top soil [11].

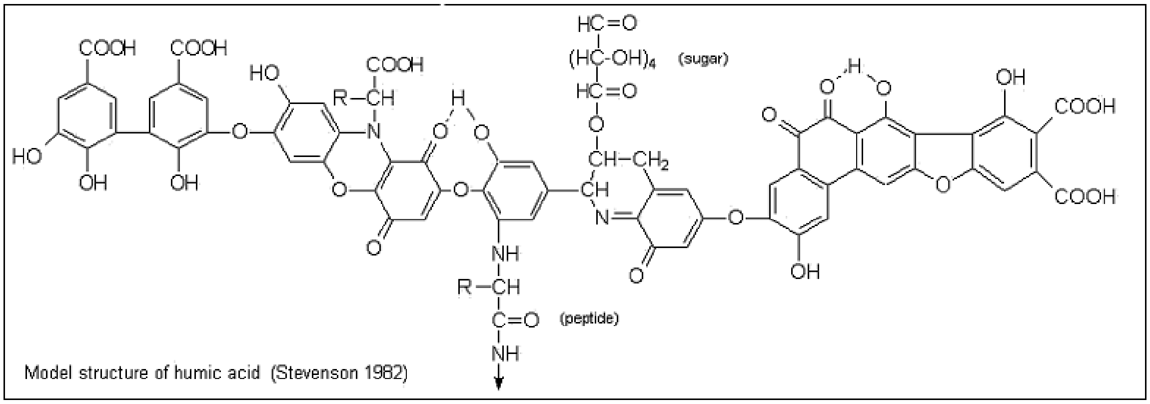

Figure 1.2: Hypothetical structure of humic acid [9]

Humic substances are strongly sorbed onto mineral surfaces and the mechanism is the specific adsorption by ligand exchange with protonated surface hydroxyl groups of the minerals [12]. Accordingly, the sorption of the radionuclides on the mineral surfaces are strongly controlled by the adsorption of humic substances on mineral surfaces [13,14]. Adsorbed humic substances may act as additional binding sites for metal ion and thus may increase metal binding to the mineral surface. In other way adsorbed humic substances may partially block sorption sites which are available for the metals ions and this may lead to decrease to metal sorption to the mineral surface. Again, the dissolved humic substances can decrease the metal ion sorption to the solid phase by forming soluble metal complexes [12]. At low pH, humic substances strongly sorbed to mineral surfaces, whereas metal cations are not strongly bound by mineral surfaces under acidic conditions. However, in higher pH, reverse phenomena happens. In both the conditions humic substances can alter the sorption behaviour of the metal ion [15, 16]. It is still a matter of ambiguity whether mineral bound humic substances do really provide additional binding sites for the metal ions without blocking the mineral surfaces for metal complexation. The probable role of humic acid in mineral interface-metal ion-humic acid ternary system is shown in **Figure 1.3.** The generalized effect of humic substances on sorption of metal ions with the variation of pH is shown in **Figure 1.4**

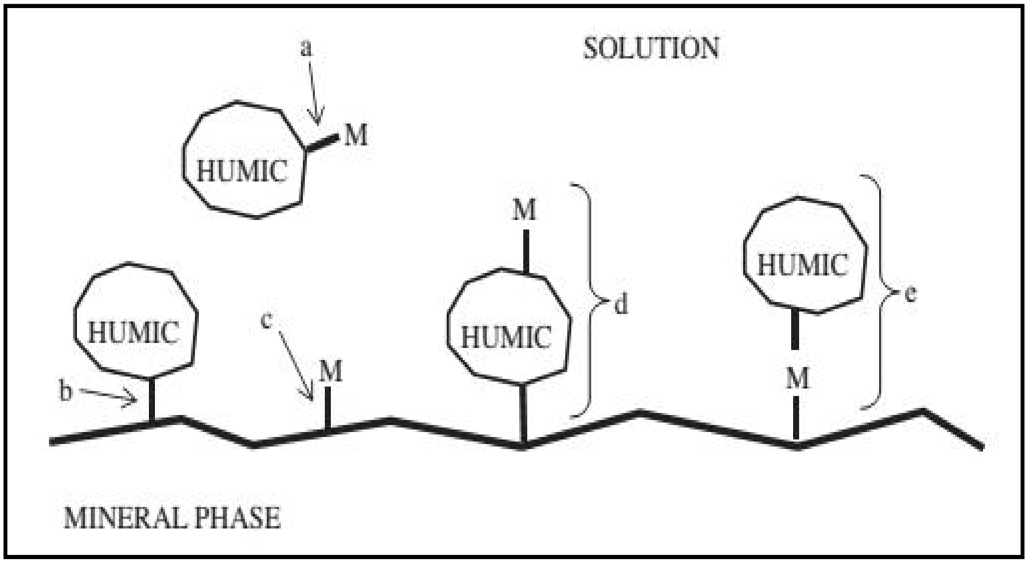

Figure 1.3: Interaction in ternary systems, binary interaction: (a) Humic acid-metal ion (b) Humic acid- mineral surface (c) Metal ion- mineral surface. Ternary interaction: (d) Humic acid as bridge between metal ion and mineral surface (e) Metal ion as bridge between humic acid and mineral surface [17]

Humic acid plays a vital role for the mobilization of radionuclides as well as non-radioactive toxic substances in the environment and this is due to their strong complexation and colloid formation ability. Along with the ligand properties, humic acids also possess redox properties and thus can influence the oxidation state of the metal ions. The change in oxidation state affects their speciation and therefore migration in the natural aquatic system. Literature reports suggest that humic acids are able to reduce most actinide ions. For example, in presence of humic acid Pu(VI) is reduced to Pu(IV), Np(VI) to Np(V) [18] and Np(V) to Np(IV) [19].

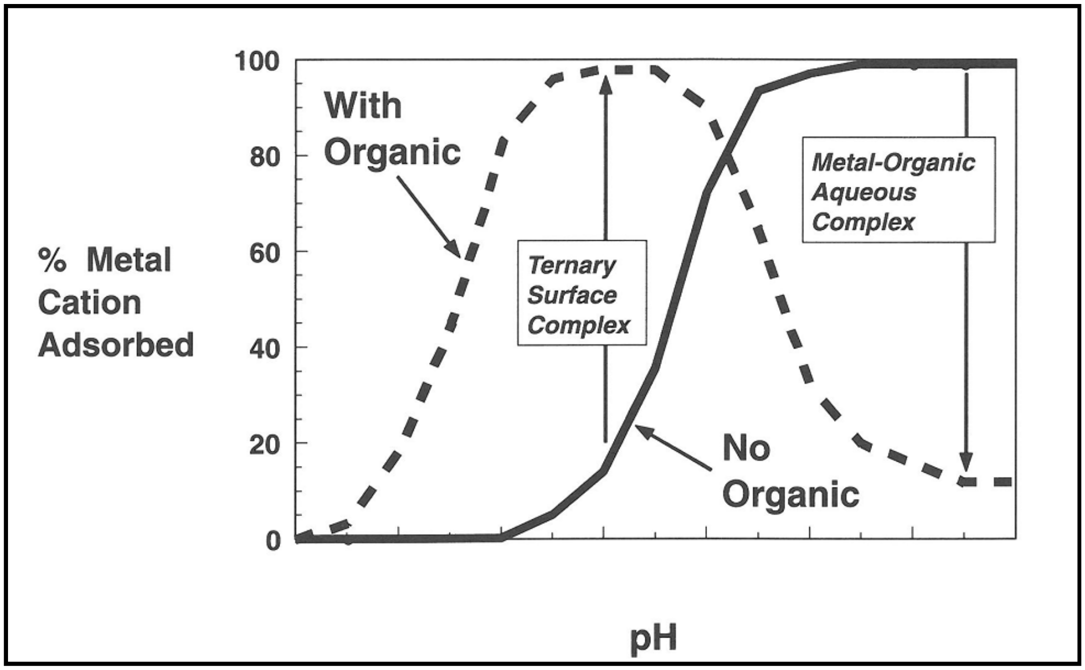

Figure 1.4: The generalized effects of dissolved organic acid anions on the adsorption of aqueous metal cations onto an oxide-type mineral surface [20].

1.6. Naturally occurring colloids

Colloids are particles in size range of 1nm to 1μm, which remain suspended in the mobile phase for a long time, until something is added in the medium which causes agglomeration of the colloid particles followed by their settling down [21]. The majority of mobile colloids that are important for contaminant migration have at least one dimension of less than 100 nm and this observation based on several reports on groundwater systems [22, 23]. They generally come into aquatic system because of the weathering and geochemical transformation of the rocks and minerals. The major oxides present in earth crust are silica (60-70 %), Alumina (13-16 %), iron oxides (5-6 %), Magnesium/Calcium oxide (~ 2%), Manganese oxide (0.15 %) and because of that silica, alumina, iron oxides are the most abundant inorganic colloids present in water [24]. Inorganic colloids present in water may be of two types (a) Intrinsic/true colloids: When the concentration of the metal ion is high, after hydrolysis of their salt they undergo polymerization, which leads to the formation of true colloids. The tendency becomes higher for those metal ions having lesser aqueous solubility and higher effective charge [25]. In case of intrinsic colloids of tetravalent actinides owing to high stability, resistance to disintegration and ability to increase the actinide concentration in solution, we need to consider this factor while predicting their migration [26, 27]. (b) Pseudo colloids: Inorganic colloids present in water those possess high surface and large number of surface functional groups. These colloids offer a good media for the contaminants or radionuclides to get sorbed. The contaminant/radionuclide sorbed inorganic colloids are termed as pseudo colloids [28, 29]. The presence of these colloids is a very important factor that must be considered during evaluation of longer and faster migration of radionuclides.

1.7. Sorption of radionuclides on mineral surfaces and on colloids

Sorption is a collective term which includes adsorption, ion exchange, absorption, inclusion and surface precipitation [30]. So sorption represents both the attachment by electrostatic means and by chemical bond formation between radionuclides and the mineral/colloid surface. The sorption of radionuclides on mineral surfaces or water-solid interfaces leads to the decrease in the concentration of the radionuclides in mobile phase thus acting as the major factor in retarding the migration of radionuclides in the near and far field from the nuclear repository [31]. But on the other hand the formation of stable intrinsic colloids of sorption of radionuclides on the surface of inorganic colloids in most cases enhance the migration of the radionuclides rather than the cases where the mobile phase conditions don't allow the colloids to remain suspended but to get agglomerated and precipitated [32, 33]. Although the sorption with above two cases results contradictory effect yet the sorption mechanism may follow the same pathway in both the cases. The generalized sorption pattern of the cations and anions on mineral surfaces with variation of pH is shown in **Figure 1.5**

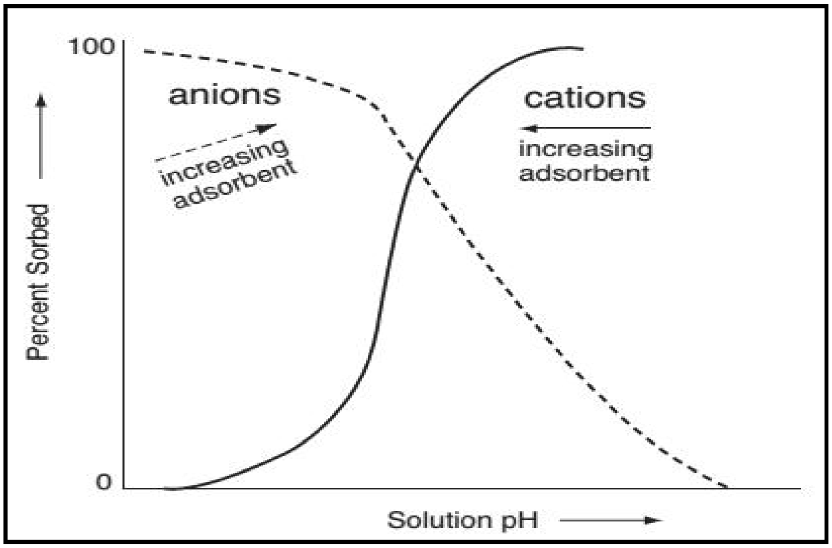

Figure 1.5: Generalized sorption pattern of cations (solid line) and anions (dashed line) on metal oxide surface [34]

Extensive study was carried out on the sorption of various radionuclides on different geological materials. Apps [35] reported the sorption of fission product radionuclides ^{137}Cs and ^{90}Sr by Savannah River site sediment impregnated with colloidal silica. Sato [36, 37] studied the sorption of Am(III), Cm(III) and Eu(III) on hematite and kaolinite and the role of humic acid. Lujanieneo [38] studied the sorption behaviour of ^{137}Cs, ^{90}Sr, ^{239,240}Pu, ^{238}Pu and ^{241}Am in the Chernobyl soil. Several other reports are also available regarding the sorption of U, Th, ^{237}Np, ^{60}Co, in different materials [39-42].

1.8. Tools for sorption mechanism evaluation

It is important to understand the mechanism of sorption of radionuclides in order to access their migration, because several parameters can alter their sorption pattern while migration takes place. The probable mechanisms which are responsible for the sorption of radionuclides on mineral surface are shown in Figure 1.6.

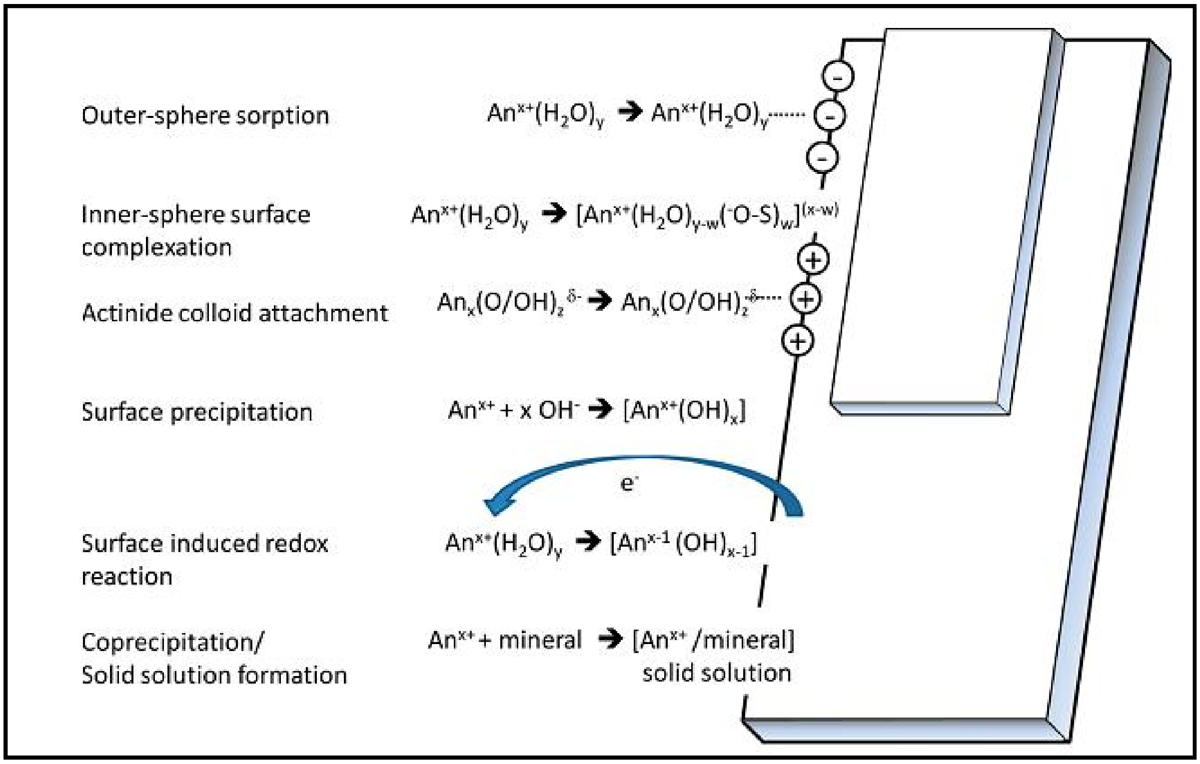

Figure 1.6: Sorption mechanisms of radionuclides on mineral surfaces [43]

There are several ways to elucidate the sorption mechanisms. In classical method, generally ionic strength effect [44, 45], temperature effect [46], and kinetic sorption data [47]) are used to understand the sorption mechanisms. In spectroscopic method, X-Ray absorption Fine Structure (XAFS) [48], Time Resolved Laser Fluorescence Spectroscopy (TRLFS) [49], Raman or Infrared spectroscopy [50], X-Ray Photoelectron Spectroscopy [51] and Laser Induced Photoacoustic Spectroscopy [52] are the commonly used experimental techniques. Out of all these techniques, XAFS and TRLFS are widely used to do the actinide speciation and sorption mechanism evaluation purposes. But the problem associated with XAFS that the concentration of the ions required is very high (10^{-1} – 10^{-4} M), which is in many cases not recommended as there is a chance of exceeding solubility limits and formation of hydrolysed polymeric species, deterring the use of this technique.

In contrast TRLFS can be carried out with much less concentration (10^{-5}-10^{-9} M) of the ions and this enable us to carry out tracer level/ molecular level speciation studies in solutions as well as on mineral surfaces [52].

1.9. Radioisotopes investigated in the present study

^{94}Nb and ^{231}Pa are the two radionuclides on which our present study is focused.

1.9.1. Generation of ^{94}Nb

Zr-Nb alloy is generally used as a pressure tube material in nuclear power reactors worldwide [53] because of its excellent mechanical strength [54] and very high resistance to hydride attack [55]. ^{93m}Nb (half-life: 16 y) and ^{94}Nb (half-life: 2.03 x 10^4 y) are the most important radioisotopes of Nb in the spent nuclear fuel, formed in the neutron activation of stable ^{93}Nb in the nuclear fuel cladding and in steel components of the fuel assemblies (Figure 1.6 & 1.7). The main route for the continuous formation of ^{93m}Nb is the decay of its long-lived parent nuclides ^{93}Zr (half-life: 1.5 x 10^6 y) and ^{93}Mo (half-life: 4 x 10^3 y). Calculation shows that after a residence time of 10 y inside a nuclear reactor having a neutron flux of 10^{14} cm^{-2}s^{-1}, discharged pressure tubes will contain about 10^{10} Bq of ^{94}Nb per kilogram of Zr-Nb alloy. Pressure tubes are removed from nuclear reactors after their lifetime or subsequent to their failure and they stored in deep tile holes with concrete cap without further processing.

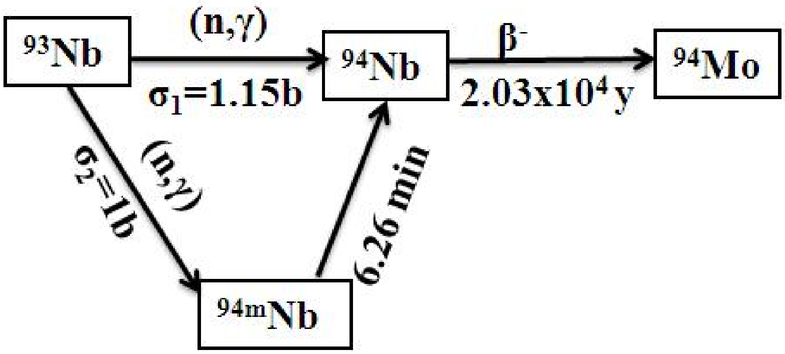

Figure 1.7: The route of generation of ^{94}Nb from ^{93}Nb in Zr-Nb pressure tube

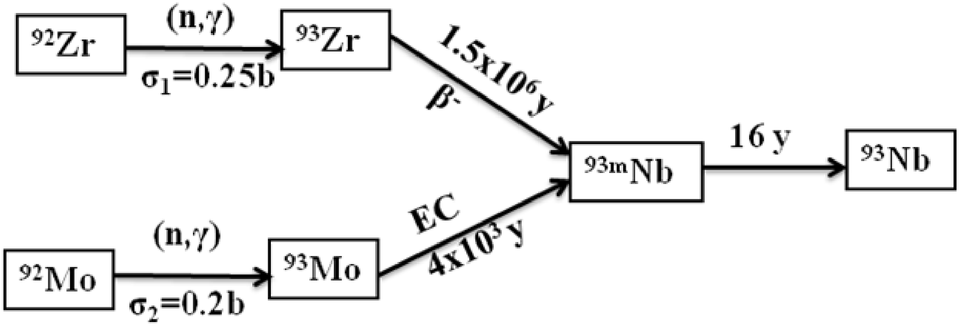

Figure 1.8: The route of generation of ^{93m}Nb in Zr-Nb pressure tube and SS components of fuel assembly

1.9.2. Generation of ^{231}Pa

Two isotopes of this element are ^{231}Pa (half-life: 3.27 x 10^4 y) and ^{233}Pa (half-life: 27 d). First one is of the natural source, generates in ^{235}U decay chain and the second one produced artificially. Both isotopes are generated in Thorium fuel cycle [56]. ^{233}Pa is produced via (n,γ) reaction of ^{232}Th where as ^{231}Pa is produced via (n,2n) nuclear reaction of ^{232}Th (Figure 1.8). The yields of ^{233}Pa and the ^{231}Pa are 0.95 % and 0.001% respectively. ^{233}Pa acting as a breeder isotope for ^{233}U fissile isotope and is not an environmental concern owing to its short half-life. ^{231}Pa is however a long-lived, alpha emitter and produced in considerable amount in the production of ^{233}U by irradiation of Th in nuclear reactor. After cooling for about 1y, ^{233}U is separated from the dissolved thoria by solvent extraction and ^{231}Pa remains in the aqueous-phase along with other actinides (THOREX process), acting as the high level radioactive liquid waste. Therefore, ^{231}Pa has long term radiological impact and the issue needs to be suitably resolved [57].

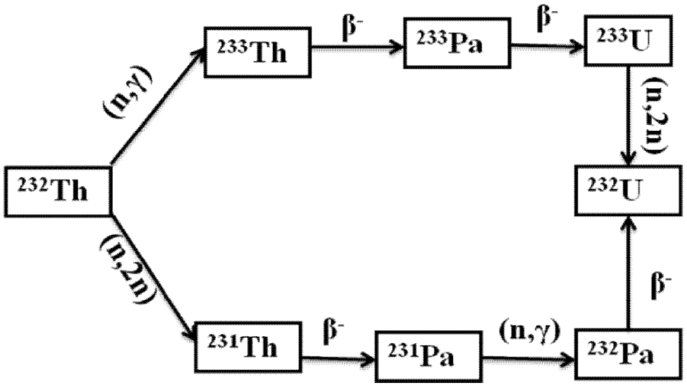

Figure 1.9: Generation of ^{231}Pa and ^{233}Pa upon neutron irradiation of Thoria

1.9.3. Associated health hazard

After getting into body system, ^{94}Nb generally pre-concentrate on liver, kidney, spleen and bone marrow. As it is a beta and gamma emitter, health hazard associated with this is less severe compared to that of ^{231}Pa.

^{231}Pa is highly toxic, for example ^{231}Pa present in air as aerosol form is 2.5×10^8 times more toxic than hydrocyanic acid. After penetration into body it generally builds up in kidney and bones. The maximum safe dose of ^{231}Pa for human is 0.03 μCi which corresponds to 0.5 μg of ^{231}Pa. So precautions must be taken while working with ^{231}Pa [58].

1.9.4. Chemistry of Nb

Niobium (Nb) belongs to second transition group in group V having electronic configuration $[Kr]4d^4 5s^1$. It can exists in several oxidation state from +I to +V but +V is the most stable one. The ionic radii of Nb(V) is 0.69Å. The solubility of Niobium hydroxide in water at pH 7 is about 1.6×10^{-5} M. Because of the higher ionic potential, Nb(V) has stronger polarizing power than Pa(V) and hence more readily hydrolyses in aqueous medium and form oxy-hydroxy species. Between 0.01-1M acid medium, Nb generally exists as singly positively charged species $Nb(OH)_4^+$ or $NbO(OH)_2^+$ or NbO_2^+ and acidity below 0.01M neutral species

$Nb(OH)_5$ or $NbO_2(OH)$ or $NbO(OH)_3$ predominates. Above pH 7 negatively charged species $Nb(OH)_6^-$ starts forming and predominating especially after pH 9. Monomeric species are abundant when the concentration is below 10^{-5} M at pH < 7.5, decreasing to almost 10^{-6} at pH ≈ 9 but concentration exceeding ~10^{-3} M, polymeric species predominates. Hardy and Scargill reported that even at [Nb] = 10^{-7} M polymeric species were present in the solution when concentration of acid was below 2 M.

Like in the case of Pa, in the case of Nb also aging effect that reduces the ion concentration in the solution is very important; even the presence of moderately strong complexing agents can't stop the process completely and because of that fresh solutions of Nb need to be prepared in 15 days intervals to get rid of the above effect. Nb undergoes strong complexation with F^- and $C_2O_4^{2-}$ and presence of such strong complexing anions make Nb solution stable for long times [59].

1.9.5. Chemistry of Pa

Pa has the electronic configuration Rn5f26d17s2. Several oxidation states of Pa are possible ranging from +III to +V but +V is the most stable one. Pa(IV) readily oxidized in solution by atmospheric oxygen. The ionic radii of Pa(IV) and Pa(V) are 0.96 Å and 0.90Å respectively. The solubility of protactinium hydroxide in water at pH 7 is about 10^{-6} M but due to aging effect solubility may decrease with time [60].

Pa(V) has strong polarizing effect on water molecules and hydroxyl ions which leads to formation of oxygen and hydroxyl group containing Pa species in aqueous solution. Most of the literature report excluded the probability of existence of hydrated Pa^{5+} ion in solution but may exist in concentrated perchloric acid medium as perchlorate has the least tendency to form complex. The first hydrolysis constant of Pa^{5+} ion in aqueous medium is about 10^3, which directly indicates the insignificant probability of this ion to exists in aqueous medium. The species of Pa exist in perchloric acid medium can be expressed as $PaO_m(OH)_n^{5-2m-n}$, where 2m + n = 4 or 3. Between 0.1-1.2 M $HClO_4$ medium Pa mainly exists as triply charged species like PaO^{3+} or $Pa(OH)_2^{3+}$. Few reports suggest that existence of doubly charged species $Pa(OH)_3^{2+}$ or $PaO(OH)^{2+}$ in $HClO_4$ concentration range 1-3 M. Welch [61] found the charge 1+ in 0.1-3 M $HClO_4$ acid medium, points towards the species PaO_2^+. Guillaumont et al. [62] reported that in the acidity range 10^{-5} to $3x10^{-2}$ N singly charged species $Pa(OH)_4^+$ or PaO_2^+ exist. Neutral species like $Pa(OH)_5$ or $PaO_2(OH)$ exist between pH 3 to 9 while above pH 9 anionic species $Pa(OH)_6^-$ predominates [63].

Aging is an important factor that must have to be taken into account while dealing with Pa in aqueous solution, because of its strong hydrolysis and polymerization tendency. Aging may affect the homogeneity, composition of the ionic species and reactivity, which leads to unexpected behaviour towards ion exchange or solvent extraction or anything else. Aging is largely controlled by the concentration of Pa in solution and the acidity of the medium used. In a freshly prepared Pa solution having acidity above 1N and the Pa concentration below 10^{-5} M, the chances of formation of polymeric species is insignificant. Solution containing Pa (~10^{-10}M) in 0.5-3.0 M $HClO_4$ is stable for 30 days but only 12 hours between pH 1-3. Pa solution in the concentration range 10^{-7}-10^{-6} in 1M $HClO_4$ is stable for a long time and in 7 M $HClO_4$ medium Pa solution with concentration in the order of 10^{-5} M is stable for about three months [60].

The complexation tendency of the inorganic ligands (anions) towards Pa can be arranged as

$$F^- > OH^- > SO_4^{2-} > Cl^- > Br^- > I^- > NO_{3-} > ClO^{4-}$$

and this complexation behaviour is similar to many metal ions. Pa readily undergoes complexation with organic complexing agents like oxalic acid, mandelic acid, trihydroxyglutaric, tartaric acid, EDTA etc. The very high enthalpy of formation may be the reason behind this strong complexation tendency with some of the inorganic and organic complexing agents. It is therefore evident that to stabilize Pa in solution for long time presence of either F^- of oxalic acid is required as they prevent the hydrolysis effectively through strong complexation.

1.10. Motivation for the work and objectives

The most advance and effective way to store and isolate the high level radioactive waste is deep geological repository. But the probable release and migration of the radionuclides from the repository are needed to be studied for safety assessment of the waste. Water is the medium via which the migration of radionuclides would take place. So speciation of the radionuclides in aquatic system is important, as it directly affects their sorption on stationary phase and thereby modulates their migration in the mobile phase. Along with the several geochemical parameters like pH, ionic strength, presence of organic as well as inorganic anions, temperature and finally the naturally occurring colloids present in mobile phase also largely affect the sorption and migration behaviour of the radionuclides. To understand the sorption and migration behaviour properly, we also need to understand the sorption mechanism, which will provide us the knowledge regarding the aquatic conditions at which the radionuclides would be strongly bonded with colloids and at the same instance suggest us the conditions that favours the colloidal migration.

The sorption and migration behaviour of different radionuclides in several geological materials have been reported in the literature as discussed in **Section 1.7**. The literature regarding the sorption and migration behaviour of ^{94}Nb and ^{231}Pa is however scanty.

Anderson et al. [64] studied the leakage of ^{94}Nb from an underground rock repository and Söderlund et al. [65] studied the sorption of Niobium on boreal forest soil. Few reports are available regarding the sorption of Pa on rapakivi granite, rock and soil [66-68]. The lack of exhaustive sorption study and non-availability of detailed mechanistic evaluation motivate us to choose these radionuclides for detailed sorption study on different hydrous oxides like silica, iron oxide, manganese oxide which present in the natural aquatic systems.

The major objectives of the present thesis are

(i) The sorption study of ^{94}Nb and ^{231}Pa on silica and understanding the effect of pH, humic acid, equilibration time, ionic strength and temperature of the sorption process. Evaluation of the sorption mechanism based on kinetic, ionic strength and temperature dependent sorption data.

(ii) The sorption study of ^{94}Nb and ^{231}Pa on different iron oxides like Goethite, Hematite and Magnetite. Understanding the effect of pH, humic acid, equilibration time, ionic strength and temperature on sorption. Evaluation of the sorption mechanism based on kinetic, ionic strength and temperature dependent sorption data.

(iii) The sorption study of ^{94}Nb and ^{231}Pa on pyrolusite and understanding the effect of pH, humic acid, equilibration time, ionic strength and temperature on the sorption process. Evaluation of the sorption mechanism based on kinetic, ionic strength and temperature dependent sorption data.

(iv) Sorption mechanism elucidation using X-Ray Absorption Fine Structure (XAFS) studies. XAFS study of the Nb sorbed silica and hematite at Nb K-edge, in acidic, neutral and basic medium.

Chapter-II

Sorption of ^{94}Nb and ^{231}Pa on Silica

2.1. Introduction

Zr-2.5 wt% Nb has been used to replace Zr-Sn alloy as pressure tube material in Pressurized Heavy Water Reactors (PHWR) because of its better mechanical strength and resistance to hydride attack. Discharged pressure tubes, made of Zr-Sn alloy, contains two long-lived radioactive isotopes, namely, ^{60}Co (half-life: 5.27 y) and ^{125}Sb (half-life: 2.77 y), which are the activation products of cobalt (present as impurity in the alloy) and tin respectively [70]. However, discharged pressure tubes, made of Zr-Nb alloy, contain a very long-lived radioactive isotope, namely ^{94}Nb (half-life: 2.03 x 10^4 y), which is an activation product of stable isotope ^{93}Nb. The presence of fission and activation products in discharged pressure tubes results in a large radiation field. After a cooling period of 8 to 10 y, short-lived and most of the medium-lived ($\leq$ 1.5 y) radioisotopes decay off [71]. The pressure tubes discharged from Indian nuclear reactors is presently kept in deep tile holes with concrete caps to get rid of these radiation hazards.

^{231}Pa, an alpha emitting isotope with a relatively long half-life (3.27 x 10^4 y) is formed during irradiation of thorium in a nuclear reactor for breeding 'fissile' isotope ^{233}U [72]. Uranium (^{233}U) and thorium are separated from fission products by thorium-uranium extraction (THOREX) process which is based on solvent extraction using tri-butyl phosphate (TBP) as an extractant. During separation by THOREX process [3, 4], ^{231}Pa along with fission products remain in the aqueous phase and forms part of the high level radioactive waste while ^{233}U goes to the organic phase. ^{231}Pa could have long term radiological impact which needs to be suitably managed and resolved [58, 73].

It has been envisaged that high level waste originating from nuclear reprocessing plant will be stored underground after suitable treatment [74]. The objective of underground storage is to isolate radioactive wastes from environment for a requisite period of time such that any possible subsequent release will not result in undue radiation exposure. It is of major concern that, if the radioactive wastes come in contact with flowing ground water, radionuclides may leach out from the repository and migrate in the environment [75]. In this scenario, the rate of radionuclide transport will depend upon the groundwater velocity as well as the distribution of radionuclides between stationary phase (aquifer solid) and mobile phase associated with the system. The greater the extent at which a radionuclide is partitioned into stationary phase, the smaller will be its average transport velocity in the groundwater. It is expected that elements with extremely low aqueous solubility and strong sorption on aquifer solid will be relatively less mobile. However, unexpected appearance of low solubility plutonium at a significant distance from its known source has been reported in the literature with great concern [21]. A three phase model of contaminant transport, known as colloidal-facilitated transport of contaminant, has been proposed to explain the enhanced migration of plutonium in ground water [76]. The three phase system consists of stationary aquifer solid, the aqueous mobile phase and the non-aqueous mobile colloids. The genesis and stabilization of ground water colloids, the factors controlling their transport through the porous media and the importance of major pathways and mechanisms to predict the role of colloids in the subsurface transport of contaminants have been discussed in detail by McCarthy and Zachara [32]. The role of chemical composition and morphology of aquatic colloids and their aggregates, their size distribution, and the factors that influence the aggregate structure and formation kinetics have been discussed by Buffle and Leppard [77]. Colloids are suspended particles with diameter less than 10 μm. Both organic and inorganic materials such as humic substances, microorganisms, mineral products and weathering products can exist as colloids in ground water system.

Both Niobium (Nb) and Protactinium (Pa) compounds readily hydrolyse in aqueous solution, forming hydrophilic colloidal systems with strong sorption properties. The solubility of niobium hydroxide is about 1.6 x 10^{-5} M in the pH range of 1-7 and increases with increase in pH. The solubility of protactinium hydroxide in water at pH 7 is about 10^{-6} M but due to aging effect solubility may decrease with time. The low solubility and tendency to form colloids make both the elements to be likely candidates for colloidal facilitated transport. The common colloids present in ground water are hydrous oxides of silica, alumina and iron, whereas the most important natural ligands are humic acids. The presence of humic acid in aquatic system may affect the sorption of radionuclides on aquifer solids and its migration in ground water [11, 78, 79]. Various aspects of colloids that affects the transport of radionuclides in natural groundwater systems have been reviewed by Bertetti (2006). The knowledge on the association of Nb and Pa with various natural colloids is one of the important parameters for predicting colloid facilitated transport of these radionuclides in ground water. Interaction of natural and anthropogenic radionuclides and actinides with components of natural water system has been surveyed by Lieser [80] and Silva and Nitsche [2] respectively.

In this chapter, we have reported the interaction of Nb and Pa with colloidal silica, investigated using ^{94,95}Nb and ^{231}Pa radiotracers. The sorption experiments were carried out in the pH range of 1 – 12, keeping the ionic strength of 0.05 M $NaClO_4$. Effects of humic acid, ionic strength and temperature on the sorption process have also been evaluated in the present study.

1.2. Experimental

2.2.1. Materials and methods

The chemicals used in the present studies are colloidal silica (commercial grade AEROSIL 200) and anion exchanger AG 1X8 (50-100 mesh, Bio-Rad Laboratories, California), sodium perchlorate (Sigma Aldrich), anion exchanger AG 1-X8 (Bio-Rad, 50-100 mesh), cation exchanger AG 50W-X8 (Bio-Rad, 50-100 mesh), perchloric acid (AR), sodium hydroxide (AR) and humic acid (Sigma Aldrich). Millipore water was used throughout the experiments.

2.2.2. X-Ray Diffraction (XRD)

XRD is a versatile non-destructive technique to characterize unknown crystalline and amorphous materials. Unlike crystalline materials, the amorphous materials do not have any sharp peak in XRD pattern because of the absence of periodicity. In crystalline materials, long range periodicity does exist and hence they have sharp peaks at particular diffraction angles. Generally Ni filtered Cu-K_α radiation used as the X-Ray source and argon filled proportional counter is used as the detector for the diffracted beam. The powder XRD pattern of silica was recorded on a Philips (PW1710 model) X-ray diffractometer with Ni filtered Cu-K_α radiation by directly placing the silica in the sample chamber.

2.2.3. Surface area measurement

The specific surface area was measured by using single point BET (Brunauer–Emmett–Teller) method [81]. About 25 mg of accurately weighed silica was heated electrically at about 110^{o}C in a glass sample cell for nearly 4 h in a continuously flowing mixture of nitrogen and helium. The sample was then cooled to liquid nitrogen temperature in a continuously flowing mixture of nitrogen and helium. The adsorbed nitrogen was desorbed by bringing the sample to room temperature. The changes in the nitrogen concentration of the flowing gas stream, consequent to the adsorption and desorption, were monitored by a thermal conductivity detector. The desorption signal was electronically integrated from which the surface area of the sample was computed.

In the present work, an indigenous surface area analyzer (BARC make) was used for the determination of specific surface area.

2.2.4. Zeta potential measurement

Colloids particles bear surface charge due to various reasons such as lattice defects, inclusion of specific ions, adsorption or desorption of surface groups. The surface charge strongly depnd upon pH and ionic strength of the medium. Oppositely charge counter ions present in the medium surrounds the particle surface and form electrical double layers. Zeta potential is the potential difference between dispersion medium and the stationary phase of the dispersion medium attached to the dispersed particle.

Zeta potential is not measurable directly but it can be calculated using theoretical models and experimentally-determined electrophoretic mobility. When an electric field is applied to colloids solution, particles move toward an electrode opposite to their surface charge. Since the velocity is proportional to the amount of charge on the particles, zeta potential can be estimated by measuring the velocity of the particles. Electrophoretic light scattering is the method most popularly used to determine the velocity of the particles suspended in a liquid medium under an applied electric field. In order to determine the speed of the particles, they are irradiated with a laser light and the scattered light from the particles is detected. Since the frequency of the scattered light is shifted (Doppler shift) from the incident light in proportion to the speed of the particles movement, the electrophoretic mobility of the particles can be measured from the frequency shift of the scattered light.

The velocity is determined using the following equation

$$\Delta\nu = \frac{2\mathrm{vn}\ \mathrm{Sin}\frac{\theta}{2}}{\lambda} \tag{2.1}$$

Where Δν is the Doppler shift in frequency, v is the velocity of the particle, n is the refractive index of the medium, θ is the angle at which scattered light detected and λ is the wavelength of the laser light.

$$V = \mu E \tag{2.2}$$

$$Z = \frac{4\pi\mu\eta}{\xi} \tag{2.3}$$

Where μ is the mobility, E is the applied electrical field, η and ξ are the viscosity and dielectric constant of the medium and Z is the zeta potential. Thus the zeta potential of a particle is determined.

Zeta potentials of silica, humic acid and silica-humic acid combined system were measured using Malvern zeta sizer nano-Z instrument (UK) by phase analysis light scattering with applied field strength of 2.5 x 10^3 V m^{-1}. The light source was He-Ne laser (632.8 nm) operated at 4 mW. The measurement was carried out using a quartz cuvette (universal 'dip' cell) with 10 mm light pathway. All the measurements were performed at 25 ± 1 ^{o}C.

2.2.5. Particle size measurement

The principle of determining particle size is the same as that for determining zeta potential. Here also velocity (v) of the colloidal particle is determined and followed by its mobility (μ). Using mobility value, diffusion constant is determined by the following equation

$$D = \mu k_B T \tag{2.4}$$

Then using the Stokes –Einstein equation hydrodynamic particle size is determined.

$$D = \frac{k_B T}{6\pi \mathrm{nr}} \tag{2.5}$$

Where, T is absolute temperature, k_B is Boltzmann's constant, n is refractive index and r is hydrodynamic radii of the colloid particles.

Dynamic light scattering (DLS) technique was used for the measurement of the particle size. The measurements were made at an angle of 130^o using Malvern 4800 Autosizer, employing a 7132 digital correlator, and the light source was He-Ne laser operated at 632.8 nm with maximum power output of 15 mW. The correlation functions were analyzed by the method of CONTIN analysis.

Silica was ultrasonicated (Retsch GmbH, Germany, 1 min, 35 kHz, power = 140 W) prior to both zeta potential and particle size measurements. It was assumed that the soft conditions of ultrasonication would not have altered particle size.

2.2.6. Preparation of ^{94}Nb radiotracer

A piece of irradiated Zr-Nb alloy coolant tube (~25 mg) was dissolved in HCl - HF acid mixture and evaporated to dryness on a water bath. The above step was repeated thrice and finally the solid residue was dissolved in 9 M HCl + 0.004 M HF. Niobium was separated from zirconium by ion exchange method described by Kraus and others [82]. Ion exchange column was made of polypropylene tube of internal diameter 10 mm. The aqueous slurry of anion exchange resin (~28 cm^3) was transferred to the column and allowed to settle, with no air bubbles trapped. Resin was preconditioned with 9 M HCl + 0.004 M HF and then solution of Zr-Nb alloy was passed through the column and effluent was collected in fraction. Gradient elution was carried out by initially using 9 M HCl + 0.004 M HF to remove zirconium followed by 9 M HCl + 0.1 M HF for niobium. Eluate was collected in volume fraction of 10 mL each. The obtained chromatogram is shown in **Figure. 2.1**.

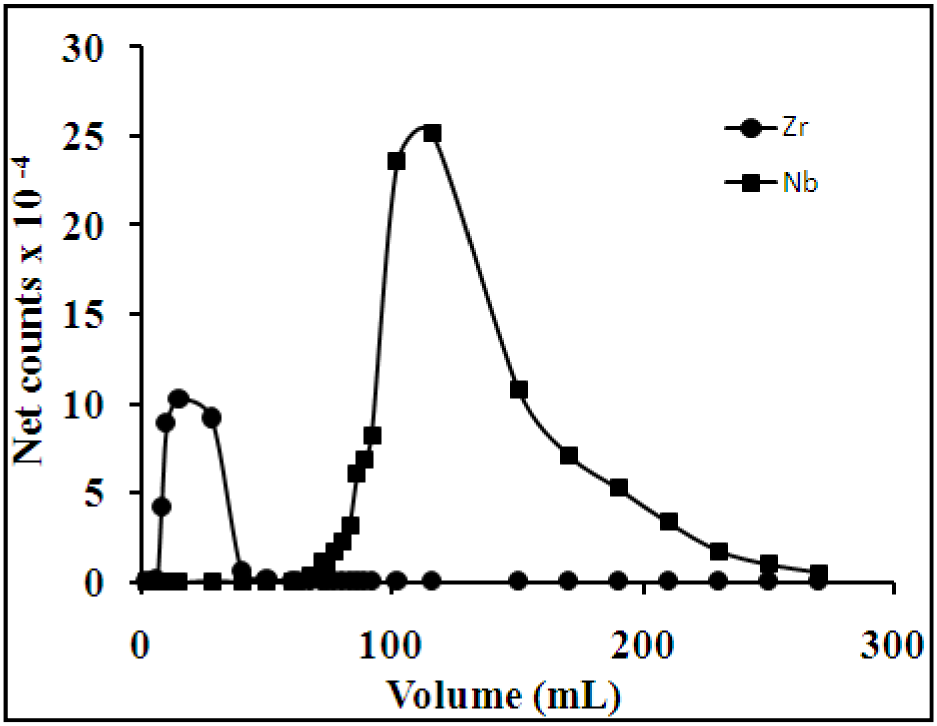

Figure 2.1: Chromatogram for the anion exchange separation of Zr and Nb

The count rate in each eluted fraction was measured using High Purity Germanium (HPGe) detector (EG&G ORTEC, relative efficiency: 30 %; resolution: 1.9 keV at 1332 keV of ^{60}Co) coupled with 8k channel analyzer. Gamma rays of ^{95}Zr (724.2 and 756.7 keV), ^{94}Nb (702.6 & 871.1 keV) and ^{95}Nb (765.8 keV) were used for activity measurement. All the fractions containing pure niobium (^{94,95}Nb) were mixed and used as the radiotracer. For sorption experiments, the required amount of radiotracer solution was converted to chlorate form by repeated treatment with perchloric acid and heating near to dryness.

2.2.7. Purification of ^{231}Pa radiotracer

Earlier in Analytical Chemistry Division, BARC, ^{231}Pa was separated from 'siliceous cake' which is the waste product of monazite processing plant and is enriched of ^{231}Pa, decayed from naturally occurring ^{235}U isotope [83]. Before starting the work, ammonium hydroxide (NH_4OH) was added to the tracer solution which led to the formation of a gelatinous precipitate. After filtration, Energy Dispersive X-ray Fluorescence (EDXRF) study of the precipitated showed the presence of Ti and Zr along with Pa. So, to purify Pa, the precipitate was again dissolved in HCl- HF mixture. Then anion exchange separation was carried out in 9MHCl + 0.004M HF medium using DOWEX-1X8 anion exchanger resin column (mesh size 50-100) and elution by the same acid mixture [84]. Activity in collected fractions also measured corresponding 283.69 keV gamma of ^{231}Pa. To check the presence of Zr and Ti in each of the fraction containing ^{231}Pa, NH_4OH was added and the fractions in which white gelatinous precipitate appeared were rejected and rest were collected. The collected fraction containing ^{231}Pa was evaporated to reduce the volume and this led to formation of NH_4Cl crystals. NH_4Cl was removed by heating on a platinum crucible and the residue was dissolved into HNO_3 and a few drop of HF.

2.2.8. Determination of ^{94}Nb and ^{231}Pa concentration in tracer solution

Before determining the tracer concentrations, efficiency calibration of the HPGe detector was carried out using ^{152}Eu source. The efficiency calibration plot is shown in **Figure 2.2**

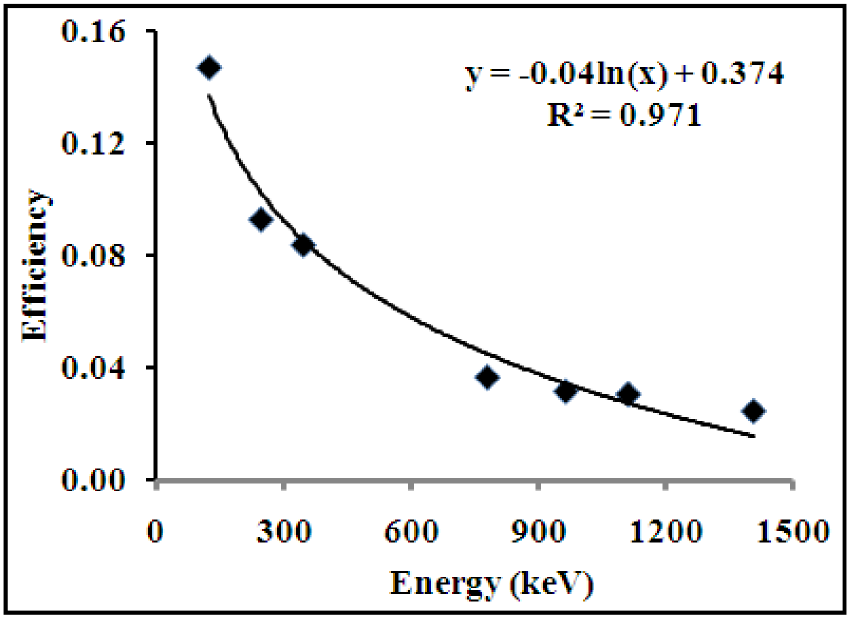

Figure 2.2: Efficiency calibration of HPGe using ^{152}Eu point source

Point sources were prepared using 50 µL of the ^{94}Nb and ^{231}Pa tracer solutions and activity of the corresponding radionuclides were measured using HPGe. From the measured activity, the concentrations of the radionuclides in the tracer solution were determined. Total Nb concentration in tracer solution was 3.12 x 10^{-5} M and the concentration corresponding to ^{94}Nb was 2.2 x 10^{-7} M. The concentration of ^{231}Pa in tracer solution was found to be 9.6 x 10^{-6} M.

2.2.9. Purification of Sodium salt of humic acids

The steps involved in the purification of commercially available sodium salt of humic acid is depicted in Figure 2.3

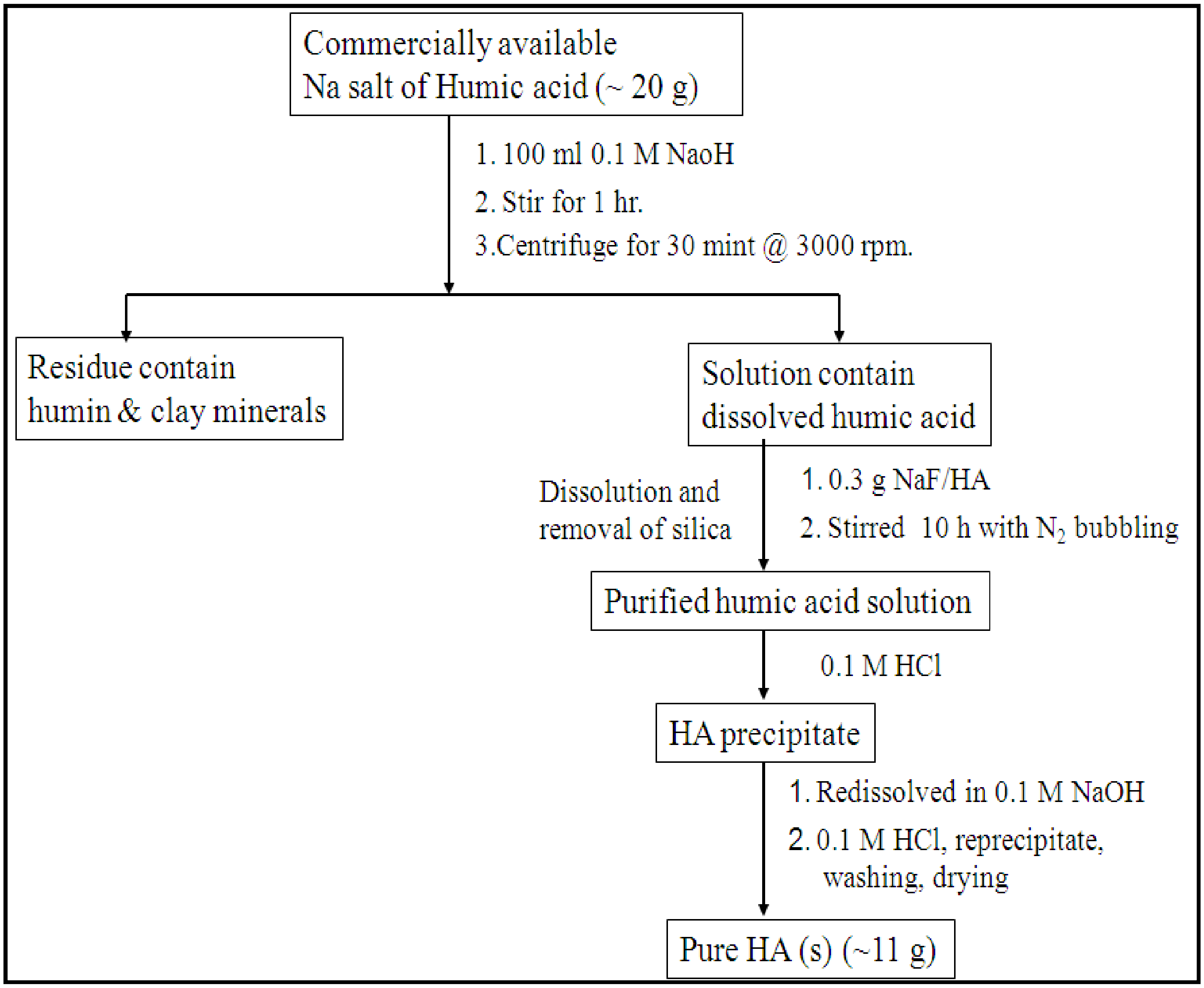

Figure 2.3: Block diagram for the purification of humic acids sodium salt [85]

Elemental compositions of the as-received and purified of humic acid samples were determined by Energy Dispersive X-ray Spectrometry (EDS) (Quanta, Model: 3D FEG-I, Switzerland). Hydrogen and nitrogen concentration in humic acid samples were determined by CHNS analyzer (Euro Vector EA3000EA-IRMS elemental analyser, Italy). The purified humic acid also characterized by UV-Vis spectrophotometry (V-530, Jasco) and FTIR (Tensor II, Bruker).

2.2.10. Determination of proton exchange capacity of humic acid

2.2.10.1. Total capacity

Total proton exchange capacity of humic acid corresponds to all the proton exchangeable groups like –COOH, phenolic-OH, Enolic-OH present in it. Baryta method is the most popular technique used to determine the total proton exchange capacity [9]. In this method, sample is allowed to react with excess barium hydroxide base, followed by the titration of the unused base by an acid of known strength. The reaction by which $Ba(OH)_2$ is consumed on its reaction with humic acids is given below

$$2HA + Ba(OH)_2 = BaA_2 + 2H_2O \qquad (2.6)$$

About 80 mg of accurately weighed purified humic acid was equilibrated with excess $Ba(OH)_2$ solution (0.01 M, 50 mL) on a mechanical shaker for about 24 h with occasional N_2 gas bubbling to remove CO_2. After equilibration, the solution was filtered and the precipitate was washed with deionised water. Filtrate and washings were combined and the solution was titrated potentiometrically using 0.5 M standard HCl (**Figure 2.4**). Then total capacity was determined using the following equation

$$\text{Total capacity } (\text{meqg}^{-1}) = \frac{(V_b - V_s)}{W_s} * N * 1000 \qquad (2.7)$$

V_b and V_s are the volume of the standard acid consumed for the titration of blank and sample.

N is the normality of the acid and W_s is the weight of the sample in mg.

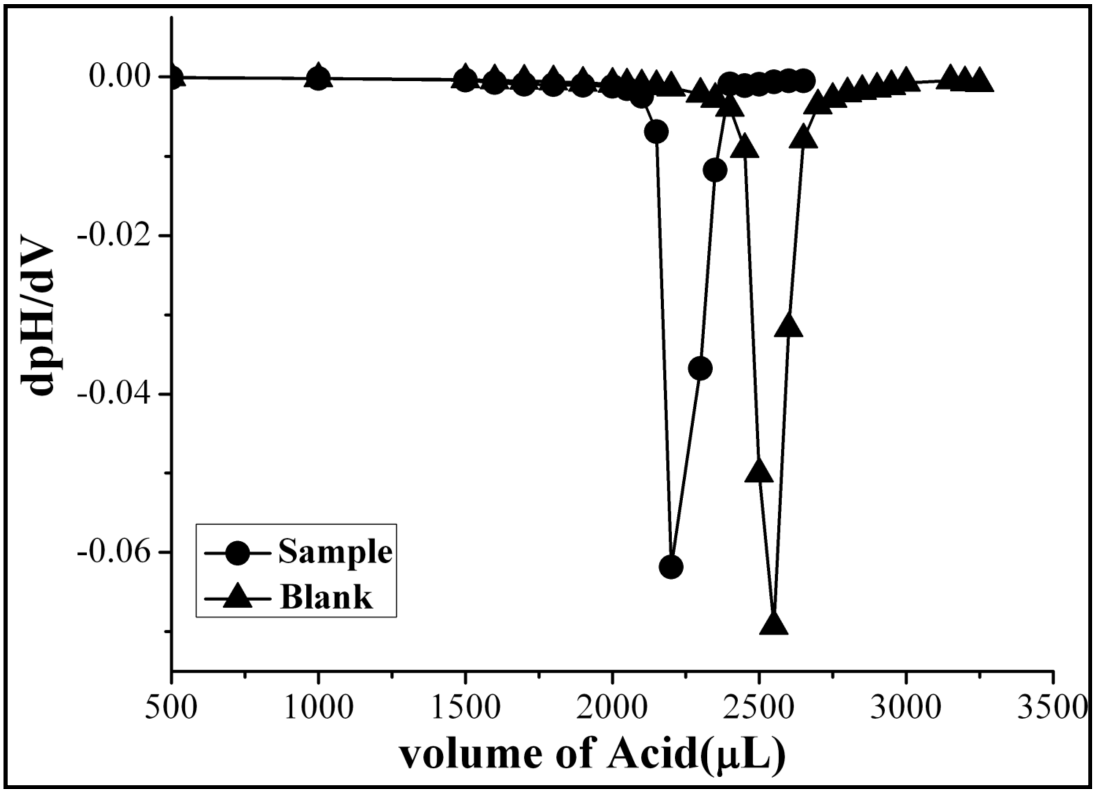

Figure 2.4: Potentiometric titration curve of blank (barium hydroxide) and HA equilibrated with barium hydroxide

2.2.10.2. Capacity corresponding to –COOH group

Carboxylic group capacity is generally determined by equilibrating humic acids with calcium acetate which leads to generation of acetic acid (Equation 2.8). This is then potentiometrically titrated using standard NaOH solution [9].

$$2R\text{-}COOH + Ca(OOCCH_3)_2 = Ca(OOC\text{-}R)_2 + 2\ CH_3COOH \qquad (2.8)$$

Purified humic acid (~ 80 mg) is equilibrated with 50 mL of 0.1 M calcium acetate solution for 24 h. After equilibration, the solution was filtered and the precipitate was washed with deionised water. The filtrate and washings were combined and the solution was titrated using 0.5 M standard NaOH. Then the –COOH group capacity was determined using the following equation

$$\text{Total capacity (meqg}^{-1}) = \frac{(\mathrm{V_s} - \mathrm{V_b})}{\mathrm{W_s}} * \mathrm{N} * 1000 \qquad (2.9)$$

2.2.11. Fourier-transform infrared (FTIR) spectroscopy

FTIR is the most useful spectroscopic method to identify the organic or inorganic molecules or species. It can also be used to quantify some components of an unknown mixture and for the analysis of solids, liquids, and gases. The Fourier Transform converts the detector output to an interpretable spectrum that provides structural insights of the sample. It is a powerful tool for identifying types of chemical bonds in a molecule by producing an infrared absorption spectrum that is like a molecular "fingerprint", as the wavelength of light absorbed is characteristic of the chemical bond of functional groups.

FTIR measurement of the purified humic acid was carried out using a Tensor II FTIR system from Bruker. Requisite amount of sample was mixed with KBr properly and then 10 mm diameter pellet was prepared using hydraulic press. The spectrum of the sample was recorded in transmission mode.

2.2.12. UV-visible spectrophotometry

Absorption spectrometry in the ultraviolet-visible spectral region is one of the simplest and widely used techniques for the qualitative as well as quantitative determination of a species or molecule. This technique is based on Lambert-Beer's law, expressed as,

$$A = ln\left(\frac{I_o}{I_T}\right) = \epsilon Cl \qquad (2.10)$$

Where, A: Absorbance, I_o: Intensity of the incident light, I_T: Intensity of the transmitted light, ε: molar extinction coefficient, C: concentration of the species, *l*: path length.

The law is valid only when the concentration of the species is low i.e $\leq 10^{-3}$M and there should not be any change in the species under measurement conditions. The wavelength corresponding to absorption maximum is the characteristic feature of the species and from the absorbance value at this wavelength the concentration of the species can be evaluated accurately.

UV-Vis spectrophotometer, V-530, Jasco, has been used in the present study to know the wavelength of absorption maximum of humic acid as well as to determine its sorption on silica at different pH following its absorbance changes.

2.2.13. Batch equilibration method for sorption studies

Batch sorption method was used to study the distribution of radionuclides between the silica surface and the aqueous phase under well defined experimental conditions of pH, ionic strength, solid/liquid ratio and temperature. Partitioning is expressed by the distribution coefficient, kd, defined as,

$$k_d(mLg^{-1}) = \frac{\left(\frac{A_s}{w_s}\right)}{\left(\frac{A_l}{V_l}\right)} \qquad (2.11)$$

Where A_s and A_l are the activities in the silica and in solution, w_s is the weight of silica and V_l is the volume of the solution.

Sorption data on specific mineral surface, generally represented in terms of % sorption and is defined as,

$$\%\ \text{sorption} = \frac{(A_i - A_f)}{(A_i)} * 100 \qquad (2.12)$$

Where A_i is the initial activity and A_f is the activity in the supernatant after phase separation.

2.2.13.1. Batch method (Silica- humic acid system)

Varying amounts of humic acid (0.5 to 15 mg L^{-1}) was added to 10 mL 0.05 M $NaClO_4$ solution and equilibrated for 30 min. The absorbance of the solution was measured at 257 nm using UV-Vis spectrophotometer and calibration curve was obtained by plotting the absorbance against the concentration of humic acid used in solution. Silica (2 g L^{-1}) was added to solution of 0.05 M $NaClO_4$ and was equilibrated for 2 h. The equilibrated solutions were made up to 10 mL with deionised water, after adjusting the pH (1 - 11) and maintaining the desired concentration of humic acid (15 mg L^{-1}). Solution was equilibrated for 48 h. Phase separation was carried out using high speed centrifuge at 6800 rpm for 1 h and the completeness of separation was checked by dynamic light scattering technique. The absorbance of the solution was measured at 257 nm and concentration of humic acid was obtained from calibration plot **(Figure 2.5)**.

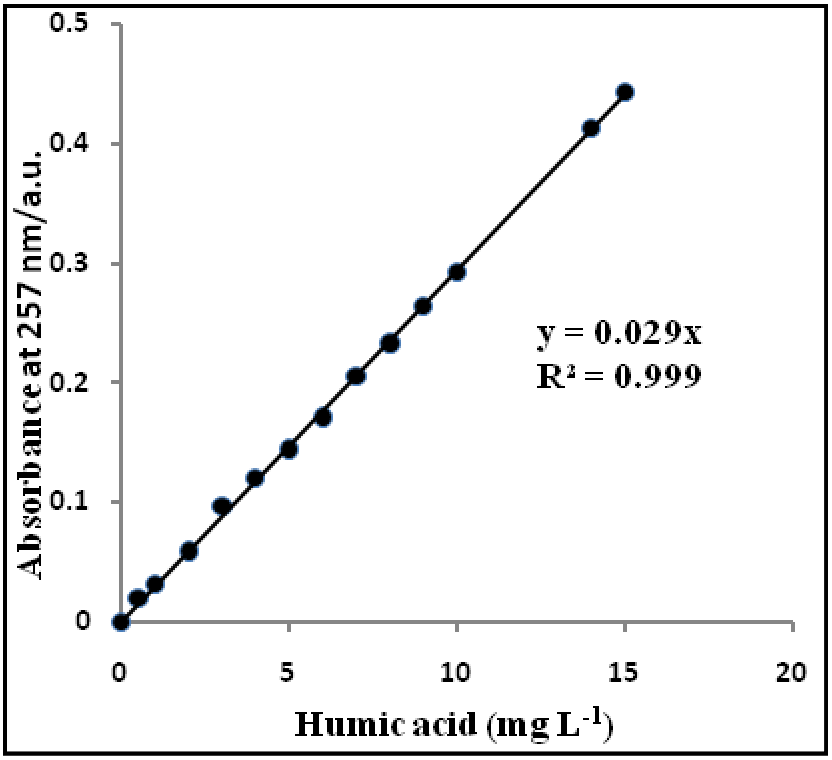

Figure 2.5: Calibration plot of the spectrophotometer at 257 nm

2.2.13.2. Batch method (Silica- Niobium/Protactinium system)

Silica (2 g L^{-1}) was added to the solution of 0.05 M $NaClO_4$ and was equilibrated for 2 h. After equilibration, pH was adjusted (2 - 11) and 100 µL each of the $^{94,95}Nb$ and ^{231}Pa radiotracers were added. Activities in the initial solutions were measured using HPGe detector and the counts at 702.6 keV (^{94}Nb) and 283.7 keV (^{231}Pa) were noted down. Then the solutions were equilibrated for 48 h and then phase separation was carried out using high speed centrifuge at 10000 rpm (Hermle Labotechnik GmbH Z383K, Germany) for 1 h. After phase separation, the activities in the supernatants were measured and finally from that % sorption of the radionuclides at different pH conditions were obtained.

2.2.13.3. Batch method (Silica-Niobium/ Protactinium-humic acid system)

Silica (2 g L^{-1}) was added to solution of 0.05 M $NaClO_4$ and was equilibrated for 2 h. After equilibration, humic acid (0-200 mg L^{-1}) was added and pH was adjusted to 1.2, 6.5 and 10.5. After addition of ^{94}Nb & ^{231}Pa radiotracers (100 µL each) and equilibration for 48 h, the subsequent steps were identical to those used for sorption of Nb/Pa on silica.

2.2.14. Determination of charge on Pa (V) species

Depending o the pH of the solution Pa(V) ion can exist as various aqua complexes with different net charges on the species. The method to determine the charge in the species based on the competition on sites on mono-functional ion exchange resins between the ions of known charge (M_1) which is used in varying amounts in large excess and the ion of the unknown charge (M_2) used in very low concentration. The precondition of this technique is that the concentration of the metal ion of unknown charge should be extremely low (nM or less) and must be in non complexing medium. The method provides only the overall average charge on the unknown metal ion [62, 86, 87].

$$m_2(R)_{m1}M_1 + m_1M_2^{m2} = m_1(R)_{m2}M_2 + m_2M_1^{m1} \tag{2.13}$$

$$D_{M_2} = C * \frac{1}{[M_1]^{m_2/m_1}} \tag{2.14}$$

$$Log(D_{M_2}) = LogC - \frac{m_2}{m_1} Log[M_1] \tag{2.15}$$

R- is the ion exchanger resin, M_1 is the ion attached to the resin and present in large excess in the medium, M_2 is the ion of unknown charge, m_1 & m_2 are absolute charge of the ions M_1 and M_2, D_{M2} is the distribution ratio of M_2. The concentration of this M_1 varies during the experiment.

About 100 µL of ^{231}Pa solution (0.061 µg mL^{-1}) and 1 g of mono-functional strong cation exchanger resin (AG 50W-X8) were added to 10 mL of $HClO_4$ solutions of desired molarities (0.1 M to 3 M). The resin was equilibrated for 2 h in a mechanical shaker. To determine the charge on Pa species in neutral and basic medium (10^{-8} to 0.5 M NaOH), ^{231}Pa tracer was equilibrated with 1 g of anion exchanger resin (AG 1-X8). The count rate at 283.7 keV gamma ray of ^{231}Pa in the solution and resin were measured using HPGe detector and the distribution ratios (D) of Pa was determined using equation 2.16.

$$D = \frac{A_{resin}}{A_{solution}} \qquad (2.16)$$

where A_{resin} and $A_{solution}$ are the counts corresponding to ^{231}Pa in resin and in solution respectively at equilibrium. The overall charge on Pa species ion was determined from the slope of Log (D) vs Log (M) plot.

2.3. Results and discussion

2.3.1. Characterization of silica and humic acids

XRD pattern (Figure 2.6) indicated that silica sample used in this study is amorphous in nature. The observed specific surface area of silica was (160 ± 20) m^2g^{-1}. The measured particle size was in the range of 160 - 310 nm.

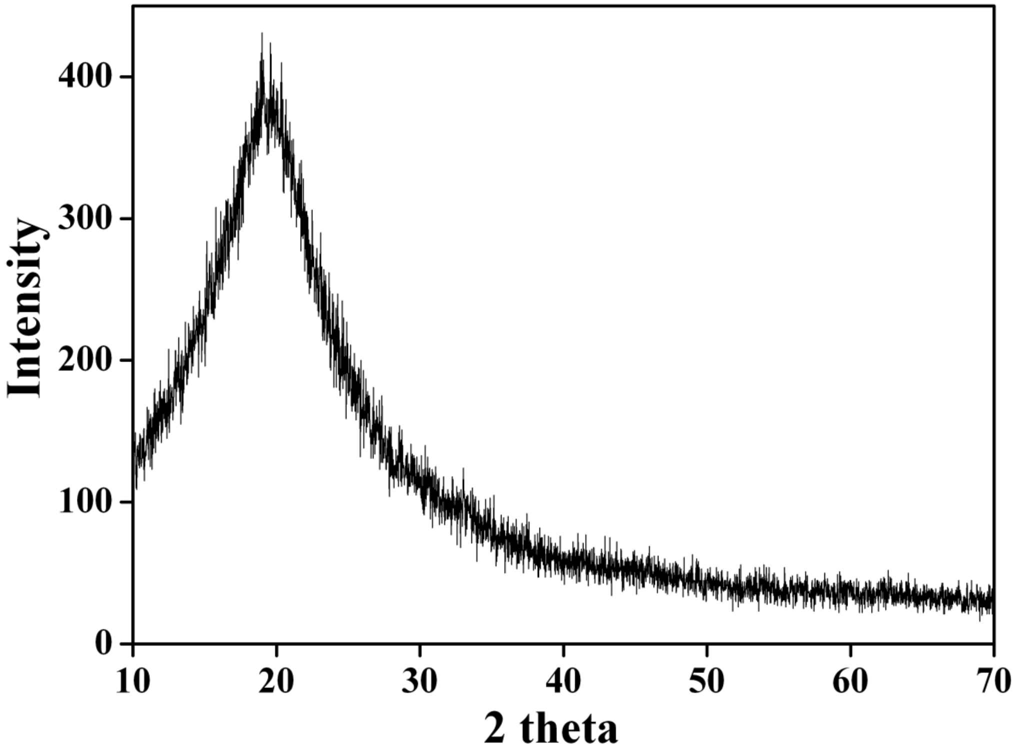

Figure 2.6: XRD pattern of silica

EDS study of unpurified humic acid indicated the presence of appreciable amount of the impurities like Al, Si along with Na. The other impurities like Fe, K, Ca, Ti were also observed. After purification, the relative contents of C, N and S increased while that of O decreased and concentration of other impurities decreased significantly (Table 2.1). The ratios of H/C, N/C and S/C did not change substantially, establishing that there was no major chemical alternation or modification of humic acid during the purification process. The large decrease in O/C ratio (Table 2.2) after purification indicates, the removal of oxygen-rich impurities such as clay and other minerals.

The proton exchange capacities of as-received and purified humic acid were (4.1 ± 0.1) meq g^{-1} and (5.4 ± 0.2) meq g^{-1} respectively. The capacity of purified humic acid corresponding to –COOH group was (3.8 ± 0.1) meq g^{-1} and hence the exchange capacity corresponds to phenolic/enolic –OH group was about 1.6 meq g^{-1}.

Table 2.1: Elemental composition of as received and purified humic acid

Element	As received humic acid (Atom %)	Purified humic acid (Atom %)
H	3.1 (±0.1)	4.7 (±0.1)
C	36.2 (±0.3)	59.9 (±0.9)
N	0.65 (±0.03)	1.20 (±0.03)
O	50.2 (±0.4)	37.9 (±1.1)
Na	9.2 (±0.2)	0.4 (±0.2)
Al	1.7 (±0.2)	0.06 (±0.03)
Si	1.7 (±0.2)	0.02 (±0.01)
S	0.3 (±0.1)	0.4 (±0.1)
K	0.2 (±0.1)	-
Ca	0.1 (±0.1)	-
Ti	0.2(±0.1)	0.07 (±0.02)
Fe	0.3 (±0.1)	0.2 (±0.1)

Table 2.2: Ratio of (H/C), (N/C), (O/C) and (S/C) before and after purification of humic acid

	Element (Atom %)				
	C	H	N	O	S
Sample		(H/C)	(N/C)	(O/C)	(S/C)
As received HA	36.20	0.086	0.018	1.387	0.015
Purified HA	59.89	0.078	0.020	0.720	0.013

The signature of purity is prominent from the FTIR spectrum (Bruker, Tensor II) of purified humic acid (Figure 2.7). The bands at 3300-3400 cm^{-1}, 2900-2940 cm^{-1} of aliphatic C-H stretching, 1720-1725 cm^{-1} of C=O stretching of –COOH and ketone group, 1630-1660 cm^{-1} of C=O stretching of amide group, quinine C=O or C=O of H-bonded conjugated ketone which is in overlap with 1600-1620 cm^{-1} of aromatic C=C or strongly H- bonded ketones, 1390-1400 cm^{-1} of O-H deformation and C-O stretching off phenolic –OH, 1200-1280 cm^{-1} of C-O stretching and OH deformation of –COOH groups are matching with the literature reported data of humic acid [9].

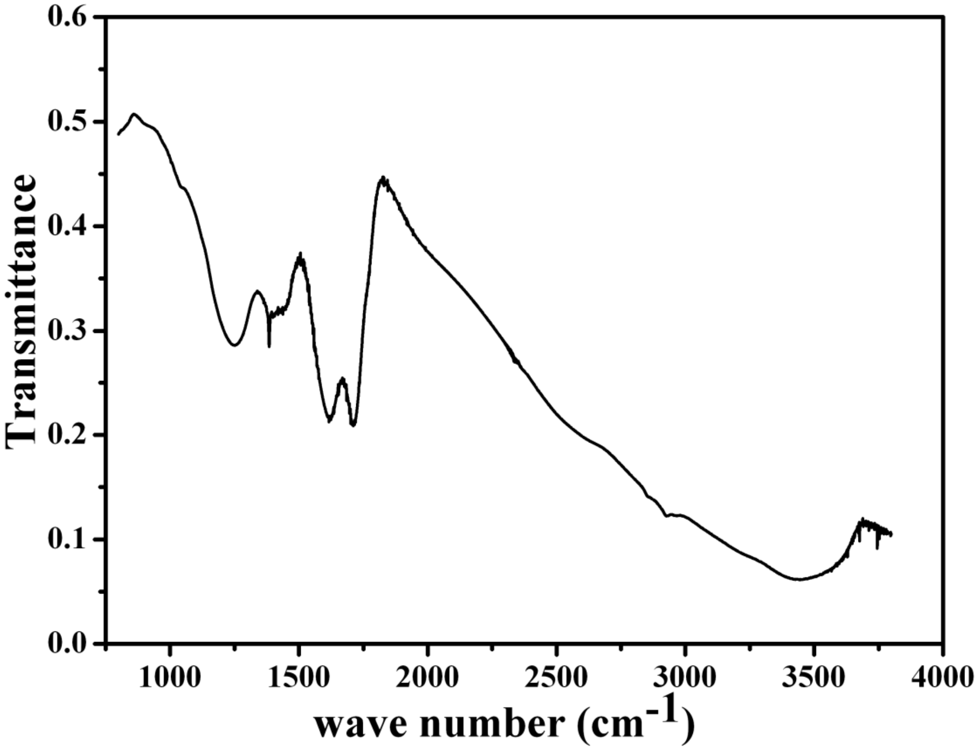

Figure 2.7: FTIR spectrum of purified humic acid

Zeta potentials of silica, humic acid and silica-humic acid were measured in the pH range of 2 - 11 in the presence of 0.05 M $NaClO_4$ and the results are shown in Figure 2.8. The point of zero charge for silica was found to be 2. The magnitude of zeta potential gradually becomes more negative with increase of pH and become saturated near about pH 10 where silanol groups of silica are supposed to be deprotonated completely ($pK_a = 9.5$) [88]. Zeta potential of humic acid was negative on starting from pH 1 and may be due to the presence of ionisable carboxylic (-COOH) and phenolic (-OH) groups. Around ~ pH 4 and 9, the change in zeta potential of HA are relatively sharp which may be associated with the dissociation of carboxylic (-COOH) and phenolic (-OH) group respectively. The zeta potential of the silica-HA mixed system (Silica 2 g L^{-1}, HA 5 mg L^{-1}) was also measured and found to be lying between those of humic acid and silica.

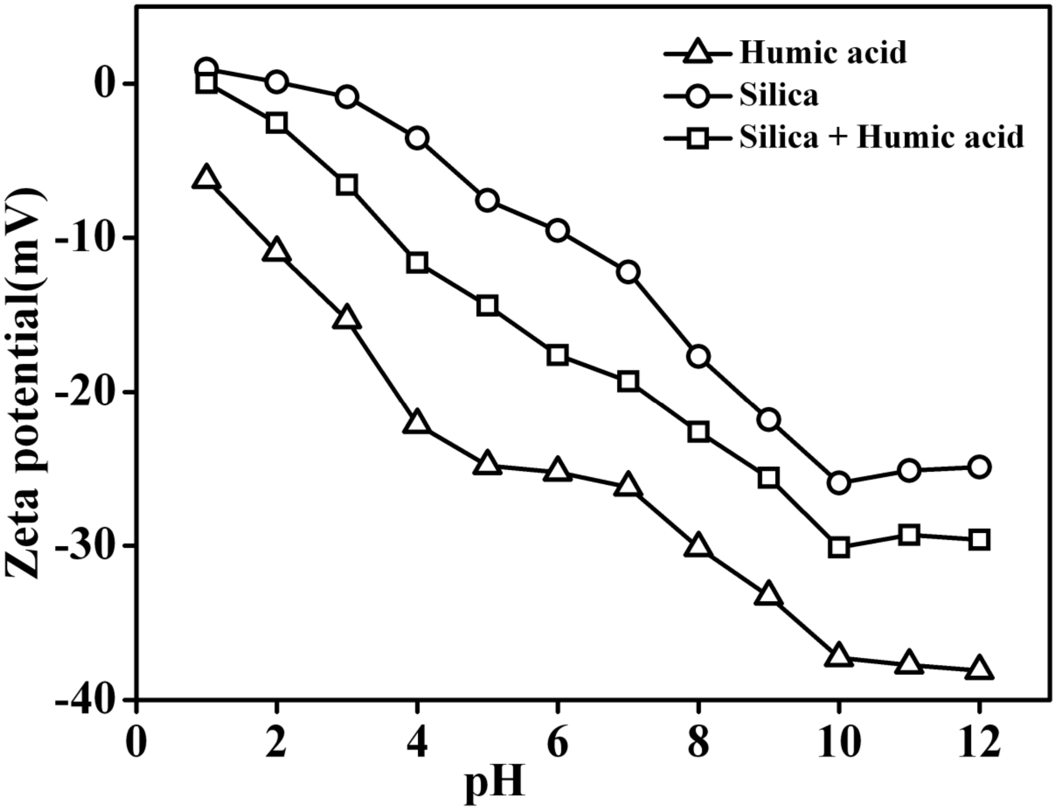

Figure 2.8: Zeta potential of silica, humic acid and silica-humic acid systems

2.3.2. Sorption of humic acid on silica

The sorption of humic acid on silica (2 g L^{-1}) was measured as a function of pH at fixed humic acid concentration (15 mg L^{-1}) in presence of 0.05M $NaClO_4$ and results are shown in Figure 2.9. Percentage sorption of humic acid decreased from 78.6% at pH 2 to 5.4% at pH 12. At lower pH (≤ 2), the zeta potential of silica is slightly positive whereas that of humic acid is negative, which is the rationale behind the observed sorption upto pH 2. Above pH 2, zeta potential of silica is negative and magnitude increases with increasing pH and at the same time zeta potential of humic acid is also negative between pH 2 - 11. Hence there is an electrostatic repulsion which explains the gradual decrease of sorption of humic acid on silica with increasing pH. As indicated in Figure 2.9, even though there was a large reduction in the sorption with increasing pH, some amount of humic acid was still sorbed on silica at very low pH, which is not fully understood and several mechanisms have been proposed in the literature to rationale such observation [85].

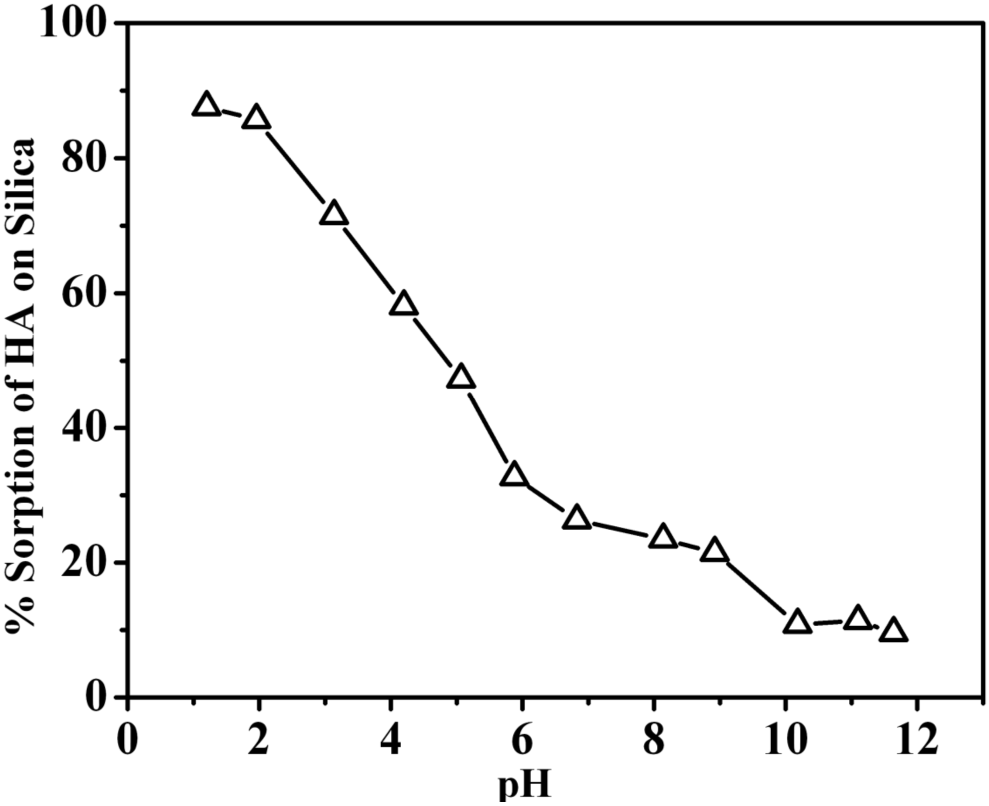

Figure 2.9: Sorption of Humic acid on silica as a function of pH

2.3.3. Determination of charge on Protactinium

The overall charge on Pa(V) ion, determined from the slope of Log (D) vs Log (M) plot (Figure 2.10) in the dilute perchloric acid medium (0.1 – 3.0 M) was about 1.12+. In the pH range 2-12, Log(D) vs Log(M) plot (Figure 2.11) has two distinct slopes, one between pH 6 to 11 and another above pH 11.

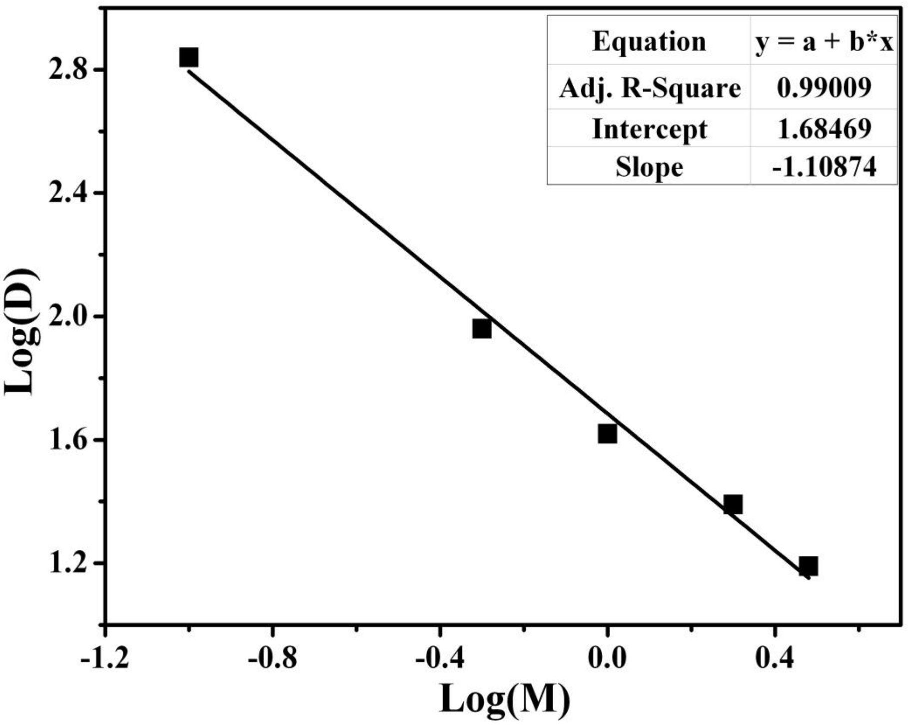

Figure 2.10: Distribution ratio (D) of Pa vs concentration(M) of $HClO_4$

Between pH 6 and 11, the charge on Pa(V) ion was 0.1-, which indicates that the major fraction of protactinium was present as neutral species and negatively charged species started forming only at higher pH. Above pH 11, the charge on Pa(V) ion was ~ 0.8-, suggesting that the protactinium predominantly existed as singly negatively charged species. It is difficult to explicitly identify Pa(V) species from the net average charge as more than one species is likely to exist simultaneously in the solution. The above findings are consistent with the literature reports [61].

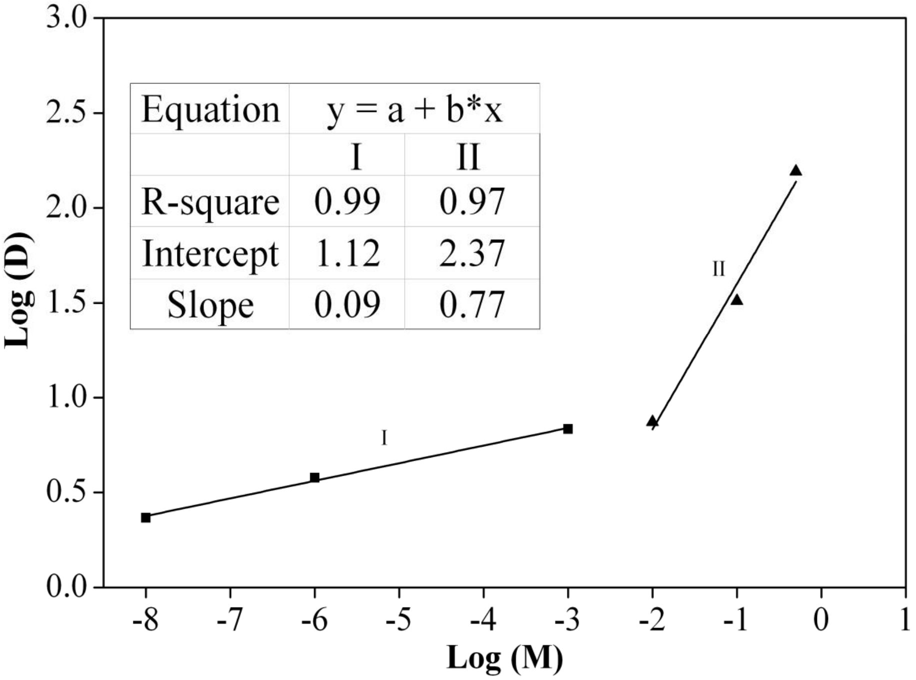

Figure 2.11: Distribution coefficient (D) of Pa vs concentration (M) of OH^-

2.3.4. Sorption of Niobium & Protactinium on silica

The hydrated pentoxide (niobic acid) is obtained as white gelatinous precipitates of the composition $Nb_2O_5.xH_2O$ or $[Nb_2O_5.xH_2O]_n$ when water soluble niobium complexes are hydrolysed or when a solution containing niobate is acidified. Hydrolysis in solutions of mineral acids results in a quantitative precipitation.

The behaviour of niobium ion in aqueous solution is very complex because of the tendency to hydrolyse and polymerize. In aqueous solutions, oxygen containing niobium species are formed because of the high ionic potential of Nb(V) ions (ionic radius = 0.69 Å). Different types of ionic species exist in aqueous solutions. The solution pH as well as niobium concentration determines the specific niobium ionic species present in the solution. Literature data on the ionic state of Nb(V) in aqueous solutions are scanty and often qualitative. Nevertheless there is a general agreement that above pH 12, mononuclear anions $NbO_2(OH)_4^{3-}$ are likely to be present in dilute solutions and at slightly lower pH, the species present are the $[H_xM_6O_{19}]^{(8-x)-}$ ions (x= 0, 1, 2, or 3) [89]. Between 0.01-1M acid medium, Nb generally exists as singly positively charged species $Nb(OH)_4^+$ or $NbO(OH)_2^+$ or NbO_2^+ and acidity below 0.01M neutral species $Nb(OH)_5$ or $NbO_2(OH)$ or $NbO(OH)_3$ predominates upto pH 7. Above pH 7 negatively charged species $Nb(OH)_6^-$ starts forming and predominates after pH 9 [60, 90].

Sorption of niobium on silica gel from 1 to 12 M HCl solutions was studied by Caletka [91] but the sorption in the pH range of 1 to 12 has not been studied. Sorption of niobium on silica as a function of pH is shown in Figure 2.12. Sorption is low (70-80%) below pH 3 but then increases and becomes almost quantitative in the pH range 5 to 9. After pH 9 there is a slight decrease in sorption. Sorption of radionuclides on solid surface is mainly due to electrostatic interaction and surface complexation reaction [92]. As niobium exists as positively charged species below pH 3 and zeta potential of silica is positive below pH 2, the electrostatic repulsion explains the observed lower sorption behaviour of niobium at low pH. Deprotonation of surface silanol groups of silica increases with increase in pH. However, surface silanol groups have pK_a close to 9.5 and hence only a small fraction will be deprotonated for the pH range below 9. Therefore, sorption of niobium can be explained on the basis of surface complexation model between pH 5 to 9, according to which hydroxo complex of niobium reacts with the surface hydroxyl groups of silica.

$$\equiv Si(OH)_{(s)} + NbO(OH)_{3(aq)} \rightarrow \equiv SiO - NbO(OH)_{2(s)} + H2O \qquad (2.17)$$

The above reaction is equivalent to condensation and the driving force of this kind of reaction is the formation of covalent bond. Vibrational spectroscopic studies of niobium oxide supported on silica showed that the interaction between niobium oxide and the surface hydroxyl groups (Si-OH) is due to acid-base type of reaction [93]. Again above pH 9, Nb exists as negatively charged species and zeta potential of silica also negative. So, Coulombic repulsion reduces the sorption of Nb on silica after pH 9.

The sorption pattern of Pa on silica follows the same trend as followed by Nb (Figure 2.12). The species of Pa(V) that exist in non-complexing media (0.1 M Na/HClO$_4$) are (a) $PaO(OH)_2^+$ or PaO_2^+ below pH 3 (c) $Pa(OH)_5$ or $PaO_2(OH)$ between pH 3 to 9 and (d) $Pa(OH)_6^-$ above pH 9. In similar way, the sorption behaviour of Pa on silica can also be explained in terms of the surface complexation and the charges on the ionic species of Pa(V) in aqueous medium and the zeta potential of silica surface.

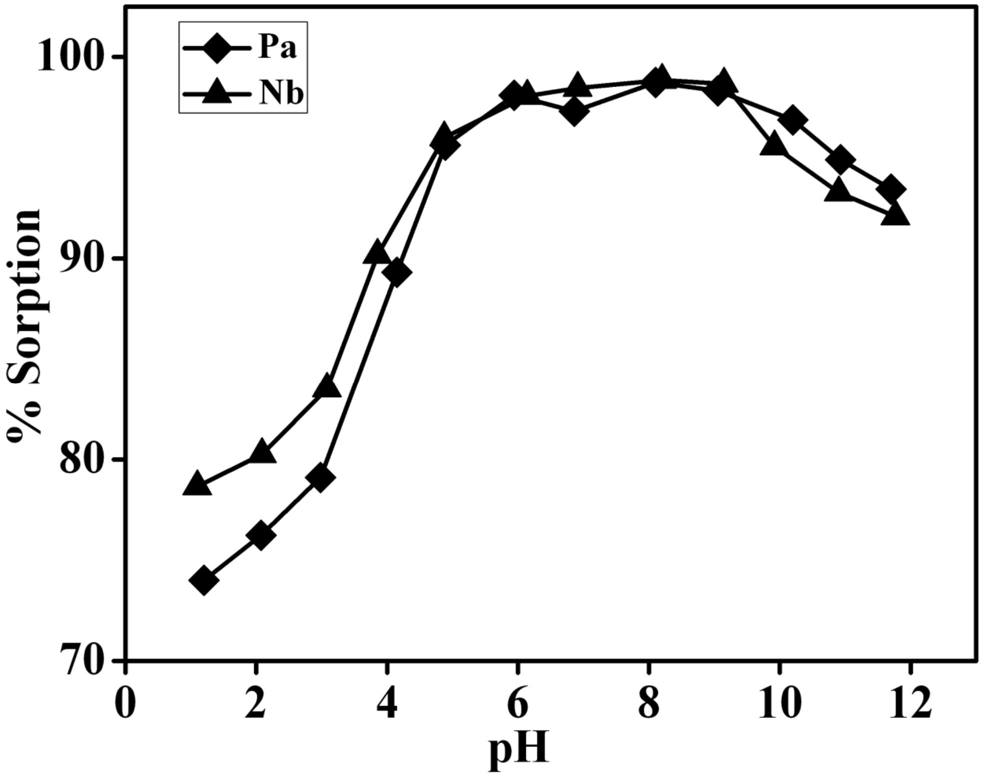

Figure 2.12: Sorption of Nb(V) and Pa(V) on silica as a function of pH

2.3.5. Effect of humic acids on sorption of Nb/Pa on silica

The result of sorption study of Nb/Pa on silica in the presence of humic acid is shown in Figure 2.13. It is evident from the figure that in acidic pH, presence of humic acid facilitates the sorption whereas in neutral pH sorption decreases mildly. In basic pH, sorption of both the element decrease substantially with increasing concentration of humic acid. In acidic pH, humic acid is strongly sorbed onto the silica surface and it is suggested that mineral bound humic acid facilitates the sorption of radionuclides on the silica. Reports are available on the complexation of humic acid with various metal ions viz. U, Np, Pb, Eu, Zn, Cu [79]. Both Nb and Pa are also having strong complexation tendency with carboxylic (-COOH) groups. At higher pH, humic acid undergoes Deprotonation and thus prefers to be in the solution rather than being sorbed on silica surface. These dissolved humic acid undergoes complexation using –COOH/COO$^-$ groups with the radionuclides, causing an increase in the concentration of Nb(V) and Pa(V) in solution, in other word, decreasing their sorption on silica surface. Self agglomeration of humic acid in acidic pH was observed above the concentration of 50 ppm and this act as an additional phase for sorption of the radionuclides. Self agglomeration may be the reason behind a comparatively steeper increase in sorption after 50 ppm concentration of humic acid at acidic pH.

2.3.6. Loss of Nb/Pa on container wall and dissolution of silica

During the present work, polypropylene containers were used instead of glass to prevent the loss of Nb and Pa on container wall due to diffusion into glass [94]. It was found that `even in polypropylene container there was (2 - 5 %) loss of Nb/Pa depending upon pH of the medium.

In a separate experiment, colloidal silica suspension (2 g L^{-1}) were prepared in acidic (pH 1), neutral (pH 7), and alkaline (pH 11) aqueous media, equilibrated on a mechanical shaker and centrifuged. The supernatant was analysed by inductively coupled plasma optical emission spectrometry (ISA Jobin Yvon - JY 2000) and contained 2 mg L^{-1} (pH 7), 14 mg L^{-1} (pH 1) and 120 mg L^{-1} (pH 11) of silica which amounted to 0.05 %, 0.35 % and 3 % of the initial concentrations respectively. So dissolution of silica has mild effect on sorption, only at high pH condition.

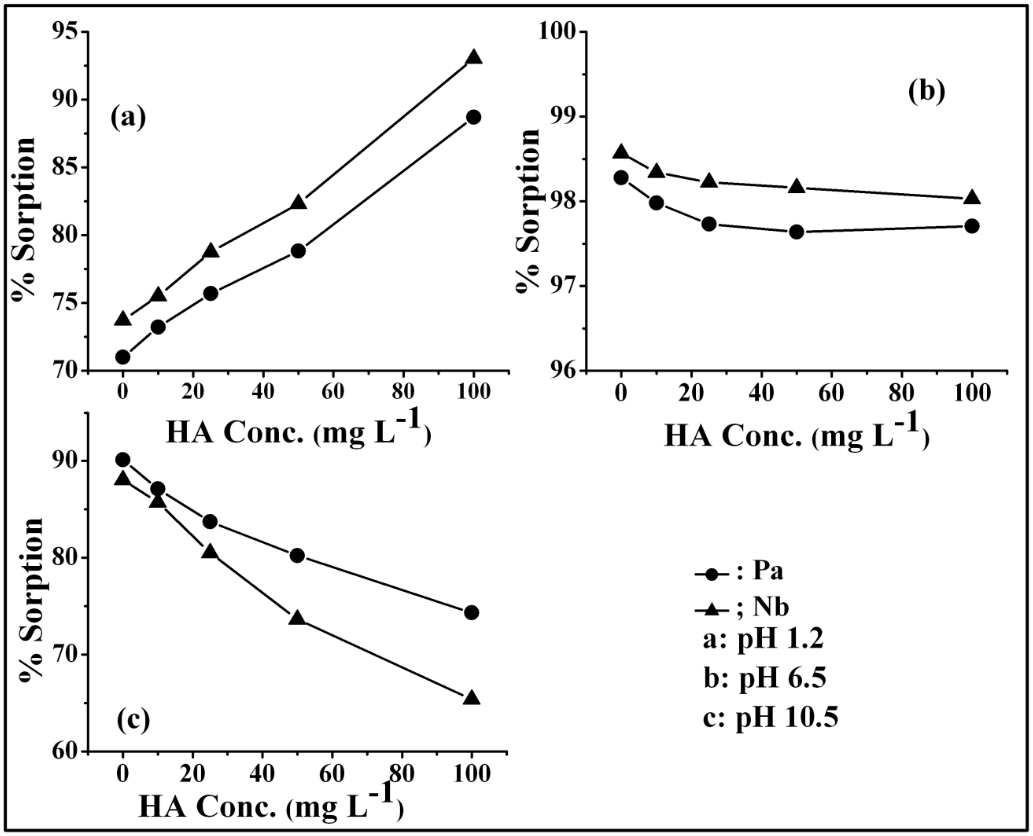

Figure 2.13: Effect of humic acid on sorption of Nb/Pa on silica

2.4. Conclusion

Silica is one of the most abundant naturally occurring inorganic colloidal particles. It displays a range of important interactions with various metal ions and radionuclides. Both Nb and Pa are strongly associated with colloidal silica, especially in the neutral to mildly basic pH region. This indicates strong probability of migration of these two radionuclides as pseudo colloid. Humic acid has negligible effect on the sorption in neutral pH but increases the sorption in acidic pH and decrease the sorption in basic pH. The results of this study will be useful for modeling the migration behaviour of both Nb and Pa.

Chapter III

Sorption of ^{94}Nb and ^{231}Pa on Iron Oxides

3.1. Introduction

The migration of radionuclides in environments became a hot topic of research in recent days specially those having (1) high yield in fission process and (2) long half-life [95]. It is of major concern if high level radioactive-waste stored underground comes in contact with flowing ground water, it may leach out and migrate [96]. In general, the factors affecting the release and migration of the radionuclides are, precipitation, complexation with organic and inorganic ligands present in aqueous medium, sorption on mineral or rock surface and colloid formation by the radionuclides by itself. Colloid formation may enhance or retard the migration process depending upon the nature of colloids and mobile phase condition [90]. Two phase model, consists of a stationary phase and a mobile phase, is used to explain the radionuclides migration based on distribution of the radionuclides between two phases and the velocity of mobile phase. However, this model is not able to explain faster and long distance migration of radionuclides especially of those, having low aqueous solubility. Then a three phase model, consists of a stationary phase, a mobile phase and colloidal phase (intrinsic or pseudo) dispersed in mobile phase, is introduced. This model is able to explain the migration of radionuclides satisfactorily [21,32]. The migration of radionuclides with very low aqueous solubility and high affinity towards stationary phase, have been explained by colloidal-facilitated transport model [76, 97]. So in this context, the sorption study of radionuclides on naturally occurring colloids (pseudo) became important. Both inorganic and organic materials such as mineral and weathering products, humic substances, and microorganisms are known to exist as colloids in groundwater. The chemical composition, size distribution, and formation kinetics of aquatic colloids and their aggregates have been discussed by Buffle and Leppard, [77]. The various aspects of colloids that facilitated the transport of radionuclides in natural groundwater systems have been reviewed by Patera et.al [98]. Sorption of radionuclides on colloidal surfaces occurs due to electrostatic forces, ion exchange, surface complexation, and surface precipitation and the rate and magnitude of sorption may depend upon the concentration of radionuclide and colloid, pH and ionic strength of solution and natural complexing species present in the solution.

^{94}Nb and ^{231}Pa, both are long lived isotopes, generated in nuclear industry. ^{94}Nb is generated from the irradiated Zr-Nb pressure tube and ^{231}Pa from the irradiated thoria as a byproduct along with the desired fissile isotope ^{233}U. Both Niobium (Nb) and Protactinium (Pa) are the high priority elements when considering its possible migration into the biosphere. This is because of their high tendency to hydrolyze in aqueous medium to form intrinsic colloids and strong affinity towards naturally occurring colloids which finally resulted to their colloid assisted migration. [99-100].

Nb occurs in soil and groundwater in +V state even in highly reducing conditions [101-103]. Niobium forms complex ions in solutions owing to its high ionic potential. In acidic solution, the principal chemical form is NbO_2^+, while neutral species ($HNbO_3$ or $Nb(OH)_5$) occur in slightly acidic to neutral solutions. Anionic species (NbO_3^- or $Nb(OH)_6^-$) are predominant above pH 7 [101, 104]. Niobium has strong tendency to form complexes with fluoride, citrate, and oxalate anions [102, 105]. Association of Nb with colloidal iron and dissolved humic substances in natural waters has been observed [106]. Niobium can also form negatively charged colloids in aqueous solutions with the chemical properties of Nb_2O_5. In 0.5 M HNO_3 medium, there is no intrinsic colloid formation of Nb at a concentration of 10 x 10^{-8} M, whereas colloids were formed at 7 x 10^{-6} M, and colloid formation increased with increase in Nb concentration [107]. Significant sorption of Nb on colloids generated from clay material has been reported [108].

The predominant and most stable form of Pa(V) in oceanic systems is PaO_2^+ ion, although it is uncertain whether the better formulation of the aqueous species is PaO_2^+ or $PaO(OH)_2^+$ [109]. PaO_2^+ is most soluble, similar to the Pu(V) ion, and sorbs to particle surfaces to a much lower extent than the tetra valent oxidation state ion, Pa(IV). It is likely that Pa(V) is first reduced to Pa(IV) before adsorption and removal from natural waters can take place, as has been seen for Np(V), which is reduced in the presence of natural organic matter such as humics [11]. Very little knowledge about its complexation and redox behaviour in aquatic systems is available. The redox potential for Pa(V) to Pa(IV) reduction is -0.05V [110]. The organic and inorganic matter present in aquatic system like humic acid (HA), bi-carbonate can facilitate the above written process in acidic to neutral medium as shown below [93].

$$Pa(V)O_2^+ + 2\,H_2O + e- = Pa(IV)(OH)_4; \qquad E_h^o = -\,0.05V \qquad (3.1)$$

In the present study we are focusing specially on three different oxides of iron, namely goethite, hematite and magnetite as they are the most abundant iron oxides present in nature. Hematite is the most stable, brown colored, highly crystalline iron oxide mostly present in red soils. Goethite is yellow colored, relatively less crystalline and dominant iron oxide mineral in red soils and humid temperature region. Magnetite is brownish-black, crystalline, dominant in beach sands but has lower abundance compared to the other two. It is observed that due to their high surface area, they are the most active in adsorption and interaction phenomenan, even these are used for the retention of pollutants in water purification and in natural system [111]. The sorption study of various radionuclides like U, ^{140}Ba, ^{90}Sr, Th(IV) on different iron oxides are reported in literature [112-115].

The lack of knowledge concerning interaction of Nb and Pa with different soil components motivated us to carry out systematic study on its sorption behaviour with natural colloids using batch method. The aim of the present work was to study the sorption of Nb and Pa on iron oxides, and effect of HA on the sorption. Sorption behaviour in neutral to slightly alkaline conditions was of special interest, where the neutral species turns into the anionic.

3.2. Experimental

3.2.1. Materials

The following chemicals were used in the sorption study: XAD-4 adsorption resin (20-60 mesh), Sodium perchlorate ($NaClO_4$) and Sodium salt of HA from Sigma Aldrich, Ferric nitrate (($Fe(NO_3)_3$: LR, Loba chemie), Sodium hydroxide (NaOH: Thomas Baker), Ammonium hydroxide (NH_4OH: SD Fine Chem.), Ferrous ammonium sulphate ($(NH_4)_2SO_4.FeSO_4.6H_2O$: Sarabhai Chemicals), Glacial acetic acid (CH_3COOH: Chemco Fine Chemicals), Acetone (Extra pure AR, Sisco Research Laboratory), and Perchloric acid ($HClO_4$: Otto Chemie Pvt. Ltd.).

3.2.2. Preparation of Iron oxides

Hematite, Goethite and magnetite are the most abundant iron oxides present in nature. So for the sorption study all these three iron oxides were synthesized in the laboratory.

3.2.2.1. Hematite

About 100 g of ferric nitrate ($Fe(NO_3)_3$) salt was taken into 500 mL beaker and then dissolved in 250 mL of DI water. Then 0.5 M Sodium Hydroxide (NaOH) solution was added gradually into the ferric nitrate solution till deep brown colored precipitate appeared. The solution was stirred continuously for 2h using magnetic stirrer. Then the precipitate was filtered and washed using deionized water until pH of the washing reached 6 to 7 and then kept overnight for drying. After that, the air dried precipitate was transferred into a silica crucible and heated at 300^oC for 36 h in muffle furnace to convert the hydroxide to crystalline hematite. Finally the brown colored crystalline material was ground thoroughly using mechanical grinder to get the hematite particle of micron size.

3.2.2.2. Goethite

About 100 g of ferric nitrate [$Fe(NO_3)_3$] salt was taken into 500 mL beaker and then dissolved in 250 mL of deionized water. Then 0.5 M sodium hydroxide solution was added gradually to the ferric nitrate solution at 60^{o}C with continuous stirring 2 h using magnetic stirrer. Then the yellowish precipitate was filtered and washed using glacial acetic acid followed by deionized water. The precipitate was kept overnight for drying and finally placed in decicator.

3.2.2.3. Magnetite

About 50 g each of the ferric nitrate and Mohr salt [$(NH_4)_2SO_4.FeSO_4.6H_2O$] were dissolved in 100 mL deionized water separately in two beakers and then mixed. After that, ammonia solution was added gradually in the mixed solution and stirred continuously at 80^{o}C for 2 h. The brownish black colored precipitate then filtered and washed using dilute ammonia solution, followed by deionized water and acetone. The precipitate was then taken into silica crucible and heated in oven at 100^{o}C for 12 h to get crystalline magnetite. Finally, the crystalline material was ground thoroughly using mechanical grinder to get the particle of micron size.

3.2.3. Characterization of Iron oxides

3.2.3.1. X-ray diffraction (XRD) measurements

The powder XRD pattern of iron oxides were recorded using a Philips X-ray diffractometer (PW1710 model) with Ni filtered Cu-K_α radiation.

3.2.3.2. Surface area measurement

The specific surface area was measured by an indigenous surface area analyzer (BARC make) using single point BET (Brunauer–Emmett–Teller) method [83].

3.2.3.3. Particle size measurement

Colloidal iron oxides were ultrasonicated (Retsch GmbH, Germany) (1 min, 35 kHz, power = 140 W) and transferred to a quartz cuvette (universal 'dip' cell). It was assumed that the soft conditions of ultrasonication would not have altered particle size. Dynamic light scattering (DLS) technique was used for measurement of particle size. The measurements were made at an angle of 130° using Malvern 4800 Autosizer employing a 7132 digital correlator, and the light source was He-Ne laser operated at 632.8 nm with maximum power output of 15 mW. The correlation functions were analyzed by the method of CONTIN analysis.

3.2.3.4. Zeta potential measurement

The zeta potentials of iron oxides (2 g L^{-1}), HA (5 mg L^{-1}) and their combined system were measured using Malvern zeta sizer nano-Z instruments, UK, by phase analysis of scattered light. The light source, He-Ne laser (632.8 nm), was operated at 4 mW. The measurement was carried out using a quartz cuvette (universal 'dip' cell) with 10 mm light pathway. All the measurements were performed at (25 ±1) °C. In all the experiments, ionic strength of the solution was maintained at 0.05 M $NaClO_4$, and pH was adjusted between 1-12 by using dilute NaOH and $HClO_4$ solutions. The pH was measured by glass electrode (Oakton, pH700, USA). Ultrasonication (1 min, 35 kHz, power = 140 W) of sample solution was carried out before zeta potential measurements to avoid aggregation.

3.2.4. Sorption experiments

3.2.4.1. Sorption of HA on iron oxides

Varying amounts of purified HA (0.5-15 mg L^{-1}) were added to 10 mL of 0.05 M $NaClO_4$

solutions and agitated for about 30 min on a mechanical shaker. Absorbance of each solution was measured at 264 nm using UV-Vis spectrophotometer (V-530, Jasco) and a calibration curve was obtained.

Synthesized iron oxide (2 g L^{-1}) were added to 25 mL of 0.05 M of $NaClO_4$ separately and agitated for 2 h on a mechanical shaker. After addition of HA (15 mg L^{-1}), the pH was adjusted between 1 and 12 and the solutions were agitated once again for 48 h on a mechanical shaker. Phase separation was carried out by centrifugation for 1 h at 10000 rpm (Hermle Labotechnik GmbH Z383K, Germany). The absorbance of the supernatant was measured at 264 nm and concentration of HA in the supernatant was obtained using the calibration function.

3.2.4.2. Sorption of Nb and Pa on iron oxides

Sorption of Nb on iron oxides was carried out in aerobic, ambient, laboratory conditions using batch method. 50 mg of each of the iron oxide were taken separately in 60 mL polypropylene containers (Tarson) containing 25 mL of 0.05 M $NaClO_4$ solution. The solution pH was adjusted between 1-12 with 0.01 or 0.1 M of $HClO_4$ or NaOH and then 100 μL of each ^{94}Nb (2.2×10^{-7} M) and ^{231}Pa (9.6×10^{-6} M) radiotracers were added. Solutions were equilibrated for 48 h on a mechanical shaker and phase separation was carried out using a high speed centrifuge (10000 rpm). The gamma ray spectrometric measurements of the solutions before and after separation were carried out using High Purity Germanium (HPGe) detector (EG&G ORTEC) coupled with 8k channel analyzer (Relative efficiency: 45%; Resolution: 1.9 keV at 1332 keV of ^{60}Co). The percentage sorptions were achieved by comparing the activities in initial solutions and in the final supernatants at 702.7 keV for ^{94}Nb and 283.7 keV for ^{231}Pa using the following equation

$$\% \text{ sorption} = \frac{(A_i - A_f)}{(A_i)} * 100 \qquad (3.2)$$

where A_i and A_f are the counts in initial solutions and supernatant respectively.

3.2.4.3. Electrochemical investigation of sorption study of Nb on magnetite

Sorption study on magnetite is more interesting compared to goethite and hematite as the previous one is the mixed valent iron oxide. Three electrode system was adopted for the experiment; where modified glassy carbon electrode (GCE) was used as working electrode, Ag/AgCl/KCl (saturated) as reference electrode and graphite rod as counter electrode. All the electrochemical experiments were carried out at room temperature and ambient conditions. Acetate buffer (0.1M) of pH 5.5 was used as supporting electrolyte. Glassy carbon electrode was polished with 5μ and 1μ alumina powder and cleaned under ultra sonication at 20 kHz for 15 mint to get clean surface. Carbon black and iron oxide composite (1:1) was prepared by mixing both (1mg mL^{-1}) at 1:1 (weight) ratio in acetone medium containing 0.1% nafion. The mixture was ultra sonicated for 5 mint at 20 kHz to disperse the solid particles in acetone medium to attain homogeneity prior to casting on the glassy carbon electrode surface. 5μL of the homogeneous mixture was drop casted on the glassy carbon electrode surface and allowed to dry. The coated electrode was rinsed with deionised water and dried in air. Experiments were carried out using Autolab Potentiostat Galvanostat 302N. Data acquisition and analysis were carried out using GPES software.

3.2.4.4. Effect of HA and equilibration time on sorption

The sorption of Nb and Pa on iron oxide in presence of HA (5 mg L^{-1}) were carried out in the pH range of 1-12. To study the effect of HA concentration, the sorption of Nb and Pa on hematite were carried out in acidic (pH 1) and basic (pH 10) region by varying HA concentration from 10-100 μg mL^{-1}.

The effect of incubation time on sorption was studied in acidic (pH 1) and basic (pH 10) media for time intervals of 5 min, 1h, 5h, 24 h, 48 h and 72 h to understand the effect of equilibration time and the kinetics followed by the sorption process in both acid and basic medium. In all the above cases, the experimental procedure was identical as described in Section 3.2.4.2.

3.2.4.5. Sorption study of Nb and Pa on XAD resin

Sorption of Nb and Pa on XAD-4 resin, an inert medium, was carried out at pH 1, 6, and 10 using 100 mg of resin and the procedure was the same as described in Section **3.2.4.2.**

3.2.4.6. Dissolution study of iron oxides at different pH

50 mg of each of the oxides were added to 25 mL solution of 0.05M $NaClO_4$ and agitated for about 1 h. After adjusting the pH between pH 1-12, solutions were agitated for 48 h on a mechanical shaker and centrifuged (10000 rpm). The supernatant was collected and iron concentration in the supernatant was measured by inductively coupled plasma mass spectrometric technique.

3.3. Results and discussion

3.3.1. Characteristics of iron oxides and HA

The XRD patterns of the synthesized iron oxides (goethite, hematite, and magnetite) are shown in the Figure 3.1 - 3.3. The peaks of the corresponding XRD pattern of each iron oxide matched with those reported in the literature [111].

The surface area, particle size and point of zero charge (PZC) of goethite, hematite, and magnetite were listed in the Table 3.1. The measured values of particle size and surface area were within the range reported in literature [111, 116-120].

Table 3.1: Surface area, particle size and PZC of goethite, hematite and magnetite

Oxide	**Surface area (m^2g^{-1})**	**Particle size (nm)**	**PZC**	**Surface area (m^2g^{-1}) Literature [111]**	**Particle size (nm) Literature**	**PZC Literature [116-120]**
Goethite	51	160-295	8	8-200	200-400	7-9.4
Hematite	18	190-340	6.5	10-70	100-500	6-6.8
Magnetite	35	180-320	6.9	4-100	50-350	6.5

Purification, compositional analysis, and proton exchange capacity of the sodium salt of HA has been reported earlier in this thesis [121]. Zeta potential of iron oxides was measured in the pH range 1-12 in 0.05M $NaClO_4$ medium (Figure 3.4**)**. Zeta potential of HA (Figure 3.5) was negative even at pH 1 and its magnitude increased with increase in pH. At about pH 4-5 and pH 8-9, the change in zeta potential of HA was relatively sharp and these may correspond to dissociation of carboxylic (–COOH) and phenolic (–OH) group respectively. The zeta potential of the iron oxide-HA combined system lay between the two individual systems but the pattern was similar to the corresponding oxide (Figure 3.5-3.7). This is obvious that, zeta potential of the mixed systems, depend on the concentration of iron oxides and humic acids in the system, apart from pH and ionic strength of the medium. The zeta potential plots shown in Figures 3.5 to 3.7 are valid for the specified concentration of iron oxides and humic acids.

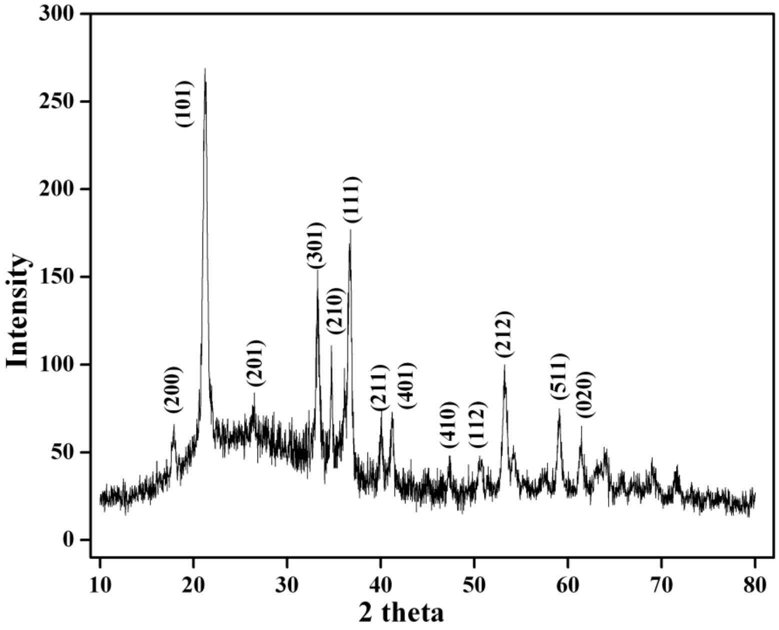

Figure 3.1: XRD pattern of Goethite

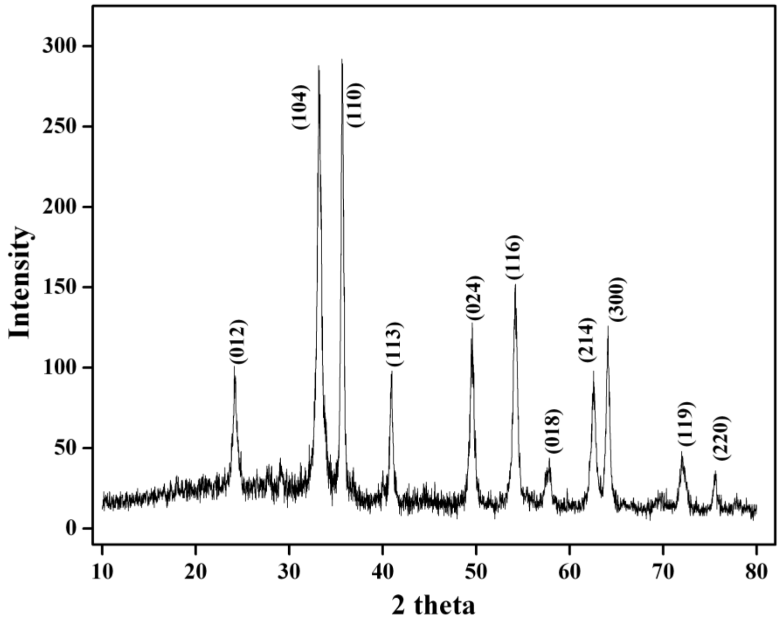

Figure 3.2: XRD pattern of Hematite

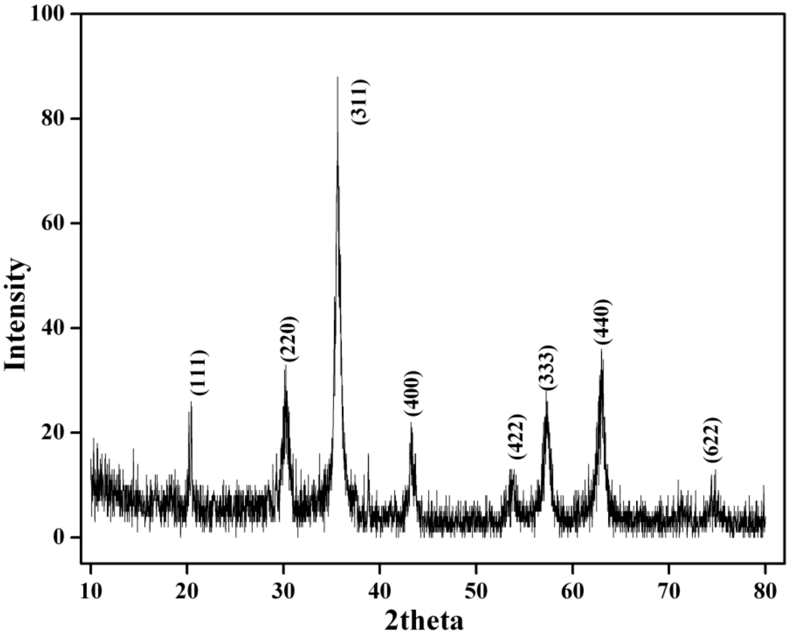

Figure 3.3: XRD pattern of Magnetite

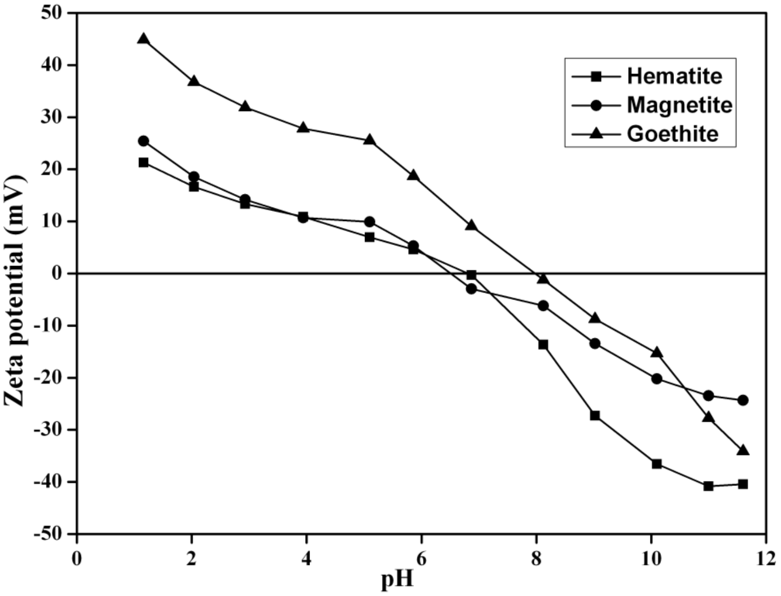

Figure 3.4: Zeta potential of iron oxides as a function of pH

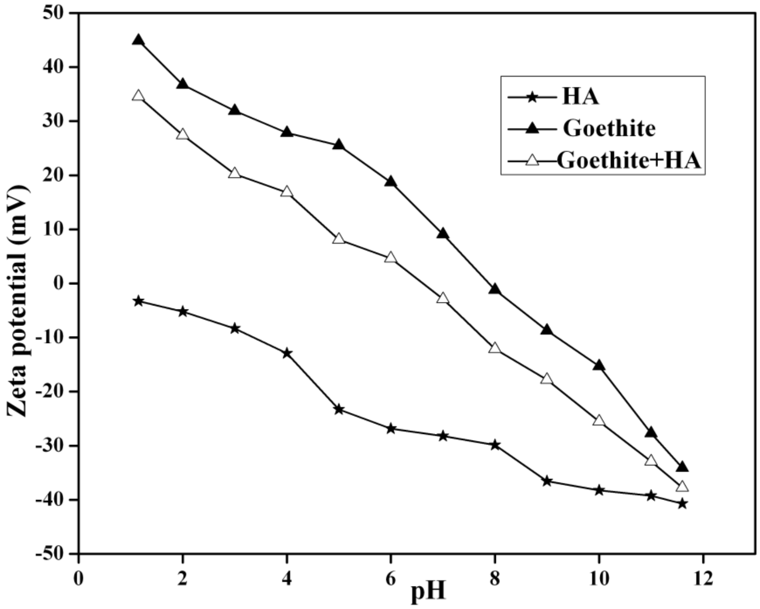

Figure 3.5: Zeta potential of goethite-HA system

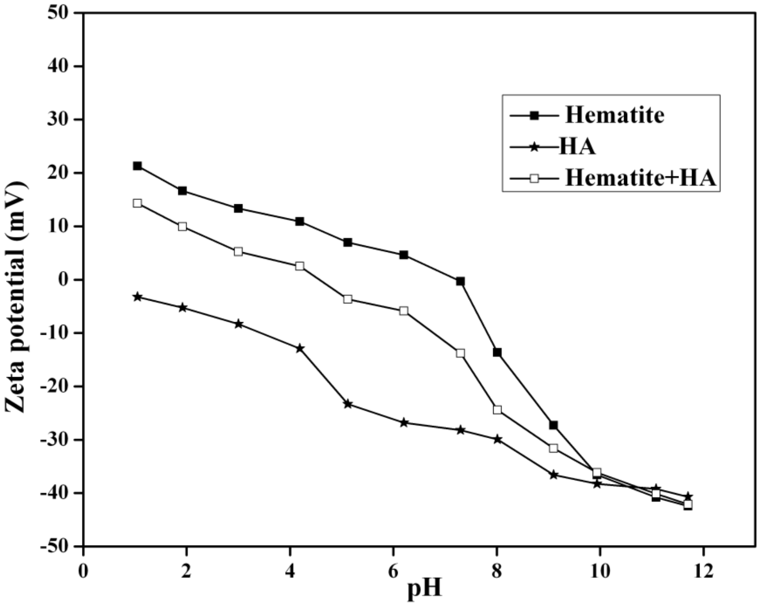

Figure 3.6: Zeta potential of hematite-HA system

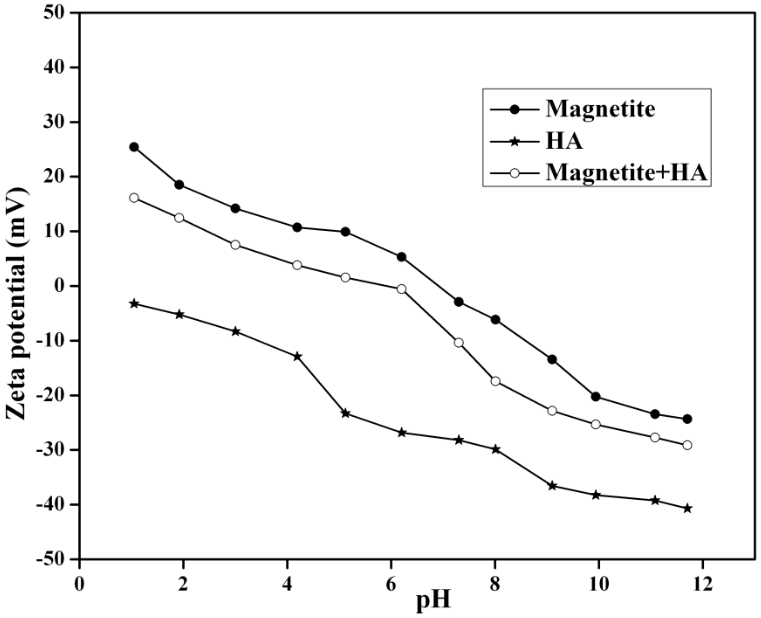

Figure 3.7: Zeta potential of Magnetite-HA system

3.3.2. Sorption behaviour of HA on iron oxides

The sorption of HA on iron oxides in the pH range 1-12 in 0.05M $NaClO_4$ medium is shown in Figure 3.8. The sorption of HA on iron oxides is very high in acidic pH, and decreases gradually with increase of pH. Several mechanisms for sorption have been reported in literature [122-124], which include electrostatic binding, specific site complexation, and ligand exchange. The infrared spectroscopic study suggested that $-COO^-$ groups on HA form complexes at the surface of the minerals [125, 126]. The mechanisms such as hydrophobicity, van der Waals forces, and hydrogen bonding may also have an effect on sorption [127]. At high pH, HA molecules are ionized and more soluble than at low pH, where they become protonated and more hydrophobic. Another contributing factor influencing HA sorption is the electrostatic repulsion at higher pH, as both HA and iron oxides bear negative charge, leading to reduced sorption with increasing pH [128]. In acidic pH, electrostatic attraction leads to very high sorption, as in this condition, iron oxides possess positive zeta potential, whereas zeta potential of HA is negative.

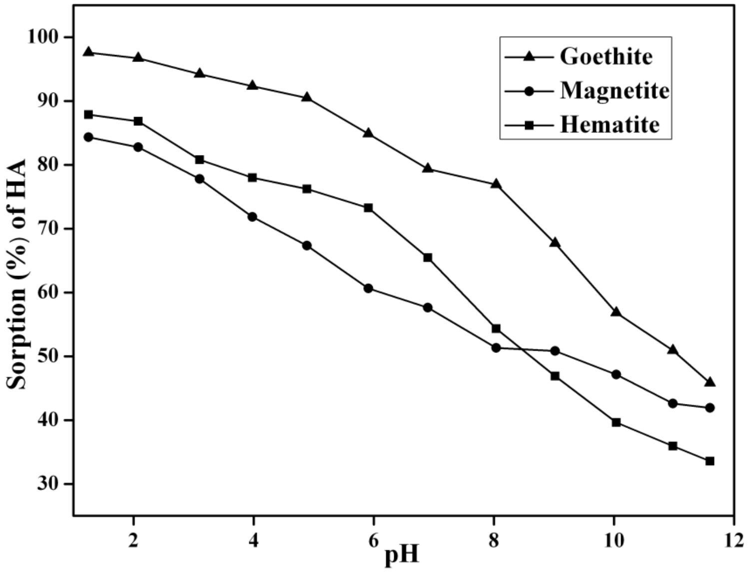

Figure 3.8: % of HA sorbed on iron oxides with variation of pH

3.3.3. Sorption behaviour of Nb and Pa on iron oxides

For the present work, polypropylene tubes were used and it was found that the sorption of Nb and Pa onto polypropylene tube were (2-5) % depending upon pH of the medium. The sorption data presented in this work was corrected for sorption on polypropylene container.

In general, the sorption of radionuclides on colloids is due to electrostatic interaction and surface complexation [2, 80, 93]. The higher the cation charge, the more strongly the cation is sorbed and the stronger the tendency of the cation to hydrolyze [129]. The pH region of the adsorption edge is usually more characteristic of the sorbing cation rather than of the sorbent material and relative placement of the adsorption edge for different metal ion is co related with the formation of hydrolysis species. The sorption of Nb and Pa on goethite, hematite, and magnetite in the presence and absence of HA, are shown in Figures 3.9 and 3.10 respectively. The sorption behaviour of Nb and Pa on iron oxides can be explained in terms of the species of Nb/Pa in solution and zeta potential of iron oxides. In aqueous solutions, oxygen containing species are formed because of their high ionic potential. The ionic species that exist in aqueous solutions are governed by the solution pH as well as the metal ion concentration. The point of zero charge (PZC) of goethite, hematite, and magnetite are 8.0, 6.9 and 6.5 respectively. High magnitude of zeta potential (+ve) of iron oxides and positively charged species of Nb/Pa results electrostatic repulsion upto pH 3 and hence the low sorption. Above pH 3, both Nb and Pa start forming neutral species which reduce the columbic repulsion, leading to increased sorption. The higher sorption between pH 6-9 can be explained in terms of surface complexation between surface hydroxyl group of iron oxides and the –OH group of the Nb/Pa oxo-hydroxy species. After pH 9, anionic species of both the elements become predominant and zeta potential of iron oxides also become negative. Thus electrostatic repulsion causes decrease in sorption after pH 9.

The percentage sorptions of Nb and Pa on magnetite are expected to be different to some extent compared to hematite and goethite, in view of higher solubility of magnetite in acidic region (pH 1-2) and due to the presence of Fe(II) site. In the present study it was observed that the sorption patterns of both Nb and Pa on magnetite are slightly lower compared to those in the other two oxides.

Nakata et al. didn’t find any change in oxidation state of Np(V) while getting sorbed onto Fe(II) containing minerals [130]. No significant difference was found in the removal of Np(V) by biotite/magnetite (Fe(II) containing mineral) and ferric oxide/hematite (Fe(III)) [131].

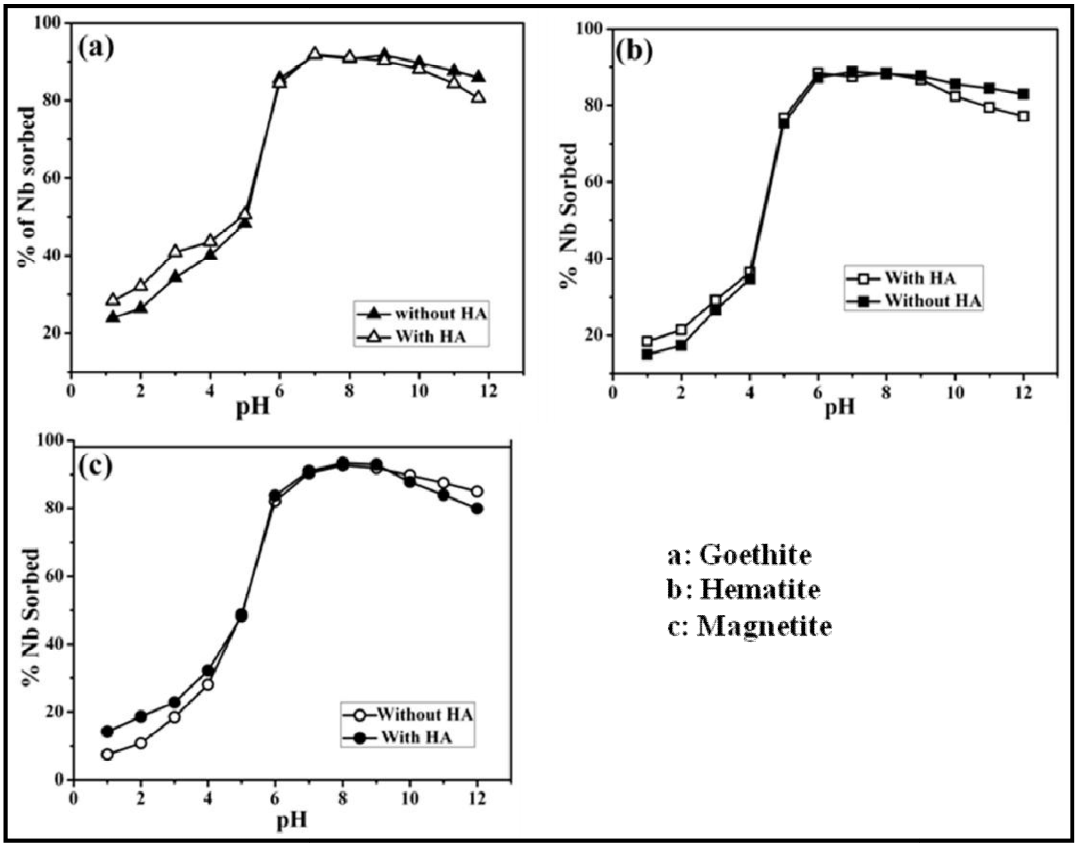

Figure 3.9: % of Nb sorbed on iron oxide (a) Goethite (b) Hematite (c) Magnetite in presence and absence of HA

Contradictory literatures are also available for the reduction of Np(V) to Np(IV) on magnetite interface under anaerobic condition. This conversion rate is faster than that by Fe(II) in homogeneous solution [132]. Similar results were reported in ORNL-5617 [133] where Np(V) was sorbed preferentially by Fe(II) containing sites, biotite, and pyrite on granite surface in aerated water. Thus, Fe(II) containing minerals catalyze and make the reduction process feasible. Again literature report showed that structural Fe(II) is a stronger reducing agent compared to aqueous Fe(II) (-0.771V). Peterson et al reported that the reduction potential of Fe(II) in magnetite had a range -0.65 to -0.34V [134]. White and Yee reported the range -0.55 to -0.34V for in Fe(II) silicate minerals [135]. These literature reports also support the special role of Fe(II) in Fe(II) containing minerals during sorption.

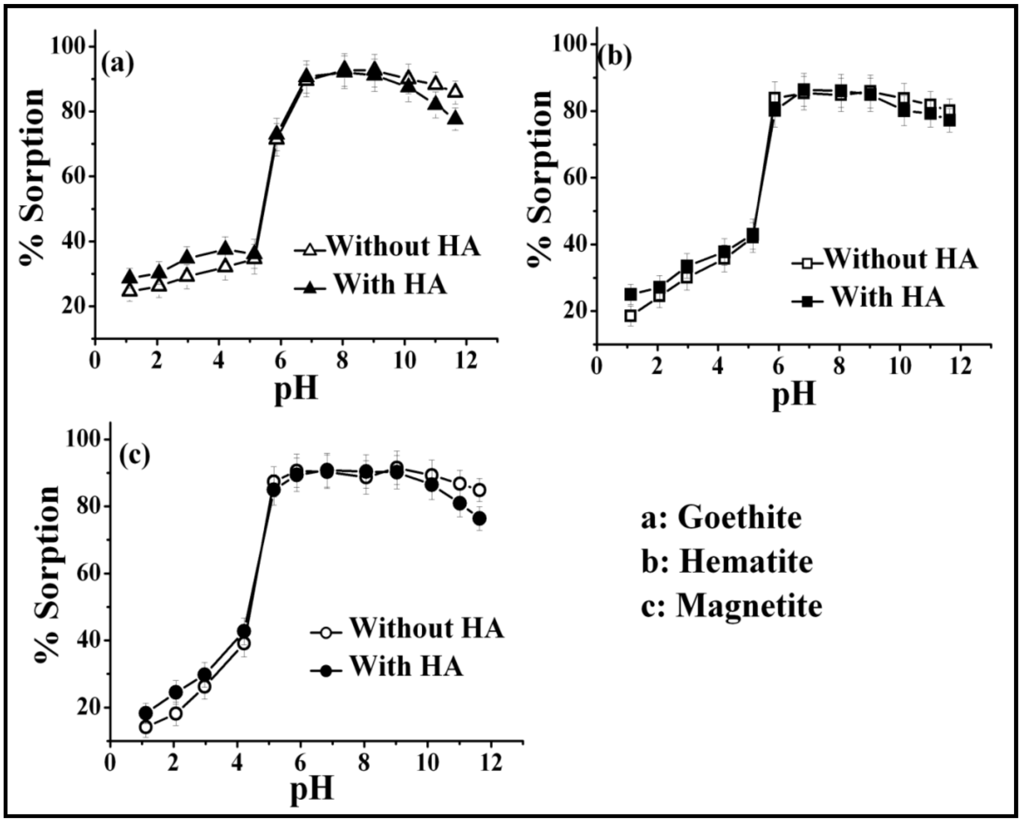

Figure 3.10: % of Pa sorbed on iron oxide (a) Goethite (b) Hematite (c) Magnetite

3.3.4. Electrochemical studies

The GCE surface was initially coated with 1:1 mixture of carbon black and synthesized magnetite and cyclic voltammetry (CV) (staring potential: 0.1V, switching potential: 1V) was performed in acetate buffer of pH 5.5 and repeated for another three times with the same surface (Figure 3.11). During anodic scanning oxidation peak was obtained around 0.72V while upon scanning in the reverse direction (cathodic) reduction peak around 0.52V was obtained. With repeated scanning the peak height of both the peaks were found to decrease gradually.

Literature reports suggest that Fe_3O_4 undergoes oxidation and reduction via liberation of Fe(II) into the aqueous solution. The electrochemical reactions of the bulk Fe_3O_4 was postulated in the following way [134, 136].

Oxidation:

$$3[Fe^{2+}Fe_2^{3+}]O_4 \rightarrow 4[Fe_2^{3+}]O_3 + Fe^{2+} + 2e^- \qquad 3.3$$

Reduction:

$$[Fe^{2+}Fe_2^{3+}]O_4 + 8H^+ + 2e^- \rightarrow 3Fe^{2+} + 4H_2O \qquad 3.4$$

During oxidation Fe_3O_4 gets converted into Fe_2O_3. The cathodic reaction results in the reductive dissolution of magnetite, the rate of which decreases with increasing pH. These may be the reason for the gradual decrease of the peak current of both the oxidation and reduction peak.

In order to check the electrochemical activity of Fe_2O_3, GCE was then coated with 1:1 mixture of carbon black and synthesized Fe_2O_3 and cyclic voltammetry was performed within the same potential window (staring potential: 1V, switching potential: 0.1V) under same electrolyte condition; Unlike the Fe_3O_4 coated electrode no redox peak was observed here (Figure 3.12). In case of Fe_2O_3 coated electrode, as Fe (III) only state of iron, it is obvious that there will not be any oxidation peak. Interestingly we did not find any reduction peak also in CV experiment within the same potential window.

Freshly prepared carbon black and Fe_3O_4 coated GCE was then dipped into 10ppm Nb(V) solution for 5 mint, washed in deionized water and then CV was performed in the same acetate buffer medium as before. Surprisingly redox peaks due to Fe^{2+}/Fe^{3+} system were not observed in this case (Figure 3.13) and this can happens only if Fe(II) is absent in Fe_3O_4 coated GCE or if the total Fe(II) has converted to Fe(III).

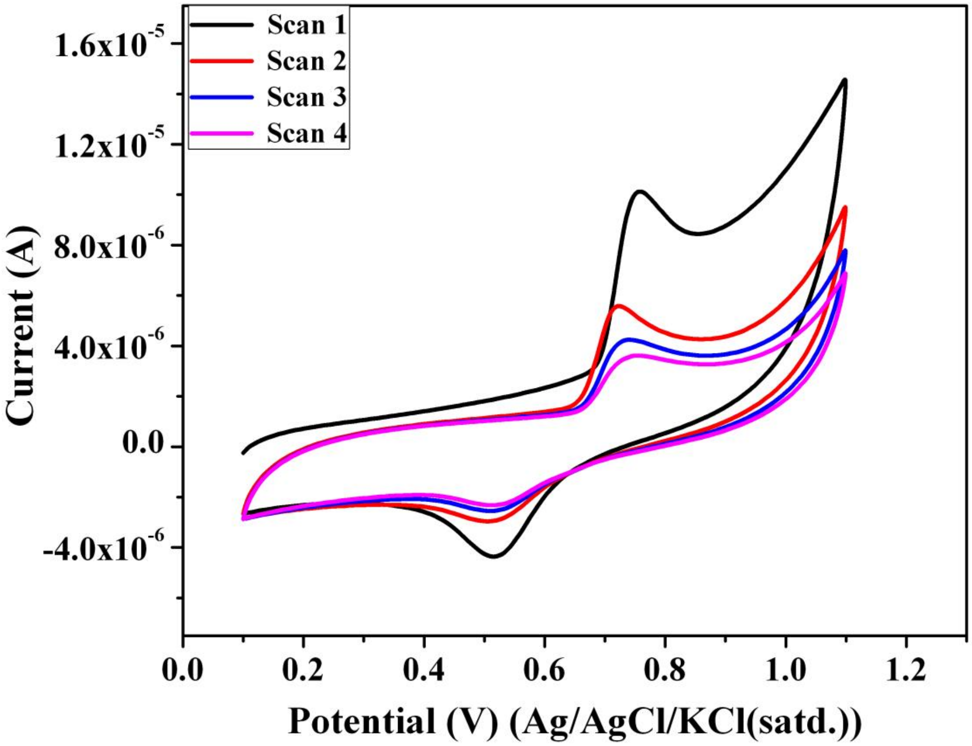

Figure 3.11: Consecutive CV of synthesized magnetite coated GCE

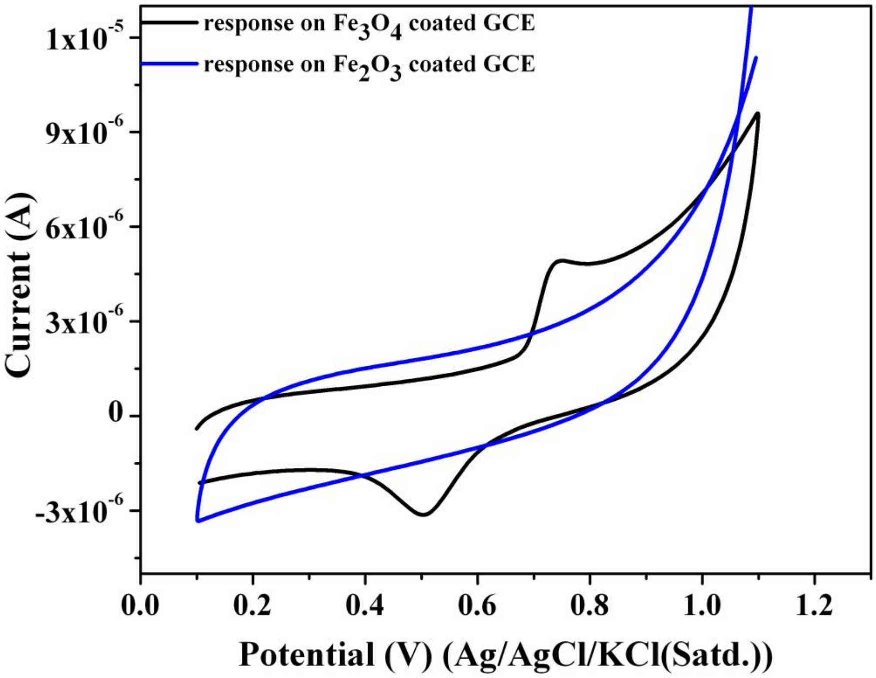

Figure 3.12: CV response of magnetite (Fe_3O_4) and hematite (Fe_2O_3) coated GCE

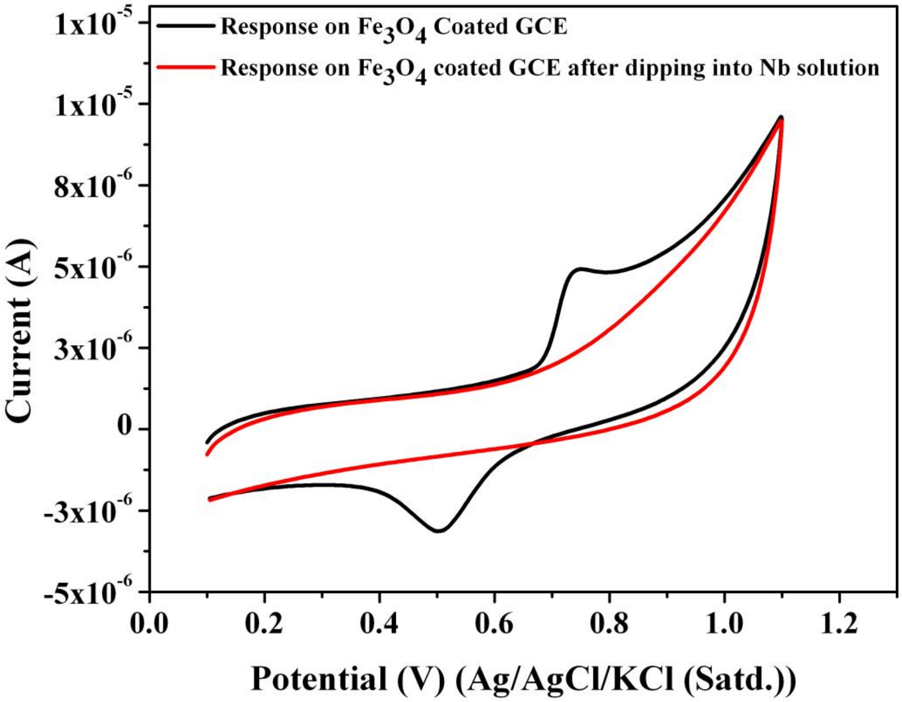

Figure 3.13: CV response of magnetite (Fe_3O_4) before and after equilibration with Nb(V) solution at pH 5.5 AcOH-NaOAc buffer

Since the electrode was dipped into the Nb(V) solution for 5 mint, free Nb(V) and Fe(II) of Fe_3O_4 coated GCE got enough time to undergo the redox reaction which resulted the reduction of Nb(V) to Nb(IV) and oxidation of Fe(II) to Fe(III). Therefore, initial Fe_3O_4 moieties are converted into Fe_2O_3 at the surface of the electrode which is often called mag-hematite as it is generated from magnetite.

3.3.5. Effect of HA on sorption behaviour of Nb and Pa on iron oxides

The sorption of Nb and Pa on iron oxides in presence of HA was different from that in its absence both in acidic and basic regions (Figure 3.9 & 3.10). Sorbed HA partially occupies sorption sites of the iron oxides, which may lead to a decrease in metal ion sorption. Again, dissolved HA can decrease sorption of metal ion to the solid phase by forming soluble metal complexes [12,137]. Considering the above fact, it is expected that HA may affect the metal cation binding to the solid phase both in acidic and basic pH conditions. At low pH, metal cations are weakly bound whereas humic substances are strongly sorbed by mineral surfaces [138, 139]. Contradictory results are also reported in literature about the sorption of metal ions in the acidic pH in presence of HA [140-142]. In the present case, sorption of Nb and Pa on iron oxides in the presence of HA increased in acidic pH. The plausible reason may be (i) complexation of Nb/Pa with HA sorbed on iron oxides, and (ii) sorption of HA on iron oxides reduced the magnitude of positive zeta potential, and consequently, the electrostatic repulsion.

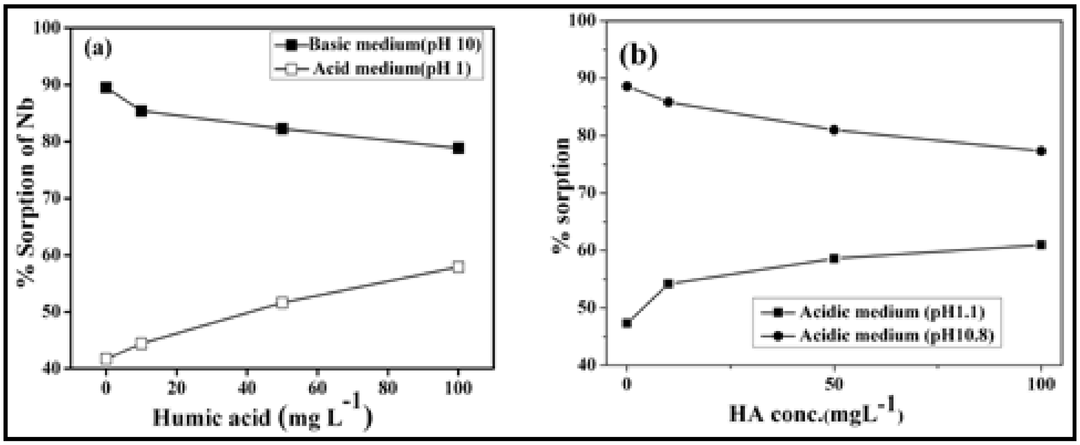

Figure 3.14: The effect of HA concentration in acidic medium (pH 1) and basic medium (pH 10) (a) Nb-hematite (b) Pa-Hematite

Again in basic pH, the sorption of Nb and Pa on iron oxides in presence HA was lower as compared to that in the absence of HA. Both Nb and Pa have strong complexation tendency with –COOH group of HA thus increase concentration of Nb/Pa in solutions or decrease the sorption on iron oxides in basic region.

The above observations were also confirmed from the sorption of Nb and Pa with varying HA concentration. The results showed the increasing trend of sorption in acidic region, and decreasing trend in basic region with increase in HA concentration (Figure 3.14).

3.3.6. Effect of equilibration time on sorption of Nb and Pa on iron oxide

The time dependent sorption of Nb and Pa on iron oxides in acidic and basic media is shown in Figures 15 and 16 respectively. The sorption kinetics is governed by surface area, porosity, and numbers and types of surface functional groups of the oxides [143]. Sorption kinetics became an important tool to determine the sorption mechanism i.e, the sorption is physisorption or chemisorption. The sorption process follows pseudo first order kinetics, corresponds to physisorption, diffusion is the rate limiting step and rate doesn't dependent on both the reactant. The sorption process follows pseudo second order kinetics, corresponds to chemisorption, involve valency forces through sharing or exchange of electron between adsorbent and adsorbate [144].

The kinetic modeling of the time dependent sorption data was studied using Lagergren's pseudo first order [145] and Ho's pseudo second order model [146]. The Lagergren equation based on pseudo-first-order adsorption kinetics is expressed as follows:

$$\frac{dC}{dt} = k_1(C_e - C_t) \qquad (3.5)$$

Where, C_e is the amount of adsorbate at equilibrium (μg mg^{-1}), C_t is the adsorbate amount at time t (μg mg^{-1}) and k_1 is the pseudo-first-order rate constant (h^{-1}). The equation simplifies to

$$\mathrm{Log}\,(\mathrm{C_e} - \mathrm{C_t}) = \mathrm{Log}\mathrm{C_e} - \frac{\mathrm{k_1 t}}{2.30\ 3} \qquad (3.6)$$

Ho's pseudo second order model expressed as

$$\frac{\mathrm{dC}}{\mathrm{dt}} = \mathrm{k_2}(C_e - C_t)^2 \qquad (3.7)$$

After integration from t=0 to t= t, the equation simplifies to

$$\frac{\mathrm{t}}{\mathrm{C_t}} = \frac{1}{\mathrm{k_2 C_e^2}} + \frac{\mathrm{t}}{\mathrm{C_e}} \qquad (3.8)$$

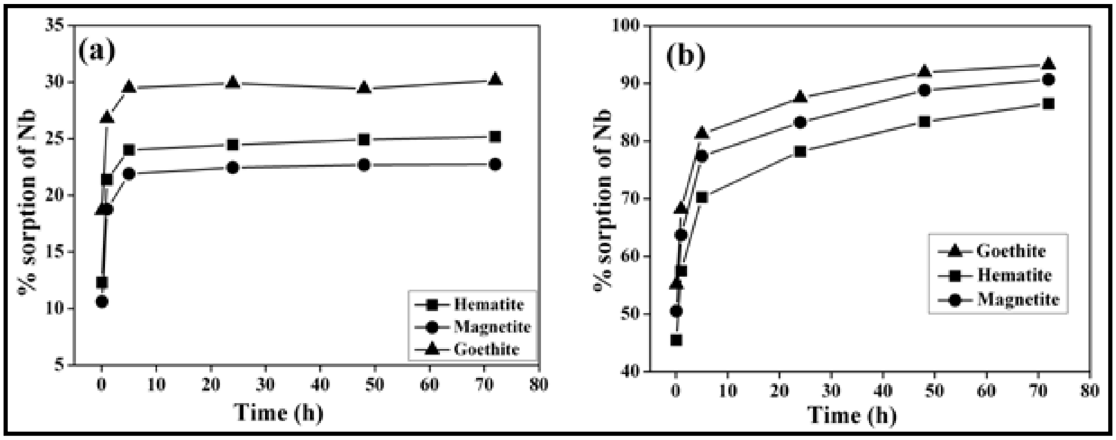

Figure 3.15: Sorption Nb on iron oxides as function of time at (a) pH 1 and at (b) pH 10

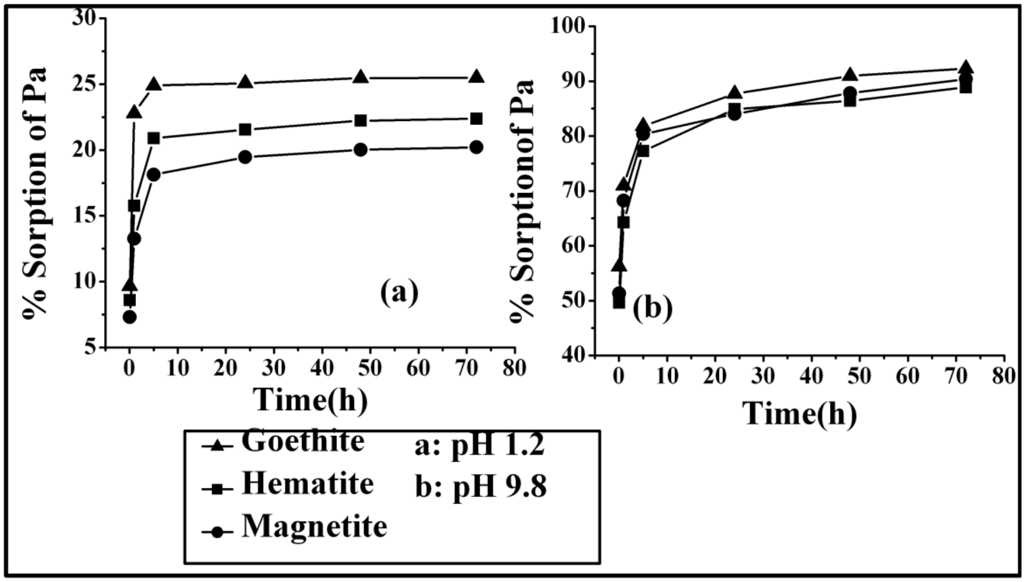

Figure 3.16: Sorption Pa on iron oxides as function of time at pH 1 and pH 10

The kinetics for the sorption of Nb/Pa on iron oxides in acidic pH is better fitted with pseudo first order rate equation. This suggests that the sorption of Nb/Pa on iron oxide in acidic pH mainly occurred through physisorption mechanism (Figure 17 & 18). The sorption kinetics of Nb and Pa on iron oxides in basic medium (pH 10) found to follow the pseudo second order kinetics (Figure 19 & 20). So the mechanism of sorption in basic medium corresponds to chemisorption.

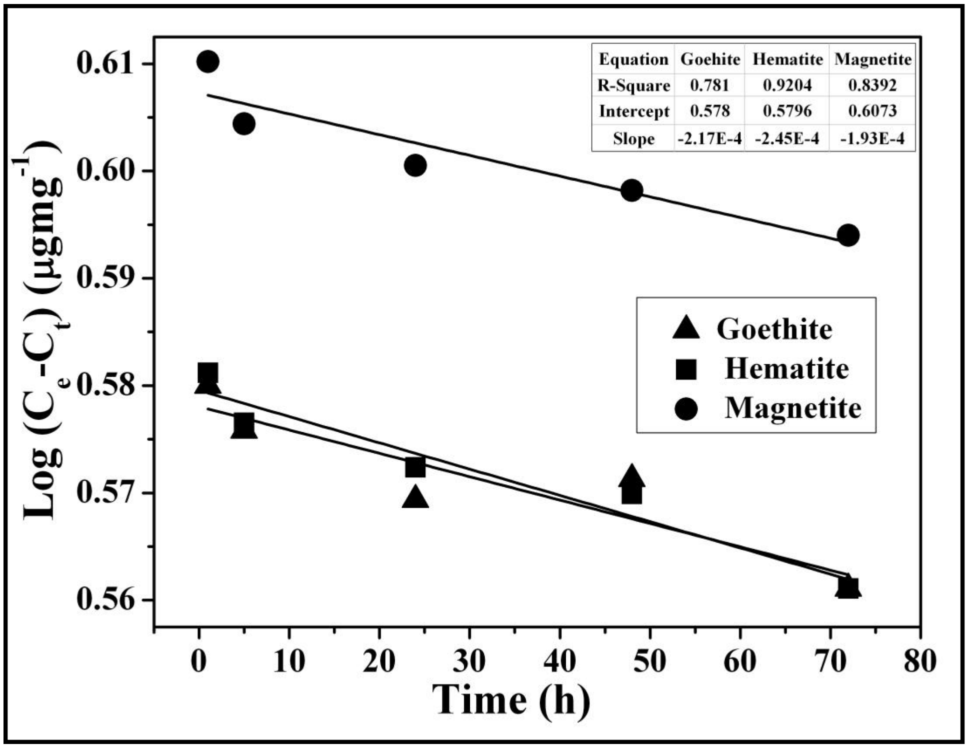

Equation	Goehite	Hematite	Magnetite
R-Square	0.781	0.9204	0.8392
Intercept	0.578	0.5796	0.6073
Slope	-2.17E-4	-2.45E-4	-1.93E-4

Figure 3.17: Pseudo first order fitting in acidic pH (Nb-iron oxide)

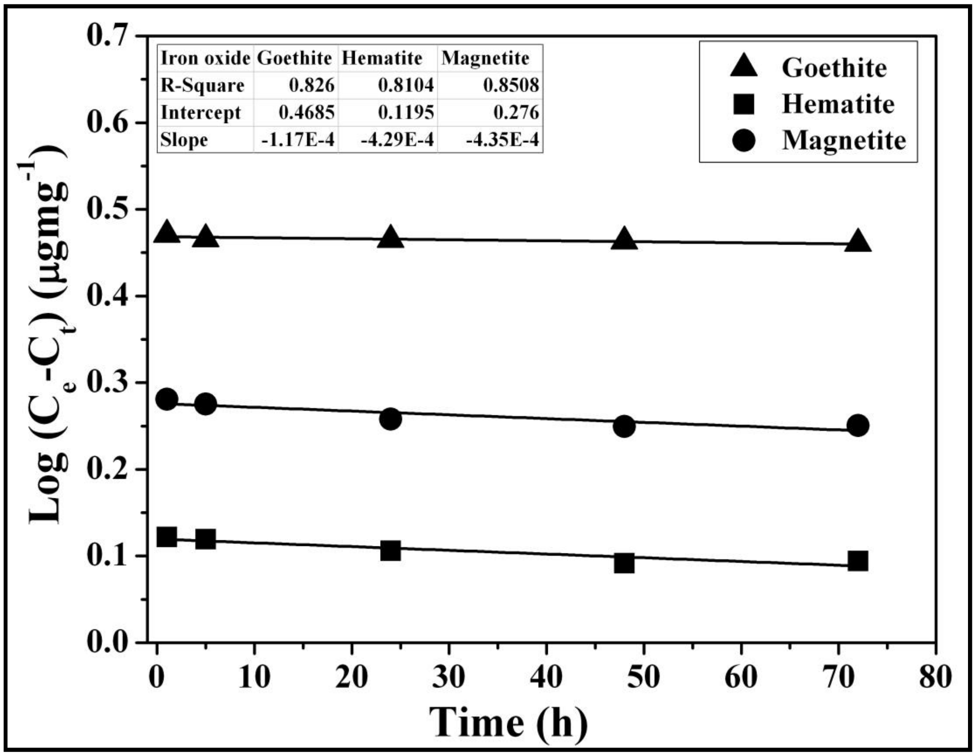

Iron oxide	Goethite	Hematite	Magnetite
R-Square	0.826	0.8104	0.8508
Intercept	0.4685	0.1195	0.276
Slope	-1.17E-4	-4.29E-4	-4.35E-4

Figure 3.18: Pseudo first order fitting in acidic pH (Pa-iron oxide)

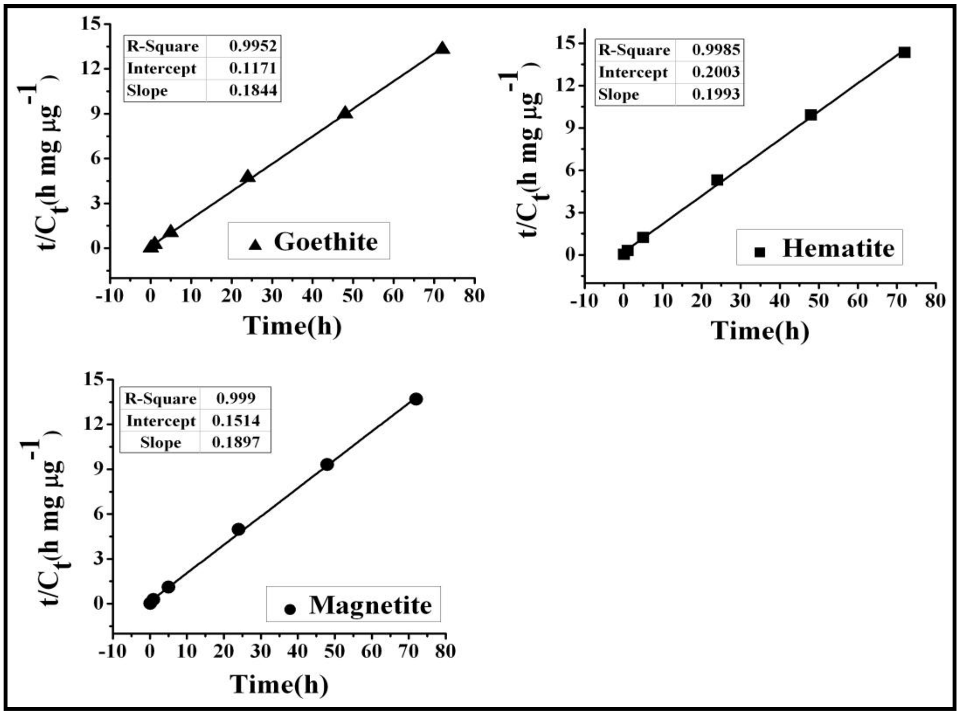

Figure 3.19: Pseudo second order fitting at pH 10 (Nb-iron oxides)

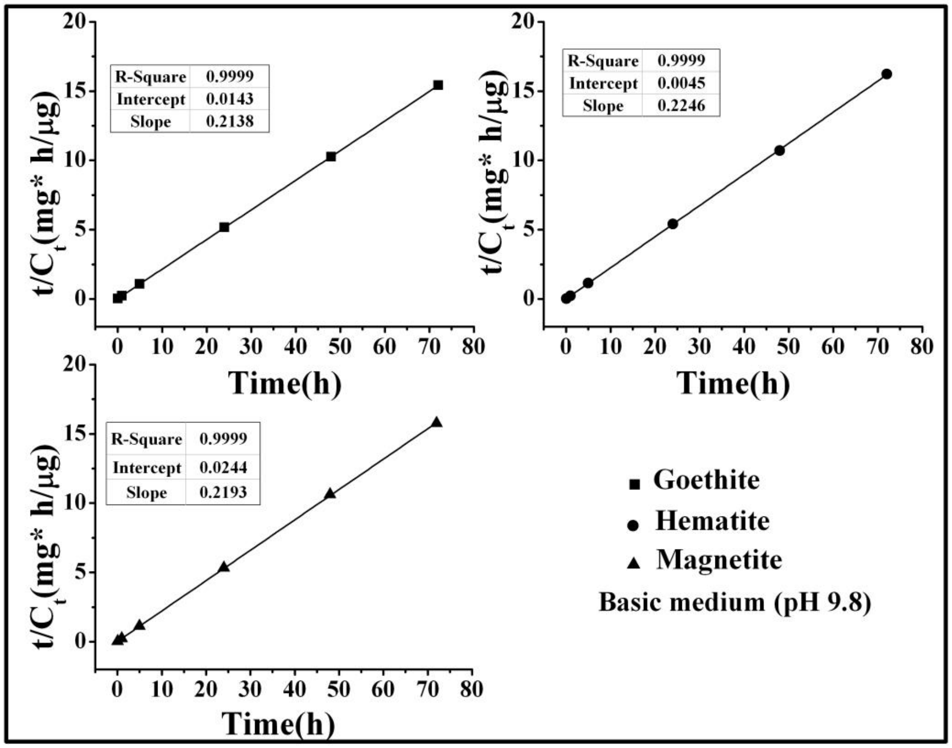

Figure 3.20: Pseudo second order fitting at pH 10 (Pa-iron oxides)

Intra particle diffusion of solute in adsorbent can be expressed by Weber- Morris model equation as below

$$q_t = k_{id}\, t^{0.5} + A \qquad (3.9)$$

k_{id} is the intra particle diffusion constant that can be obtained from the q_t vs $t^{0.5}$ plot and A is the intercept of the plot. The model assumes that if the plot stands straight line and passes through the origin then sorption is pore diffusion controlled and solute ions diffuse within the pores of the adsorbent material. If plot is non linear, then film diffusion process considered to be the rate limiting [147, 148]. In present study, the plots obtained for intra particle diffusion for the sorption of Nb/Pa on different iron oxides in acidic medium (pH 1.2), seem to exhibit two straight lines which demonstrate about the involvement of two stage adsorption. The intra-particle diffusion curve appears to be divided into two distinct linear regions (Figures 3.21 and 3.22). The first curve that obtained during the initial time period of 5 to 60 mint. indicates external mass transfer which involves movement of Nb/Pa from liquid phase to the solid interface. After 60 mint the second line indicates the gradual diffusion of the metal ions to the pores of iron oxides.

Again, the sorption kinetics both in acidic and basic medium at different temperature, the activation energy of the sorption process can be determined using the Arrhenius equation

$$k = Ae^{-\frac{E_a}{RT}} \qquad (3.10)$$

where k, A, E_a, R, and T are rate constant, frequency factor, activation energy, universal gas constant, and absolute temperature respectively.

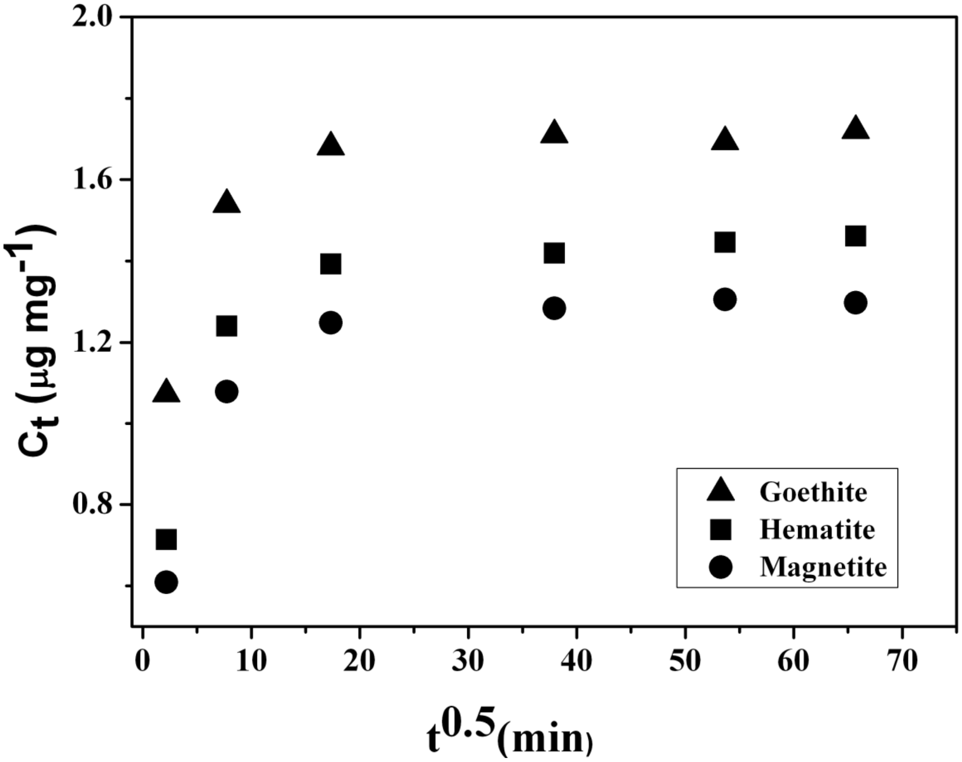

Figure 3.21: Intra particle diffusion plots: Nb-iron oxides in acidic medium (pH 1)

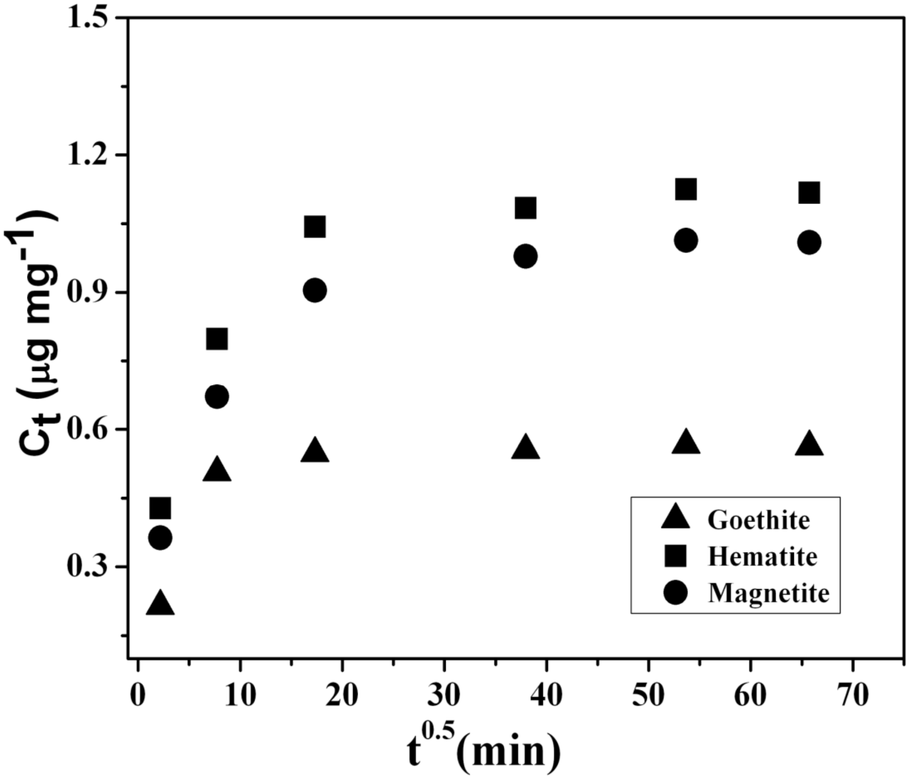

Figure 3.22: Intra particle diffusion plots: Pa- iron oxides in acidic medium (pH 1)

The activation energy of the sorption reaction was determined using rate constant values of two different temperatures. The values of the activation energy are given in Table 3.2 & 3.3. From the activation energy data, it is clear that minimum energy is required for the sorption both for Nb and Pa on iron oxides in acidic pH. In basic medium, the activation energy for the sorption process is negative and that is why, it is not mentioned in Table 3.2 and 3.3. This indicates, in basic medium, the sorption reactions do not require any activation energy.

The Sticking probability (S^*) is the chance of adsorption per molecular collision with the adsorbent surface i.e, it is a function of adsorbate/adsorbent system. It depends on of the temperature and the surface structure of the adsorbent [149]. It can be expressed in terms of modified Arrhenius equation [150, 151]

$$S^* = (1-\theta)e^{-\frac{E_a}{RT}} \tag{3.11}$$

where θ indicates the surface coverage factor, and other terms have been explained earlier. θ is given by the equation

$$\theta = \frac{(C_0 - C_e)}{C_0} \tag{3.12}$$

where C_0 and C_e are the initial and equilibrium concentrations of adsorbate in the solution respectively. The sticking probability can be determined from the intercept, $\log(S^*)$, of the $\log(1-\theta)$ vs. 1/T plot. The values of sticking probability for both Nb and Pa with goethite, hematite and magnetite are given in the following Table 3.2 & 3.3. As the value of S^* are near to zero, we can conclude that the sorption mechanism is chemisorption [152].

Table 3.2: Activation energy and sticking probability values (Nb-iron oxides)

Niobium	**Goethite**	**Hematite**	**Magnetite**
Condition	Activation energy(kJ M^{-1})		
pH 1	11.58	15.86	39.65
	Sticking probability (S^*)		
pH 1	0.1494	0.2260	0.0587
pH 10	0.001	0.0008	0.0003

Table 3.3: Activation energy and sticking probability values (Pa-iron oxides)

[Note: Negative activation energy in basic pH not included in the table]

Protactinium	**Goethite**	**Hematite**	**Magnetite**
Condition	Activation energy(kJ M^{-1})		
pH 1	16.65	19.03	44.41
	Sticking probability (S^*)		
pH 1	0.2427	0.1975	0.0964
pH 10	0.0002	0.0009	0.0007

3.3.7. Sorption study of Nb/Pa on inert sorbent (XAD resin)

Percentage sorption of Nb/Pa on XAD-4 at pH 1, pH 6 and pH 10 are given in the following Table 3.4. The sorption values are slightly higher than those for polypropylene tube as discussed in **section 3.3.3.** XAD-4 does not contain any functional group and has very large surface area (725 m^2 g^{-1}). The sorption of Nb/Pa has resemblance with the low sorption of both the element on iron oxides and this indirectly proves that the sorptions of both Nb and Pa on iron oxides are physisorption type phenomena at pH 1. The sorptions of both Nb and

Pa on iron oxides are very high compared to their sorption on XAD-4 at pH 6 and 10. This indicates the sorption of Nb/Pa at pH 6 and 10 supposed to follow chemisorption mechanism.

Table 3. 4: % sorption of Nb and Pa on XAD-4 at pH 1, pH 6 and pH 10

pH	% of Nb sorbed on XAD-4	% of Pa sorbed on XAD-4
1	3.9	7
6	4.8	12
10	6.9	11

The Fourier transform-infrared spectroscopy (FTIR) and Raman spectroscopic studies on Nb-iron oxides system at different pH were also carried out but it did not provide any useful information as the concentrations of Nb (~10^{-8} M) was close to the detection limit of the technique. It is known that the speciation of a hydrolysable metal ion is solely governed by its concentration and the pH of the solution. Hence, inferences drawn by carrying out spectroscopic studies at higher concentration of Nb will not be valid at very low concentrations.

3.3.8. Dissolution of iron oxides

The dissolution study showed that the Fe concentrations in supernatant in case of goethite and hematite were negligible throughout the pH range studied, whereas 3 % magnetite got dissolved in acidic pH (Figure 3.23).

The plot of Fe concentration (μg mL^{-1}) in supernatant vs. pH (Figure 3.23) showed that all the three iron oxides were stable in basic region whereas goethite and hematite were much more stable compared to magnetite in acidic region [111, 153]. The lesser stability of magnetite in acidic region may be due to presence of Fe(II) in its structure.

From the above study, it is clear that sorption would not have been influenced by the dissolution of iron oxides even in acidic pH and very large contact time for goethite and hematite but mildly affect the sorption behaviour in acidic medium (pH ≤2) in the case of magnetite.

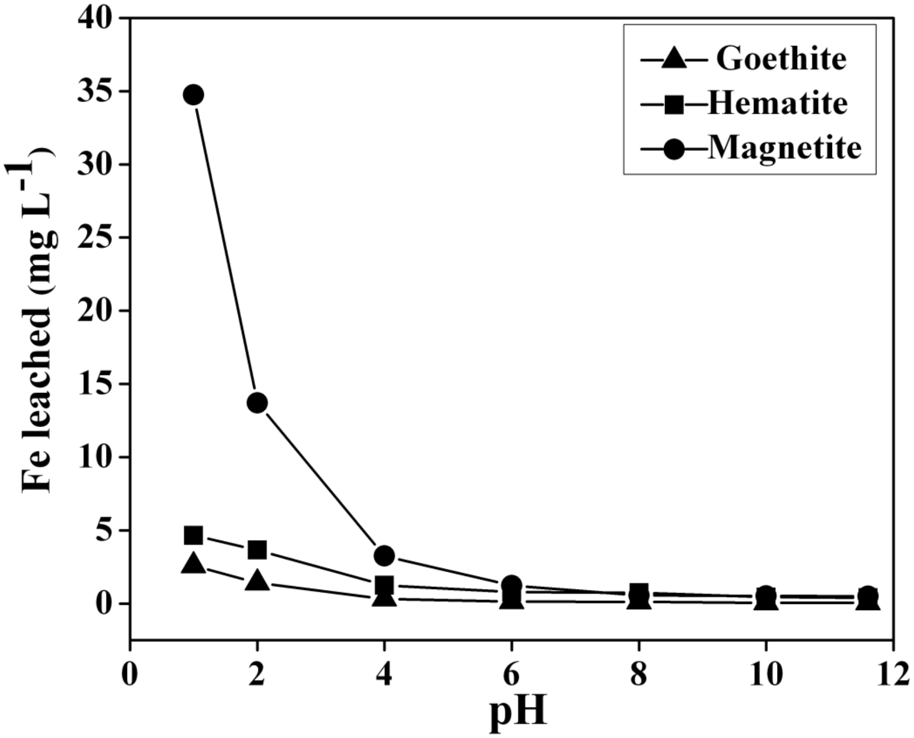

Figure 3.23: Dissolution of iron oxides with variation of pH

3.4. Conclusion

The sorption of Nb/Pa on all the three iron oxides was low (~ 10-20 %) at pH 1, increased to ~ 90% at pH 8 and decreased marginally above pH 9. HA increases the sorption at pH 1 where as decreases the sorption at pH 10. In acidic medium, the sorption decreases with increase in ionic strength, whereas in basic medium the effect is negligible. The sorption followed pseudo-first order-order kinetics at acidic pH but pseudo second order in basic pH conditions. The sticking probability values indicate that the sorption follow physisorption mechanism at acidic pH and chemisorption mechanism at basic pH. The sorption is not influenced by the dissolution of hematite and goethite but do mildly in case of magnetite. This study is important to understand the probable migration of ^{94}Nb and ^{231}Pa during underground storage of radioactive waste.

Chapter IV

Sorption of ^{94}Nb and ^{231}Pa on Manganese dioxide

4.1. Introduction

The migration behaviour of radioisotopes released to the environments has to be known for trustworthy, long term assessment of nuclear waste repository. Repositories for nuclear waste should meet the norm that radionuclides from repository should not come into the human habitation in thousand years. Their presence in upper layer of soil and sediment are two main sources for their introduction to the food chain. If the radionuclide contamination occurs in water, it will have nasty effects because of both chemical as well as radiological toxicities.

The migration of the radionuclides depend on solubility of radionuclides in underground waters, complexation with anions present in aqueous stream, sorption on components of engineered and geochemical barriers (rocks and minerals) and the colloid formation (pseudo or true). Among all of these parameters, sorption of radionuclides at the water rock interface retards the migration in natural systems. Thus, the factors that administer the radionuclides sorption on mineral surfaces have to be studied thoroughly [154]

A lot of work has been carried out to understand the sorption of various radionuclides on different minerals, which includes hydrous oxides of Fe [155-157], Si and Al [158], clay [159]. According to most of the existing literature, tri- and tetravalent actinides did not impart hazardous effects, as they have high tendency to get sorbed onto the components used for their isolation and host rocks and owing their extremely low solubility [154]. However, recent studies suggest the possibility of colloidal migration of these radionuclides in groundwater [32,160,161]. Several evidences are also available regarding fast and long distant migration of the radionuclides in the ground water system [7,76]. The reports indicate that colloids dispersed in groundwater act as an auxiliary phase and enhance the transport of radionuclides. A three phase model, consisting of a stationary phase, a mobile phase and colloids (intrinsic or pseudo) dispersed in mobile phase was introduced and able to explain the migration of radionuclides satisfactorily [21, 32, 76]. So in this context the sorption study of radionuclides on naturally occurring colloids (pseudo) in aqueous stream became relevant and the need of the modern era, as the atomic power production is increasing day by day.

Pyrolusite is the most common and most stable oxide of manganese, present in nature. Because of its high surface area and low isoelectric point, the radionuclides easily get sorbed onto pyrolusite surface even at acidic pH conditions. These features make pyrolusite very strong contender to make colloid facilitate transport of radionuclides although having much lesser abundance in natural aquatic system, compared to other mineral oxides like iron oxides. Pyrolusite ubiquitously present in clays, soils and sediments which are the most prominent absorber of the radionuclides from aqueous stream. The sorption study of several radionuclides like ^{90}Sr, ^{137}Cs, ^{60}Co, U, Pu, Np, Am, Cm and Th on manganese dioxide or manganese dioxide based different ores are reported in the literature [162-168]. Manganese oxides are considered as the foremost scavenger of the environmental contaminants. It is observed that the radionuclides, adsorbed strongly in the soil, are initially contained by manganese oxide present in the soil. For this reasons, it is proposed to mix finely grounded manganese oxide with high level waste before vitrification [169]. Apart from the sorption of radionuclides, manganese based ore also facilitate the migration of radionuclides or heavy metals. Under anaerobic conditions, manganese dissolves as Mn(II) hydroxide and then precipitates as oxide of higher oxidation state under aerobic condition. This phenomenon plays an important role in the transportation of radionuclides and heavy metals from anaerobic to aerobic region in geosphere [170].

The most common natural organic ligand present along with inorganic anions in aquatic system, is humic acid (HA). Presence of HA in ground water can alter the sorption as well as migration behaviour of radionuclides either by complexing with the radionuclides or by changing their oxidation states. It is also reported that HA itself get sorbed onto colloid surfaces and thus affect the radionuclides sorption on colloid surfaces [11, 171].

The protocols for the management of discharged Zr-Nb pressure tubes from Pressurized Heavy Water Reactor (PHWR) is to store in deep tile holes with concrete caps. In present study, we are dealing with ^{94}Nb, a long lived radioisotope (half-life: 2.03 x 10^4 y), which generates from ^{93}Nb stable isotope during neutron irradiation of Zr-Nb pressure tube or cladding material. ^{231}Pa is generated as the byproduct during production of fissile ^{233}U from ^{232}Th upon irradiation by neutron in nuclear reactor. ^{231}Pa, a long lived (half-life: 3.27 x 10^4 y), alpha emitting isotope which is present in high level liquid waste after extraction of ^{233}U from irradiated Thoria.

Here we report the sorption phenomenon of niobium (Nb) and protactinium (Pa) on laboratory synthesized manganese dioxide and the detailed investigation regarding the effect of different physico-chemical parameters like pH, ionic strength, equilibration time, humic acid and temperature on sorption.

4.2. Experimental

4.2.1. Chemical reagents

Sodium salt of humic acid (Sigma Aldrich), Sodium hydroxide (AR, Thomas baker), Sodium perchlorate (Sigma Aldrich), AR grade Manganese nitrate (S D Fine Chem), Extra pure AR Acetone (Sisco Research laboratory) and AR grade Perchloric acid (Otto Chemie Pvt. Ltd.) were used in the present study.

4.2.2. Preparation of manganese dioxide

About 100 g of manganous nitrate ($Mn(NO_3)_2$) was dissolved in 250 mL of deionized water in 500 mL beaker. Then the solution was evaporated on a hot plate near to dryness with continuous stirring, which was resulted in the formation of thick blackish solution. The blackish solution was then transferred into a silica crucible and then heated in a muffle furnace at 180°C for 48 h. Then the black crystalline material was ground and washed with deionized water. Finally the black powder is heated for another 24 h at 102°C in an oven for the removal of water [172].

4.2.3. Characterization of manganese dioxide

4.2.3.1. X-Ray diffraction (XRD)

X-ray diffraction pattern of the synthesized manganese oxide was recorded using powder X-ray diffractometer (rotating anode, Rigaku, Japan) utilizing CuKα (λ=1.5406 and 1.5444 Å) radiation. The angle range was 10 - 70° between which diffraction data were collected with a step width of 0.02° and time 5 s.

4.2.3.2. Fourier transformed Infra red (FTIR)

FTIR of the sample was carried out using a Tensor II FTIR system from Bruker. The requisite amount of manganese dioxide was mixed with KBr and then pellet was prepared using hydraulic press. The spectrum of the sample-KBr pellet was recorded in transmission mode.

4.2.3.3. Surface area measurement

Specific surface area of manganese dioxide was measured using single point BET (Brunauer–Emmett–Teller) surface area analyzer (BARC make). The method is based on the adsorption and desorption of nitrogen gas on sample at liquid nitrogen and room temperature respectively and subsequent determination of the desorbed nitrogen gas using thermal conductivity detector.

4.2.3.4. Scanning electron microscopy (SEM)

Scanning electron microscope coupled with energy dispersive X-Ray spectrometry (SEM-EDS, Instrument Model No. VEGA MV 2300T) was used to obtain the surface morphology of the synthesized manganese oxide.

4.2.3.5. Zeta potential and particle size measurement

Particle size and Zeta potential of the oxide were measured using the Litesizer^{TM}500, Anton-Paar instrument. Zeta potential measurement is based on the electrophoretic light scattering (ELS), related to the speed of the particle under electric field which is directly proportional to the surface charge of the particle or zeta potential. Particle size was measured by Dynamic Light Scattering (DLS) where the measurement of random motion of the particle is measured which directly associated with the particle size.

4.2.4. Batch sorption experiments

4.2.4.1. Binary sorption (HA - manganese dioxide)

Before studying the sorption of Nb and Pa on manganese dioxide, we need to study the sorption behaviour of humic acid on manganese oxide. For that, we have prepared a set of purified humic acid solution of concentration 0.5-15 mg L^{-1} in 0.05M $NaClO_4$ medium and UV-Vis spectrophotometric measurement (V 530, Jasco) was carried out to obtain the calibration plot.

Afterwards another set of humic acid solutions of known concentration (15 mg L^{-1}) were prepared in the same medium mentioned above and 50 mg of manganese dioxide was added to each of the solutions. pH of the solutions were adjusted between 1 to 12 using dilute $NaOH/HClO_4$ and measured using pH meter (Oakton, pH700, USA) calibrated using buffer solutions of pH 4, 7 and 9. Then solutions were equilibrated for 48 h and followed by centrifugation for 1 h at 4000 rpm. The concentrations of humic acid in supernatant solutions were determined using UV-Vis spectrophotometer and hence the percentage sorption of HA on manganese dioxide was calculated.

4.2.4.2. Binary sorption (Nb/Pa - manganese dioxide)

Sorption of Nb and Pa on manganese oxide was carried out separately using ^{94}Nb and ^{231}Pa radiotracers having concentrations $2.2\mathrm{x}10^{-7}$ M and $9.6\mathrm{x}10^{-6}$ M respectively. 50 mg of manganese oxide was taken separately in 60 mL polypropylene containers (Tarson) containing 25 mL solution of ionic strength 0.05 M $NaClO_4$. About 100µL of the tracer solution was added to each of the set and pH adjustment was carried out. The experiments were performed under ambient condition at 25^{o} C and rests of the experimental parameters were same as mentioned above. The activities in initial solutions and in supernatants (solution after centrifugation) were measured using High Purity Germanium (HPGe) detector (Canberra, France) coupled with 8k channel analyzer (Relative efficiency: 30%; Resolution: 1.9 keV at 1332 keV of ^{60}Co). The activity corresponding to 702.7 keV gamma ray of ^{94}Nb and 283.7 keV gamma of ^{231}Pa were utilized to obtain the percentage sorption of Nb and Pa on manganese dioxide using the following equation 4.1.

$$\%\,\mathrm{Sorption} = \frac{(\mathrm{A_i}-\mathrm{A_f})}{\mathrm{A_i}}\,\mathrm{X}\,100 \tag{4.1}$$

Where A_i and A_f are the activities of ^{94}Nb/^{231}Pa in initial solution and in the supernatant after phase separation.

4.2.4.3. Ternary sorption (Nb/Pa - manganese dioxide - HA)

Ternary sorption experiment is similar to that of the process described in the section 4.4.2 and the only difference is, the sorption experiments were carried out in the presence of humic acid. For better understanding of the effect of humic acid on sorption, humic acid concentration was varied from 5 mg L^{-1} to 200 mg L^{-1}, both in acidic (pH 1) and basic medium (pH 9).

4.2.5. Effect of ionic strength, temperature and equilibration time

The effect of ionic strength on the sorption of Nb and Pa on manganese dioxide was studied in the range of 0.01 M to 1.0 M $NaClO_4$. Similarly the effect of equilibration time on sorption was studied for time intervals of 1 h, 5 h, 10 h and 20 h to understand the kinetics of the sorption process. The temperature effect was also studied by carrying out sorption experiment at 5°C, 25°C, 50°C and 75°C. The distribution ratio (k_d) was obtained using the equation 4.2. All the above three sets of experiments were performed both in acidic (pH 1) and basic (pH 9) medium.

$$k_d = \frac{(A_i - A_f)}{A_f} \text{ X } \frac{V}{m} \qquad (4.2)$$

Where m is the mass (mg) of manganese dioxide and V is the total volume (mL) of the solution.

4.3. Results and discussion

4.3.1. Characterization of manganese dioxide

The XRD pattern of the laboratory synthesized manganese dioxide is shown in Figure 4.1. The XRD peaks are well matched with the ICDD diffraction pattern of pyrolusite or β-MnO_2. FTIR spectrum Figure 4.2 data is in accordance with the literature reported data for pyrolusite [173]. The specific surface area of the oxide is about $9m^2g^{-1}$.The hydrodynamic particle size is in the range 410-650 nm. SEM image given in Figure 4.3 shows the surface morphology of manganese dioxide. The zeta potential of manganese dioxide was measured in the pH range of 1 to 12 and it is observed that the point of zero charge (PZC) is about pH 4 which is in accordance with literature [174]. Above pH 4, zeta potential becomes negative and the magnitude increases with increase in pH of the medium. At pH 1, the negative zeta potential of HA may be because of the partial dissociation of carboxylic groups.

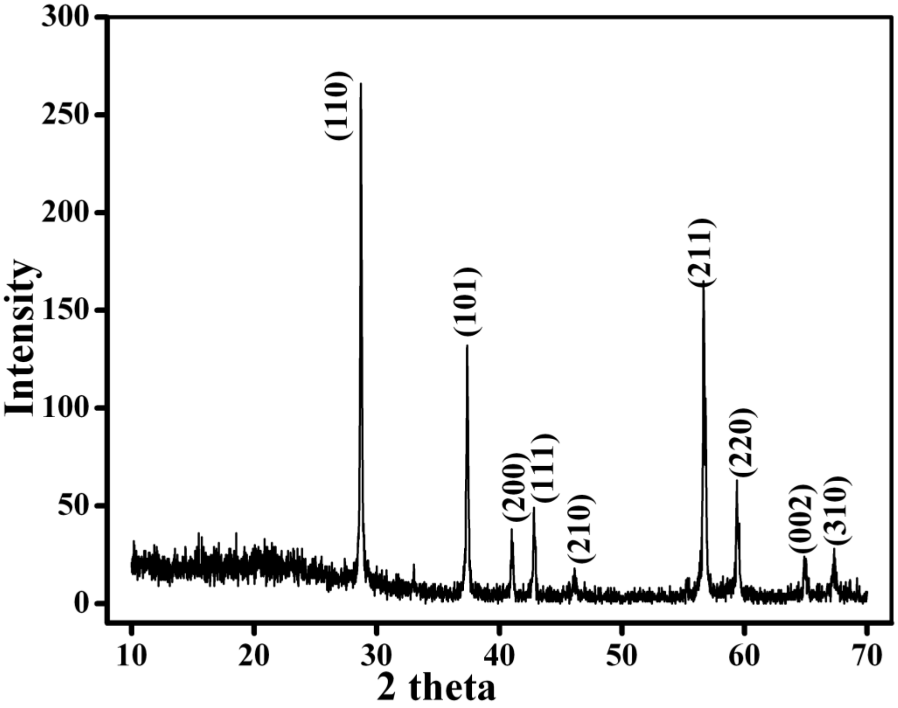

Figure 4.1: XRD pattern of manganese dioxide

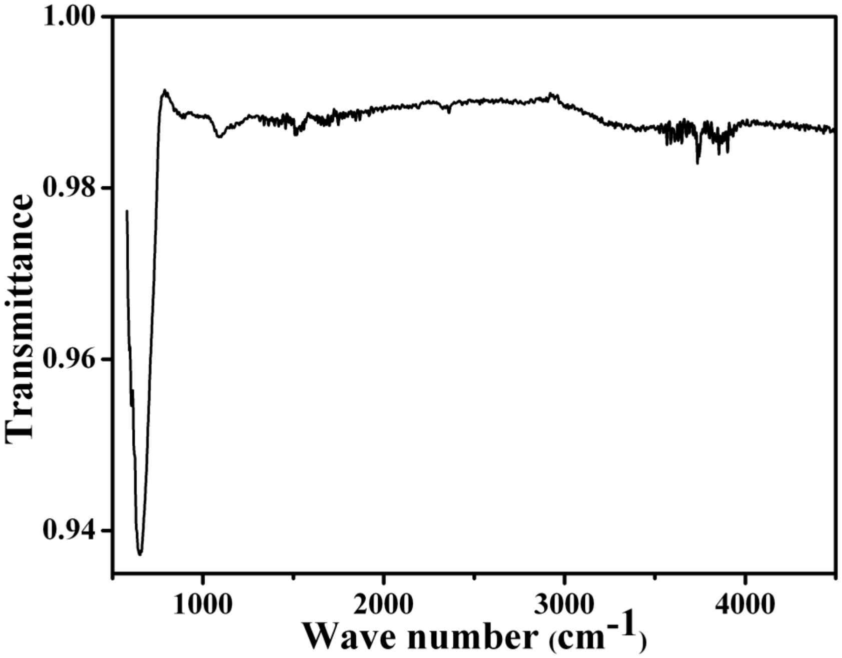

Figure 4.2: FTIR spectrum of manganese dioxide

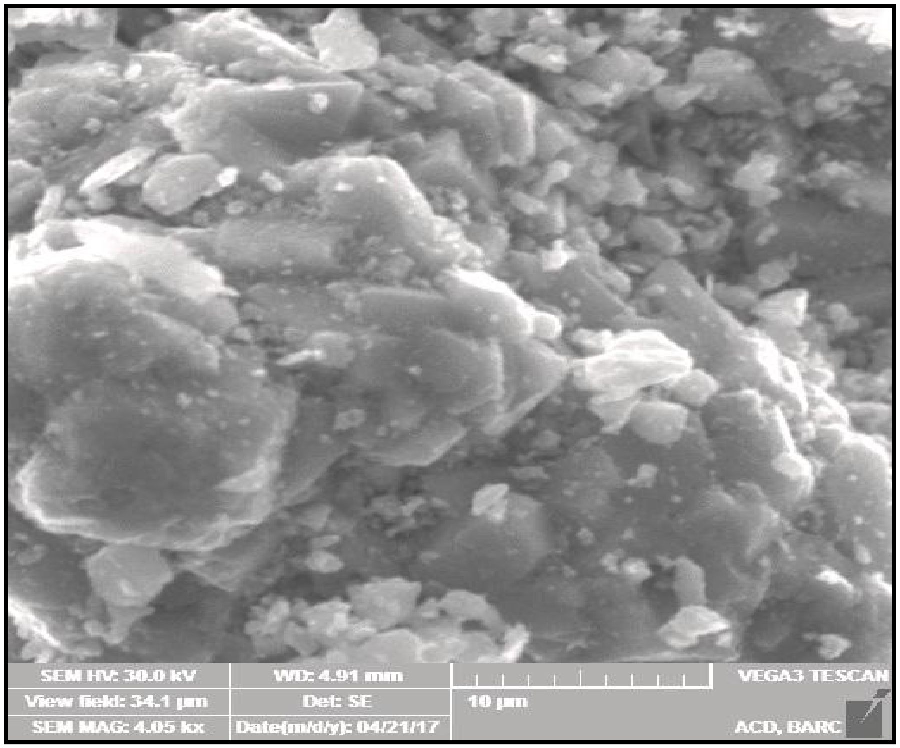

Figure 4.3: SEM image of synthesized manganese dioxide

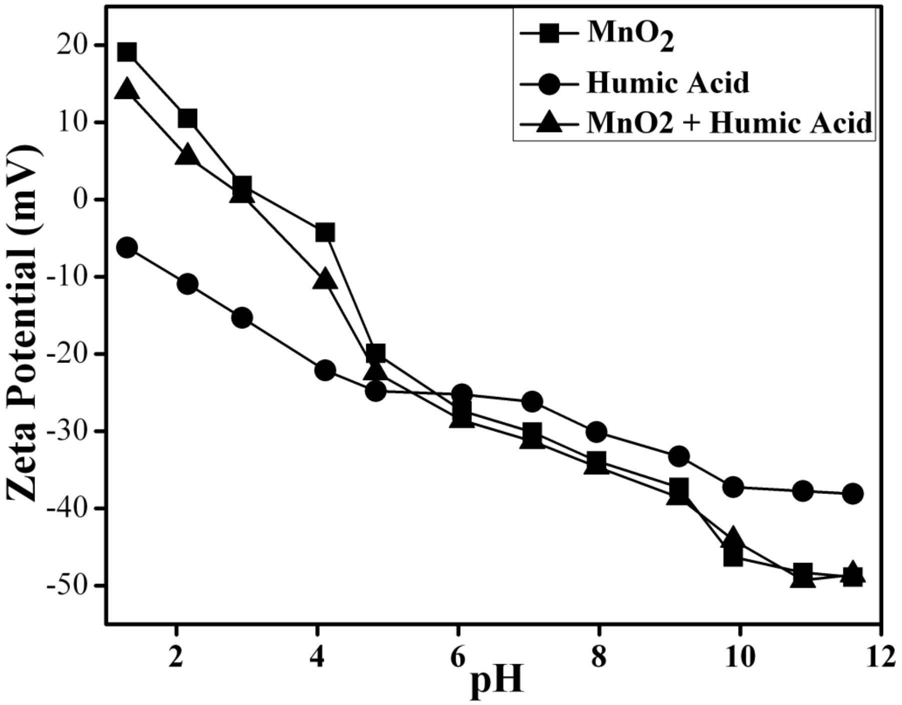

Figure 4.4: Zeta potential of manganese dioxide, humic acid and mixed system

Relatively steeper change in zeta potential of HA at pH 4-5 and pH 8-9, are attributed to the dissociation of carboxylic (–COOH) and phenolic (–OH) groups respectively. The zeta potential of the manganese dioxide-HA combined system was also measured and found to lie between the two individual systems (Figure 4.4) but the PZC of manganese dioxide is slightly shifted towards lower pH.

4.3.2. Sorption studies

4.3.2.1. Binary sorption (HA-Manganese dioxide)

The sorption of HA on manganese dioxide, in the pH range 1-12 in 0.05 M $NaClO_4$ medium is shown in Figure 4.5. At low pHs as the surface of hydrous manganese dioxide is protonated and obviously the surface remains positive charged whereas HA bears negative charge on it throughout the whole pH range studied. Hence the electrostatic attraction explains the near quantitative sorption of HA on manganese dioxide (90%). The surface charge of manganese dioxide decreases with increasing pH, then after pH 4 (Point of Zero Charge) it becomes negative, and therefore HA sorption decreases, and this observation is in accordance with literature report [175]. Excluding the electrostatic attraction/repulsion factor, several mechanisms of sorption of HA on mineral surfaces were reported in literature. These includes, ligand switch over phenomenon between active sites on the mineral surfaces and the functional groups of HA, hydrophobic interaction and sorption associated with conformational changes of HA. In addition with that, others factors like solubility and concentrations of HA and surface area mineral oxides can also affect the HA sorption on mineral surface.

4.3.2.2. Binary sorption (Nb/Pa - manganese dioxide)

The sorption of Nb and Pa on manganese dioxide is shown in Figure 4.6. Generally, two factors, namely the electrostatic interaction and the surface complexation control the sorption of the radionuclides on colloid surfaces [2, 80, 93,176]. Electrostatic interaction depends upon the charge on the colloid surfaces, and the species of the metal ions exist in different pH conditions. The principal chemical forms of Nb and Pa in acidic solution are NbO_2^+ and PaO_2^+ respectively. While in mild acidic to mild basic solutions, the neutral species like $NbO_2(OH)$ or $NbO(OH)_3$ for Nb and $PaO_2(OH)$ or $PaO(OH)_3$ for Pa predominates.

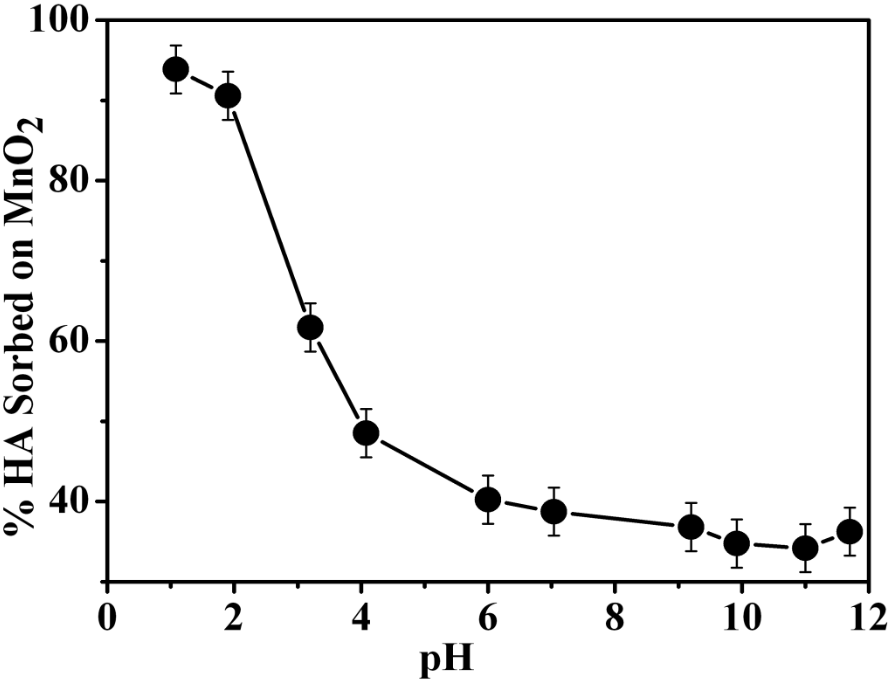

Figure 4.5: Sorption of humic acid on manganese dioxide with variation of pH

The anionic species like $NbO(OH)_4^-$ or $Nb(OH)_6^-$ are the most stable above pH 9 and for Pa the species like $Pa(OH)_6^-$ persists [61,101, 104]. In the pH range 1-3, the sorption is low as the surface charge on manganese dioxide is positive and both Nb and Pa bear positive charge and whatever the sorption observed may be due to physisorption or ion exchange phenomenon between surface –OH group of manganese dioxide and the positively charged

Nb species. Again the same electrostatic repulsion above pH (9-12) between the negatively charged manganese dioxide surface and the negatively charged species of Nb and Pa explains their low sorption on manganese dioxide above pH 9. If we see more carefully, it is clear that the sorption above pH 9 is higher compared to the sorption in the pH range 1-3. This indicates physisorption alone is not responsible for the sorption of Nb and Pa on manganese dioxide above pH 9, some other mechanism also involved through which they get sorbed onto manganese dioxide surface.

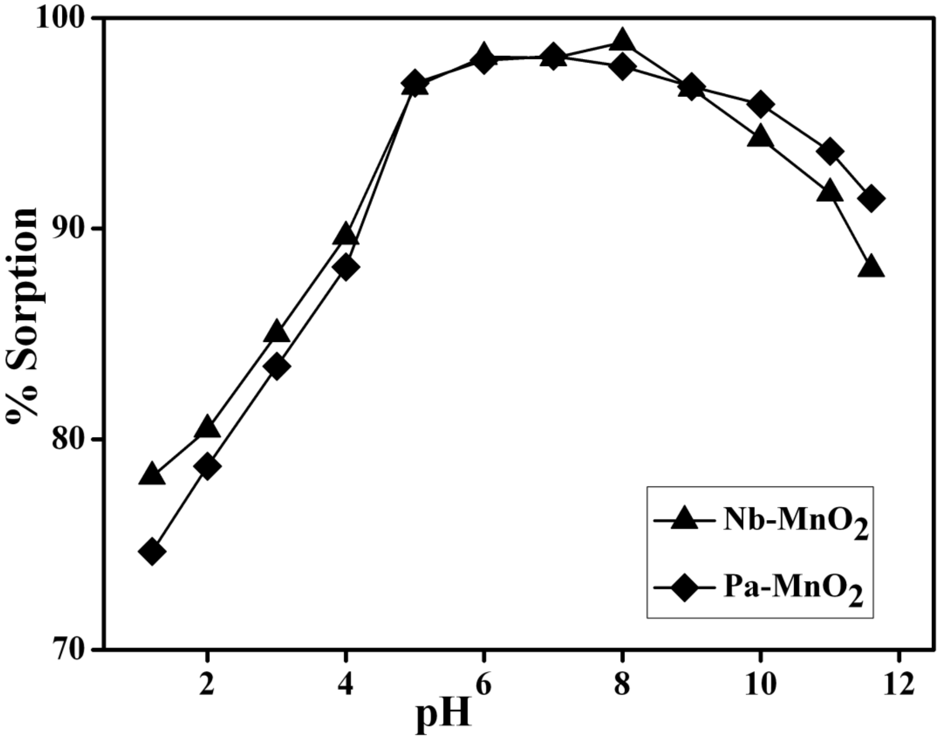

Figure 4.6: Sorption of Nb and Pa on manganese dioxide as a function of pH

However, it is very difficult to explain the very high sorption value in the pH range 5-9, where the surface charge on manganese dioxide is negative and neutral species of Nb and Pa are predominating. The very high sorption in this pH range can only be explained by the surface complexation between the hydroxyl group of neutral Nb/Pa species and the surface hydroxyl group (-OH) of manganese dioxide.

4.3.2.3. Ternary sorption (Nb/Pa - manganese dioxide-HA)

The presence of humic acid increase the sorption in acidic pH, but the reverse effect is observed in basic pH. HA is found to have insignificant effect on sorption in neutral pH region (Figure 4.7). The effect becomes more severe with increase in concentration of humic acid. At low pH, metal ions are feebly bound, whereas humic acid is firmly sorbed by manganese dioxide surface. Hence mineral bound humic acid facilitate the sorption of Nb and Pa on manganese dioxide surface. However, in basic pH, owing to its higher solubility, humic acid prefers to stay in solution rather than on hydrated MnO_2 surface. The dissolved humic acid undergoes complexation with Nb and Pa using the carboxylic groups, causing increased concentration of Nb and Pa in solution and hence lowered sorption. The role of humic acid perceive here in agreement with several literature where it is stated that metal cations are weakly bound to mineral surface but raises in presence of HA [138, 177] but contradictory literature also available pointing that sorbed HA on surface reduces the available sites for metal ion and hence reduced sorption of metal ion in presence of humic acid in acidic pH [178].

At pH 1, it is observed that as the HA concentration exceeds 50 mg L^{-1}, HA starts to agglomerate and itself form a new colloidal phase which is not observed in the basic medium. Therefore, above HA concentration of 50 mg L^{-1}, the surface of manganese dioxide is totally covered by humic acid and this surface coated manganese dioxide causing the higher sorption and in the mean while HA colloids also offer an additional phase for Nb and Pa to get sorbed. Thus the steeper enhancement of sorption for both the metal ion in presence of high concentration of humic acid is justified.

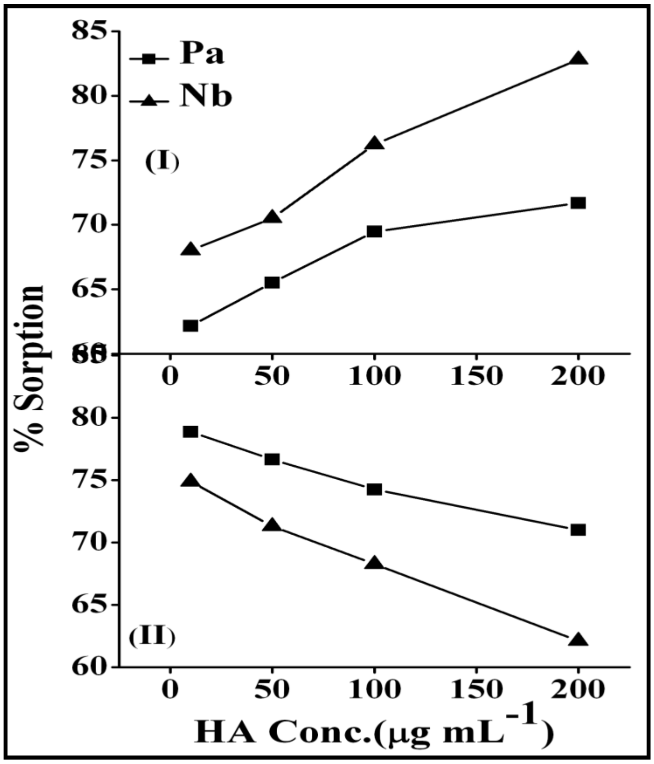

Figure 4.7: Effect of humic acid concentration on sorption of Nb and Pa on manganese dioxide at (I) pH 1 and (II) pH 9

4.3.3. Effect of ionic strength on sorption

Figure 4.8 shows the sorption of Nb and Pa on manganese dioxide, as a function of ionic strength. At pH 1, increase of ionic strength resulted in decrease the sorption value, whereas mild enhancement of sorption was observed at pH 9. This ionic strength dependent sorption study is utilized to differentiate between inner sphere and outersphere complexation. According to Hayes et al [179] variation of ionic strength can affect the sorption in the case of outersphere complexation. The principle rationale behind the above observation is the solution electrolyte can engage itself with the nonspecific sorption of the ions on present binding sites of the surface. The other reason is the change of interfacial potential due to change in ionic strength. This affect the activity of the adsorbing species as the solution electrolyte and the outer sphere complexes of adsorbing species are positioned at same plane in the triple layer model. In the case of inner-sphere complexation, the adsorbing species situate much closer to the surface as compared to background electrolyte and hence ionic strength can not affect this type of complexation. The inference that can be drawn from the above observation is the possibility of physisorption or ion exchange or outersphere mechanism in acidic pH [180]. In basic pH, the effect of ionic strength is less prominent or nearly insensitive compared to in acidic pH. This observation indicates the possibly may be chemisorption mechanism at pH 9.

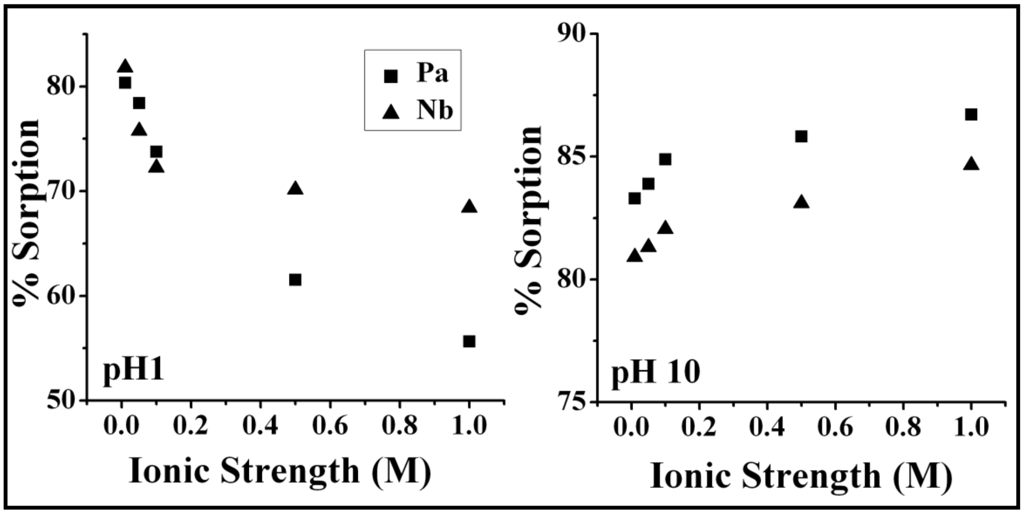

Figure 4.8: Effect of ionic strength on sorption at pH 1 and at pH 9

4.3.4. Effect of temperature on sorption

Temperature is a critical parameter in sorption study, as it can directly affect the distribution ratio (k_d) of the ion and finally kinetics of the sorption process. The temperature dependent variation of distribution ratio both in acidic and basic pH is given in Table 4.1. This phenomenon can be utilized in Van't Hoff equation to deduce the thermodynamic parameters of the sorption process.

$$\log(k_d) = \frac{\Delta S}{2.303R} - \frac{\Delta H}{2.303RT} \qquad (4.3)$$

The values of enthalpy, ΔH^o, and entropy, ΔS^o, were calculated from the slopes and intercepts of the log(k_d) vs.1/T plot (Figure 4.9 & 4.10). Then The Gibbs free energy, ΔG^o, of the sorption process is calculated from the equation:

$$\Delta G = \Delta H - T\Delta S \qquad (4.5)$$

Where R is the universal gas constant (8.314 J mol^{-1} K^{-1}) and T is absolute temperature (K).

Table 4.1: k_d values of Nb and Pa on manganese dioxide in acidic (pH 1) and basic medium (pH 9) at different temperatures

	Nb		**Pa**	
Temp (K)	**k_d (Lkg^{-1}) (pH 1)**	**k_d (Lkg^{-1}) (pH 9)**	**k_d (Lkg^{-1}) (pH 1)**	**k_d (Lkg^{-1}) (pH 10)**
278	685	7065	1123	16513
298	981	3648	1870	4103
323	1210	2008	2258	2046
348	1069	1120	784	1571

The thermodynamic parameters (Table 4.2) help in understanding the mechanism concerning the adsorptive interaction of Nb and Pa with manganese dioxide. The positive ΔH^o value indicates the adsorption process is endothermic in acidic pH. One possible explanation of the endothermic process is that both Nb and Pa are in +V oxidation state and are highly solvated in aqueous medium and before sorption on colloid surface, rupture of the hydration sphere occurred to some extent, and the process requires energy. It is also assumed that the energy required for the dehydration exceed the exothermicity of Nb and Pa ions fixing on manganese dioxide surface and makes the whole process endothermic. The Gibbs free energy change (ΔG) is negative, indicating that the process is spontaneous under the experimental conditions.

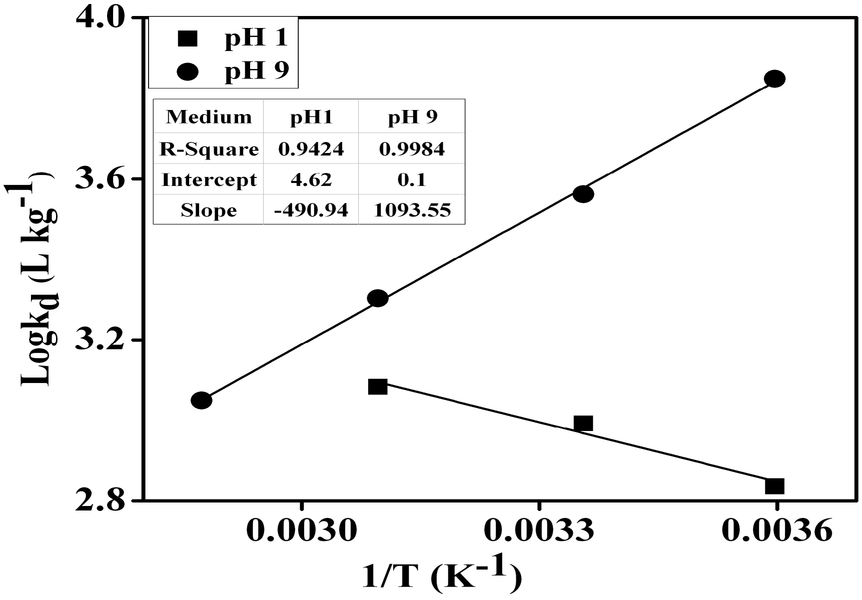

Figure 4.9: Log kd vs 1/T plot for Nb on manganese dioxide both in acidic (pH 1) and basic medium (pH 9)

The positive values of entropy change (ΔS) reflect the increase of randomness at the solid/liquid interface during the sorption process. The partial removal of water molecule due to the ion exchange process between the adsorbate and surface functional groups is the responsible factor behind positive entropy change [181]. Slightly different observation of reduction in k_d at 75°C in acidic pH was observed (Table 4.1), suggesting weak interaction between the Nb/Pa and manganese dioxide colloids at that pH condition. The decrease in K_d is exactly in accordance with the phenomenon of decreased physisorption at higher temperature.

At pH 9, ΔH^o is negative; designates the sorption process is exothermic. With increase of pH, the hydration sphere around Nb and Pa gets weaker as the oxo-hydroxy species are most favorable. This causes the reduction in energy required for the rupture of weak hydration sphere surrounding the metal ions. At the same instant, the energy liberated because of the chemical bond formation between Nb/Pa oxo-hydroxy species and surface hydroxyl group of manganese dioxide, over compensates the energy required for the rupture of hydration sphere and hence makes the process exothermic.

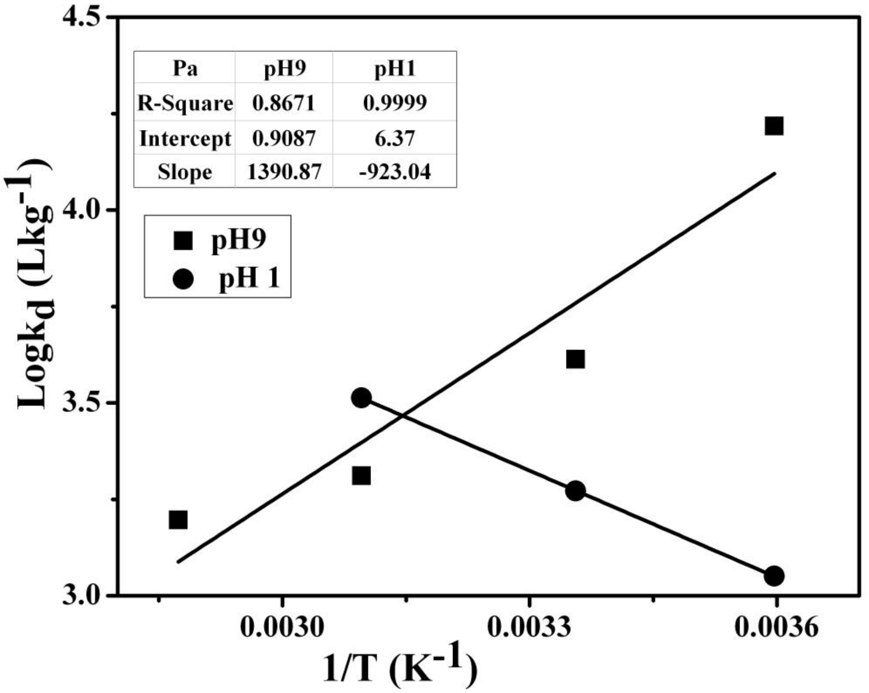

Figure 4.10: Log kd vs 1/T plot for Pa on manganese dioxide both at pH 1 and pH 9

Although there are no hard and fast rules regarding the ΔH^{o} values to interpret the sorption nature, the enthalpy change of the sorption process, ranging from 2.1- 20.9 kJ mol^{-1} (0.5- 5 kcal mol^{-1}) is considered to follow the physisorption mechanism. The enthalpy change in the range of 20.9 - 418.4 kJ mol^{-1} (5.0 and 100 kcal mol^{-1}) is associated with the charge sharing or formation of coordinate/covalent bond between metal surfaces and metal ions (chemisorption) [182-184].

The enthalpy change, associated with sorption process at pH 1, is significantly low (13.4 kJ mol^{-1}) and indicates towards physisorption mechanism in acidic pH. At pH 9, the high enthalpy change (-29.8 kJmol^{-1}) indicates the chemisorption mechanism.

Table 4.2: The values of the thermodynamic parameters obtained for the sorption process

at 273K

	Nb(V)		
pH	**ΔG^{o} (kJM^{-1})**	**ΔH^{o} (kJM^{-1})**	**ΔS^{o} (JK^{-1} M^{-1})**
1	-10.9	13.4	88.42
9	-31.5	-29.84	1.9
	Pa(V)		
1	-15.88	18.15	124.65
9	-31.38	-26.63	17.4

The combined uncertainties in kd values are calculated by considering the uncertainties arise from the counting statistics, the volumetric operations and the weighing. The uncertainty contribution from counting statistics is maximum and then from volumetric operation and weighing. The standard error propagation method was employed to get the final uncertainties associated with the measured parameters [185-187]. The uncertainty equation for % sorption (Equation 4.5) and k_d (Equation 4.6) were derived based on the equations 4.1 and 4.2.

$$u_{(\%\ \mathrm{Sorption})} = (\%\ \mathrm{Sorption})\sqrt{\left[\left(\frac{u_{A_o - A_f}}{A_o - A_f}\right)^2 + \left(\frac{u_{A_o}}{A_o}\right)^2\right]} \qquad (4.5)$$

$$u_{k_d} = k_d\sqrt{\left[\left(\frac{u_{A_o - A_f}}{A_o - A_f}\right)^2 + \left(\frac{u_V}{V}\right)^2 + \left(\frac{u_{A_f}}{A_f}\right)^2 + \left(\frac{u}{W}\right)^2\right]} \qquad (4.6)$$

Where 'u' represents the uncertainty in the respective parameters discussed in equations 4.1 and 4.2. As the pH changed from 1 to 12, the relative uncertainties for % sorption and k_d varied 3-6 % and 4-8 % respectively.

4.3.5. Effect of equilibration time on sorption

The kinetic modeling of the time dependent sorption data was achieved using Lagergren's pseudo first order [188] and Ho's pseudo second order model [189]. The details regarding these two kinetic model has been discussed in section 3.3.6. in chapter III.

The observations of time dependent sorption of Nb and Pa on manganese dioxide both in acidic (pH 1) and basic media (pH 9) are shown in Figure 4.11 & 4.12. In acidic pH the kinetic data best fitted when we follow pseudo first order kinetics (regression coefficient: 0.9999 and 0.9649 respectively for Nb and Pa) (Figure 4.13). This indicates in acid medium, the sorption of Nb and Pa on manganese dioxide follows pseudo first order kinetics and the sorption occurring predominantly via physisorption or the outersphere complexation predominant. But the kinetic sorption data for basic medium is well fitted with pseudo second order model (regression coefficient: 0.9999 for both Nb and Pa) rather than pseudo first order model (regression coefficient: 0.9519 and 0.9047 for Nb and Pa respectively) (Figure 4.14 & 4.15). This infers that chemisorption is the predominant mechanism of sorption at pH 9.

Based on the ionic strength and temperature dependent data and the kinetic model fitting, the probable mechanism of sorption of Nb on manganese dioxide is shown in schematic manner in Figure 4.16. The sorption mechanism for Pa follow the same manner as described in previous figure for Nb.

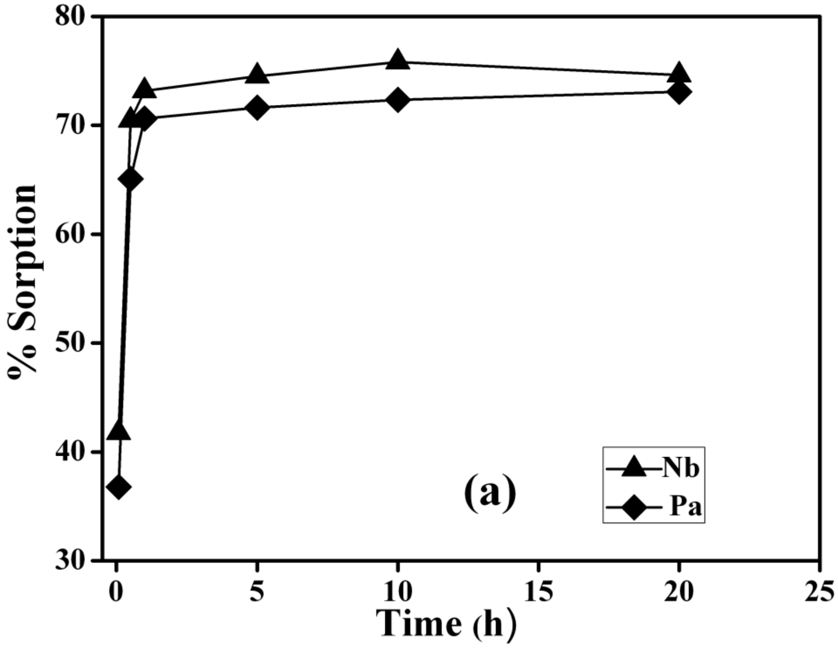

Figure 4.11: Effect of equilibration time on sorption in acidic medium (pH 1)

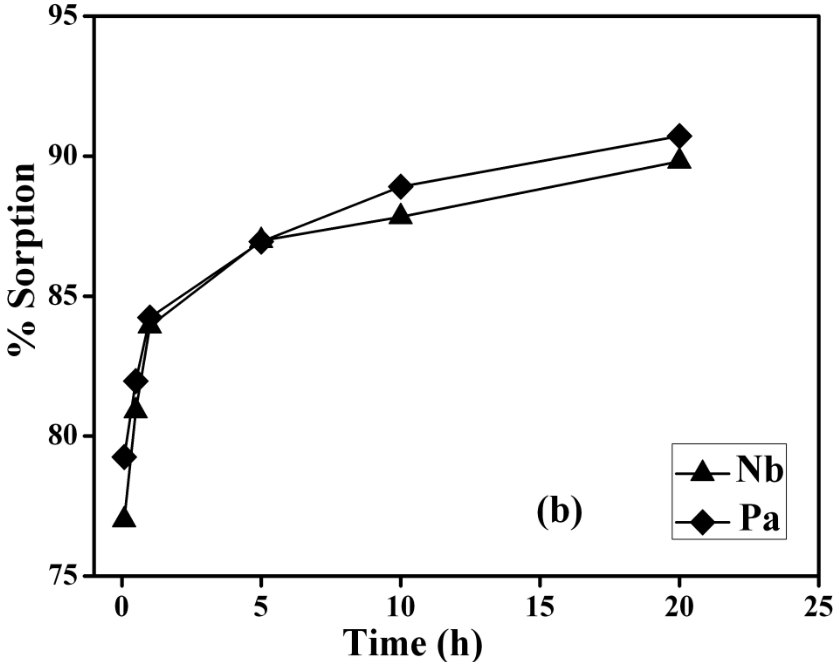

Figure 4.12: Effect of equilibration time on sorption in basic medium (pH 9)

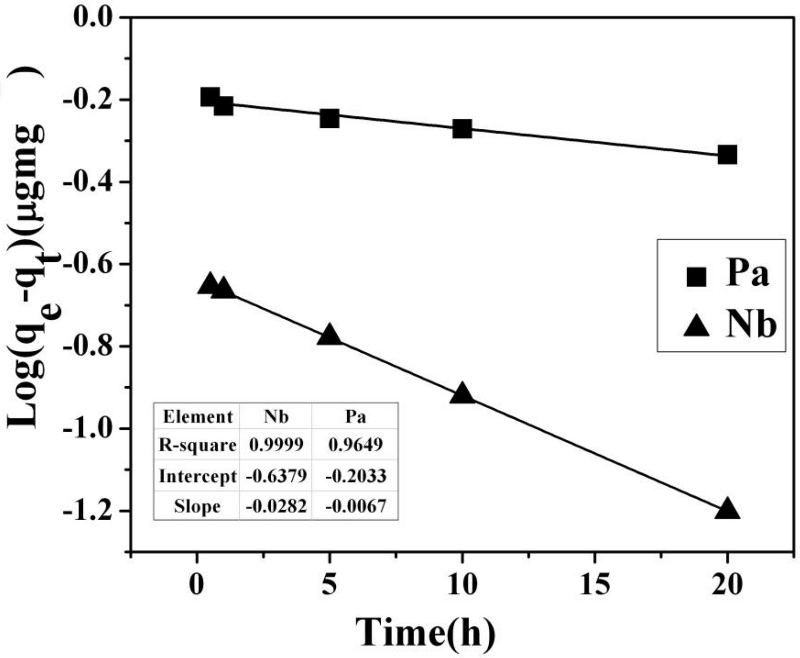

Element	Nb	Pa
R-square	0.9999	0.9649
Intercept	-0.6379	-0.2033
Slope	-0.0282	-0.0067

Figure 4.13: Pseudo first order kinetic fitting in acid medium (pH 1)

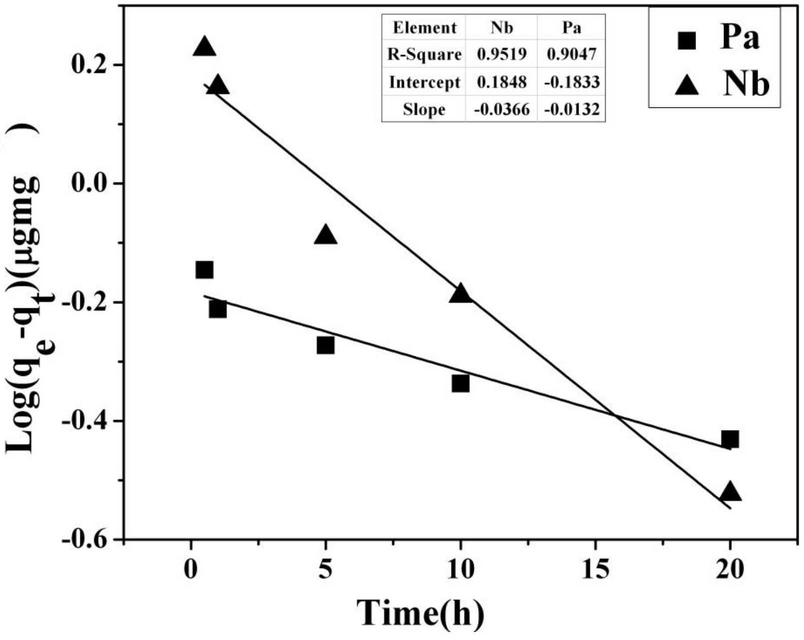

Element	Nb	Pa
R-Square	0.9519	0.9047
Intercept	0.1848	-0.1833
Slope	-0.0366	-0.0132

Figure 4.14: Pseudo first order kinetic fitting in basic medium (pH 9)

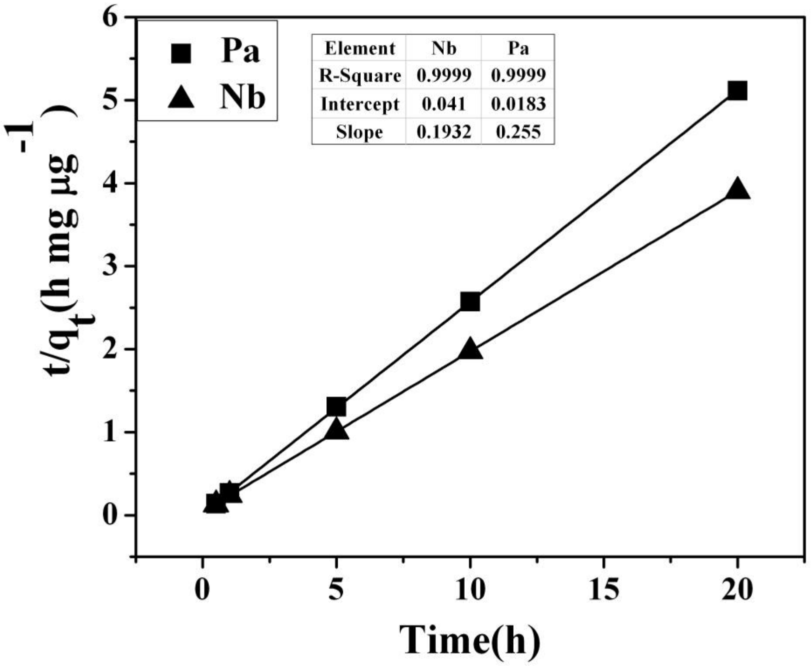

Element	Nb	Pa
R-Square	0.9999	0.9999
Intercept	0.041	0.0183
Slope	0.1932	0.255

Figure 4.15: Pseudo second order kinetic fitting in basic medium (pH 9)

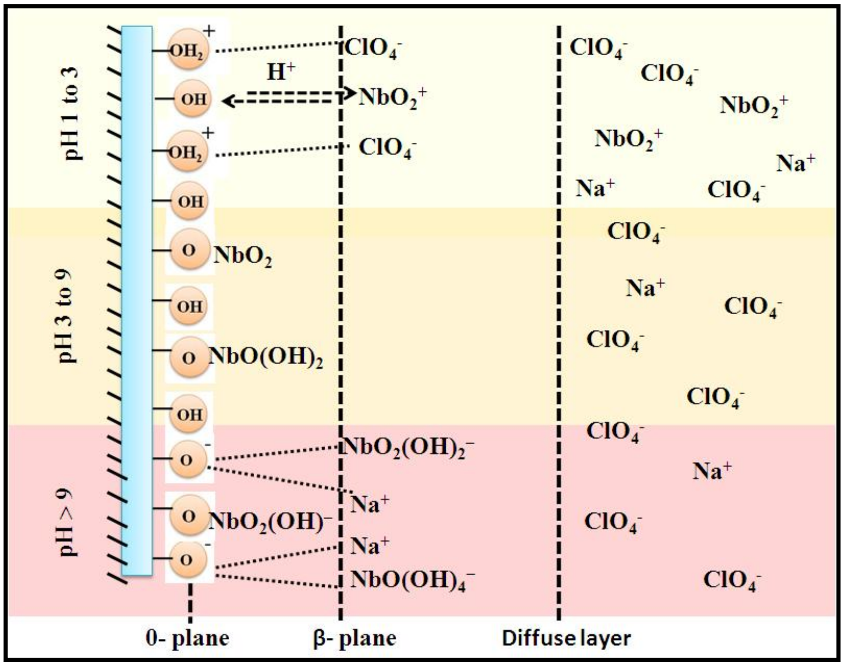

Figure 4.16: Triple layer model for the sorption of Nb(V) on manganese dioxide

4.4. Conclusion

The knowledge that can be gathered from the above sorption studies are (1) The sorption of Nb and Pa on manganese dioxide is quantitative in neutral to near neutral pH region. (2) In low pH, mineral bound humic acid enhances the sorption of Nb and Pa. In higher pH, dissolved humic acid complexes with Nb/Pa and reduced the sorption. (3) As the sorption is strongly dependent on ionic strength, it follows outer sphere complexation in low pH but the mild dependence in basic pH, reinforces the probability of innersphere complexation. (4) The positive entropy change of the sorption process in acidic pH makes the endothermic sorption process spontaneous. (5) Pseudo first order fitting in low pH suggests the high probability of physisorption, whereas pseudo second order kinetic fitting proposes the probability of chemisorption mechanism at high pH.

Chapter V

Evaluation of sorption mechanism using Thermodynamic studies and X-Ray Absorption Fine Structure (XAFS)

5.1. Introduction

The generation of ^{94}Nb and ^{231}Pa in nuclear industry, the probable migration of these radionuclides as pseudo colloids and their speciation are discussed in Chapter I. In view of their probable colloid assisted migration, the sorption studies of ^{94}Nb and ^{231}Pa was carried out on naturally occurring colloids like silica and iron oxides (goethite, hematite and magnetite) and the effect of pH, humic acid, and equilibration time on the sorption have been studied in detail. The aim of this study was to obtain percentage sorption or solid/liquid distribution ratio of the isotopes for understanding performance assessment of nuclear waste repositories. It is realized that clear concept regarding the sorption species and the reaction mechanisms are required for prediction of their behaviour in environment as well as their migration in aquatic system. This will help in modeling of the migration and bio-availability of the radionuclides in environment. This knowledge will help in interpreting the conditions at which their migration is supposed to most probable and according measures can be taken to minimize the effect [190].

Several classical as well as spectroscopic methods are reported in the literature to understand the sorption mechanism and actinide surface speciation. In classical method, ionic strength [191, 192] and thermodynamic data [45, 193] have been used by different authors to understand these aspects. Generally, the spectroscopic techniques are supposed to offer more detailed structural information of sorption mechanism at the molecular level. As the sorption reactions generally occur at the solid-water interface, the spectroscopic techniques can be used for the in situ characterization of the surface complexes directly avoiding any undue alteration or disruption of structure in the complexes. In spectroscopic techniques, Time Resolved Laser Fluorescence spectroscopy (TRLFS) [194, 195], Raman or Infrared spectroscopy [196], X-ray Photoelectron spectroscopy (XPS) [197,198], X-ray Reflectivity [199] and X-ray Absorption Fine structure (XAFS) [200, 201] have been used extensively for the above said purposes.

Actinide speciation by TRLFS is based on the characteristic luminescence properties arising from their f−f electronic transitions. The identification and characterization of the species are based on the shift in the fluorescence peak and change in the fluorescence life time, as these parameters are strongly dependent on the hydration state of the actinides ion. This technique is highly sensitive, allows for molecular-level understanding of surface speciation and is considered to be one of the best technique for the said purpose at very low concentration level [43]. XPS being surface sensitive technique and measurements are performed in vacuum; there is a chance of alteration the species under experimental conditions of XPS study. Thus the technique become self limited for the speciation and sorption mechanism study along with the requirement of higher concentration of the sorbed species [43]. In comparison to XPS, attenuated total reflection Fourier transform infrared (ATR FTIR) spectroscopy is a more useful tool for the in-situ characterization of species sorbed on mineral surfaces, but the strong absorption band of water may interfere in these measurements [49].

XAFS cite the ways through X-rays are absorbed by an atom at absorption edge energy or at slightly higher energy than that of absorption edge. The technique is based on the absorption probability by the atom. This absorption probability directly depends on the chemical and physical state o the atom. The technique provides the formal oxidation state, co-ordination number, type of neighbours, inter-atomic distance and structural disorders surrounding the selected element. XAFS spectra can be measured virtually for all the elements in the periodic table. The main advantage of this technique is that, it does not require crystallinity of the sample and can be carried out in air. Because of that the technique has become one of the few useful structural probes available for characterizing non-crystalline and highly disordered materials and even for liquid sample. These advantages make the XAFS a versatile technique for the analysis of amorphous samples, liquids, biological samples, homogeneous and heterogeneous catalysts and obviously a very useful experimental technique in material science [202].

The X-ray absorption spectrum is typically divided into two distinct regions: X-ray Absorption Near Edge Spectroscopy (XANES) and Extended X-ray Absorption Fine Structure (EXAFS). Though the origin of both is the same, but distinction is required for better interpretation. XANES is sensitive to oxidation state, while EXAFS is sensitive to coordination number, neighbouring species and their distance from the absorbing element. The main constraint of the technique is, it requires an intense tunable X-ray source which only can be offered by synchrotron radiation. The other limitations are: (a) the local structure determination is limited by mean free path of the photo-electron in the matrix, which is generally lie between 5-10Å radius from the selected element, (b) the concentration of the element required for the technique, is relatively high. The technique is widely used in the speciation study of actinides in mineral-water interface [43, 203].

In the present study, we have tried to elucidate the sorption mechanism of Nb(V) on colloidal silica and hematite in different pH conditions using XAFS. We have tried to correlate the ionic strength and temperature dependent sorption data with the findings from XAFS of Nb(V) sorbed silica and hematite at different pH conditions.

Because of the constraints of handling radioactivity at the facility and unavailability of Pa(V) tracer solution of high concentration, EXAFS study of Pa(V) sorbed silica or hematite were not carried out in the present scenario. But as Nb(V) is considered as chemical analogue of Pa(V), so from the XAFS study of Nb(V) sorbed silica and hematite, we can have superficial idea regarding the sorption mechanism of Pa(V) on silica and hematite at different pH conditions.

5.2. Materials and methods

5.2.1. Materials

Sodium perchlorate (Sigma Aldrich), sodium hydroxide (NaOH) and perchloric acid ($HClO_4$) of AR grade, colloidal silica (commercial grade AEROSIL 200), sodium salt of humic acid (Sigma Aldrich) were used in the experiments. Ultrapure water (Mili-Q gradient system, resistivity: 18.2 MΩ cm^{-1}) was used throughout the experiments. Silica was purchased and hematite, goethite and magnetite were synthesized in the laboratory. ^{94}Nb and ^{231}Pa radiotracers were used throughout the experiments. As both the elements are strongly hydrolysable in nature, the initial stocks were kept in 0.5M HF solutions. Prior to experiments, measured volume (1 mL) of the primary stock was taken into Teflon dish and evaporated to dryness eight times in 1:1 Perchloric acid medium. Finally the tracers were prepared in perchlorate medium (5 mL) and the process was repeated in 15 days interval as the tracers were not so stable in perchlorate medium (hydrolysis causes inhomogeneity of the tracer solution).

5.2.2. Batch sorption studies

The sorption experiments were carried out in batch mode. Polypropylene container was used to minimize the loss of the tracer on container wall. These experiments were conducted at a mass loading of 2g L^{-1} of SiO_2, 2g L^{-1} of Fe_2O_3,100μL of each 2.2 $\times 10^{-7}$ M of ^{94}Nb, 9.6$\times 10^{-6}$

M of ^{231}Pa keeping the ionic strength at 0.05M $NaClO_4$. The experiments were performed under ambient atmospheric condition at 25^{o}C. The equilibration time was maintained for 48 h in a mechanical shaker (125 rpm) and the phase separation was carried out by high speed centrifugation at 10000 rpm for 1 h.

The sorption of the radionuclides were measured by monitoring the corresponding activities in initial solution and the supernatant after phase separation using the gamma energies of 702.7 keV for ^{94}Nb and 283.7 keV for ^{231}Pa. The activity measurement was carried out using High Purity Germanium (HPGe) detector (Canberra) coupled to 8k channel analyzer (Relative efficiency: 30%, Resolution: 1.9 keV at 1332 keV of ^{60}Co).

pH dependent sorption was studied in pH range 1-12 and the pH of the solutions were adjusted using of 0.001 M or 0.1 M NaOH/$HClO_4$ solutions in different cases so that volume addition of NaOH/ $HClO_4$ is the minimum possible for any of the solutions. The pH was measured in the supernatant without agitation using pH meter (Oakton, pH700, USA), calibrated with commercially available buffer solutions of pH 4.01, 7.00 and 9.21. The effect of ionic strength on sorption was studied by varying the ionic strength from 0.01 M to 1.0 M $NaClO_4$ in acidic (pH 1.2), neutral (pH 6.5) and basic medium (pH 10.5) for silica and at pH 1.2 and pH 10.5 for iron oxides.

For thermodynamic evaluation of the sorption process for Nb/Pa on silica, temperature dependent studies were carried out at four different temperatures 5^{o}C, 25^{o}C, 50^{o}C and 75^{o}C at acidic (pH 1.2), neutral (pH 6.5) and basic (pH 10.5) conditions, keeping all other parameters unchanged. Similar studies were also carried out for Nb/Pa- iron oxides at pH 1 and at pH 10.

5.2.3. Sample preparation for XAFS

The batch experiments were carried out using tracer solutions in nano-molar (nM) concentration which was not sufficient for XAFS studies. Therefore to overcome the constraints, inactive Nb solution was used in elevated concentrations (mM) for the sample preparations. Samples were prepared by adding 2.5 mL Nb solution (0.01M) to 25 mL well-dispersed silica solution (4 g L^{-1}) keeping the rest of the parameters identical as in the case of batch experiments. The initial solutions were adjusted to the desired pH values (pH 1.2, pH 6.5 and pH 10.5) with either dilute NaOH or $HClO_4$, as mentioned before. Allowing the samples to equilibrate for 48 h in mechanical shaker and following centrifugation, Nb loaded silica sample at three different pHs were separated from supernatant but kept hydrated to keep the bonding feature intact, because bonding features usually changes on drying. The Nb sorbed hematite samples at different pH were also prepared in the similar manner. Hematite is chosen over goethite and magnetite for the XAFS study because, in hematite, Fe has well defined oxidation state (III) and does not impart any redox reaction at the surface as reported for the other two iron oxides [204-206] which unnecessarily complicate the XAFS data interpretations.

5.2.4. XAFS methodology

The XAFS measurements were carried out at the Energy-Scanning XAFS beamline (BL-9) at the Indus-2 Synchrotron source (2.5 GeV, 100 mA) in Raja Ramanna Centre for Advanced Technology (RRCAT), Indore, India [207].The operating energy range was 4 keV to 25 keV. The beamline optics consists of a Rh/Pt coated collimating meridional cylindrical mirror and the collimated beam reflected by the mirror is monochromatized by a Si (111) (2d=6.2709) based double crystal monochromator (DCM). The second crystal of DCM is a sagittal cylinder used for horizontal focusing while a Rh/Pt coated bendable post mirror, facing down, was used for vertical focusing of the beam at the sample position. Rejection of the higher harmonics in the X-ray beam was performed by de-tuning the second crystal of DCM. In the present case, X-ray absorption spectrometry (XAS) measurements were performed in transmission mode by putting the slurry sample in transparent glass cuvette in the beam path. The experiments were performed at Nb K-edge energy (18.9856 keV). For the transmission measurements, three ionization chambers (300 mm length each) were used for data collection, one ionization chamber for measuring incident flux (I_0), second one for measuring transmitted flux (I_t) and the third one for measuring X-ray absorption spectrum of a reference metal foil for energy calibration. Appropriate gas pressure and gas mixtures were chosen to achieve 10-20% absorption in first ionization chamber and 70-90% absorption in second ionization chamber to improve the signal to noise ratio.

In order to take care of the oscillations in the absorption spectra $\mu(E)$ has been converted to absorption function $\chi(E)$ defined as given in following equation (5.1) [208]

$$\chi(E) = \frac{\mu(E) - \mu_0(E)}{\Delta\mu_0(E_0)} \tag{5.1}$$

where, E_0 is absorption edge energy, $\mu_0(E_0)$ is the bare atom background and $\Delta\mu_0(E_0)$ is the step in $\mu(E)$ value at the absorption edge. The energy dependent absorption coefficient $\chi(E)$ has been converted to the wave number dependent absorption coefficient $\chi(k)$ using the relation given in equation (5.2).

$$k = \sqrt{\frac{2m(E-E_0)}{\hbar^2}} \tag{5.2}$$

where, m is the electron mass. $\chi(k)$ is weighted by k^2 to amplify the oscillation at high k and the $\chi(k)k^2$ functions are Fourier transformed in R space to generate the $\chi(R)$ versus R spectra in terms of the real distances from the center of the absorbing atom. The set of EXAFS data analysis programme available within Demeter software package was used for EXAFS data analysis [209]. This includes background reduction and Fourier transform to derive the $\chi(R)$ vs R plot from the absorption spectra (using ATHENA software), generation of the theoretical EXAFS spectra starting from an assumed crystallographic structure and finally fitting of experimental data with the theoretical spectra using ARTEMIS software.

5.3. Results and discussion

5.3.1. Batch sorption

The sorption of Nb and Pa on silica as a function of pH is already shown in Figure 2.12 in chapter II. The sorption of both the elements on silica in acidic pH is about 70% and it become almost quantitative between pH 6-9 and then slightly decreased in basic pH. The pH dependent sorption trends for both the elements have similarities with those reported in the literature on various sorbents [210, 211]. In our case sorption is higher in acidic region as compared to those reported in the literature and this may be attributed to very high surface area of silica. Somewhat reduced sorption below pH 3 as compared to pH range 6-9, is explained by electrostatic repulsive interaction between positively charged silica surface and the positively charged species of Nb and Pa exist at the acidic pH condition. Between pH 6-9, almost quantitative sorption is explained by surface complexation model where chemical bond formation is supposed to take place between surface silanol group of colloidal silica and hydroxyl groups of the oxo-hydroxy species of Nb/Pa. Beyond pH 9, the sorption slightly decreases but the reduction is not as much as in acidic pH condition. This infers that in basic pH, the electrostatic interaction may not be the main controlling parameter behind the sorption phenomenon.

The solubility of the colloidal silica was checked to understand that its solubility have any severe effect on the observed sorption process. The Si content in the solutions was found to about 1 mg L^{-1}, 7 mg L^{-1} and 60 mg L^{-1} at pH 1, pH 6.5 and pH 11, respectively, which amounted to 0.05 %, 0.35 % and 3 % of the total silica uses in these experiments. So Silica dissolution can have only a mild effect on sorption process, especially at higher pH.

The sorption of Nb and Pa on hematite is shown in Figure 3.9 and 3.10 in chapter III. The sorption in acidic pH (upto pH 5) is very low (~15-20 %), showing marked difference as compared to the sorption of the elements on silica. Beyond pH 5, the sorption increases sharply and reach about 90% till pH become 9. After that, the sorption decreases again slightly with further increase in pH of the medium and the pattern is almost similar to penta valent element Np on hematite-water interface as reported in the literature [212]. The very low sorption in acidic pH may be due to the very high positive zeta potential of hematite surface below pH 6. Accordingly, this imparts strong Coulombic repulsive force between hematite surface and positively charged species of Nb/Pa causing a large reduction in sorption. The sorption pattern in neutral and basic region can be explained in the similar fashion as in case of Nb/Pa - silica system. The solubility of hematite throughout the working pH range is negligible over a large contact time. So the solubility of hematite does not affect the sorption behaviour of Nb/Pa on hematite in the studied pH conditions.

5.3.2. Ionic strength effect

The effects of ionic strength on sorption of Nb and Pa on silica at different pH are shown in Figure 5.1. In general, investigation of ionic strength effects on sorption of metal ion on hydrous oxides is a benchmark method to differentiate between outer sphere surface complex (OSSC) and inner sphere surface complex (ISSC). If the sorption of metal ion decreases with increase of ionic strength, the mechanism is supposed to follow OSSC and is valid in those cases where the cation get sorbed on to positively charged oxide surfaces. Inertness of sorption to ionic strength has been considered as the indication of ISSC [43,179]. Literature on stimulating effect of ionic strength on sorption and adequate explanation about the observed trend is scanty [213, 214]. In the present study, it is observed that, ionic strength causes reduction of sorption in acidic medium (pH 1.2), indicating OSSC mechanism to be operative. In neutral medium (pH 6.5), sorption is effectively invariant with varying ionic strength suggesting ISSC mechanism.

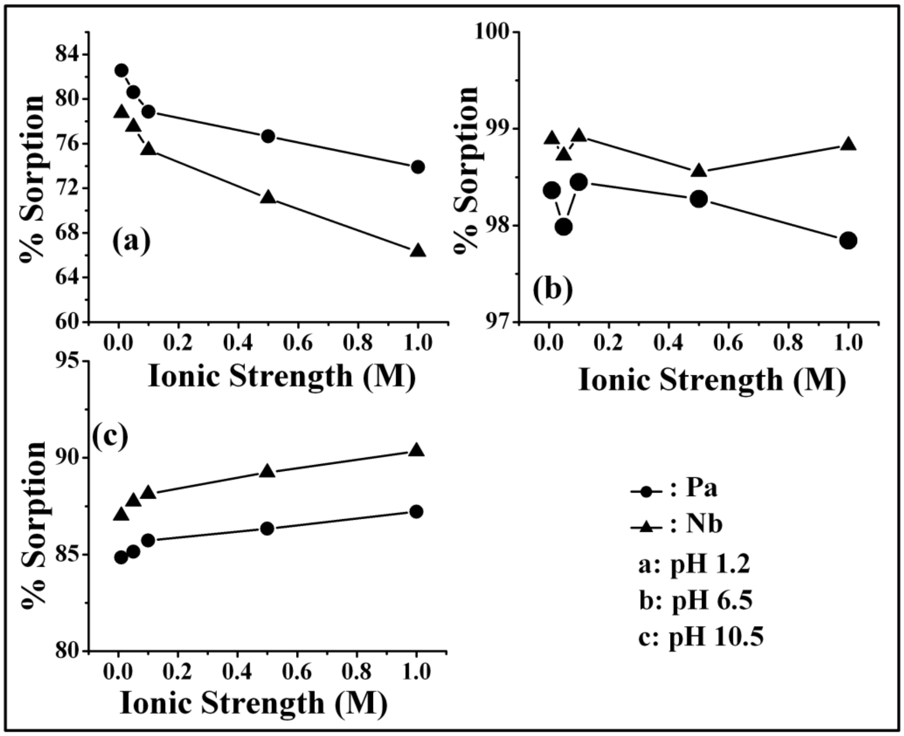

Figure 5.1: Effect of ionic strength on sorption of Nb and Pa on silica at (a) pH 1, (b) pH 6.5 and (c) pH 10.5

In basic medium (pH 10.5), mild enhancement of sorption with increase of ionic strength was observed but the interpretation regarding this unconventional observation is very clear. The probable reason behind the promotive effect of ionic strength is the formation of ion pairs between the charged metal inner sphere surface complex and the counter ions present in the medium. In other words, high ionic strength effectively stabilises the highly charged surface complexes [43].

The effect of ionic strength on sorption of Nb and Pa on different iron oxides at pH 1 and pH 10 is shown in Figure 5.2 and 5.3.

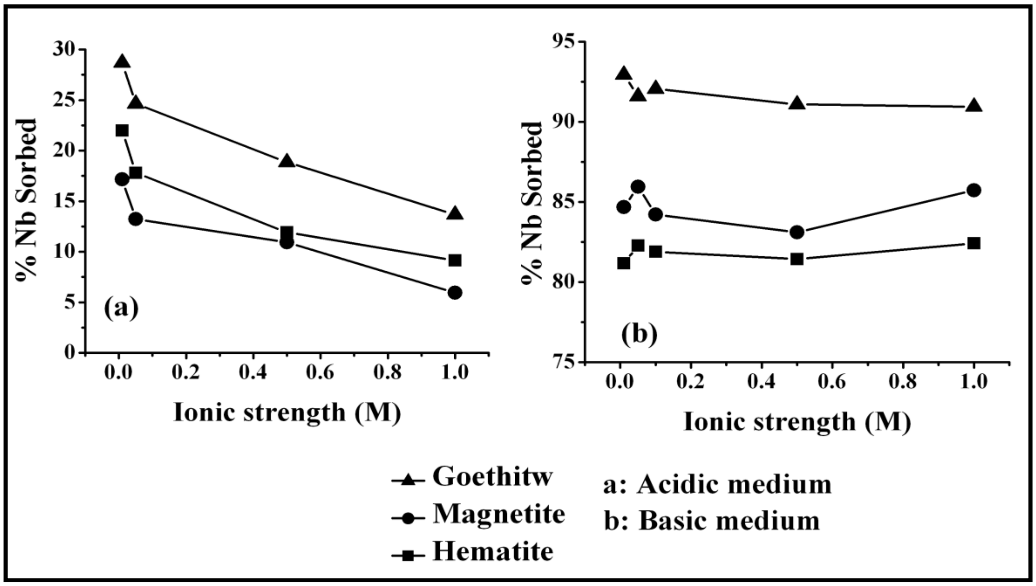

Figure 5.2: Effect of ionic strength on sorption of Nb on iron oxides at pH 1 and at pH 10.

It is observed that at pH 1, sorption strongly depends upon ionic strength whereas at pH 10, the sorption is almost insensitive with respect to change in ionic strength. This infers that the sorption follows OSSC in acidic pH and ISSC in basic pH.

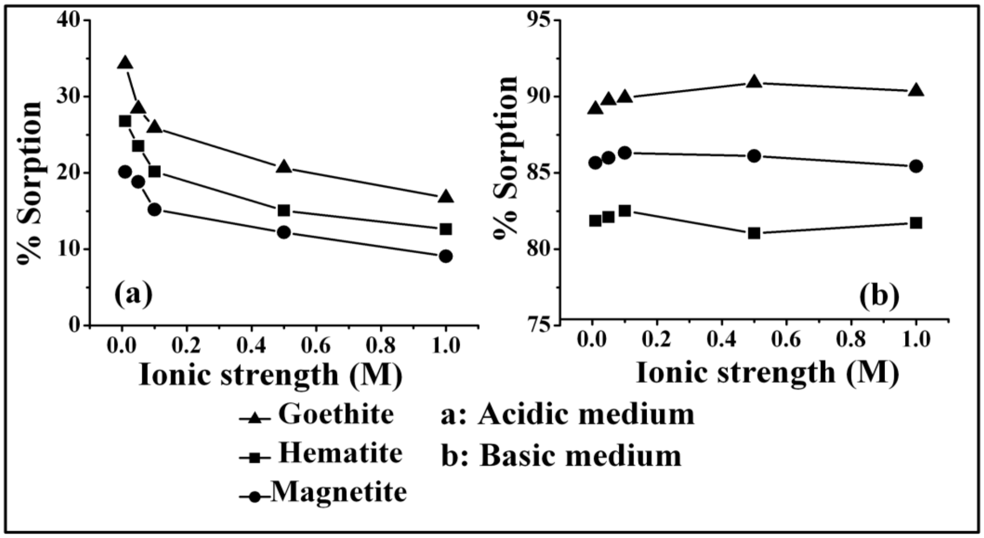

Figure 5.3: Effect of ionic strength on sorption of Pa on iron oxides at pH 1 and at pH 10.

5.3.3. Sorption thermodynamics

Temperature is an extremely important parameter in sorption study, as it can affect the sorption processin different ways through altering equilibrium among solution species, change in the point of zero charge (PZC) of sorbent, change in distribution ratio (k_d) of the ion and finally influencing the kinetics of the process involved. In general, PZC of hydrous metal oxides decreases with increase in temperature. In the present work, the different thermodynamic parameters like enthalpy, entropy and free energy chnages were calculated using Van't Hoff equation,

$$Log(k_d) = \frac{\Delta S^o}{2.303R} - \frac{\Delta H^o}{2.303RT} \tag{5.3}$$

where, kd is the distribution ratio (L kg^{-1}), T is absolute temperature, R is the universal gas constant (8.314 J $mole^{-1}$), ΔH^o and ΔS^o are the standard changes in enthalpy and entropy associated with the sorption reaction. After linear fitting of log k_d vs 1/T plot (Figure 5.4), ΔH^o and ΔS^o were obtained from the slope and intercept respectively. Free energy change was subsequently determined using the following equation

$$\Delta G^{O} = \Delta H^{O} - T\Delta S^{O} \tag{5.4}$$

The values of ΔH^{o}, ΔS^{o} and ΔG^{o} for different media (pH 1.2, 6.5 and 10.5) are given in Table 5.1. Although there is no well defined criteria to relate ΔH^{o} values with the mechanism of sorption, as a general guide, the heat of sorption values ranging from 2.1- 20.9 kJ mol^{-1} (0.5-5 kcal mol^{-1}) are considered to correspond the physical sorption process and the values in the range of 20.9 - 418.4 kJ mol^{-1} (5.0 and 100 kcal mol^{-1}) are considered to be associated with the sharing or formation of coordinate/covalent bond between mineral surfaces and the metal ions (chemisorption) [215-217]. In acidic medium, positive ΔH^{o} suggests the sorption process is endothermic but the ΔG^{o} value is negative, making the process spontaneous. To be mentioned that similar phenomenon was observed in Sb(V) sorption on kaolinite [218]. Slightly different and unlikely observation like a reduction in sorption at 75°C was observed, suggesting a weak interaction between the metal ion and silica colloids. This may be due to increased tendency of the metal ions to escape from the silica surface after a certain temperature. The ΔG^{o} value in acidic region is in accordance with the results of the ionic strength experiments which suggested purely electrostatic interaction or OSSC.

In neutral (pH 6.5) and basic (pH 10.5) media, almost quantitative sorption of Nb and Pa were observed on silica surface. The sorption reactions are exothermic (ΔH^{o} negative) in nature and high magnitude of enthalpy (> 20.9 kJ mol^{-1}) indicate that there is a possibility of charge sharing or bond formation which was supported by insignificant or mild effect of ionic strength on sorption at these pH conditions.

The k_d vs 1/T plot for the sorption study of Nb/Pa on iron oxides systems in acidic and basic pH are shown in Figure 5.5 to 5.7 respectively. The values of the thermodynamic parameters obtained from the temperature dependent sorption experiments are listed in Table 5.2 and

5.3. The sorption in acidic pH is endothermic but the positive entropy change makes the free energy of the sorption process negative and hence the sorption in acidic pH also becomes spontaneous.

Table 5.1: Thermodynamic parameters of the sorption of Nb and Pa on silica at different pH (at 273K)

pH	**Nb - Silica**			**Pa - Silica**		
	ΔG^o (kJM^{-1})	ΔH^o (kJM^{-1})	ΔS^o ($JK^{-1}M^{-1}$)	ΔG^o (kJM^{-1})	ΔH^o (kJM^{-1})	ΔS^o ($JK^{-1}M^{-1}$)
1.2	-17.3	7.0	89.0	-16.7	6.6	85.6
6.5	-25.5	-24.4	4.12	-24.6	-23.0	5.9
10.5	-20.25	-21.5	-4.44	-19.84	-22.13	-8.4

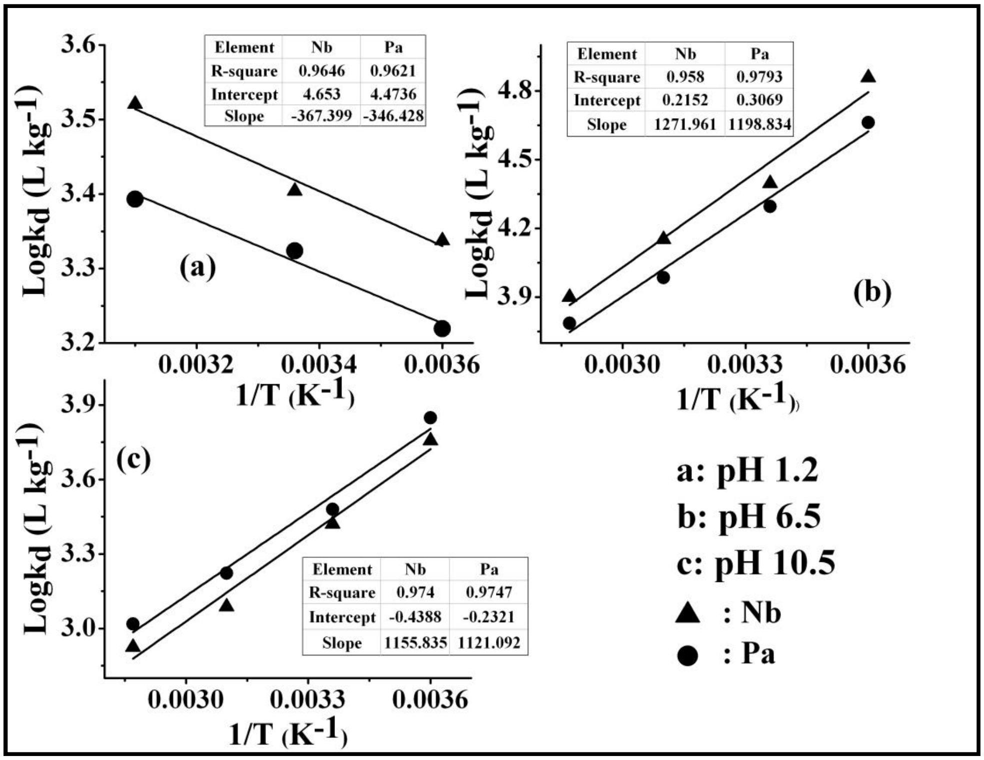

Figure 5.4: k_d vs 1/T plot for the sorption of Nb and Pa on silica at (a) pH 1.2, (b) pH 6.5 and (c) pH 10.5

For magnetite the enthalpy change is very high which indicates some other phenomenon also taking place simultaneously along with the sorption process. Electrochemical studies on magnetite - Nb system suggest the occurrence of the redox reaction between Fe(II) site of magnetite and Nb which is getting sorbed onto the magnetite from the solution. The details regarding this electrochemical study and related observations have already been discussed in chapter III elaborately. In basic medium sorption in exothermic and the very large change in enthalpy suggest that the sorption of both Nb and Pa on all three iron oxides follow chemisorption mechanism i.e., covalent bond formation occurs between iron oxides surface and the species of Nb/Pa.

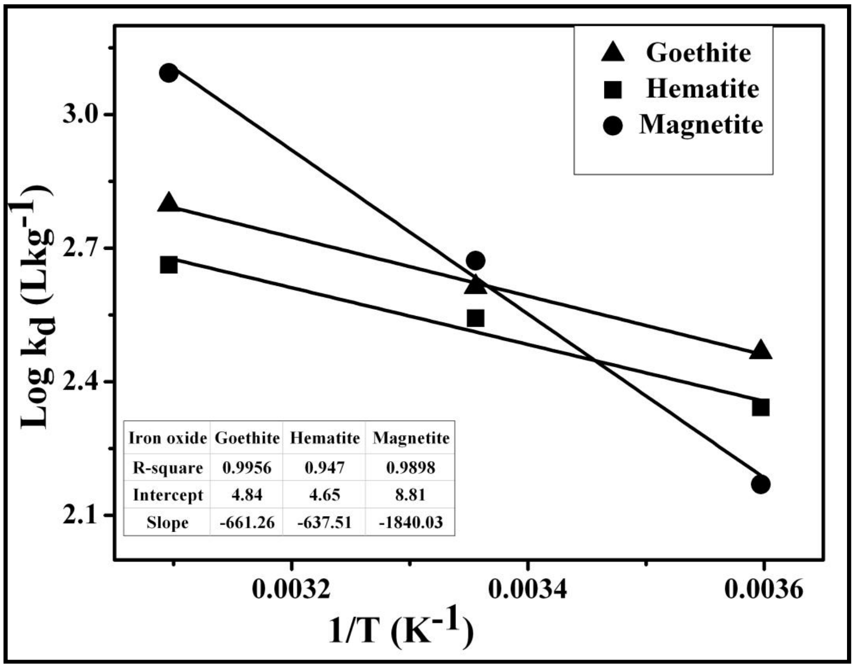

Iron oxide	Goethite	Hematite	Magnetite
R-square	0.9956	0.947	0.9898
Intercept	4.84	4.65	8.81
Slope	-661.26	-637.51	-1840.03

Figure 5.5: k_d vs 1/T plot for the sorption of Nb on iron oxides at pH 1

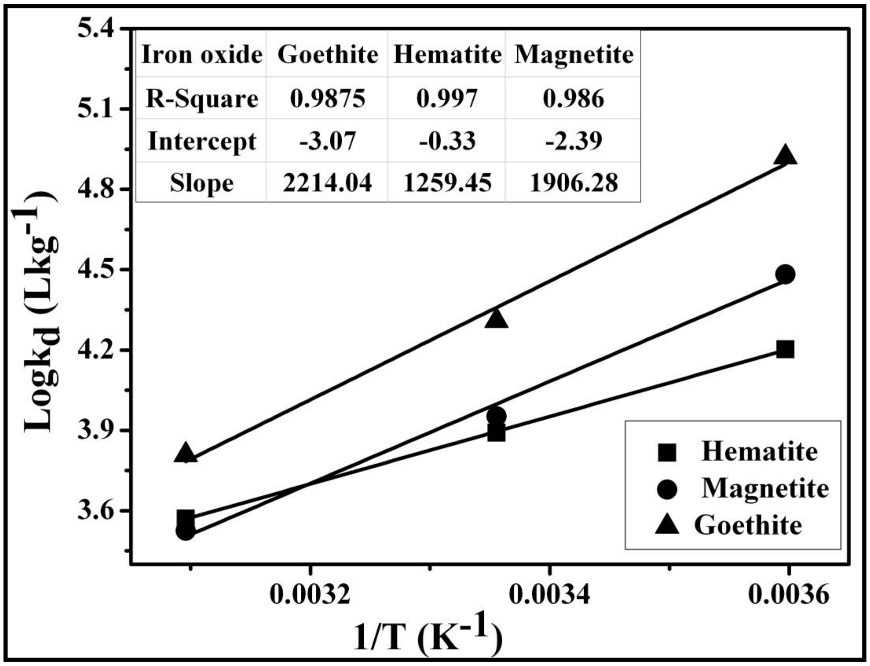

Iron oxide	Goethite	Hematite	Magnetite
R-Square	0.9875	0.997	0.986
Intercept	-3.07	-0.33	-2.39
Slope	2214.04	1259.45	1906.28

Figure 5.6: k_d vs 1/T plot for the sorption of Nb on iron oxides at pH 10

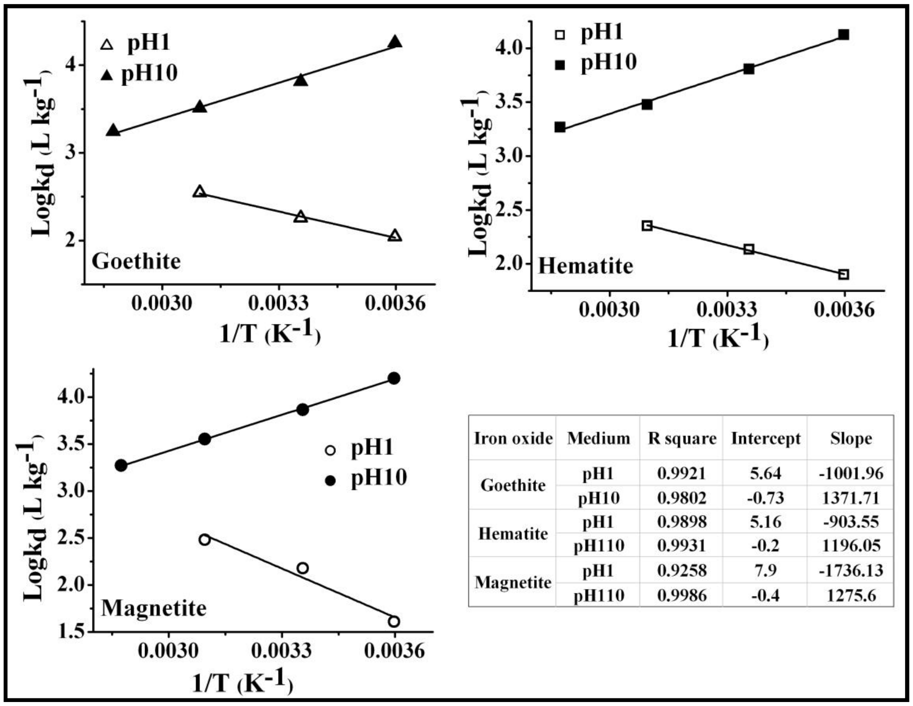

Iron oxide	Medium	R square	Intercept	Slope
Goethite	pH1	0.9921	5.64	-1001.96
	pH10	0.9802	-0.73	1371.71
Hematite	pH1	0.9898	5.16	-903.55
	pH110	0.9931	-0.2	1196.05
Magnetite	pH1	0.9258	7.9	-1736.13
	pH110	0.9986	-0.4	1275.6

Figure 5.7: k_d vs 1/T plot for the sorption of Pa on iron oxides at pH 1 and pH 10

Table 5.2: Thermodynamic parameters of the sorption of Nb on iron oxides at pH 1 and pH 9 (at 273K)

Iron oxides	**pH**	**ΔG^o(kJM^{-1})**	**ΔH^o(kJM^{-1})**	**ΔS^o(JK^{-1}M^{-1})**
Goethite	1	-7.25	18.05	92.67
	9	-44.32	-42.4	-7.07
Hematite	1	-12.1	12.21	89.03
	9	-31.38	-24.11	-6.31
Magnetite	1	-10.82	35.23	168.68
	9	-50.0	-36.5	-45.76

Table 5.3: Thermodynamic parameters of the sorption of Pa on iron oxides at different pH (at 273K)

	Goethite		
pH	**ΔG^o(kJM^{-1})**	**ΔH^o(kJM^{-1})**	**ΔS^o(JK^{-1}M^{-1})**
1	-10.30	19.18	107.99
10	-30.08	-26.26	-13.97
	Hematite		
1	-9.67	17.3	98.79
10	-23.95	-22.95	-3.83
Magnetite			
1	-8.05	33.24	151.26
10	-26.51	-24.41	-7.65

5.3.4. XAFS data interpretation

XAFS spectroscopic study of Nb in different kind of matrix like silica, alumina are available in the literature where Nb is present in the percentage level and the analysis has been carried out in solid state [219, 220]. The XAFS study of Nb in colloid type matrix in mM concentration level is really scanty. The normalized X-ray absorption near edge structure (XANES) spectra at Nb K-edge is shown in Figure 5.8 for all the three pH conditions namely pH 1, 6.5 and 10.5. The same absorption edge positions for all three pH systems suggest identical oxidation state of Nb. XANES spectra are in general highly sensitive to the oxidation state and coordination geometry of the absorbing atom and any difference in absorption edge and spectra, suggests different coordination environment around Nb atom sorbed on silica at different pH conditions.

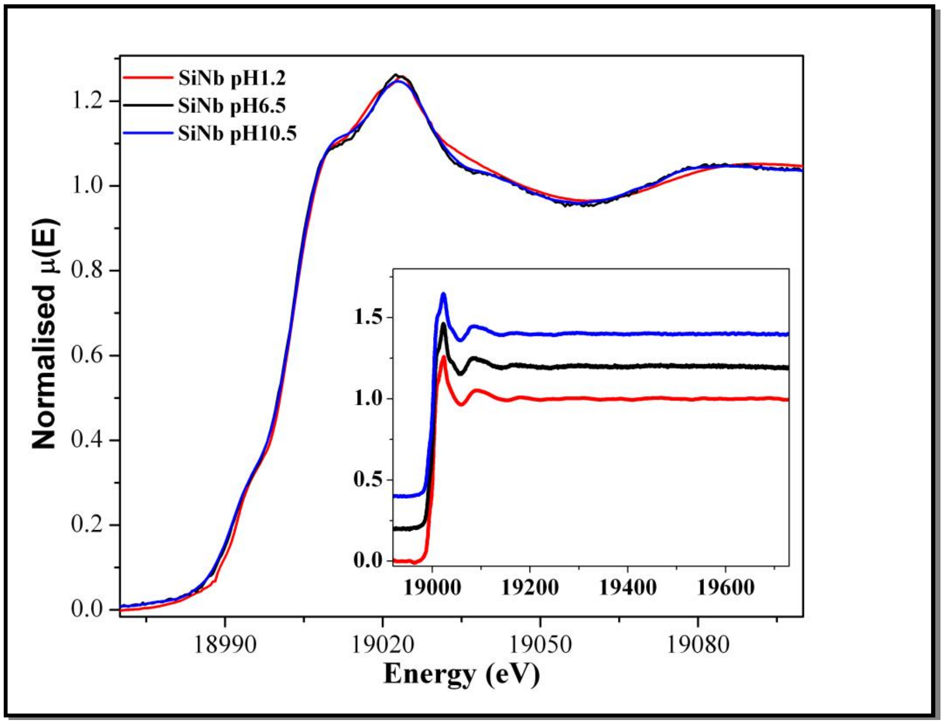

Figure 5.8: Normalised XANES spectra at Nb K edge of Nb-SiO_2 at different pH. The inset shows EXAFS spectra.

$\chi(R)$ vs R plots generated at Nb K-edge using Fourier transform range of k=3.0-9.5 Å^{-1} from the μ(E) vs E spectra following the methodology described above are shown in Figure 5.8. The theoretical backscattering amplitudes of Nb-O and Nb-Si are calculated assuming

$K_2Nb_2Si_4O_{14}$ structure since after extensive search it has been found that the Nb-O and Nb-Si bond lengths of the above compound more or less agree with that obtained in the present case [221]. However, it should be noted here that assumption of the above structure has only been used as an initial guess structure of the fitting process and does not critically affect the final results. During the fitting, bond distances, co-ordination numbers (including scattering amplitudes) and disorder (Debye-Waller) factors (σ^2), which give the mean square fluctuations in the distances, have been used as fitting parameters. The best fit $\chi(R)$ versus R plots (Range R=1.0-3.5 Å) of the samples have been shown in Figure 5.9 along with the experimental data. The best fitting results are tabulated in Table 5.4 at Nb K-edge.

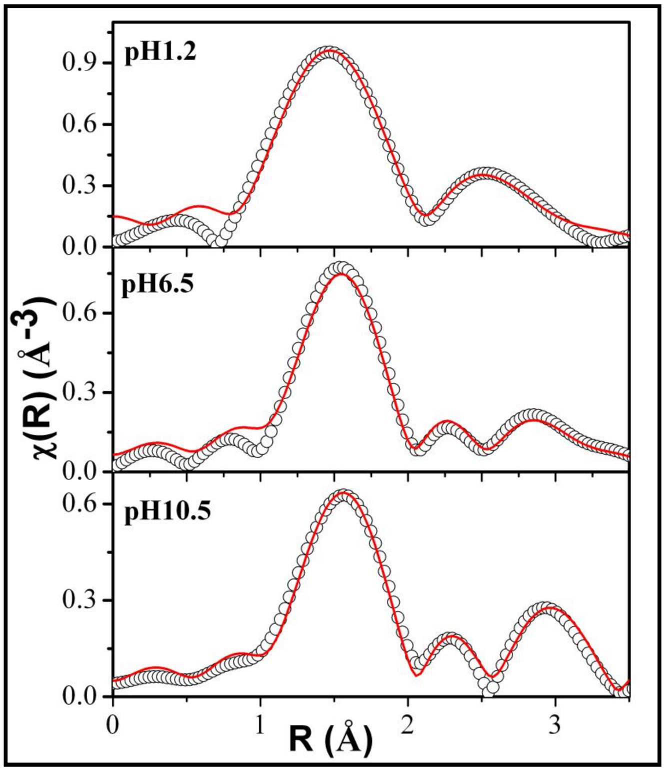

Figure 5.9: Fourier transformed EXAFS spectra of Nb-SiO_2 at Nb K edge at different pH (Scatter points) and theoretical fit (Solid line).

The Fourier transform EXAFS spectra shown in Figure 5.9 is phase uncorrected, which shows coordination peaks at lower R, however the fitting results are obtained after phase correction. In case of Nb-SiO_2 (pH 1.2) system, there are two peaks at 1.5 Å and 2.5 Å as depicted in Figure 5.9, which corresponds to at least two shells of atoms in the vicinity of Nb atom, in our case (aqueous medium) these might be O atoms at different distance. Phase corrected fitting results indicate that, there are two O atom nearest to Nb at a distance 1.98 Å, suggesting the presence of Niobyl group present as $[O=Nb=O]^+$ in hydrated condition. The other two O atoms at 2.08 Å may correspond to Nb-O bond which is less rigid and longer (Table 5.4).

The contribution of oxygen in the second coordination peak is identified using multiple k-weight procedure for the pH 1.2 systems (Figure 5.10). The same amplitudes of different k-weighted spectra for the first and second peaks confirmed similar atomic species in both coordination shells [222]. The second shell also contains two O atoms with an average distance of 2.43 Å which are characteristics of the equatorial water molecules around Nb (Table 5.4).

From the EXAFS data analysis for the system at pH 1.2, it is obvious that there is no nearby Si atom upto 3.46 Å and the EXAFS data could be fitted satisfactorily with O coordination shells (Table 5.4). The observation infers that there is no chemical bond formation between colloidal silica and Nb present in aqueous media. The finding also explains the low sorption of Nb on colloidal silica at pH 1.2. Hence the sorption at lower pH may be due to physisorption or ion exchange type interaction.

Similar to Nb-SiO_2 (pH 1.2) system, Nb-SiO_2 (pH 6.5) and Nb-SiO_2 (pH 10.5) also have two shells. For Nb-SiO_2 (pH 6.5) system, the first peak at ~1.5 Å (Figure 5.10) corresponds to 1.8 oxygen atoms at both 2.0Å and at 2.07Å distance respectively. For Nb-SiO_2 (pH 10.5) system, the first peak at ~1.5 Å (Figure 5.10) corresponds to 1.63 and 1.67 oxygen atoms at

2.01Å and at 2.07Å distance respectively. However, the second peak appeared at 3.0 Å, showed disparity from the system at pH 1.2 (Table 5.4).

Table 5.4: Bond length, coordination number and disorder factor obtained by EXAFS fitting for Nb-SiO_2 at Nb K edge

Sample	**Paths**	**R(Å)**	**N**	**σ^2**
SiNb(pH 1.2)	Nb-O	1.98±0.01	1.89±0.08	0.0018±0.0003
	Nb-O	2.08±0.01	1.80±0.08	0.0018±0.0003
	Nb-O	2.43±0.01	1.80±0.14	0.0010±0.0009
	Nb-O	3.46±0.01	3.92±0.28	0.0030±0.0010
SiNb(pH 6.5)	Nb-O	2.0±0.01	1.80±0.06	0.0020±0.0006
	Nb-O	2.07±0.01	1.80±0.06	0.0020±0.0006
	Nb-Si	3.44±0.02	1.32±0.12	0.0030±0.0010
SiNb(pH 10.5)	Nb-O	2.01±0.01	1.63±0.08	0.0027±0.0006
	Nb-O	2.07±0.01	1.67±0.08	0.0027±0.0006
	Nb-Si	3.50±0.01	1.65±0.21	0.0017±0.0010

At pH 6.5, different amplitudes for different k-weighted spectra for second peak have been found, which suggests different species than oxygen in second peak (Figure 5.11). The second peak has contributions from Si at the distance of 3.44 Å.

In the case of the system at pH 6.5, EXAFS data analysis clearly showed the presence of O atoms in first coordination sphere and Si atoms in the second coordination sphere of Nb (Table 5.4). This implies the formation of chemical bond between silica and Nb atoms, present in aqueous media via oxygen bridge.

The formation of chemical bonds between Nb and Si leads to high sorption of Nb onto silica at this pH condition. The Si atom density around Nb atom at pH 6.5 is about 1.32, which indicates that majority of the Nb species get bonded with silica through one silanol group (-Si-OH), and rest through two silanol groups. To be mentioned here that the EXAFS study of transuranic element, neptunium (V), in different sorbents like goethite and hematite, are reported in the literature for neutral or slightly basic medium [203,223]. The studies reveal the formation of the inner sphere complexes at the neutral pH conditions.

In basic medium (pH 10.5), the NbO_2^+ species are more disrupted than at pH 6.5 which is evident from the decreased number of O atom (N= 1.67) at 2.01 Å. Alike the system at pH 6.5, there are also the presence of Si atoms (N= 1.65) at 3.5 Å away from Nb atom, which is confirmed by k-weighted test (Figure 5.12), and suggest the probability of bond formation between Nb species and surface silanol groups of silica. As at pH 10.5, the Si atom density around Nb is 1.65, which suggests that the maximum probability with which the Nb species get attached with silica through two silanol groups.

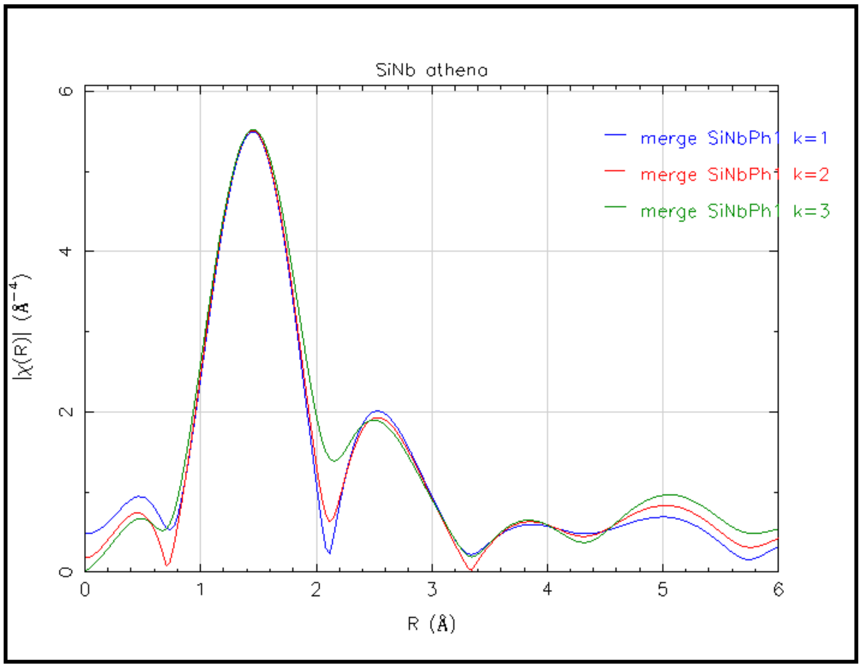

Figure 5.10: K-weight test for SiO_2-Nb system at pH 1

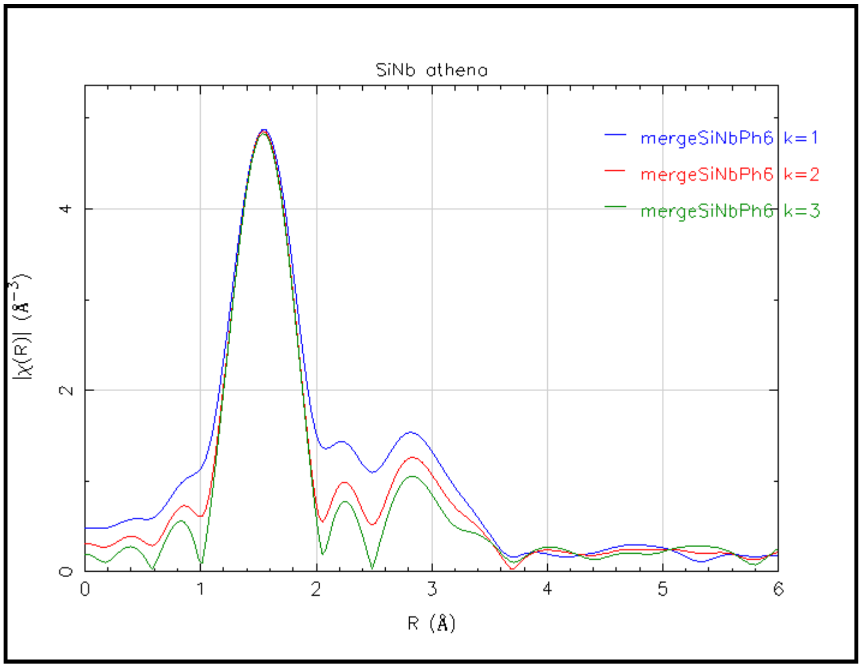

Figure 5.11: K-weight test for SiO_2-Nb system at pH 6.5

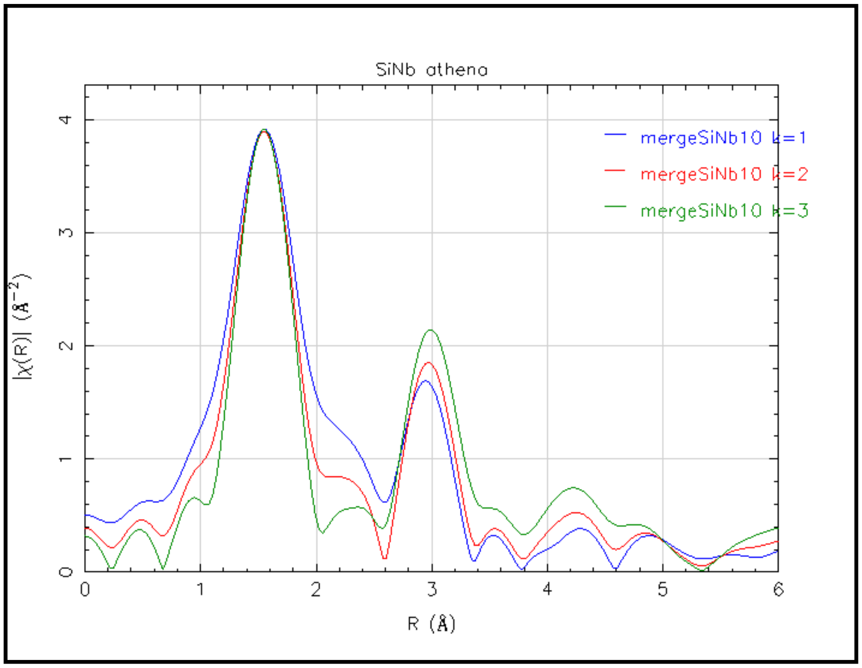

Figure 5.12: K-weight test for SiO_2-Nb system at pH 10.5

The parity among the ionic strength data, thermodynamic data and spectroscopic data together established the probable mechanism of sorption of Nb on silica in acidic, neutral and basic medium. In acidic medium, the mechanism is supposed to be outersphere complexation, whereas in neutral and basic medium, it is innersphere complexation. As Nb is considered as the chemical analogue of Pa(V) and from the experimental sorption data it is anticipated that both the elements follow the similar sorption mechanism at different pH conditions.

The probable sorption mechanism of Nb on silica in different pH is presented schematically in the Figure 5.13.Quite similar mechanism can also be suggested for Pa at different pH conditions

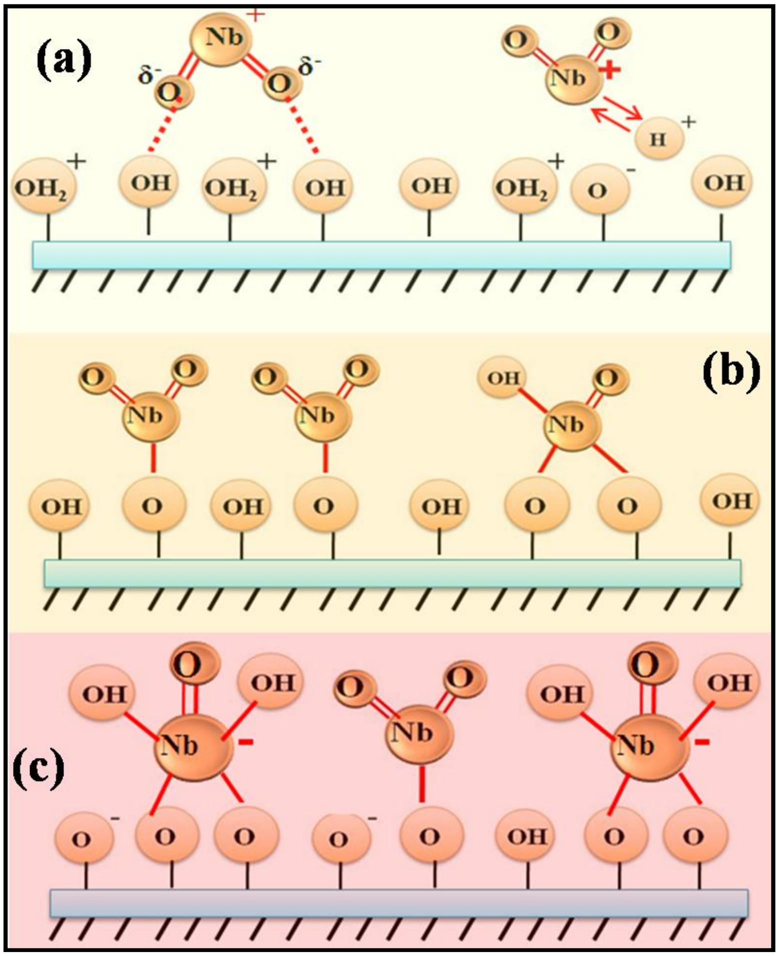

Figure 5.13: Probable sorption mechanism of Nb on silica at (a) pH 1 (b) pH 6.5 and (c) pH 10.5

The normalized X-ray absorption near edge structure (XANES) spectra at Nb K-edge for Nb-Fe_2O_3 system is shown in Figure 5.14 for all three pH conditions. The best fit $\chi(R)$ versus R plots (fitting range R=1.0 - 6 Å) of the samples have been shown in Figure 5.15 along with the experimental data. The details of the EXAFS data analysis of Nb sorbed hematite at different pH (1, 6 and 10) is given in Table 5.5. The Nb-Fe_2O_3 system at pH 1 shows that 1.88 numbers of oxygen atom at a distance of 1.76 Å, corresponds two NbO_2^+ group. The second and third peaks corresponds to the longer and less rigid Nb-O bond with the oxygen atoms from water molecules, satisfying the coordination number of Nb.

The contribution of oxygen in second coordination peak is identified using multiple k-weight procedure. The same amplitudes of different k-weighted spectra for the first and second peaks confirmed similar atomic species in both coordination shells. With increase of pH, the NbO_2^+ species becomes less stable which is evident from the decreasing number of oxygen atom in the first co-ordination shell of Nb.

For the Nb-Fe_2O_3 system at pH 6.5, there are 1.62, 2.02 and 1.97 numbers of oxygen atoms at 1.76 Å, 1.93 Å and 2.15 Å distances respectively surrounding Nb atom. The contribution from oxygen atoms confirmed by the multiple k-weighted test. The test shows that, the forth peak does not correspond to oxygen atom. The atom is identified as Fe with number density of 0.5 at a distance of 2.93 Å. This infers that the formation of chemical bond between hematite surface and the Nb during the sorption at pH 6.5.

The Nb-Fe_2O_3 system at pH 10 shows almost similar bonding features as that in the case of system at pH 6.5. The main difference is that the Fe atom density around Nb atom is higher in pH 10 system compared to system at pH 6.5. Thus there are 2 numbers of iron atoms at a distance of 2.72 Å.

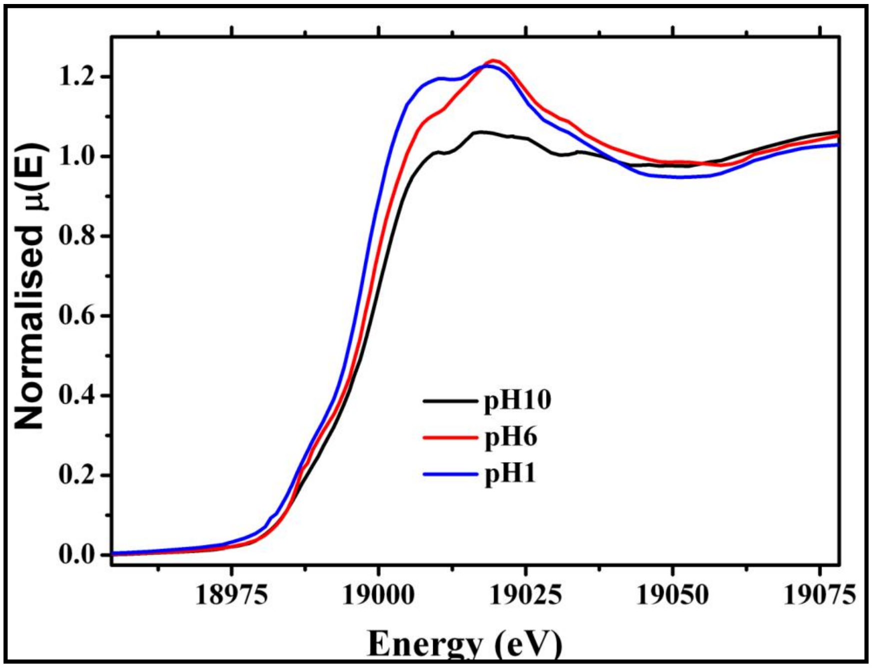

Figure 5.14: Normalised XANES spectra at Nb K edge of Nb-Fe_2O_3 at different pH. The inset shows EXAFS spectra

Table 5.5: Bond length, coordination number and disorder factor obtain by EXAFS fitting for Nb-Fe_2O_3 at Nb K edge

Sample	Paths	R(Å)	N	σ^2
Nb-Fe_2O_3 (pH 1)	Nb-O	1.76±0.01	**1.88**±0.90	0.0065±0.0012
	Nb-O	1.87±0.01	2.08±0.90	0.0065±0.0012
	Nb-O	2.07±0.01	2.94±0.60	0.0056±0.0023
Nb-Fe_2O_3 (pH 6)	Nb-O	1.76±0.02	**1.62**±0.36	0.0012±0.0010
	Nb-O	1.93±0.02	2.02±0.36	0.0012±0.0010
	Nb-O	2.15±0.02	1.97±0.36	0.0012±0.0010
	Nb-Fe	2.93±0.03	0.46±0.28	0.0015±0.0009
Nb-Fe_2O_3 (pH 10)	Nb-O	1.77±0.01	0.98±0.27	0.0010±0.0008
	Nb-O	1.97±0.01	2.98±0.27	0.0010±0.0008
	Nb-O	2.34±0.01	3.30±0.61	0.0049±0.0018
	Nb-Fe	2.72±0.02	2.01±0.48	0.0078±0.0022

This finding also proves the chemical bond formation at pH 10 between hematite surface and Nb which is getting sorbed. Similar type of observation is reported by Bots et al [224] where the authors found that Np(V) is coordinated with one iron atom at 2.88 Å distance for Np-Fe_2O_3 system at pH 11.

These findings support the physisorption mechanism in acidic pH and chemisorption mechanism at neutral and basic pH conditions. The probable sorption mechanism of Nb/Pa on hematite surface will be very similar to that as presented for Nb on silica in Figure 5.13.

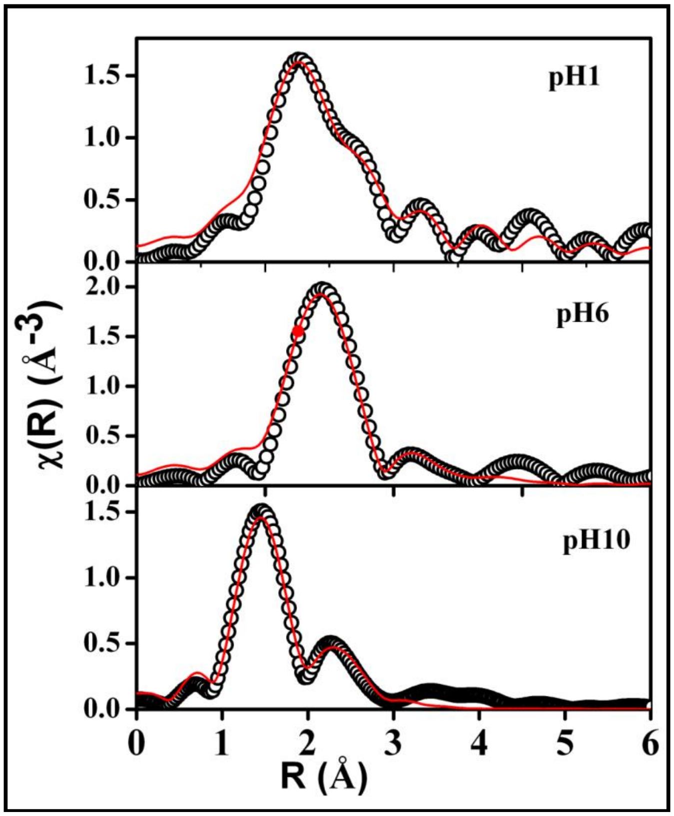

Figure 5.15: Fourier transformed EXAFS spectra of Nb-Fe_2O_3 at Nb K edge at different pH. (Scatter points) and theoretical fit (Solid line).

5.4. Conclusions

From the present study, major conclusions drawn are: (a) The ionic strength dependent sorption of Nb and Pa on silica and hematite under acidic pH conditions is primarily due to the Outer Sphere Surface complexation, which is solely governed by electrostatic forces. On the contrary, the insensitive nature of sorption with ionic strength in neutral and alkaline pH conditions indicates Inner Sphere Surface Complexation, which is governed by electron sharing or bond formation. (b) Enthalpy changes associated with the sorption process at different pH further supports the observation of the ionic strength dependent results. (c) XAFS study of the Nb sorbed colloidal silica at different pH clearly shows that in acidic pH, Nb is not coordinated with Si atoms and the whole coordination is satisfied by oxygen atoms only. In neutral and basic medium Nb is bonded with one to two Si atoms indicating Nb-O-Si type co-ordinations and thus supporting chemisorption mechanism. In the case of hematite also, in acidic pH, there is no evidence of Nb and Fe bonding, oxygen atom satisfying the whole coordination sites of Nb. In neutral and basic medium, however Nb is coordinated with Fe atoms suggesting Nb-O-Fe type coordination and hence chemisorption mechanism. So in the present study, there is a good agreement among the chemical, thermodynamic and spectroscopic data which together establish the physisorption nature in acid medium and chemisorptions in neutral and basic medium.

LIST OF ABBREVIATION

Nuclear Fuel Cycle	NFC
Ammonium Di-uranate	ADU
Fast Breeder Test Reactor	FBTR
Pressurized Heavy Water Reactor	PHWR
Low Level Waste	LLW
Intermediate Level Waste	ILW
High Level Waste	HLW
High Efficiency Particulate Absorber	HEPA
Humic Substances	HS
Humic Acids	HA
X-Ray Absorption Fine Structure	XAFS
Time Resolved Laser Fluorescence Spectroscopy	TRLFS
X-Ray Photoelectron Spectroscopy	XPS
Distribution Coefficient	k_d
X-Ray Diffraction	XRD
Brunauer-Emmett-Teller	BET
High Purity Germanium Detector	HPGe
Dynamic Light Scattering	DLS
Energy Dispersive X-Ray Fluorescence	EDXRF
Energy Dispersive X-Ray Spectrometry	EDS
Fourier Transfomed Infrared Spectroscopy	FTIR

SYNOPSIS

Since the discovery of radioactivity, it finds application in various fields of science & technology. It has enriched our society in several areas namely power production, medical science, agriculture, industry and strategic applications. In the field of power production, the term Nuclear Fuel Cycle (NFC) is used to describe the entire cycle starting from the mining of uranium to the reprocessing of spent fuel and the final disposal of the radioactive waste. The process from mining to fuel fabrication is called Nuclear Front End, whereas the reprocessing and waste management is termed as Nuclear Back End of the NFC. The main source of high-level radioactive waste is the fission products in the spent fuel from nuclear reactors. Other sources of radioactive waste arise from nuclear weapons testing, decommissioning of nuclear facilities and the waste from radioactive laboratories. It has been envisaged that high-level waste originating from the nuclear reprocessing plant will be stored underground in geological repositories after suitable treatment [1]. The main objective of underground storage of radioactive waste is to isolate it from the environment for a long period of time to avoid any possible release to cause any undue radiation exposure [2].

Nowadays, the back end of the NFC has become the most concerned and challenging research area in the nuclear industry, although there are standard protocols in place for the management and disposal of radioactive waste. The concern is due to any possible unwanted release and migration of radionuclides [3], more specifically those radioisotopes that have high yield in the fission/activation process and long half-life [4]. In general, the factors affecting the release and migration of the radionuclides in the environment are precipitation, complexation and sorption processes. Precipitation process takes the radionuclides in solid phase, thereby limits the concentration in the solution phase and thus retards their release and migration. Complexation of the radionuclides with organic and inorganic ligands present in aqueous medium can increase the release and migration of the species due to increased solibilization of the complexes. This increases the concentration of the radionuclides in the mobile phase. Attachment of radionuclides to mineral or rock surfaces in contact with aqueous phase, called the sorption process, can reduce the migration process substantially [5]. Based on the above three processes, most of the existing literature suggests that the tri and tetravalent radioisotopes cause no major hazard, as they have very high tendency to get sorbed onto the material engineered for their isolation and also in host rocks [6]. Earlier, a two-phase model, consisting of a mobile and a stationary phase, was used to explain the migration of radionuclides in aquatic system. However, a recent study reveals the migration of ^{239}Pu upto a distance of about 1.3 km in 30 years from the Nevada test site [7]. Penrose et al. [8] have studied the behaviour of Pu and Am in the Mortandad canyon and observed the migration rate of these radionuclides of about 0.5 km y^{-1} from the source. The two-phase model was unable to explain such fast and long-distance migration of radionuclides observed in previous cases. Another drawback of the two-phase model is its inability to explain the migration of radionuclides which have very low aqueous solubility. It was suggested that the colloids present in groundwater provide an additional phase causing enhanced migration [7]. Therefore, a three-phase model consisting of a mobile phase, a stationary phase and suspended colloids in mobile phase has been introduced to explain the enhanced migration of radionuclides and other contaminants in groundwater [9, 10].

The most important natural ligands found in groundwater are the humic acids. The presence of humic acid may affect the sorption and migration of radionuclides in the groundwater [11, 12]. It is reported that the anthropogenic actinides are about 10 times more concentrated in humic acid fraction than in the overall topsoil [13]. The complexation of humic acids with radionuclides increases the mean residence time of actinides in the mobile phase, which in turn reduces the sorption of the radionuclides to the stationary phase and thus enhances their migration. Humic acids can also affect the sorption behaviour of radionuclides by altering the oxidation state e.g. U(VI) to U(IV) and Np(V) to Np(IV) [13].

Oxides, especially those of Si, Al, and Fe, occur as colloids in groundwater. Various aspects of colloids that facilitate the transport of radionuclides in natural groundwater systems have been reviewed by Patera et al. [14]. Extensive work has also been carried out to understand the sorption of radionuclides on several minerals which include hydrous oxides of Fe [14-17], Mn [18], Si and Al [19], montmorillonite [20], bentonite [21] etc., studied for several radioisotopes like U, ^{239}Pu, ^{244}Cm, ^{241}Am, ^{60}Co, ^{152}Eu, ^{230}Th, ^{90}Sr, ^{137}Cs and so on.

Literature regarding leaching, sorption and migration of niobium (^{94}Nb) and protactinium (^{231}Pa) [22-24] are scanty and this motivated us to carry out extensive sorption studies for these two radionuclides in different hydrous oxides of Si, Fe and Mn, present in aquatic systems. The effect of pH, naturally occurring humic acid ligands, ionic strength, equilibration time and temperature on the sorption behaviour of ^{94}Nb and ^{231}Pa nuclides on silica, iron oxides and manganese dioxide have been evaluated. The sorption mechanism has been elucidated based on the classical sorption data (ionic strength and temperature dependent sorption study) and the spectroscopic evidences (Extended X-ray Absorption Fine Structure) obtained from the present study. In the PhD thesis, the work has been presented and discussed in six chapters, briefly described as follows.

Chapter 1: Introduction

This chapter provides the general introduction of the thesis encompassing the basic aspects of the element niobium (Nb) and protactinium (Pa). The course, in which ^{94}Nb and ^{231}Pa are generated in the nuclear industry, may be described as follows. Zirconium-niobium (Zr-Nb) alloy is used as pressure tubes in nuclear power reactors [25] because of its excellent mechanical strength [26] and very high resistance to hydride attack. ^{94}Nb (half-life: 2.03 x 10^4 y) is generated in the pressure tube by the (n,γ) reaction of the stable isotope ^{93}Nb. The presence of ^{94}Nb, along with other fission and activation products in discharged pressure tubes, results in large radiation field. The short and medium-lived radioisotopes (half-life: ≤ 1.5 y) decay off after 8-10 years of cooling [27]. ^{94}Nb activity remains for a prolonged period due to the long half-life.

Thoria is irradiated in a nuclear reactor for the production of fissile isotope ^{233}U via (n, γ) nuclear reaction of ^{232}Th and subsequent beta decay of ^{233}Th. Along with ^{233}U, ^{231}Pa (half-life: 3.27 x 10^4 y) is also generated via (n, 2n) nuclear reaction of ^{232}Th and consecutive beta decay [28]. After extraction of ^{233}U, ^{231}Pa remains in the aqueous phase along with other actinides. This aqueous phase is considered as high-level radioactive liquid waste. The severe concern in the handling and management of this high-level waste is the presence of ^{231}Pa, because the isotope is both long-lived and alpha-emitting [29]. ^{94}Nb and ^{231}Pa are thus two important radionuclides in radioactive waste and could have long term radiological impact. Chemical properties of these two elements and their comparisons are discussed in this chapter, which are the basis of the present thesis work.

Chapter 2: Sorption of ^{94}Nb and ^{231}Pa on colloidal silica

Sorption of niobium (Nb) and protactinium (Pa) on silica colloids was studied using radiotracer (^{94}Nb and ^{231}Pa) in the pH range of 2-11 in $NaClO_4$ medium, adopting batch equilibration method. Gamma activity measurements were carried out using high purity germanium (HPGe) detector coupled to 8k channel analyzer. Silica was characterized using X-ray diffraction (XRD), light scattering and surface area measurements. The point of zero charge for silica colloids was about pH 2. It is found that both Nb and Pa were strongly sorbed on silica colloids in the pH range of 3 to 9 in $NaClO_4$ medium. The sorption is lower (70-80 %) below pH 3 and above pH 9. There is no significant change in the sorption behaviour of both Nb and Pa on silica colloids in the presence of humic acid between pH 3 to 9. However, there is a small increase in the sorption below pH 2 and a small reduction in sorption above pH 10.

The pH dependent sorption phenomenon observed can be explained in terms of the chemical species of Nb and Pa exist at different pH condition and the variation in the zeta potential of silica at different pH. Literature reports suggest that both the elements exist as single positively charged species below pH 3 and this was confirmed in the case of Pa by determining the average charge (~ +1) in dilute $HClO_4$ medium (0.1 to 3M). Coulombic repulsion between the positively charged Pa and positive surface charge on silica colloids may be the reason for the lower sorption below pH 3. The strong sorption on silica colloids in the pH range 3 to 9 was assigned to the surface complexation between neutral species of Nb/Pa with the silanol groups of silica colloids. In basic pH, both Nb and Pa exist as negatively charged species and the zeta potential of silica is highly negative. Therefore, coulombic repulsion between them reduces the sorption of Nb/Pa on silica colloids in the alkaline condition.

The slight increase of sorption below pH 2 in the presence of humic acid (HA) may be due to sorption of humic acid on silica causing a reduction in surface charge of the colloids. In basic medium, carboxylate groups of humic acid may undergo complexation with Nb/Pa, increasing the concentration of the metal ions in the solution, and thus reducing their sorption on silica colloids.

Chapter 3: Sorption of ^{94}Nb and ^{231}Pa on various iron oxides

In this Chapter, results on the sorption of Nb and Pa on various iron oxide colloids are reported along with the effect of pH, ionic strength, humic acid and temperature on the sorption process. Iron oxides viz. goethite (FeOOH), hematite (α-Fe_2O_3), and magnetite (Fe_3O_4) were chemically synthesized and characterized by XRD, particle size, surface area, and zeta potential measurements. Results show that the sorption of Nb on all the three iron oxides was low (10-20 %) at pH 1, increased to ~ 90% at pH 8 and decreased marginally above pH 8. Presence of humic acid resulted in increased sorption of Nb/Pa on iron oxides in acidic medium, whereas the reverse was observed in basic medium. In acidic medium (pH 1), it is observed that the sorption is decreased with an increase in the ionic strength, and the effect of ionic strength is found to be strongest in the case of goethite, and least in the case of hematite. In basic medium (pH 10), the effect of ionic strength on sorption is quite negligible for all three oxides. From the above observations, it is inferred that the sorption in acidic pH occurs mainly due to ion-exchange between positively charged species of Nb/Pa and the surface –OH groups on the iron oxides. In basic pH, ion exchange phenomenon cannot contribute to the sorption, because the existence of Nb/Pa as the anionic species, causing a reduction in the sorption. Thermodynamic parameters viz. activation energy, enthalpy, entropy, free energy, and sticking probability were estimated to understand the mechanism of the sorption process. Although the enthalpy is found to be positive, the free energy change is overall negative, suggesting the sorption process to be an entropy-driven phenomenon. The sorption process followed pseudo-second-order kinetics and the sticking probability model of sorption indicated that the process is indeed chemisorption. The dissolution study of iron oxides shows that the iron concentrations in the supernatant in the case of goethite and hematite are negligible throughout the pH range, whereas ~3 % magnetite got dissolved in acidic pH. The solubility of magnetite in the acidic region may be due to the presence of Fe(II) in its structure which partially goes to the solution phase. From the above studies, it is clear that sorption is not influenced by the dissolution of goethite and hematite in acidic pH, though a mild effect exists in the case of magnetite.

Chapter 4: Sorption of ^{94}Nb and ^{231}Pa on manganese dioxide

The sorption of Nb/Pa on synthesized manganese dioxide has been described in this Chapter. The effects of pH, ionic strength, humic acid, temperature and equilibration time were investigated in a series of batch equilibrium experiments. The synthesized oxide was characterized using XRD, Fourier transform infrared (FTIR) spectroscopy, Scanning electron microscopy (SEM), surface area, particle size, and zeta potential measurements. The sorption is found to be affected by solution pH, ionic strength and humic acid. The sorption is high in neutral and near neutral pH zone (~ 96 %) but lower sorption is observed both in acidic pH (70-80 %) and basic pH (~ 85 %) conditions. Sorption decreases in acidic pH with an increase in ionic strength and reverse effect is seen in basic pH, although the effect in the latter case is less prominent. From the above results, it is inferred that the mechanism of sorption is the physisorption or outer sphere complexation at acidic pH and chemisorption or innersphere complexation at basic pH conditions. Presence of humic acid enhances the sorption in acidic pH, which indicates that mineral bound humic acid facilitates the sorption process at low pH whereas at higher pH, the dissolved humic acid complexes with Nb/Pa causing a decrease in sorption on manganese dioxide. The sorption process is found to be endothermic in acid medium but the positive entropy change makes the free energy of the sorption process negative and hence the process is spontaneous. However, the sorption in basic medium is exothermic and the high magnitude of enthalpy change indicates that the sorption process follows the chemisorption mechanism. Kinetics of the sorption is found to follow pseudo first order rate under acidic pH whereas pseudo second order rate under basic pH. Pseudo first order fitting under low pH condition suggests the physisorption mechanism whereas pseudo second order kinetic fitting proposes the chemisorption mechanism at high pH condition.

Chapter 5: Evaluation of sorption mechanism using Extended X-ray Absorption Fine Structure (EXAFS)

The sorption experiments discussed in the previous chapters were carried out using tracer solutions of ^{94}Nb and ^{231}Pa in nanomolar (nM) concentration, which is not sufficient for EXAFS studies as the method require higher concentration. Due to the constraints of handling radioactivity at the EXAFS facility, inactive Nb solution was used in elevated concentration (mM) for the sample preparation. Nb sorbed silica samples at pH 1.2, 6.5 and 10.5 were prepared and kept hydrated, to keep the bonding feature intact. Complete drying of the samples were avoided because it may change the binding features.

The EXAFS measurements were carried out at the Energy-Scanning EXAFS beamline (BL-9) at the Indus-2 Synchrotron Source (2.5 GeV, 100 mA) in Raja Ramanna Centre for Advanced Technology (RRCAT), Indore, India. X-ray absorption spectrometry (XAS) measurements were performed in transmission mode placing the slurry sample in a transparent glass cuvette in the beam path. The experiments were performed at Nb K-edge energy. The same absorption edge position for all three pH condition suggests identical oxidation state for Nb.

The Fourier transform EXAFS spectra of Nb-SiO_2 at pH 1.2 suggests that there are two O atoms nearest to Nb at a distance 1.98 Å, indicating the presence of niobyl group as $[O{=}Nb{=}O]^+$ in hydrated condition. The other two O atoms at 2.08 Å may correspond to Nb-O bond which is longer and less rigid. The same amplitudes of different k-weighted spectra for the first and second peaks confirm similar atomic species in both the coordination shells. The second co-ordination shell also contains two O atoms with an average distance of 2.43 Å, which are the characteristics of equatorial water molecules around Nb. From the analysis of the EXAFS data at pH 1.2, it is obvious that there is no nearby Si atom upto 3.46 Å and the EXAFS data could be fitted satisfactorily with oxygen coordination shells.

It is inferred that there is no chemical bond formation between colloidal silica and Nb present in aqueous media. This finding also explains the low sorption of Nb on colloidal silica at pH 1.2. Hence the sorption at lower pH may be attributed to physisorption or ion exchange mechanism.

Although the systems at pH 6.5 and pH 10.5 have the same type of environment in the first coordination shell, the analysis suggests the presence of Si atom in the second coordination sphere. This implies the formation of chemical bond between silica and Nb atoms via oxygen bridge. The formation of chemical bonds between Nb and Si leads to high sorption of Nb onto silica at these pH conditions. The Si atom density around Nb atom at pH 6.5 and pH 10.5 are found to be about 1.32 and 1.65, respectively.

The EXAFS data of Nb sorbed hematite at three different pH (1, 6 and 10) also confirmed that at pH 1, Nb is not coordinated with Fe atom whereas at pH 6 and at pH 10, Nb is coordinated with 0.5 and 2 numbers of Fe atoms at 2.93 Å and 2.72 Å distances, respectively. These findings support the physisorption mechanism in acidic pH and chemisorption mechanism at neutral and basic pH conditions.

Chapter 6: Summary and future perspectives

In this Chapter, a brief summary of the research work carried out under the PhD programme has been presented, highlighting the major observations and suggesting the future perspectives of the present investigation.

The major outcomes of the present study are as follows:

(i) The sorption of both ^{94}Nb and ^{231}Pa in the acidic range is low and follow physisorption mechanism. The sorption is however quantitative in neutral or near neutral pH region and suggested to chemisorption mechanism. These propositions have been established based on ionic strength and temperature dependent sorption data as well as from the EXAFS spectroscopic evidences.

(ii) The quantitative sorption in neutral to near neutral pH region indicates that in the natural aquatic condition the migration of these two radionuclides is mainly assisted by the colloids present in the medium.

(iii) The naturally occurring complexing ligand i.e. humic acid, can alter the Nb/Pa sorption both in acidic and basic region, either by its self-absorption onto the colloids or by its complexation with the radionuclides at those respective pH conditions.

Future perspective of the present investigation:

(i) EXAFS investigation in Nb sorbed pyrolusite systems can provide more information on the sorption mechanism.

(ii) More detailed spectroscopic investigations on the sorption behaviour of Nb/Pa on iron oxides of mixed oxidation state (magnetite) and studies in regards to changing of metal ion oxidation states can provide more insight of the sorption process.

(iii) Utilization of laser-based fluorescence techniques to study the sorption mechanisms in very low concentration level of the radionuclides can provide more relevant information.

(iv) Sorption study of ^{94}Nb and ^{231}Pa on naturally occurring bentonite, clay minerals and soil samples are worth to be investigated in regard to the migration of radionuclides in aquatic systems.

References

1. Geological disposal of radioactive waste: An overview of the current status of understanding and development. Organization for economic cooperation and development (OECD), 1984, OECD publication service, Paris.
2. F.R. Rinderknecht, H. Geckies, T. Schafe, Bentonite erosion and colloid mediated transport of radionuclides in advection controlled system, Dissertation Karlsruher, Karlsruher Institut fur Technologie (KIT) (2017).
3. M.J. Apted, Radionuclide release from high-level nuclear-waste packages, J. Radioanal. Nucl. Chem. 142/1 (1990) 321-330.
4. D.J. Wiggins, J.A. Franz, Mobility of organic complexes of some NON-TRU fission and activation products: A selective review, PNL-2607 (UC-70), (1978) Pacific Northeast Laboratory, USA.
5. W. Stumm, J.J. Morgan, Aquatic Chemistry: Chemical Equilibria and Rates in Natural Waters. 3rd Edition, (1996) John Wiley & Sons, New York.
6. A.B. Khasanova, N.S. Shcherbina, S.N. Kalmykov, Yu. A. Teterin, A.P. Novikov, Sorption of Np(V), Pu(V), and Pu(IV) on colloids of Fe(III) oxides and hydrous oxides and MnO_2, Radiochemistry 49/4 (2007) 419-425.
7. A.B. Kersting, D.W. Efurd, D.L. Finnegan, D.J. Rokop, D.K. Smith, J.L. Thompson, Migration of Plutonium in ground water at the Nevada test site, Nature 397 (1999) 56-59.

8. W.R. Penrose, W.L. Polzer, E.H. Essington, D.M. Nelson, K.A. Orlandilini, Mobility of Plutonium and Americium through shallow aquifer in a Semiarld region, Environ. Sci. Technol 24/2 (1990) 228-234.
9. J.F. McCarthy, J.M. Zachara, Subsurface transport of contaminants, Environ. Sci. Technol. 23/5 (1989) 496-502.
10. B.D. Honeyman, Colloidal culprits in contaminants, Nature 397 (1999) 23-24.
11. S. Sachs, G. Bernhard, Influence of humic acids on the actinide migration in the environment: suitable humic acid model substances and their application in studies with uranium-a review, J. Radioanal. Nucl. Chem. 290 (2011) 17-29.
12. H. Geckies, T. Stumpf, Annual report on waste disposal, KIT SR-7617 (2011) KIT Scientific Publishing, Karlsruhe, Germany.
13. G. Buckau, Humic substances in performance assessment of nuclear waste disposal: actinide and iodine migration in the far field, 3rd Technical progress report, FZKA 7070 (2005) Karlsruhe Institute of Technology, Karlsruhe, Germany.
14. E.S. Patera, D.E.Hobart, A. Meijer, R.S. Rundberg, Chemical and physical processes of radionuclide migration at yucca mountain Nevada, J. Radioanal. Nucl. Chem. 142/1 (1990) 331-347.
15. T.D. Waite, J.A. Davis, T.E. Payne, D.A. Waychunas, N. Xu, U(VI) adsorption on ferrihydrite: application of a surface complexation model, Geochim. Cosmochim. Acta. 58/24 (1994) 5465-5478.
16. A.L. Sanchez, J.W. Murray, T.H. Sibley, The adsorption of Pu (IV)/(V) on goethite, Geochim. Cosmochim. Acta 49 (1985) 2297-2307.

17. B.A. Powell, R.A. Fjeld, D.I. Kaplan, J.T. Coates, M.S. Steven, Pu(V)O_2^+ adsorption and reduction by hematite and goethite, Environ. Sci. Technol. 39/7 (2005) 2107-2114.
18. J.L. Means, D.L. Krerer, M.R. Borcsik, D.O. Duguid, Radionuclide adsorption by manganese oxides and implication for radioactive waste disposal, Nature 274 (1978) 44-47.
19. E.R. Sylwestera, E.A. Hudsona, P.G. Allen, The structure of uranium (VI) sorption complexes on silica, alumina, and montmorillonite, Geochim. Cosmochim. Acta 64/14 (2000) 2431-2438.
20. E. Hartmann, H. Geckeis, T. Rabung, J. Lützenkirchen, T. Fanghäne, Sorption of radionuclides onto natural clay rocks, Radiochim. Acta 96 (2008) 699-707.
21. S.C. Rasai, J.W. Juang, Comparison of linear and nonlinear forms of isotherm models for Strontium sorption on sodium bentonite, J Radioanal and Nucl. Chem, 243/3 (2000) 741-746.
22. S. Kulmala, M. Hakanen, Sorption of protactinium on rocks in ground waters from Posiva investigation sites (POSIVA 98-12) (1998) University of Helsinki, Finland.
23. Y. Sakamoto, T. Ishii, S. Inagawa, Y. Gunji, S. Takebe, H. Ogawa, T. Sasaki, Sorption characteristics of actinium and protactinium onto soils, J. Nucl. Sci. and Technol., S3 (2002) 481-484.
24. H. Ervanne, M. Hakanen, J. Lehto, Modelling of niobium sorption on clay minerals in sodium and calcium perchlorate solutions, Radiochim. Acta, 102/9 (2014) 839-847.
25. H.G. Weidinger, Zr-Alloys, the nuclear material for water reactor fuel: A survey and update with focus on fuel for pressurized water reactor systems, 7th Int. Conf. on WWER Fuel Performance, Modelling and Experimental Support (2007) Albena, Bulgaria.
26. M. Howe-Grant, Kirk–Othmer encyclopedia of chemical technology, Vol-17, 4th ed. (1996) Wiley, New York, pp. 449-450.

27. S. Gangotra, P.M. Ouseph, S. Anantharaman, K.C. Sahoo, Gamma spectrometry studies on irradiated zircaloy pressure tubes, ZIRC-2002 (2002) BARC, Mumbai, India, pp. 658-674.
28. R.H. Rainey, J.G. Moore, Laboratory development of the acid Thorex process for recovery of consolidated edison Thorium reactor fuel. Oak Ridge National Laboratory, U.S. Atomic Energy Commission, ORN L-3155 (1962).
29. IAEA TECDOC-1450, Thorium fuel cycle - Potential benefits and challenges. Vienna, Austria (2005).

References

1. M. Salvatores, I. Slessarev, A. Tchistiakov (1998) The transmutation of long lived fission products by neutron irradiation. Nuclear Science and Engineering. 130: 309-319.
2. R. J. Silva, H. Nitsche (1995) Actinide environmental chemistry. Radiochim. Acta. 70(71): 377-396.
3. J.R. Oliver (1958) Thorex process: Third Uranium cycle studies. ORN L-2473, U.S. Atomic Energy Commission,USA.
4. K. Raj, K. K. Prasad, N. K. Bansal (2006) Radioactive waste management practices in India, Nucl. Eng. Des. 236: 914-930
5. P. K. Wattal (2013) Indian programme on radioactive waste management. Sadhana (Indian Academy of Science). 38(5): 849-857
6. P. K. Dey, N. K. Bansal (2006) Spent fuel reprocessing: a vital link in Indian nuclear power program. Nucl. Eng. Des. 236: 723-729
7. W. R. Penrose, W. L. Polzer, E. H. Essington, D. M. Nelson, K. A. Orlandilini (1990) Mobility of Plutonium and Americium through shallow aquifer in a Semiarld region. Environ. Sci. Technol 24(2): 228-234.
8. G. R Choppin (2007) Actinide speciation in the environment. J. Radioanal. Nucl. Chem. 273**:** 695.
9. F. J. Stevenson (1982) Humus Chemistry: Genesis, Composition, Reactions. John Wiley & Sons.
10. G. R. Choppin, L. Kullberg (1978) Protonation Thermodynamics of Humic acid. Inorg. Nucl. Chern. 40: 651-654.
11. G. Buckau (2005) Humic substances in performance assessment of nuclear waste disposal: actinide and iodine migration in the far field. 3rd Technical progress report, FZKA 7070,

Karlsruhe, Germany.

12. E. M. Murphy, J. M. Zachara (1995) The role of sorbed humic substances on the distribution of organic and inorganic contaminants in groundwater. Geoderma 67: 103-124.
13. J. A. Davis, J. O. Leckie (1978) Effect of adsorbed complexing ligands on trace metal uptake by hydrous oxides. Environ. Sci. Technol.12: 1309-1315.
14. J. A. Davis (1984) Complexation of trace metals by adsorbed natural organic matter. Geochim Cosmochim Acta. 48: 679-691.
15. M. M. Benjamin, J. O. Leckie (1981) Multiple-site adsorption of Cd, Cu, Zn, and Pb on amorphous iron oxy-hydroxide. J. Colloid and Interface Sci. 79: 209-221.
16. P. W. Schindler, P. Liechti, J. C. Westall (1987) Adsorption of copper, cadmium and lead from aqueous solution to the kaolinite/water interface. Netherlands J. Agricultural Science. 35: 219-230.
17. N. D. Bryan, L. Abrahamsen, N. Evans, P. Warwick, G. Buckau, L. Weng, W. H. Van Riemsdijk (2012) The effects of humic substances on the transport of radionuclides: recent improvements in the prediction of behaviour and the understanding of mechanisms. Appl.Geochem. 27: 378-389.
18. G. R. Choppin (1999) Role of humics in actinides behaviour in ecosystem. In: Chemical separation technologies and related method for nuclear waste management (G. R. Choppin and M. Kh Khankhasayev edn), Kluwer academic publishers, 247.
19. P. Zeh, J. I. Kim, C. M. Marquardt, R. Artinger (1999) The reduction of NP(V) in groundwater rich in humic substances. Radiochim Acta. 87: 23-28.

20. J. B. Fein (2002) The effects of ternary surface complexes on the adsorption of metal cations and organic acids onto mineral surfaces. The Geochemical Society, Special Publication No.7, 365-378. Editors: R Hellmann and S. A. Wood

21. B. D. Honeyman (1999) Colloidal culprits in contamination. Nature. 397: 23-24

22. W. Hauser, H. Geckeis, J. I. Kim, T. Fierz (2002) A mobile laser-induced breakdown detection system and its application for the in situ-monitoring of colloid migration. Colloids Surf. A 203: 37–45.

23. S. N. Kalmykov, V.V. Kriventsov, Y. A. Teterin, A. P. Novikov (2007) Plutonium and neptunium speciation bound to hydrous ferric oxide colloids. Comptes Rendus Chimie 10:1060.

24. J. M. Zachara, C. T. Resch, S. C. Smith (1994) Influence of humic substances on Co^{2+} sorption by a subsurface mineral separate and its minealogic components. Geochim. Cosmochim. Acta 58(2): 553-566.

25. D.A. Ramsay (1988) The role of colloids in the release of radionuclides from nuclear waste. Radiochim. Acta 44(45): 165-170.

26. V. Neck, M. Altmaier, T. Fanghanel (2007) Solubility of plutonium hydroxides/hydrous oxides under reducing conditions and in the presence of oxygen. Comptes Rendus Chimie 10: 959-977.

27. M. Altmaier, V. Neck, T. Fanghanel (2004) Solubility and colloid formation of Th (IV) in concentrated NaCl and $MgCl_2$ solution. Radiochim. Acta, **92:** 537-543.

28. A. L. Sanchez, J. W. Murray, T.H. Sibley (1985) The adsorption of plutonium IV and V on goethite. Geochim. Cosmochim. Acta 49: 2297.

29 A. P. Novikov, S. N. Kalmykov, S. Utsunomiya, R. C. Ewing, F. Horreard, A. Merkulov, S.

B. Clark,V.V. Tkachev, B. F. Myasoedov (2006) Colloid transport of Plutonium in the far-field of the Mayak Production Association, Russia. Science. 314: 638–641.

30. T. Schafer, F. Huber, H. Seher, T. Missana, U. Alonso, M. Kumke, S. Eidner, F. Claret, F. Enzmann (2012) Nano particles and their influence on radionuclide mobility in deep geological formations. Appl. Geochem. 27: 390-403.
31. H. Geckeis, T. Rabung (2008) Actinide geochemistry: From the molecular level to the real system. J. Contam. Hydrol. 102: 187.
32. J. F. McCarthy, J. M. Zachara (1989) Subsurface transport of contaminants: mobile colloids in the subsurface environment may alter the transport of contaminants Environ. Sci. Technol. 23: 497-502.
33. K. J. Wilkinson, J.R. Lead (2006) Environmental colloids and particles behaviour, separation and characterisation. In: IUPAC Series on Analytical and Physical Chemistry of Environmental Systems. John Wiley & Sons, New York.
34. K. S. Smith (1999) Metal sorption on mineral surfaces: an overview with examples relating to mineral deposits. The Environmental Geochemistry and Mineral Deposits, US Geological Survey. 161-182.
35. J. A. Apps (2004) Sorption of fission product radionuclides ^{137}Cs and ^{90}Sr by Savannah River site sediment impregnated with colloidal silica. Radiochim Acta. 92: 419-432
36. S. Sato (2000) Effects of humic acid on the sorption of Am(III) and Cm(III) on Kaolinite. Radiochim Acta 88: 717-721.
37. S. Sato (2004) Am(III) and Eu(III) uptake on hematite in the presence of humic acid. Radiochim Acta. 92: 697-702.
38. G. Lujanieneo, A. Plukis, E. Kimtys, V. Remeikis, D. Jankünaiteo,B. I. Ogorodnikov

(2002) Study of ^{137}Cs, ^{90}Sr, ^{239,240}Pu, ^{238}Pu and ^{241}Am behaviour in the Chernobyl soil. J. Radioanal. Nucl. Chem. 251(1): 59-68

39. Hongxia Z, Chao Y, Zuyi T (2009) Effects of phosphate and fulvic acid on the sorption and transport of uranium(VI) on silica column. . J. Radioanal. Nucl. Chem. 279(1): 317-323
40. Y. Iida, T. Yamaguchi, T. Tanaka, K. Hemmi (2016) Sorption behaviour of thorium onto granite and its constituent minerals. J Nucl. Sci. Technol. 53(10): 1573-1584.
41. S. Nagasaki, S. Tanaka, A. Suzuki (1999) Sorption of neptunium on bentonite and its migration in geosphere. Colloids and Surfaces A: Physicochemical and Engineering Aspects. 155: 137–143.
42. W. Dong, X. Wang, S. Yi, X. Zhao, Z. Tao (2000) Sorption of radiocobalt on bentonite and kaolinite. J. Radioanal. Nucl. Chem. 245(2): 431-434
43. H. Geckeis, J. Lützenkirchen, P. Robert, R. Thomas, S. Moritz (2013) Mineral- Water Interface Reactions of Actinides. Chem. Rev.113: 1016-1062.
44. A. W. Miller, Y. Wang (2012) Radionuclide Interaction with Clays in Dilute and Heavily Compacted Systems: A Critical Review. Environ. Sci. Technol. 46(4): 1981-1994.
45. H. Geckeis, T. Rabung (2002) Solid-Water Interface Reactions of Polyvalent Metal Ions at Iron Oxide-Hydroxide Surfaces. Marcel Dekker, Inc. New York.
46. T. C. Hsu (2009) Experimental assessment of adsorption of Cu^{2+} and Ni^{2+} from aqueous solution by oyster shell powder. J. Hazard. Mater. 171: 995-1000.
47. Yuh-Shan Ho (2006) Review of second-order models for adsorption systems. J. Hazard Mater B136: 681–689
48. F. Seco, C. Hennig, J. D. Pablo, M. Rovira, I. Rojo, V. Marti, J. Gimenez, L. Duro, M. Grive, J. Bruno (2009) Sorption of Th(IV) onto Iron Corrosion Products: EXAFS Study.

Environ. Sci. Technol. 43(8): 2825-2830.

49. K. J. Chung, R. Klenze, K. K. Park, P. Paviet-Hartmann, J.I Kim (1998) A Study of the Surface Sorption Process of Cm(III) on Silica by Time-Resolved Laser Fluorescence Spectroscopy. Radiochim. Acta. 82: 215-219.
50. K. Muller, H. Foerstendorf, V. Brendler, G. Bernhard (2009) Sorption of Np(V) onto TiO_2, SiO_2, and ZnO: An in Situ ATR FT-IR Spectroscopic Study. Environ. Sci. Technol. 43(60): 7665-7670.
51. A. T. Yu, K. I. Maslakov, S. I. Kalmykov, K. E. Ivanov, L. Vukcevic, A. B. Khasanova, N. S. Shcherbina (2006) Interaction of Neptunyl with goethite (α-FeOOH), maghemite (γ-Fe_2O_3), and hematite (α-Fe_2O_3) in water as probed by X-ray photoelectron spectroscopy. Russ. J. Inorg. Chem. 51(12): 1937-1944.
52. J. I. Kim, R. Stumpe, R. Klenze (1991) Laser Induced Photoacoustic Spectroscopy for the speciation of transuranic elements in natural aquatic system. Top. Curr. Chem. 157: 129 - 179.
53. G. R. Choppin (2006) Actinide speciation in aquatic systems. Marine. Chemistry 99: 83-92.
54. H. G. Weidinger (2007) Zr-Alloys, the Nuclear Material for Water Reactor Fuel. A Survey and Update with Focus on Fuel for Pressurized Water Reactor Systems. 7th International Conference on WWER Fuel Performance, Modelling and Experimental Support Albena, Bulgaria.
55. M. Howe-Grant (1996) Kirk–Othmer encyclopedia of chemical technology, vol-17, 4th ed. Wiley, New York, 449-450.
56. D. H. Lister (1992) Coolant technology for water cooled reactors. IAEA-TECHDOC-667, vol. 2, IAEA, Vienna.

57. R. H. Rainey, J. G. Moore (1962) Laboratory development of the acid Thorex process for recovery of consolidated Edison Thorium reactor fuel. Oak Ridge National Laboratory, U.S. Atomic Energy Commission, ORN L-3155
58. IAEA (2005) Thorium fuel cycle- potential challenges and benefits. IAEA TECDOC-1450, Vienna, Austria
59. K.W. Bagnall (1996) The Chemistry of Weighable Amounts of Polonium and Protactinium. Radiochim Acta. 5(1): 1-5
60. I. M.Gibalo (1968) Analytical chemistry of niobium and tantalum. Israel program for scientific translations, Jerusalem, pp. 9-10.
61. A. V. Davydov, E.S. Pal'shin (1967) Oxalte complexes of Pa(V). Atomnaya Energiya, 22(5): 389-392
62. G. A. Welch (1953) The Protactinyl ion. Nature, 172: 458
63. R. Guillaumont (1965) Bull. Soc. Chim France. 132
64. B. Fourest (2004) The Hydrolysis of Protactinium (V) studied by Capillary Diffusion. *J.* Solution Chem. **33**(8): 957-973.
65. K. Andersson, B. Torstenfelt, J. Rydberg (1979) Leakage of Niobium-94 from an underground rock repository. Department of Nuclear Chemistry, Chalmers University of Technology, Göteborg, 1979-11-05.
66. M. Söderlund, M. Hakanen, J. Lehto (2015) Sorption of Niobium on boreal forest soil. Radiochim Acta. 103(12): 859-869.
67. T. Huitti, M. Hakanen (1996) Sorption of cesium, radium, protactinium, uranium, neptunium and plutonium on rapakivi granite. Laboratory of Radiochemistry Department of chemistry University of Helsinki, Finland

68. S. Kulmala, M. Hakanen (1996) Sorption of protactinium on rocks in ground waters from Posiva investigation sites. Laboratory of Radiochemistry Department of Chemistry University of Helsinki, Finland

69. Y. Sakamoto, T. Ishii, S. Inagawa, Y. Gunji, S. Takebe, H. Ogawa, T. Sasaki (2002) Sorption Characteristics of Actinium and Protactinium onto Soils. J. Nucl. Sci. Technol. S3: 481-484.

70. P. S. Remya Devi, S. Joshi, R. Verma, A. V. R. Reddy, A. M. Lali, L. M. Gantayet (2010) Ion-exchange separation of ^{60}Co and ^{125}Sb from zirconium for radioactive waste management. Nuclear Technology 171**:** 220-227.

71. S. Gangotra, P. M. Ouseph, S. Anantharaman, K. C. Sahoo (2002) Gamma spectrometry studies on irradiated zircaloy pressure tubes. ZIRC-2002, BARC, Mumbai, India, p 658

72. Organization for economic cooperation and development(OECD) (2015). Perspectives on the Use of Thorium in the Nuclear Fuel Cycle. NEA No. 7228.

73. M. Srinivasan, K. Subba Rao, M.V. Dingankar (1990) The actinide waste problem in perspective. Proceedings of the Indo-Japan seminar on Thorium Utilization, Bombay, India, pp.184-196.

74. Organization for Economic Cooperation and Development (OECD) (1984) Geological disposal of radioactive waste: An overview of the current status of understanding and development, Organization for economic cooperation and development. Paris.

75. H. Basu, R, K. Singhal, M. V. Pimple, A. Kumar, A. V. R. Reddy (2015) Association and migration of uranium and thorium with silica colloidal particles in saturated subsurface zone. J. Radioanal. Nucl. Chem. 303(3): 2283-2290.

76. A. B. Kersting, D. W. Efurd, D. L. Finnegan, D. J. Rokop, D. K. Smith, J. L. Thompson

(1999) Migration of plutonium at Nevada test site. Nature 397:56-59.

77. J. Buffle, G. G. Leppard (1995) Characterization of aquatic colloids and macromolecules. 1. Structure and behaviour of colloidal material. Environ. Sci. Technol 29(9): 2169-2175.
78. S. Sachs, G. Bernhard (2011) Influence of humic acids on the actinide migration in the environment: suitable humic acid model substances and their application in studies with uranium-a review J. Radioanal. Nucl. Chem 290:17-29.
79. H. Geckeis, T. Stumpf (2009) Institute for Nuclear waste disposal. Annual Report. KIT-SR 7559 14.
80. K. H. Lieser (1995) Radionuclides in geosphere: Sources, reactions in natural waters and interaction with solids. Radiochim. Acta 70(71**):** 355-375.
81. G. Fagerlund (1973) Determination of specific surface by the BET method. Matériaux et Construction. 6(3): 239-245.
82. K. A. Kraus, G. E. Moore (1951) Anion exchange studies I. Separation of zirconium and niobium in HCl-HF mixtures. J. Am. Chem. Soc 73**:** 9-13.
83. S. Sethi, P. Anupama, L. M. Gantayet (2001) Pilot plant experience of recovery of rare, natural protactinium from the insoluble muck: installation and operation. TSM-203 CHEMCON, Chennai.
84. K. A. Kraus, G. E Moore (1951) Anion Exchange Studies-III: Protactinium in Some HCl-HF Mixtures: Separation of Niobium, Tantalum and Protactinium. J. Am. Chem. Society. **73**(6): 2900-2902.
85. M. Samadfam, T. Jintoku, H. Ohashi, T. Mitsugashira, M. Har, Y. Suzuki (2000) Effects of humic acid on the sorption of Am(III) and Cm(III) on kaolinite. Radiochim. Acta 88: 717-721.

86. J. D. H. Strickland (1952) Use of Ion exchanger resin to determine charge of an ion in aqueous solution. Nature. 169: 620.
87. M. Marhol (1982) Ion exchanger in analytical chemistry, their properties and use in inorganic chemistry. Vol. XIV. P 57.
88. W. Stumm, J.J. Morgan (1970) An Introduction Emphasizing Chemical Equilibria in Natural Waters, Wiley Interscience, p. 481.
89. F. A. Cotton, G. Wilkinson, C. A. Murillo, M. Bochmann (1999) Advanced inorganic chemistry, 6th edn., John Wiley & sons, Inc, p 897.
90. H. Ervanne, E. Puukko, M. Hakanen (2013) Modeling of sorption of Eu, Mo, Nb, Ni, Pa, Se, Sn, Th and U on kaolinite and illite in olkiluoto groundwater simulators. Working report 2013-31. University of Helsinki, Finland.
91. R. Caletka (1970) Separation of ^{95}Zr and ^{95}Nb by means of sorption on silica gel from hydrochloric acid solutions. J. Radioanal. Nucl. Chem 6(1): 5-10.
92. W. Stumm, J. J. Morgan (1996) Aquatic Chemist*,* John Wiley & Sons, Inc., USA, p 516
93. J. B. Burcham, J. Datka, I. E. Wachs (1999) In situ vibrational spectroscopy studies of supported niobium oxide catalysts. J. Phys. Chem. B 103(29): 6015-6024.
94. H. W. Kirby (1960) The radiochemistry of Protactinium. NAS-NRC. USA.
95. 95. D. J. Wiggins, J. A. Franz (1978) Mobility of organic complexes of some non-TRU fission and activation products: a selective review. Battelle Pacific Northwest Labs., Richland, Wash. (USA)
96. M. J. Apted (1990) Radionuclide release from high-level nuclear-waste packages. J. Radioanal. Nucl. Chem. 142 (1): 321-330.

97. D. M. Nelson, K. A. Orlandini (1986) Source effects on actinides movement in ground water, NL 86-15, Argonne National Laboratory, Argonne, Illinois 60439, USA.
98. E. S. Patera, D. E. Hobart, A. Meijer, R. S. Rundberg (1990) chemical and physical processes of radionuclide migration at yucca mountain Nevada. J. Radioanal. Nucl. Chem. 142(1): 331-347.
99. R. Haapanen, L. Aro, J. Helin, T. Hjerpe, A. Ikonen, T. Kirkkala, S. Koivunen, A. M. Lahdenperä, L. Puhakka, M. Rinne, T. Salo (2009) Olkiluoto Biosphere Description. Posiva Report 2009-2.
100. T. Hjerpe, A. T. K. Ikonen, R. Broed (2010) Biosphere Assessment Report 2009. Posiva Report 2010-03.
101. J. Lehto, X. Hou (2010) Chemistry and analysis of radionuclides: laboratory techniques and methodology. Wiley-VCH 2010, Germany.
102. E. P. Steinberg (1961) The Radiochemistry of niobium and tantalum. Clearing House for Federal Scientific and Technical Information NAS-NS 3039, USA.
103. C. F. Jr. Baes, R. E. Mesmer (1976) The hydrolysis of cations. John Wiley & Sons, New York.
104. K. Andersson, B. Torstenfelt, J. Rydberg (1979) Leakage of niobium-94 from an underground rock repository. SKB Technical Report 79-26.
105. D. Charles, D. Prime (1983) Desorption behaviour of artificial radionuclides sorbed on to estuarine silt: (I) caesium-137 and ruthenium-106, (II) zirconium-95 and niobium-95. Environ. Pollut. B5: 273-295.

106. M. E. Åström, P. Peltola, J. J. Virtasalo, A. T. Kotilainen, R. Salminen (2008) Niobium in boreal stream waters and brackishwater sediments. Geochem. Explor. Environ. Anal. 8: 139-148.

107. C. Lin, C. Zhang, X. Zhang (1990) Study of the behaviour of niobium colloid in nitric acid solution by electro dialysis. J. Radioanal. Nucl. Chem.12: 140-145**.**

108. G. M. N. Baston, J. A. Berry, A. K. Littleboy, N. J. Pilkington (1992) Sorption of activation products on London clay and Dungeness aquiver grave. Radiochim. Acta 58(59): 225-233.

109. G. R. Choppin (1983) Solution Chemistry of the Actinides. Radiochim Acta. 32: 43-53.

110. N. N. Greenwood, A. Earnshaw (1997) Chemistry of the Elements. 2nd Edition. Oxford Butterworth-Heinemann in Oxford, Boston.

111. U. Schwertmann, R. M. Cornell (2004) The Iron oxidex: Structure, properties, reaction and uses. Wiley-VCH, New York.

112. E. K. Papynov, A. S. Portnyagin, A. I. Cherednichenko, I. A. Tkachenko, E. B. Modin, V. Y. Maiorov, A. N. Dran'kov, T. A. Sokol'nitskaya, K. A. Kydralieva, Sh. Zh Zhorobekova, V. A. Avramenko. (2016) Uranium sorption on reduced porous iron oxides. J. Radioanal. Nucl. Chem. 468(1): 67-71.

113. L. Yan, F. Wu, Q. Wangsuo (2011) Sorption of Th(IV) on goethite: effects of pH, ionic strength, FA and phosphate. J. Radioanal. Nucl. Chem. 289(3): 865-871.

114. C. Dinga, W. Chenga, Y. Suna, X. Wang (2015) Novel fungus-Fe_3O_4 bio-nano-composites as high performance adsorbents for the removal of radionuclides. J. Hazardous Materials. 295:127-137.

115. Z. Guo, D. Xu, D. Zhao, S. Zhang, J. Xu (2011) Influence of pH, ionic strength, foreign ions and FA on adsorption of radiocobalt on goethite. J Radioanal Nucl Chem. 287:505-512.

116. M. Mohapatra, S. Anand (2010) Synthesis and applications of nano-structured iron oxides/hydroxides: a review. Int. J. Eng. Sci. Technol. 2(8): 127-146.

117. L. S. Balistrieri, J. W. Murray (1981) The surface chemistry of goethite (α-FeOOH) in major ion in seawater. Am. J. Sci. 281: 788-806.

118. M. Kosmulaski, E. Maczka, E. Jartych, J. B. Rosenholm (2003) Synthesis and characterization of goethite and goethite–hematite composite: experimental study and literature survey. Advances in Colloid and Interface Science. 103: 57-76.

119. J. J. Carlson, S. K. Kawatra (2013) Factors affecting zeta potential of iron oxides. Mineral Processing & Extractive Metall. Rev. 34: 269-303.

120. T. M. Petrova, L. Fachikov, J. Hristov (2011) The magnetite as adsorbent for some hazardous species from aqueous solutions: a review. Int. Rev. Chem. Eng. 3: 134-152.

121. M. Ghosh, P. S. Remya Devi, R. Verma, A. V. R. Reddy (2015) Sorption of niobium on colloidal silica and the effect of humic acid. J. Radioanal. Nucl. Chem. 306: 147-153.

122. J. A. Davis, R. Gloor (1981) Adsorption of dissolved organics in lake water by aluminum oxide. Effect of molecular weight. Environ. Sci. Technol. 15: 1223-1229.

123. E. M. Murphy, J. M. Zachara, S. C. Smith (1990) Influence of mineral-bound humic substances on the sorption of hydrophobic organic compounds. Environ. Sci. Technol. 240: 1507-1516.

124. R. Amal, J. A. Raper, T. D. Waite, T (1992) Effect of fulvic acid adsorption on the aggregation kinetics and structure of hematite particles. J. Colloid Interface Sci. 151: 244-257.

125. B. Gu, J. Schmitt, Z. Chen, L. Liang, J. F. McCarthy (1994) Adsorption and desorption of natural organic matter on iron oxide: Mechanisms and models. Environ. Sci. Technol. 28: 38-46.

126. K. H. Tan (1976) Complex formation between humic acid and clays as revealed by gel filtration and infrared spectroscopy. Soil Biol. Biochem. 8: 235-239.

127. J. L. Zhou, S. Rowland, R. Fauzi, C. Mantoura, J,. Braven (1994) The formation of humic coatings on mineral particles under simulated estuarine conditions-A mechanistic study. Water Res. 28: 571-579.

128. G. McD.Day, B. T. Hart, I. D. McKelvie, R. Beckett (1994) Adsorption of natural organic matter onto goethite.Colloids & Surfaces A: Physicochem. Eng. Aspects 890: 1-13.

129. D. A. Dzombak, F. M. M. Morel (1987) Adsorption of inorganic pollutants in aquatic systems. J. Hydraulic Engineering.113: 430–475.

130. K. Nakata, T. Tanaka, S. Nagasaki, S. Tanaka, A. Suzuki, Y. Sakamoto, H. Ogawa (1998) Sorption characteristics of Np on Fe(II) + Fe(IH) oxides. JAERI-Conf 99-004: 634-642, Japan.

131. S. Nakayama, Y. Sakamoto (1991). Sorption of neptunium on naturally-occurring iron-containing minerals. Radiochim. Acta 52(53): 153-157.

132. K. Nakata, S. Nagasaki, S. Tanaka, Y. Sakamoto, T. Tanaka, H. Ogawa (2004) Reduction rate of neptunium(V) in heterogeneous solution with magnetite. Radiochim. Acta 92: 145-149.

133. G. W. Beali, G. D. O'Kelley, B. Allard (1980) An autoradiographic study of actinide sorption on climax stock granite, ORNL-5617, Oak Ridge, Tennessee 37830.

134. F. A. White, M. Peterson (1996) Reduction of aqueous transition metal species on the surface of Fe(II) containing oxides. Geochim. Cosmochim. Acta. 60: 3799-3814.

135. F. A. White, A. Yee (1985) Aqueous oxidation reduction kinetics associated with coupled electron cation transfer from iron containing silicates. Geochim. Cosmochim. Acta. 49:1263-1275.

136. A. F. White, M. L. Peterson, M. F. Jr. Hochella (1994) Electrochemistry and dissolution kinetics of magnetite and ilmenite. Geochim Cosmochim Acta. 58(8): 1859-1875.

137. R. D. Harter, R. Naidu (1995) Role of metal-organic complexation in metal sorption by soils. Advances in Agronomy 55: 210-263.

138. M. M. Benjamin, J. O. Leckie (1981) Multiple-site adsorption of Cd, Cu, Zn, and Pb on amorphous iron oxyhydroxides. J. Colloid and Interface Science. 79: 209-221.

139. P. W. Schindler, P. Liechti, J. C. Westall (1987) Adsorption of copper, cadmium and lead from aqueous solution to the kaolinite/water interface. Netherlands J. Agri. Science. 35: 219-230.

140. B. K. Singh, A. Jain, S. Kumar, B. S. Tomar, R. Tomar, V. K. Manchanda, S. Ramanathan (2009) Role of magnetite and humic acid in radionuclide migration in the environment. J. Contaminant Hydrology 106: 144-149.

141. X. Tan, Q. Fan, X. Wang, B. Grambow (2009) Eu(III) Sorption to TiO_2 (Anatase and Rutile): Batch, XPS, and EXAFS Studies. Environ. Sci. Technol. 43: 3115-3121.

142. A. Fairhurs, J. P. Warwick, S. Richardson (1995) The influence of humic acid on the adsorption of europium onto inorganic colloids as a function of pH. Colloids and Surfaces A: Physicochemical and Engineering Aspects. 99: 187-199.

143. K. S. Smith (1999). Metal sorption on mineral surfaces: an overview with examples relating to mineral deposits, U.S. Geological Survey, Box 25046, MS 973, Federal Center, Denver

144. H. Yuh-Shan (2006) Review of second-order models for adsorption systems. J. Hazardous Materials. B136:681-689.

145. S. Lagergren (1898) Zur theorie der sogenannten adsorption geloster stoffe. 591. Kungliga Svenska Vetenskapsakademiens, Handlingar 24 (4): 1-39.

146. Y. S. Ho (1995) Adsorption of heavy metals from waste streams by peat, Ph.D. thesis, University of Birmingham, Birmingham, U.K.

147. W. J. Weber, J. C. Morris (1963) Kinetics of adsorption on carbon from solution. J. Sanit. Eng. Div. Am. Soc. Civ. Eng.89(2): 31-60.

148. S. S. Gupta, K. G. Bhattacharyya (2011) Kinetics of adsorption of metal ions on inorganic materials: a review. Adv Coll Inter Sci.162: 39-58.

149. IUPAC., 2014.Compedium of Chemical Terminology, Gold Book, version 2.3.3.

150. S. Sundaram, N. Viswanathan, S. Meenakshi (2008) Defluoridation chemistry of synthetic hydroxyapatite at nano scale: Equilibrium and kinetic studies, J. Hazardous Materials. 155: 206-215.

151. S. Ananta, S. Banerjee, V. Vijay (2015) Adsorption isotherm, thermodynamic and kinetic study of arsenic (III) on iron oxide coated granular activated charcoal. Int. Res. J. Environ. Sci. 4(1): 64-77.

152. M. Jnr. Horsfall, A. I. Spiff (2005) Effects of temperature on the sorption of Pb^{2+} and Cd^{2+} from aqueous solution by Caladium bicolor (Wild Cocoyam) biomass. Electronic J Biotechnol. 8(2): 162-169.

153. T. Missana, M. García-Gutiérrez, C. Maffiotte (2003). Experimental and modeling study of the uranium (VI) sorption on goethite. J. Colloid and Interface Science 260: 291-301.

95. A. B. Khasanova, N. S. Shcherbina, S. N. Kalmykov, Yu, A. Teterin, A. P. Novikov (2007) Sorption of Np(V), Pu(V), and Pu(IV) on Colloids of Fe(III) Oxides and Hydrous Oxides and MnO_2. Radiochemistry 49(4): 419-425.

155. T. D. Waite, J. A. Davis, T. E. Payne, D. A. Waychunas, N. Xu (1994) U(VI) adsorption on ferrihydrite: application of a surface complexation model. Geochim. Cosmochim. Acta. 58(24): 5465-5478.

156. A. L. Sanchez, J. W. Murray, T. H. Sibley (1985) The adsorption of Plutonium IV and V on goethite. Geochim. Cosmochim. Acta 49: 2297-2307.

157. B. A. Powell, R. A. Fjeld, D. I. Kaplan, J. T. Coates, M. S. Steven (2005) $Pu(V)O_2^+$ adsorption and reduction by Hematite and Goethite. Environ. Sci. Technol. 39(7): 2107-2114.

158. E. R. Sylwestera, E. A. Hudsona, P. G. Allen (2000) The structure of uranium (VI) sorption complexes on silica, alumina, and montmorillonite. Geochim. Cosmochim. Acta. 64(14): 2431-2438.

159. E. Hartmann, H. Geckeis, T. Rabung, J. Lützenkirchen, T. Fanghänel (2008) Sorption of radionuclides onto natural clay rocks. Radiochim. Acta. 96: 699–707.

160. S. B. Clark, W. H. Johnson, M. A. Malek, S. M. Serkiz, T. G. Hinton (1996) A comparison of sequential extraction technique to estimate geochemical controls on the mobility of

fission products, actinides and heavy metal contaminants in soil. Radiochim. Acta. 74: 173-179.

161. E. L. Cooper, M. K. Haas, J. F. Mattie (1995) Studies of the speciation of Plutonium and other actinides in natural groundwater using anion exchange resin. Appl. Radiat. Isot. 46(11): 1159-1173.

162. L. Axe, T. Tyson, P. Trivedi, T. Morrison (2000) Local structure analysis of strontium sorption to hydrous manganese oxide. J. Colloid and Interface Sci. 224: 408-416.

163. L. Al-Attar, A. Dyer (2002) Sorption behaviour of uranium on birnessite, a layered manganese oxide. J. Mater Chem. 12: 1381-1386.

164. A. Dyer, M. Pillinger, R. Harjula, S. Amin (2000) Sorption characteristics of radionuclides on synthetic birnessite-type layered manganese oxides. J.l of Mater Chem 10(8): 1867-1874.

165. M. C. Duff, D. B. Hunter, I. R. Triay, P. M. Bertsch, D. T. Reed, S. R. Sutton, G. Shea McCarthy, J. Kitten, P. Eng, S. J. Chipera, D. T. Vaniman (1999) Mineral associations and average oxidation states of sorbed Pu on tuff. Environ. Sci. Technol. 33: 2163-2169.

166. W. L. Keeney-Kennicutt, J. W. Morse (1984) The interaction of Np(V) O_2^+ with common mineral surfaces in dilute aqueous solutions and seawater. Marine Chemistry 15: 133-150.

167. J. L. Means, D. A. Crerar, M. P. Borcsik, J. O. Duguid (1978) Adsorption of Co and selected actinides by Mn and Fe oxides in soils and sediments. Geochim Cosmochim Acta 42: 1763-1773.

168. P. Misaelides, T. Katranas, A. Godelitsas, H. Lkewe-Nebenius, I. Anousis (2002) The chemical behaviour of the natural microporous manganese-oxide todorokite in actinides (Th, U, Pa) aqueous solutions. Separation Science and Technology 37 (5): 1109-1121.

169. J. L. Means. D. L. Krerer, M. R. Borcsik, D. O. Duguid (1978) Radionuclide adsorption by

manganese oxides and implication for radioactive waste disposal. Nature 274: 44-47.

170. A. Mohammad, A. K. R. Rao, B. A. Siddiqui (1995) Adsorption studies and the removal of dissolved metals using pyrolusite as adsorbent. Environ Monitoring and Assessment. 38(1): 25-35.

171. T. Xiaoli, W. Xiangke, C. Changlun, S. Aihua (2007) Effect of soil humic and fulvic acids, pH and ionic strength on Th(IV) sorption to TiO_2 nanoparticles. Appl. Radiat. isot. 65: 375-381.

172. R. M. Mckenzi (1971). The synthesis of birnessite, cryptomelane and some other oxides and hydroxides of manganese. Mineralogical magazine 38: 493-502.

173. Pyrolusite R040153 - RRUFF Database: Raman spectra, X-ray Diffraction and chemistry data for minerals

174. E. Cristiano, J. H. Yung, S. Matthew, K. Daniel, H. Nitsche (2011) A comparison of point of zero charge measurement methodology. Clay and Clay Minerals. 59(2): 107-115.

175. A. J. Fairhurst, P. Warwick, S. Richardson (1995) The influence of humic acid on the adsorption of Europium onto inorganic colloids as function of pH. Colloids & Surfaces A: Physicochemical and Engineering aspects. 99: 187-199.

176. Z. Lang, Z. Huyuan, Y. Ming, C. Hang, Z. Ming (2013) Laboratory determination of migration of Eu(III) in compacted bentonite–sand mixtures as buffer/backfill material for high-level waste disposal. Appl. Radiat. isot. 84: 139-144.

177. X. Wang, D. Xu, L. Chen, X. Tan, X. Zhou, A. Ren, C. Chen (2006) Sorption and complexation of Eu(III) on alumina: Effects of pH, ionic strength, humic acid and chelating resin on kinetic dissociation study. Appl. Radiat. isot. 64: 414-421.

178. E. M. Murphy, J. M. Zachara, S. C. Smith, J. L. Phillips, T. Wietsma (1994) Interaction of

hydrophobic organic compounds with mineral-bound humic substances. Environ. Sci. Technol. 28:1291-1299.

179. K. F. Hayes, Ch. Papelis, J. O. Leckie (1988) Modeling ionic strength effects on anion adsorption at hydrous oxide/solution interfaces. J. Coll. Interf. Sci. 125: 717-726.

180. S. Xiaoping, W. Suowei, C. Lei, Z. Maolian, D. Yunhui (2009) Effect of pH, ionic strength and temperature on the sorption of radionickel on Na-montmorillonite. Appl. Radiat. isot. 67: 1007-1012.

181. Li. Yan-Hui, Di. Zechao, D. Jun, Wu. Dehai, L. Zhaokun, Z. Yanqiu (2005) Adsorption thermodynamic, kinetic and desorption studies of Pb^{2+} on carbon nanotubes. Water Research 39: 605-609.

182. J. M. Smith (1981) Chemical engineering kinetics. 3rd ed., McGraw-Hill, New York.

183. A. Ozcan, A. S. Ozcan, S. Tunali, T. Akar, I. Kiran (2005) Determination of the equilibrium, kinetic and thermodynamic parameters of adsorption of Cu(II) ions onto seeds of Capsicum annuum. J. Hazard. Mater. B124: 200-208.

184. N. Unl, M. Ersoz (2006) Adsorption characteristics of heavy metal ions onto a low cost biopolymeric sorbent from aqueous solutions. J. Hazard. Mater. B136: 272-280.

185. D. A. Skoog, D. M. West, F. J. Holler, S. R. Crouch (2010) Fundamentals of analytical chemistry. India edition (8th), p.128.

186. IAEA TECDOC 1401(2004), Quantifying uncertainty in nuclear analytical measurements, IAEA, Vienna.

187. S. L. R. Ellison, A. Williams (2012) Quantifying Uncertainty in Analytical Measurements, Eurachem/CITAC Guide CG 4, QUAM, 3rd edn.

188. S. Lagergren (1898) Zur theorie der sogenannten adsorption geloster stoffe. 591. Kungliga

Svenska Vetenskapsakademiens, Handlingar 24 (4); 1-39.

189. Y. S. Ho (1995) Adsorption of heavy metals from waste streams by peat, Ph.D. thesis, University of Birmingham, Birmingham, U.K.

190. X. Tan, M. Fang, X. Wang (2010) Sorption Speciation of Lanthanides/Actinides on Minerals by TRLFS, EXAFS and DFT Studies: A Review. Molecules. 15: 8431-8468.

191. G. D. Turner, J. M. Zachara, J. P. Mckinley, S. C. Smith (1996) Surface-charge properties and UO_2^{2+} adsorption of a subsurface smectite. Geochim Cosmochim Acta. 60(18): 3399-3414.

192. K. F. Hayes, J. O. Leckie (1987) Modeling Ionic Strength Effects on Cation Adsorption at Hydrous Oxide/Solution Interfaces. J. Coll. Interf. Sci. 115(2): 564-572.

193. A. Ozer, D. Ozer (2003) Comparative of the bio-sorption of Pb(II), Ni(II) and Cr(VI) ions onto S. cerevisiae: determination of biosorption heats. J. Hazard. Mater. 100: 219-229.

194. T. Rabung, M. C. Pierret, A. Bauer, H. Geckeis, M. H. Bradbury, B. Baeyens (2005) Sorption of Eu(III)/Cm(III) on Ca-montmorillonite and Na-illite. Part I: Batch sorption and time-resolved laser fluorescence spectroscopy experiments. Geochim. Cosmochim. Acta. 69: 5393-5402.

195. U. Gabriel, L. Charlet, C. W. Schläpfer, J. C. Vial, A. Brachmann, G. Geipel (2001) Uranyl surface speciation on silica particles studied by time-resolved laser-induced fluorescence spectroscopy. J.Colloid Interface Sci. 239: 358-368.

196. G. Lefèvre, J. F. Kneppers, M. Fédoroff (2008) Sorption of uranyl ions on titanium oxide studied by ATR-IR spectroscopy. J. Colloid. Interface Sci. 327: 15-20.

197. R. Chowdhury, E. K. Yanful, A. R. Pratt (2011) Arsenic removal from aqueous solutions by mixed magnetite/maghemite nanoparticles, Environ. Earth Sci 64: 411-423.

198. X. L. Tan, X. K. Wang, H. Geckeis, T. Rabung (2008) Sorption of Eu(III) on humic acid or fulvic acid bound to alumina studied by SEM-EDS, XPS, TRLFS and batch techniques. Environ. Sci. Technol. 42: 6532-6537.

199. M. Schmidt, P. J. Eng, J. E. Stubbs, P. Fenter, L. Soderholm (2011) A new x-ray interface and surface scattering environmental cell design for in situ studies of radioactive and atmosphere-sensitive samples. Rev. Sci. Instrum. 82: 075105 (1-10).

200. W. C. Lee, S. O. Kim, J. Ranville, S. T. Yun, S. H. Choi (2014) Sequestration of arsenate from aqueous solution using 2-line ferrihydrite: equilibria, kinetics, and X-ray absorption spectroscopic analysis. Environ Earth Sci 71(8): 3307-3318.

201. M. N. Denecke (2006) Actinide speciation using X-ray absorption fine structure spectroscopy. Coord. Chem Rev. 250(7/8):730-754.

202. G. Vlaic, L. Olivi (2004) EXAFS spectroscopy: a brief introduction. Croatica Chemica Acta. 77(3): 427-433.

203. J. N. Combes, C. J. Chisholem-Brause, G. E. Brown, G. A. Parks (1992) EXAFS spectroscopic study of Np(V) sorption at the α-FeOOH/water interface. Environ. Sci. Technol. 26(2): 376-381.

204. P. Zhao, J. D. Begg, M. Zavarin, S. J. Tumey, R. Williams, Z. R. Dai, R. Kips, A. B. Kersting (2016) Plutonium(IV) and (V) Sorption to Goethite at Sub-Femtomolar to Micromolar Concentrations: Redox Transformations and Surface Precipitation Environ. Sci. Technol. 50(13): 6948-6956.

205. T. Peretyazhko, J. M. Zachara, S. M. Heald, B. H. Jeon, R. K. Kukkadapu, C. Liu, D. Moore, C. T. Resch (2009) Heterogeneous reduction of Tc(VII) by Fe(II) at the solid–water interface. Geochim Cosmochim Acta. 72: 1521-1539.

206. M. L. Peterson, G. E. Brown, Jr., G. A. Parks (1995) Direct XAFS evidence for heterogeneous redox reaction at the aqueous chromium magnetite interface. Colloids and surfaces A: Physico chem. Eng. Aspects. 107: 77-88.

207. S. Basu, C. Nayak, A. K. Yadav, A. Agrawal, A. K. Poswal, D. Bhattacharyya, S. N. Jha, N. K. Sahoo (2014) A comprehensive facility for EXAFS measurements at the INDUS-2 synchrotron source at RRCAT, Indore, India. J. Phys.: Conf. Ser. 493: 012032 (1-4).

208. D. C. Konigsberger, R. Prince (1988) X-Ray Absorption: Principles, Applications, Techniques of EXAFS, SEXAFS and XANES. Wiley, New York.

209. M. Newville, B. Rave, B. Haskel, J. J. Rehr, E. A. Stern, Y. Yacoby (1995) Analysis of multiple scattering XAFS data using theoretical standards. Physica B. 208(209): 154-156.

210. S. Dierking, S. Amayri, T. Reich (2008) Actinide Sorption Studies Using the Isotopes ^{237}Np and ^{239}Np. J. Nucl. Sci. Technol. S6: 133-137.

211. O. Tochiyama, S. Endo, Y. Inoue (1995) Sorption of Neptunium(V) on various iron oxides and hydrous iron oxides. Radiochim. Acta. 68: 105-111.

212. K. Muller, A. Groschel, A. Rossberg, F. Bok, C. Franzen, V. Brendler, H. Foerstendrof (2015) In situ spectroscopic identification of Np(V) inner-sphere complexes on hematite-water interface. Environ. Sci. Technol. 49: 2560-2567.

213. S. Ardizzone, L. Formaro, J. Lyklema (1982) Ionic Strength Effects on Cation Sorption to Oxides: Macroscopic Observations and Their Significance in Microscopic Interpretation. J. Electroanal. Chem. 133: 149-155.

214. P. Venema, T. Hiemstra, W. H. van Riemsdijk (1996) Multisite adsorption of Cadmium on Goethite. J. Colloid Interface Sci. 183: 515-527.

215. J. M. Smith (1981) Chemical Engineering Kinetics. 3rd ed., McGraw-Hill, New York.

216. A. S. Ozcan, S. Tunali, T. Akar, I. Kiran (2005) Determination of the equilibrium, kinetic

and thermodynamic parameters of adsorption of Cu(II) ions onto seeds of Capsicum annuum. J. Hazard. Mater. B124: 200-208.

217. N. Unl, M. Ersoz (2006) Adsorption characteristics of heavy metal ions onto a low cost bio-polymeric sorbent from aqueous solutions. J. Hazard. Mater. B136: 272-280.

218. X. Jianhong, H. Mengchang, L. Chunye (2010) Adsorption of antimony (V) on kaolinite as a function of pH, ionic strength and humic acid. Environ Earth Sci 60: 715-722. DOI 10.1007/s12665-009-0209-z

219. Y. Hisao, T. Tsunehiro, Y. Tomoko, F. Takuzo, Y. Satohiro (1996) Control of the structure of niobium oxide species on silica by the equilibrium adsorption method. Catal. Today 28: 79-89.

220. K. Asakura, Y. Iwasawa (1991) Synthesis, characterization, and catalytic properties of SiO_2 attached One-atomic-layer Niobium oxide catalysts. J. Phys. Chem 95: 1711-1716.

221. M. P. Crosnier, D. Guyomard, A. Verbaere, Y. Piffard, M. Tournoux (1992) The Potassium Niobyl Cyclotetrasilicate $K_2(NbO)_2Si_4O_{12}$. J. Solid State Chem. 98: 128-132.

222. S. D. Kelly, D. Hesterberg, B. Ravel (2008) Analysis of soils and minerals using X-ray absorption spectroscopy, Chapter-14, USA, pp. 387-463.

223. Y. Aria, P. B. Moran, B. D. Homeyman, J. A. Davis (2007) In situ spectroscopic evidence for Np(V)-Carbonate innersphere and outer sphere ternary surface complexes on hematite surfaces. Environ. Sci. Technol. 41(11): 3940-3944.

224. P. Bots, S. Shaw, G. T. Law, T. A. Marshall, J. Frederick, W. Mosselmans, K. Morris (2016) Controls on the Fate and Speciation of Np(V) During Iron (Oxyhydr) oxide Crystallization. Environ. Sci. Technol. 50: 3382-3390.

Thesis Highlight

Name of the student: MADHUSUDAN GHOSH

Name of the CI/OCC: Bhabha Atomic Research Centre **Enrolment no.:** CHEM 01201304020

Thesis title: Studies on interaction of niobium and protactinium with hydrous oxides

Discipline: Chemical Sciences

Date of viva voce: January 06, 2020

In this thesis, the sorption studies of ^{94}Nb and ^{231}Pa on silica, iron oxides and manganese dioxides and effect of different physico-chemical parameters were described. The sorption mechanism is evaluated based on ionic strength and temperature dependent sorption phenomena and EXAFS spectroscopic investigation of the Nb sorbed silica and hematite at different pH. Both Nb and Pa are strongly associated with colloidal silica, iron oxides and manganese dioxide especially in the neutral pH to mildly basic pH region. In acidic pH the sorption of both the radionuclides is low for iron oxides but quite high for silica and manganese dioxide. Humic acid affects the sorption in acidic and basic medium either by its self-absorption onto the colloids or its complexation with the radionuclides at those respective pH conditions. There is mild effect of dissolution of iron oxides in acidic region (pH1-2) but for silica effect was observed above pH 10. Dissolution doesn't affect the sorption in case of manganese dioxide.

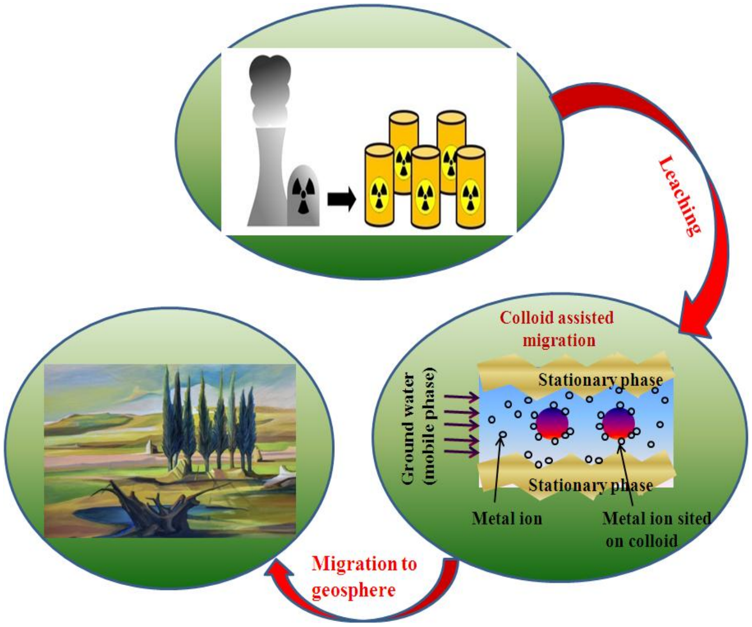

EXAFS study of the Nb sorbed silica at different pH clearly shows that in acidic pH, Nb is not coordinated with Si atom, whole coordination is satisfied by oxygen atom only. In neutral and basic medium, Nb is bonded with Si atom at 3.44 Å and 3.50 Å distances respectively. In the case of hematite in acidic pH, there is no evidence of Nb and Fe bonding but in neutral and basic medium, Nb is coordinated with 0.5 and 2 numbers of Fe atoms at 2.72 Å and 2.88 Å distances respectively.

The quantitative sorption in neutral to near neutral pH region indicates that in the natural aquatic conditions the migration of ^{94}Nb and ^{231}Pa is mainly assisted by the colloids present in the medium.